April 2022

Sediment Buffering and Recycling on an Annual to Centennial Scale Along the Mississippi River

Nikki E. Neubeck
Louisiana State University and Agricultural and Mechanical College

SEDIMENT BUFFERING AND RECYCLING ON AN ANNUAL TO CENTENNIAL SCALE ALONG THE MISSISSIPPI RIVER

A Thesis

Submitted to the Graduate Faculty of the
Louisiana State University and
Agricultural and Mechanical College
in partial fulfillment of the
requirements for the degree of
Masters of Geology

in

The Department of Geology and Geophysics

by
Nikki Elizabeth Neubeck
B.A., Louisiana State University, 2020
May 2022

ACKNOWLEDGMENTS

I would like to start off by thanking my graduate advisor, Dr. Peter Clift. I am beyond grateful for all the wonderful experiences I have gained from his guidance. I would like to believe that if I never went on the Ireland trip my freshman year of undergrad, I wouldn't be here with Dr. Peter Clift today, and I am so thankful. I am also thankful for my committee members, Dr. Carol Wilson, and Dr. Achim Herrmann, for their advice during laboratory work and helpful criticism along the way. I want to thank USU OSL Laboratory, Geosep Services, LSU lab facilities, and the London Geochronology Centre for analyzing my samples to produce the data in this study. I also would like to thank all the students I have met throughout the years in the geology department for being great friends and peers throughout my time here. Lastly, I would like to give a huge thank you to my father for believing in me and giving me opportunities to travel through LSU and have an amazing educational experience.

TABLE OF CONTENTS

ABSTRACT v

CHAPTER 1. INTRODUCTION 1

CHAPTER 2. BACKGROUND 3
2.1. Sediment Buffering During Transport 3
2.2. Basement Terrains of North America 4
2.3. Holocene Climatic History 8
2.4. Geology of the Lower Mississippi Valley 10
2.5. History of Levees 12
2.6. Study Area 13

CHAPTER 3. METHODS 15
3.1. Geoprobe Coring/Grab Bag 15
3.2. Optically Stimulated Luminescence 17
3.3. Zircon U-Pb Dating 19
3.4. Grain Size 22
3.5. Geochemical Analysis 23

CHAPTER 4. RESULTS 25
4.1. OSL Dating 25
4.2. Zircon U-Pb Dating 26
4.3. Grain Size Analysis 29
4.4. Geochemical Analysis 29

CHAPTER 5. DISCUSSION 33
5.1. Geochemical Analysis 33
5.2. Zircon U-Pb Dating 34
5.3. Grain Size Analysis 40
5.4. OSL Dating 43
5.5. Sediment Buffering 47
5.6. Efficiency of Zircon as a Provenance Method 47
5.7. Future Research Recommendations 51

CHAPTER 6. CONCLUSION 52

APPENDIX A. SUPPLEMENTARY FIGURES 53

APPENDIX B. ANALYTICAL DATA FOR GRAIN SIZE 56

APPENDIX C. OSL GEOCHEMISTRY DATA 62

APPENDIX D. ANALYTICAL DATA FOR ZIRCON U-PB DATING 67

APPENDIX E. XRF EXTENDED DATA 130

APPENDIX F. MONTE CARLO ZIRCON U-PB UNMIXING DATA 132

APPENDIX G. CUMULATIVE FREQUENCY PLOTS: K-S FORWAD MODELS 137

APPENDIX H. CUMULATIVE FREQUENCY PLOTS: KUIPER FORWARD MODELS....139

REFERENCES...141

VITA...150

ABSTRACT

Although the Mississippi River and its tributaries have been investigated for many years, the alteration of the river through dams, levees, and diversions has affected how sediment is transported from source to sink (>10^3 y). Previous provenance research using detrital zircon U-Pb dating indicates a slow transport time from source-to-sink, but recent anthropogenic alterations of the river may potentially diminish the transportation time of heavy minerals due to an increase in flow efficiency. The objective of this study is to analyze the degree of buffering and recycling of Mississippi River sediment over a range of short time scales, spanning months to centennial scale over the last approximately 2500 years. I will be using deposits that pre-date levee construction and are preserved in meandering river point bars, such as the False River point bar in southern Louisiana. First, optically stimulated luminescence dating is used to accurately date the accretion history of the False River point bar. Secondly, detrital U-Pb zircon dating is used to define provenance and constrain variations in modern flux and possible anthropogenic influences on coarse-grained sediment within the Mississippi River. The importance of zircon U-Pb dating is also analyzed to determine if this method is suitable for large river systems with a statistically robust number of grains analyzed. Grain size is used to determine if the late Holocene False River point bar is similar to Modern River samples and if bias is created amongst grain size data. Lastly, to achieve further provenance discrimination, major element bulk sediment geochemical compositions are determined and compared to previous analyses in the Gulf of Mexico to determine short-term variability.

CHAPTER 1. INTRODUCTION

Understanding what controls the development of landscape and the erosion and transport of sediment is fundamental to our interpretation of the sedimentary record. Unless we understand how the sedimentary record is built and to what extent signals generated in sources are lost or deleted during transport, it is impossible to interpret the deposits that are preserved in major sedimentary basins and form the basis of our reconstruction of ancient climate as well as the development of tectonic systems. Although tectonics is important in the process of sediment production over long periods of geological time ($>10^6$ y) (Fildani, McKay et al. 2016), large river systems are generally affected only by climate over timescales of up to 100,000 years. More recently, erosion has also been affected by human activities, particularly due to the installation of dams and the development of agriculture which have affected the amount erosion and the ability of sediment to reach marine depocenters (Montgomery 2007, Syvitski and Milliman 2007, US Army Corps of Engineers 2017).

Modelling of large drainage systems with extensive floodplains suggests that deposition and reworking of sediment on these floodplains has an important influence in removing short-term variations in the composition of river sediment. In this study, I use Optically Stimulated Luminescence (OSL) dating to constrain the accretionary age history of the False River point bar, located in the lower reaches of the Mississippi. Additionally, detrital zircon (DZ) U-Pb dating is used as a provenance method by repeatedly analyzing sediment samples collected monthly from a single point along the lower reaches of the river to understand if there is statistically significant annual or centennial variability. This would have serious implications for those using modern river sediments to compare with ancient deposits in the offshore, as well as provide a test of how well buffered the river is. I further use the opportunity to compare zircon

crystallization ages with grain size to understand the degree of potential bias that may be introduced by the preferential analysis of fine sand. My work has significance for all those who use this widespread method to constrain sediment provenance by better defining the actual uncertainties inherent in the method.

CHAPTER 2. BACKGROUND

2.1. Sediment Buffering During Transport

Sediments deposited in fluvial settings record environmental conditions during the time of sedimentation, and can also reflect accumulation rates, erosion, climate, and even seasonality of transport. In theory, fluvial sediments deposited and preserved in the rock record can be used to reconstruct a variety of geologic processes, such as growth and erosion of mountain belts, development of regional climate, or the evolution of sedimentary basins. However, to interpret the sediment record we need to understand how sediment is transported from source to sink. It is necessary to understand if sedimentary signals created in the source hinterland are diluted or destroyed by storage and recycling of older sediments in floodplain environments, en route to the ocean depocenter. Low gradient floodplains in the lower reaches of major rivers represent an important stage of the transport process and may store large amounts of sediment over long periods (10^3–10^5 y) of time. Many sediment provenance studies use modern rivers as baseline samples against which to assess changing erosion, but do random modern samples reliably image the state of the modern catchment? In theory such delta plain areas may act as long-term records of how the drainage basin evolves under the impact of climate and sea level change.

Transport and storage of sediment through large river systems can be complicated by the behavior of different grain sizes in suspension and bedload. Fine grained sediment is usually transported as suspended sediment, while zircons, reflecting their high density usually travel as bedload, especially if they are sand sized (Benyon, Leier et al. 2014). Since zircon grains tend to be transported as bedload, the travel time from source to sink will be much slower than the suspended sediment in the river. For example, U-series isotope work in the Ganges suggests that the coarse sediment load takes approximately 80,000 years to travel from the source to the delta,

which provides ample time for storage and reworking of the sediment (Granet, Chabaux et al. 2007). Provenance data from the Indus delta is consistent with long term buffering of sediment flux, but implies shorter zircon transport spanning ~7000 years (Clift and Giosan 2014). However, recent zircon analysis from the Indus Canyon showed major short-term variations in silt-sized sediment spanning 100–300 years which suggests that the signal is not entirely lost, despite the affected drainage system by seasonal and climate events, such as monsoons.

The Mississippi River largely drains a more vegetated and less erosive source than the Himalayan rivers and provides a chance to test the applicability of source-to-sink models formulated in those areas. For example, DZ U-Pb ages in the Mississippi River show response times to environmental forcing of 1000-10,000 years (Fildani, McKay et al. 2016, Mason, Fildani et al. 2017). This implies rapid transport times which agrees with data from South Asia (Paola, Heller et al. 1992, Paola, Heller et al. 1992, Castelltort and Driessche 2003). This lag effect may be diminished in modern river systems where levees confine and transport sediment more efficiently. The degree of sediment buffering, and recycling may be best studied using deposits that pre-date levee construction, and are preserved in meandering river point bars, such as the False River point bar in southern Louisiana (Fig. 4).

2.2. Basement Terrains of North America

U-Pb dating of DZ grains is commonly used to describe the source terrain, determine the depositional age of the host strata, or determine provenance (Gehrels 2000). Zircon ages of North American source terrains are well known, but interpretation of DZ data can be complicated due to sediment reworking from uplift, erosion, and transport (Romans, Castelltort et al. 2016). The availability of zircon grains, as well as the analysis of either younger rims or older cores can also complicate data interpretation by yielding different inheritance ages (Blum and Pecha 2014). The

Mississippi River derives sediment from eight basement terrains or major tectonic blocks (Fig. 1): the Superior Province (>2.5 Ga; (Hoffman 1988, Corfu, Krogh et al. 1989)), the Trans-Hudson Province (1.8–2.3 Ga; (Dahl, Holm et al. 1999, Ross and Villeneuve 2003)), the Yavapai-Mazatzal Province (1.6–1.8 Ga), the Granite-Rhyolite Province (1.34–1.48 Ga; (Whitmeyer and Karlstrom 2007)), the Grenville Province (1000–1250 Ma; (Blum and Pecha 2014), the Peri-Gondwana Province (500–650 Ma; (Mueller, Heatherington et al. 1994) the Taconic Province (380–500 Ma; (Drake Jr, Sinha et al. 1989, Park, Barbeau Jr et al. 2010) and lastly the Cordilleran Province (<300 Ma).

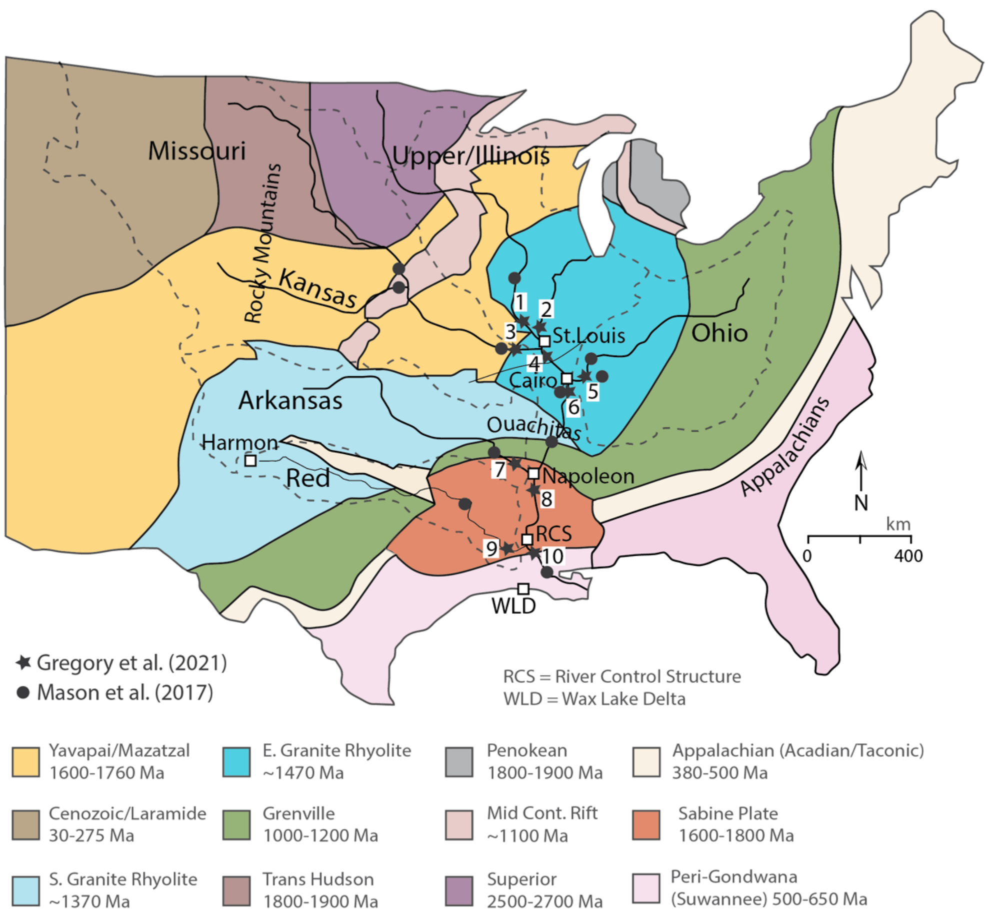

Figure 1. Tectonic map of North America showing the major blocks that comprise the primary sources of the Mississippi River. Dashed lines indicate the locations of major drainage basins. Modified from Gehrels and Dickinson (Gehrels, Dickinson et al. 1995).

The Superior Province (>2.5 Ga) spans approximately 1,500,000 km^2 of land and is the largest Archean terrestrial craton of North America. This stable crustal block covers most of central Canada, as well as the northern edge of the United States. This craton underwent a series of tectonic/magmatic events which included growth, deformation, and accretion of both oceanic and continental crust (Percival, Skulski et al. 2012). The Superior Province formed as a result of major tectonic blocks colliding, specifically the Slave-Rae-Hearne cratons with the Superior craton (Hoffman 1988).

The Trans-Hudson Province (1.8–2.3 Ga) spans approximately 500 km wide and is bound by the Hearne-Wyoming and Superior Province. These three provinces eventually formed the core of the North American continent, otherwise known as Laurentia (Hoffman 1988). The Hearne-Wyoming and Superior Province sutured together to form a network of Paleoproterozoic orogenic belts which include the margins of three supercontinents: Laurasia, Pangaea, and Kenorland (Stauffer 2006).

The Yavapai-Mazatzal Province (1.6–1.8 Ga) represents two cycles of crustal development during the Early Proterozoic which underly the southwestern and midcontinental regions of North America (Hoffman 1988). The Yavapai crustal development cycle (1.79–1.69 Ga) consolidated rocks during an episode of deformation, metamorphism, and plutonism and spans from Arizona through Colorado into the northeast of the United States. The Mazatzal crustal development cycle (1.71–1.62 Ga) stretches from northern Mexico into Canada and includes volcanic rocks, arenites, and turbidites which experienced folding and thrusting, followed by plutonism (Hoffman 1988).

The Granite-Rhyolite Province (1.34–1.48 Ga) lies in the Midwest region and extends east into the northern United States (Muehlberger, Denison et al. 1967, Bickford and Van

Schmus 1985). Felsic magmatism is present throughout the midcontinental United States, but in the southwest region, this magmatism intruded the Yavapai-Mazatzal Province. The early magmatism represents anorogenic or A-type granites, which resulted from three separate magmatic events (Anderson 1983, Barnes, Anthony et al. 2002).

The Grenville Province (1000–1250 Ma) extends from northern parts of Mexico, into the northern Midwest and central Canada (Dalziel 1991, Moores 1991). The tectonic history included early magmatism, metamorphism, and arc accretion with Laurentia (Karlstrom, Harlan et al. 1999). Overall, this terrain emerged from multiple collisional events, ultimately resulting in the formation of Rodinia (Dalziel 1991, Moores 1991).

The Peri-Gondwana Province (500–650 Ma) includes the Appalachian Mountains, which were constructed from a series of collisional events accreted with Laurentia. Also, the Peri-Gondwana Province includes the Suwannee Block which accounts for the Gondwana accumulations of basement terrains in Florida (Mueller, Heatherington et al. 1994).

The Taconic Province (380–500 Ma) lies in the eastern portion of the United States and affected both the northern and southern portions of the Appalachian Mountains during the Ordovician-Devonian Period. Events that occurred in the Northern Appalachians include disconformities of carbonates, deformation of volcanic rocks, gravity slides from uplift, and widespread deformation. The southern portion of the Appalachians were affected greatly by the Taconic but with greater influence from the later Alleghenian Orogeny (Rodgers 1971).

The Cordilleran Province (<250 Ma) stretches from southern California through the northwestern United States into southwest Canada. The terrain was altered through many orogenic processes throughout the mid-Mesozoic and Eocene and was subsequentially modified during the Cenozoic Basin and Range extension from gravitational collapse (Constenius 1996,

DeCelles 2004, Dickinson 2004). The Cordilleran Province no longer falls within the catchment of the Mississippi, but earlier work indicates that Cordilleran zircons are found within the Sevier foreland basin from which they have been reworked following uplift related to the Laramide Orogeny (Laskowski, DeCelles et al. 2013, Balgord, Yonkee et al. 2021).

2.3. Holocene Climatic History

Holocene climate change has had a significant impact on human settlement across the globe. Specific changes in climate during this time were driven by different forcing mechanisms such as solar insolation, ocean circulation, and atmospheric variability. Paleoclimate reconstructions of events during the Holocene (~11.5 ka) indicate that this time frame has been far from stable (Moossen, Bendle et al. 2015). Three distinct climatic shifts occurred during the Holocene (Early, Mid, Late), but prominent events during this time frame that affect my study start in the Roman Warm Period and end in the Medieval Warm Period, as well as an intervening cold climate period, such as the Little Ice Age.

The Early Holocene (11.7–7.8 ka) is characterized by warm temperatures and cold sea-surface temperatures (SSTs) caused from glacial melt, and relatively low precipitation (Briere and Gajewski 2020). Large ice sheets were still heavily present during this time, for example the Laurentide Ice Sheet collapsed near the end of the Early Holocene, transitioning to the Mid-Holocene period (Briere and Gajewski 2020). The transition from the Late Glacial to Early Holocene period shows changes from braided to single-thread channels observed around the globe, but was also observed in the Lower Mississippi Valley (Fisk 1944). Deposition of sediment also fluctuated during the Early Holocene due to periodic flooding events (Kesel 2008). The Mid-Holocene (7.8–3.2 ka) is characterized by peak SSTs, declining atmospheric temperatures, and an increase in precipitation (Moossen, Bendle et al. 2015). In the Lower

Mississippi Valley, rapid sea-level rise caused the alluvial valley to fill with sediment and the Maringuin delta (~6 ka) stepped landward until the rate of sea level rise plateaued. But transitioning into the Late Holocene, sea-level rise decelerated and deltas were constructed along the inner shelf and shelf margin of the gulf coast (Blum and Roberts 2012). The Late Holocene (after ~4.0 ka) is characterized by an increase in temperatures, sea-level rise, and land subsidence (Wanner, Beer et al. 2008, Karegar, Dixon et al. 2016). During the Late Holocene, the Mississippi River avulsed three times which later resulted in the Mississippi-Atchafalaya diversion representing the fourth avulsion (Aslan, Autin et al. 2005).

The Roman Warm Period (2.5–1.6 ka; Holmquist, Booth et al. 2016) corresponds to the Iron Age/Roman time. The climate during this time varied greatly with periodic episodes, of dry/humid conditions, as well as wet/humid conditions. The Medieval Warm Period (1.2–0.7 ka; (Campbell, Campbell et al. 1998)) roughly coincides with the Medieval Ages in Europe. Data varies on a global scale regarding the extent of the climatic variations, but consists of relatively warm temperatures in several regions which include the North Atlantic, Europe, and parts of North America (Campbell 1998, Rafferty 2014). Possible drivers of increased temperatures include an increase in solar radiation paired with an absence in volcanic activity, as well as warmer sea water delivered in the North Atlantic region (Rafferty 2014). The Little Ice Age (0.5–0.1 ka; (Campbell, Campbell et al. 1998)) is characterized by a decrease in the amount in solar insolation, due to orbital forcing, an increase in the amount in volcanic eruptions and a minimal amount of solar activity (Wanner, Beer et al. 2008).

The exact date of the start of the Anthropocene is widely debated but there are some estimates based on different proxies. For example, SSTs indicate that the Anthropocene to begin around 1950 AD, sea-level rise about 1870 AD, and about 1750 AD for global atmospheric

complications (IPCC. 2007). The Anthropocene is defined as a geologic epoch due to the global impact on the Earth's surface from humans (Lewis and Maslin 2015). Technological advances and farming have heavily impacted sediment flux in rivers, especially the Mississippi River (Wang, Fu et al. 2016). Also, sediment flux has been trapped through the construction of damns, which mostly have been constructed since the 1940's in the United States (Meade and Moody 2010). This has impacted both suspended and bedload sediment throughout rivers by potentially causing slower transport times, as well as trapping sediment behind the dam walls. Prior to the construction of dams, the combined Mississippi-Atchafalaya River system was estimated to have transported an annual average of 400 million metric tons of sediment into the Louisiana basin, but as of 2006, the annual sediment delivery to the coastline is about 170 metric tons, a 60% decrease (Meade and Moody 2010). These human alterations in agriculture, industry, and extraction has caused a drastic change in sediment flux through the river, which is important to understand in order to determine the rate at which zircon grains are being transported.

2.4. Geology of the Lower Mississippi Valley

The Mississippi River originates in Minnesota and spans almost 4,000 km until termination in southern Louisiana, into the Gulf of Mexico (Syvitski and Milliman 2007). It is the largest river system in North America and comprises five main drainage systems that flow across a geologically diverse terrain. Most of the sediment discharge in the Mississippi River has historically come from the Missouri River (56.9 Mt/yr, 40.5% of total), while the largest portion of the water discharge is derived from the Ohio River (8000 m^3/s compared to 2400 m^3/s in the Missouri) (Fig. 2) (Meade and Moody 2010, Alexander, Wilson et al. 2012). Mason et al. (2017) used DZ data and mixing models to estimate a "negligible" contribution from the Ohio to the Mississippi Fan during the LGM (Fildani, McKay et al. 2016), compared with an estimated 14–

17% Ohio contribution to the modern lower Mississippi River. That study emphasized flux from the Missouri River of 59–67% to the net flux to the ocean. More recently Gregory et al. (2022) used DZ data to estimate ~5% of the sediment in the lower reaches was derived from the Ohio River, but with 34% and 31% coming from the Missouri and Upper Mississippi respectively. It is apparent that recent studies derive quite different estimates for competing source contributions. It is not clear from these studies whether they represent real time changes in the composition of the river, caused by either the cut off of tributaries, such as the Red River following installation of the Old River Control Structure (RCS), or whether they might represent pulses of different compositions flowing through the mainstem in the wake of changing erosion upstream over short timescales, and not eliminated by recycling in the floodplains.

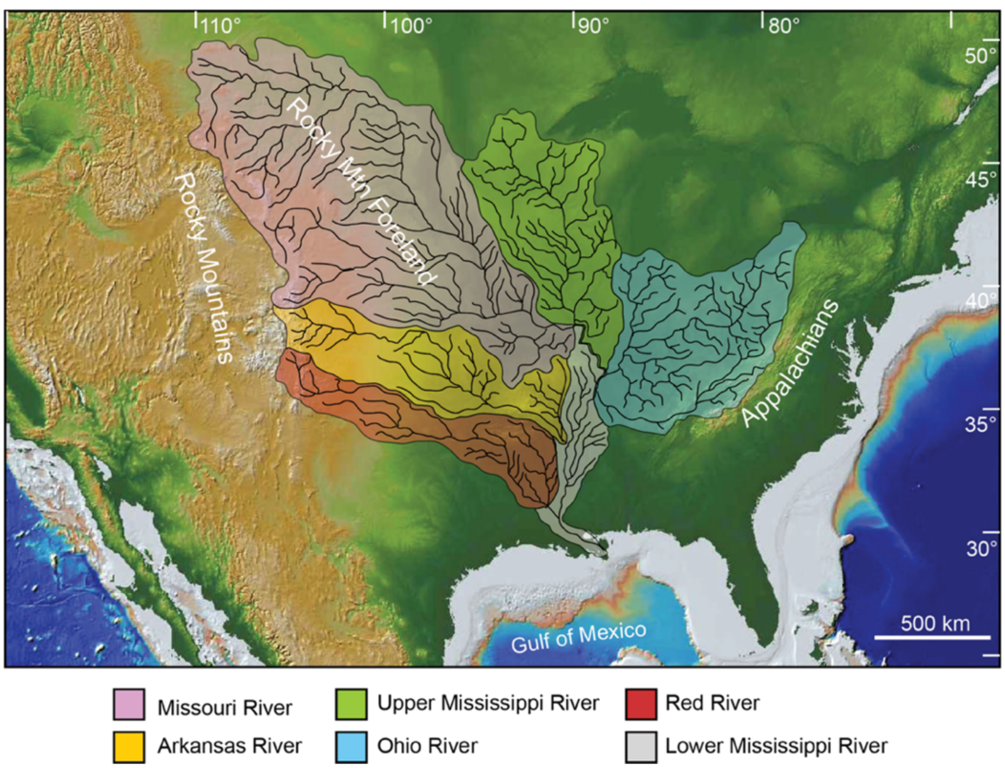

Figure 2. Shaded topographic map of North America showing the extent of the Mississippi catchment and the major tributaries that are supplying sediment to the lower reaches of the river. Data is Shuttle Radar Topography Mission (SRTM) from NASA.

The role that dams have played in controlling the transport of coarse-grained sediment (bedload) in the Mississippi River has been debated. The reduced sediment supply to the river mouth requires a significant reduction in fine-grained sediment transport. However, it is not clear whether the sand is affected in the same way, and this is often the type of sediment most typically used in provenance studies. Nittrouer and Viparelli (2014) argued that sand capture behind dams is not affecting the coarse bedload supply because the Mississippi River scours its own bed to maintain a constant supply, a process that might also buffer the composition of sediment in the lower reaches. However, gauging data (Heimann, Sprague et al. 2011) shows a fall in silt and coarser sediment transport the Mississippi, suggesting that coarser material is being sequestered behind dams (Blum and Pecha 2014).

While dams affect the overall sediment supply in the Mississippi, the RCS has also completely cut off the connection of the Red River to the mainstem of the lower Mississippi River, thus impacting the provenance of the sediment downstream (Gregory, Herrmann et al. 2022). Prior to the late Holocene the Red River joined the Mississippi-Teche channel belt on the western side of the alluvial valley (Aslan, Autin et al. 2005).

2.5. History of Levees

The amount of recycling in the lower reaches of the Mississippi Valley has reduced substantially as the river has been engineered for safety of human life, and flooding impacts on urbanization. The first levees were installed around New Orleans during the early 18th century, and the extension upstream was closely linked to intensifying regulations for civilization safety (US Army Corps of Engineers 2017). It was not until the late 19th century that the river was heavily leveed as far upstream as the Arkansas River confluence (Fig. 2) (US Army Corps of Engineers 2017). Nonetheless, over the last couple of centuries the ability of the Mississippi

River to incise its floodplain has been substantially curtailed due to the changes in erosion of the headwaters, floodplain recycling, or even anthropogenic levee installation, so that changes in sediment supply from the upper reaches might be more susceptible to being transmitted into the lower reaches of the river in modern times. Changes in sediment composition can be the result of changing patterns of erosion in the headwaters, whether these are caused by climate, or human activity. It remains questionable whether single large weather events, such as major storms, can produce and propagate erosional pulses through the river that would be recognisable in the lower reaches. Alternatively, sediment mixing and buffering during transport might make it only possible to identify changes in the sediment supply caused by processes operating over longer timescales, such as climatic episodes like the Mediaeval Warm Period or the Little Ice Age.

2.6. Study Area

False River is located about 35 km northwest of Baton Rouge, in Pointe Coupee Parish, Louisiana, and joins the towns of Jarreau and Ventress (Fig. 3) (Farrell 1987). The point bar system formed prior to approximately around 1720 AD when a meander loop of the Mississippi River was abandoned (Fisk 1944, Sternberg 1956, Sternberg 1956, False River Watershed Study 2013, Fenstermaker 2013). False River is an approximately 3,060 acre oxbow lake which has a steep outer bank and a gradually sloping inner bank (Ensminger 1999). Evidence of point bar reorientation surfaces can be seen and formed during the migration of the point bar to the south and then southwest as accretion occurred (Fig. 4). The sediment of the False River point bar is reflective of the first Holocene meander belt sequence indicating it is Holocene age sediment (Saucier and Snead 1989, Blum and Roberts 2012, Blum and Roberts 2012). Neck cut-off of the meander loop was determined by the presence of the oxbow lake bounded by an accretionary point bar and a natural levee through aerial photographs (Fisk 1947). False River was completely

isolated from the Mississippi River due to levee construction in the 1930's (Fenstermaker 2013). Though much research has been conducted on the evolutional history of the Mississippi River, False River has not been researched enough to understand the age of the deposition or to see if there have been seasonal/temporal variations in the sediment between the Mississippi River and False River, prior to cutoff.

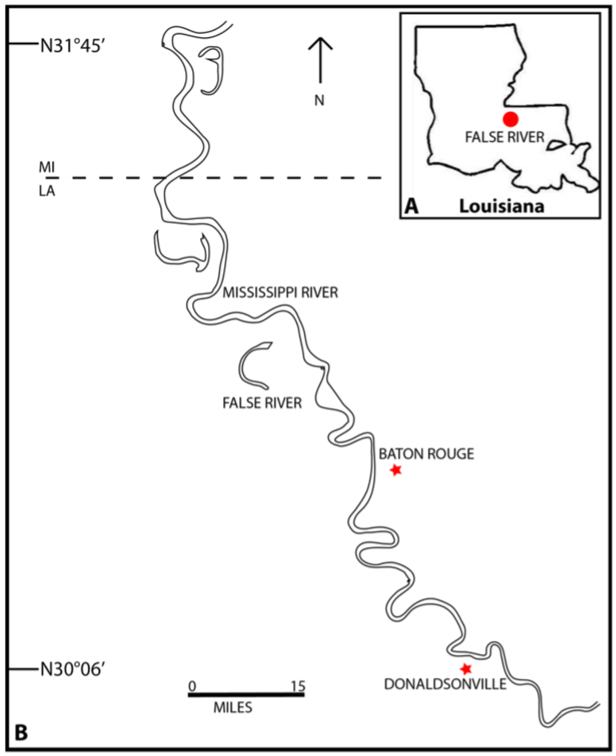

Figure 3. (A) Image of the state of Louisiana marking the location of the False River with a red dot. (B) Map of the Lower Mississippi River valley showing the major cities with a red star, and the False River in the middle of the image (Lechnowskyj 2015).

Sediment grab bag samples were also collected in Reserve, Louisiana, which is about 81km southeast from Baton Rouge, Louisiana. Samples were collected annually along the Mississippi Riverbank at 30.053060°N, 90.555560°W to establish a seasonal scale for zircon provenance variation. The data collected will help determine the depositional history of the river as well as seasonal/temporal changes of the sediment flux.

CHAPTER 3. METHODS

3.1. Geoprobe Coring/Grab Bag

Sediment cores were collected using a shallow environmental geological coring unit: Geoprobe MC5 Soil Sampling System. This type of machine employs a direct push system that involves a hammering force to advance the core liners unto the subsurface to extract sediment cores. The outer diameter of the rod used was 1.25 inches which housed a plastic core liner for sediment sampling. Before sampling, the plastic core liners were painted black using black spray paint to prevent future error amongst OSL data. Each location was drilled twice, and each core liner was 1.5 m in length, totaling a maximum depth of 3 m. After the cores were extracted from the subsurface, I carefully pulled the plastic core liner from the core rod into a black trash bag as another precaution for OSL data. False River core samples are labeled using the property name abbreviation (i.e., B=Beuche, J=Jumonville, W=Woody, Table 1)

Modern grab bag samples were collected on the riverbank in Reserve, Louisiana. Approximately two gallons of sediment was collected from the surface and transported back to LSU for analysis to be complete. (Table 1)

Table 1. List of samples collected from both the False River Point Bar and the modern river samples collected in Reserve, Louisiana. Depth (m), date collected, depositional age (from OSL, zircon, or estimations), sediment type, coordinates, and zircon or OSL selected samples analyzed for this study.

Sample	Depth (m)	Date collected	Depositional age (y BP)	Sediment type	North (°)	West (°)	Zircon	OSL
21100901	0	9-Oct-21	0.3	Fine sand	30.053060	90.555560	X	
BLBR21	0	9-Oct-21	0.3	Silt	30.297220	91.227500	X	
21022001	0	20-Feb-21	0.8	Silt	30.053060	90.555560	X	
21012501	0	25-Jan-21	0.9	Fine sand	30.053060	90.555560	X	
20121501	0	15-Dec-20	1.0	Fine sand	30.053060	90.555560	X	
20110101	0	10-Nov-20	1.1	Silt-Fine Sand	30.053060	90.555560	X	
20092401	0	9-Sep-20	1.3	Fine sand	30.053060	90.555560	X	
18020401	0	4-Feb-18	4.0	Fine sand	30.053060	90.555560	X	
LA1701	0	1-Sep-17	4.8	Fine sand	30.053060	90.555560	X	
17093001	0	3-Sep-17	4.8	Fine sand	30.053060	90.555560	X	
B3-2	3.0	5-Oct-20	700	Silt	30.628333	91.466389	X	X
B2-14, B2-16	15.8-19.5	9-Feb-17	860	Fine sand	30.630500	91.464317	X	
B2-2	3.0	5-Oct-20	940	Silt	30.630278	91.465278		
B1-2	3.0	5-Oct-20	1010	Silt	30.632500	91.463889	X	X
W1-17, W1-18	19.5-21.9	11-Feb-17	1370	Med sand	30.624750	91.384172	X	
W11-2	3.0	5-Oct-20	1430	Fine sand	30.625680	91.387940	X	
W2-5	4.9-6.1	12-Feb-17	1500	Silt-Fine Sand	30.627569	91.387664	X	
W10-2	3.0	5-Oct-20	1500	Silt	30.627570	91.390230	X	X
W9-2	3.0	5-Oct-20	1690	Silt	30.630530	91.394500	X	X
W3-10, W3-11	10.9-13.4	13-Feb-17	1780	Med sand	30.632081	91.394200	X	
W3-18	21.3	13-Feb-17	1790	Fine sand	30.632081	91.394200	X	
J2-11, J2-10	12.8	1-Feb-17	2200	Fine sand	30.656072	91.389936	X	
J4-2	3.0	6-Oct-20	2230	Silt	30.648460	91.407270	X	X
J7-2	3.0	6-Oct-20	2420	Silt	30.656650	91.389950		X
J5-2	3.0	6-Oct-20	2433	Silt	30.658980	91.389670	X	
J6-2	3.0	6-Oct-20	2460	Silt	30.664070	91.388470	X	X

3.2. Optically Stimulated Luminescence

The age of the initial cutoff of the False River point bar is estimated from literature to be around 1720 AD, which was determined through satellite imagery and topographic analysis, in relation from previous historical accounts of French navigators/settlers (Fisk 1947, Saucier 1969). OSL dating is a technique used to provide an age estimate of the last exposure of sunlight or heat to siliciclastic sediment, presumably during transport. Exposure of sunlight or heat resets the luminescence signal and creates a timestamp of deposition (Rittenour 2018). Brief heating of about 200 °C–400 °C or short daylight exposure of about 1–100 s is sufficient to bleach the sample, which reduces the electron trap populations in turn resetting the OSL age. Following burial, trapped charges increase over time due to radiation from radioactive isotopes in the surrounding sediment. These trapped charges are then measured to determine the age of last exposure (Rhodes 2011).

OSL dating can be challenging in fluvial environments, but deposits from these settings can be accurately dated by selecting depositional facies which are most likely to have been reset by sunlight exposure (Fuchs and Owen 2008, Rittenour 2008). Specifically, river systems can have turbid water conditions, rapid transport times, and even sediment buffering from the floodplains which can be associated with partial bleaching of the sediments. The importance of using OSL dating in fluvial deposits is the key to understand how rivers respond to external forcings such as climate and sea level fluctuations (Rittenour 2018).

Eleven core samples were collected using the Geoprobe MC5 Soil Sampling System along the False River point bar in the southeastern part of Pointe Coupee Parish, Louisiana (Fig. 4). Seven of the eleven samples collected, which can be seen in Table 1, were sent to the Luminescence Laboratory at Utah State University for OSL analysis. Procedures for sample

processing and small-aliquot OSL age analysis are as follows: all samples were opened and processed under dim amber safelight conditions within the lab. Sample processing OSL dating followed standard procedures involving sieving, HCl and bleach treatments, heavy mineral separation at 2.72 g/cm^3, and acid treatments with HCl and HF to isolate the quartz component of a narrow grain-size range, 75–125 μm. The purity of the quartz samples was checked by measurement with infra-red stimulation to detect the presence of feldspar. The USU Luminescence Lab follows the latest single-aliquot regenerative-dose (SAR) procedures for OSL dating of quartz sand (Murray and Wintle 2000, Murray and Wintle 2003, Wintle and Murray 2006). The SAR protocol includes tests for sensitivity correction and brackets the equivalent dose (DE) the sample received during burial by irradiating the sample at three different doses (above the DE, plus a zero dose and a repeated dose to check for recuperation of the signal and sensitivity correction). The resultant data are fit with a linear curve from which the DE is calculated on the Minimum Age Model (MAM) (Galbraith and Roberts 2012). The OSL age is reported at 1σ standard error and is calculated by dividing the DE (in grays, Gy) by the environmental dose rate (Gy/kyr) that the sample has been exposed to during burial. The contribution of cosmic radiation to the dose rate was calculated using sample depth, elevation, and latitude/longitude following(Prescott and Hutton 1994). Dose rates are calculated based on water content, sediment chemistry, and cosmic contribution (Aitken and Xie 1990, Aitken 1998).

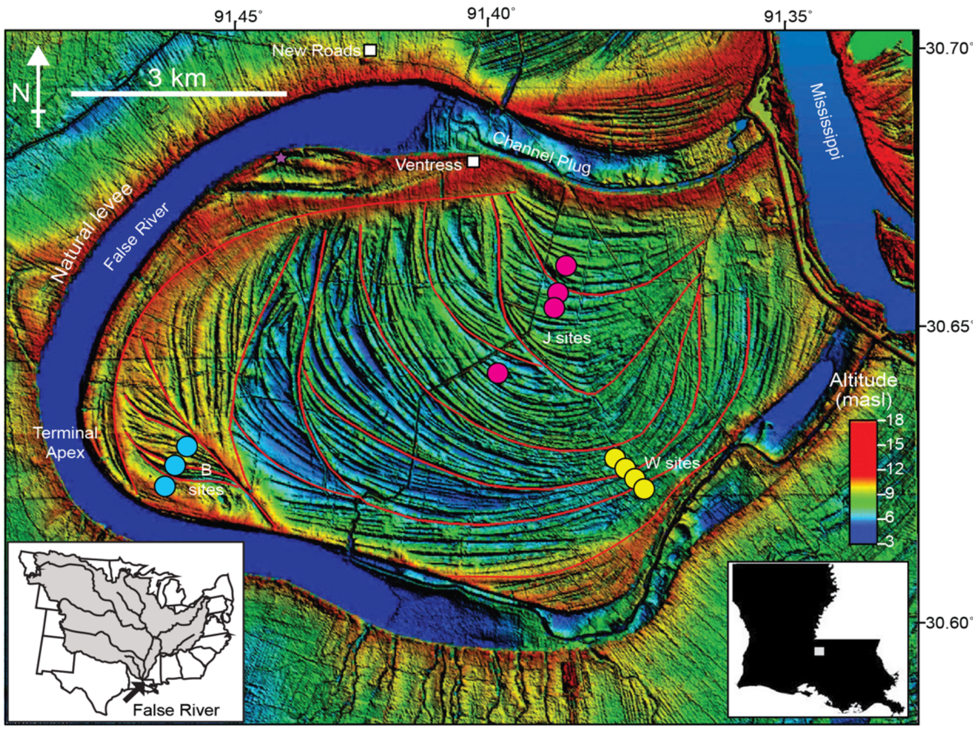

Figure 4. Lidar image of the False River point bar. The red lines indicate scroll bars. The colored circles indicate core sites (pink: J Sites, blue: B Sites, yellow: W Sites). A more detailed lidar image is highlighted in the results section (Fig. 9).

3.3. Zircon U-Pb Dating

Nine of eleven samples from False River, two samples from previous MS research conducted by Lechnowskyj (2015), and four modern grab bag samples were sent to GeoSep Services for heavy mineral separating. GeoSep Services processed the samples by the following procedure: sieve, wash with water to remove lighter particles, separate in Lithium Metatungstate to remove particles with a specific gravity less than 2.95 g/cm^3, remove magnetic grains with a Frantz^{TM} magnetic separator, separate in Di-iodomethane to remove particles with a specific gravity less than 3.33 g/cm^3 (GeoSepServices). After receiving the separates from GeoSep Services, zircon grains were mounted in epoxy rounds at Louisiana State University.

Half of the amount of zircon separates of each sample were sprinkled in the center of circular epoxy silicon molds. These molds were placed into a vacuum chamber and degassed to

release as much air to the surface in the form of bubbles. The molds cured for 48 hours and then polished using 2,000 grit sandpaper, 0.3µm and 0.05µm MicroPolish Alumina polishing powder. Between each polishing process, the epoxy round was put into a sonicated bath to prevent scratching during the next polishing process from loose zircon grains.

A total of seven mounts were sent to the London Geochronology Centre and two mounts were sent to GeoSep Services for Zircon U-Pb chronology. The London Geochronology Centre's methodology is as follows: samples were analyzed by a Laster Ablation-Inductively Coupled Mass Spectrometer (LA-ICPMS) using a New Wave 193nm excimer laser ablation system coupled to an Agilent 7900 quadrapole-based ICP–MS. The laser was set up to produce an energy density of ca 2.5 J/cm^2 at a repetition rate of 10 Hz. The time-resolved mass spectrometer data was processed using GLITTER 4.5 data reduction software. Data was filtered to exclude mixed rations, non-zircons based on zirconium concentrations (>10 counts per second) and a –5/+15% discordance threshold was applied. Repeated measurements of external zircon standard PLESOVIC (TIMS reference age 337.13 ± 0.37 Ma; (Sláma, Košler et al. 2008)) and NIST 612 silicate glass (Pearce, Perkins et al. 1997) were used to correct for instrumental mass bias and depth-dependent inter-element fractionation of Pb, Th and U. 91500 (Wiedenbeck, Hanchar et al. 2004) and Temora (Black, Kamo et al. 2003) zircon were used as secondary age standards. Data was filtered using standard discordance tests with a 15% cutoff. The $^{206}Pb/^{238}U$ ratio was used to determine ages where <1000 Ma and the $^{207}Pb/^{206}Pb$ ratio for older grains. IsoplotR software was used for data plotting (Vermeesch 2018).

GeoSep Services U-Pb dating methodology is as follows: isotopic analyses were performed with a New Wave UP-213 laser ablation system in conjunction with an Agilent 7700x quadrapole LA-ICP-MS in the GeoAnalytical Lab at Washington State University. For all laser

analyses, the beam diameter was 30 μm and the frequency was set at 5 Hz, yielding ablation pits ~12–15 μm deep. He and Ar gas were used to deliver the ablated material into the plasma source. Each analysis of 32 cycles took approximately 30 s to complete and consisted of a 6 s integration on peaks with the laser shutter closed (for background measurements) followed by a 24 s integration with the shutter open and the laser ablating zircon material. A 20 s delay occurred between analyses. The isotopes measured included ^{202}Hg, $^{204}(Hg + Pb)$, ^{206}Pb, ^{207}Pb, ^{208}Pb, ^{232}Th, ^{235}U, and ^{238}U. Several zircon U-Pb age standards were used during analysis for calibration purposes. These included the 1099 ± 0.6 Ma FC zircon (FC-1 of Paces and Miller, 1993) as the primary age standard. The secondary age standard was the 61.2 ± 0.1 Ma Tardree Rhyolite zircon (Dave Chew, personal communication). Third-level age standards included the Fish Canyon Tuff with an age of 28.20 ± 0.1 Ma (Lanphere and Baadsgaard 2001), the Mount Dromedary Syenite with an age of 99.1 ± 0.1 Ma (Renne, Swisher et al. 1998), and the Temora[2] diorite with an age of 416.8 ± 0.3 Ma (Black et al., 2004). At the beginning of the LA-ICPMS session, zircon standards (TR and FC1) were analyzed until fractionation was stable and the variance in the measured $^{206}Pb/^{238}U$ and $^{207}Pb/^{206}Pb$ ratios was at or near one percent. To correct for inter-element fractionation during the session, these standards were generally reanalyzed after each 15–25 unknowns. Uranium decay constants and the $^{238}U/^{235}U$ isotopic ratio reported in (Steiger and Jäger 1977) were used. Uranium decay constants and the $^{238}U/^{235}U$ isotopic ratio reported in (Steiger and Jäger 1977) were used in this study. $^{207}Pb/235Uc$ ($^{235}Uc = 137.88^{238}U$), $^{206}Pb/^{238}U$, and $^{207}Pb/^{206}Pb$ ages were calculated for each data scan and checked for concordance; concordance here was defined as overlap of all three ages at the 1σ level (the use of 2σ level was found to skew the results to include scans with significant common Pb). The background-corrected isotopic sums of each isotope were calculated for all concordant scans. The precision

of each isotopic ratio was calculated by using the background and signal errors for both isotopes. The fractionation factor for each data scan, corrected for the effect of accumulated α-damage, was weighted according to the ^{238}U or ^{232}Th signal value for that data scan; an overall weighted mean fractionation factor for all concordant data scans was used for final age calculation. If the number of concordant data scans for a spot was greater than zero, then either the $^{206}Pb/^{238}U$ (for ages <1.5 Ga) or $^{207}Pb/^{206}Pb$ (for ages >1.5 Ga) age was chosen as the preferred age. If zero concordant data scans were observed, then the analysis was deleted. Common Pb was subtracted out using the (Stacey and Kramers 1975) common Pb model for Earth. Ages and common Pb ratio were determined iteratively using a pre-set, session-wide minimum common Pb age value (default for each session was the age of the oldest age standard which for both Ap and Zrn was 1099 Ma FC-1 and/or FC-5z).

3.4. Grain Size

A total of twenty-five samples from both the False River point bar and Reserve, Louisiana were analyzed following the procedure of Hülse and Bentley Sr. (Hülse and Bentley Sr 2012). About 2 g of sample was placed in a 50 ml plastic centrifuge tube with 5.75 mL of $NaPO_3$ solution. The tube was capped and vortexed to deflocculate clay sized sediment and separate organic particles. The sample was poured through an 850 μm sieve to help remove large particles of organic matter. The glass tube was placed into a centrifuge to settle the sediment at the bottom of the vial. The vials were then run at ~25 RPM for 60 minutes and then the supernatant was removed. About 2 mL of $NaPO_3$ was then added to the centrifuged sample as well as 5 mL of H_2O_2. The H_2O_2 reacted with the sample for about 20-30 minutes. Small amounts of acetone were sprayed in the vials to stabilize the reaction and once the reactions settled, the samples were placed into a hot bath set at level 70 °C over night. Once removed from

the hot bath the supernatant was removed from the vials and the sample was then transferred into plastic tubes with caps to be vortexed for analysis. The samples were then analyzed using a Beckman-Coulter (LS 13-320SW) Laser Diffraction Particle Size Analyzer Single Wavelength.

3.5. Geochemical Analysis

X-Ray Fluorescence (XRF) analysis was completed at Louisiana State University in collaboration with Dr. Matthew Loocke. The methodology is as follows: loss on ignition was determined by weighing out 2.0000 ± 0.02 g of sample powder, igniting it in a furnace at 950°C for two hours, and then re-weighing the sample powder. Glass fusion disks were then created by mixing 0.600 ± 0.006 g of the ignited sample powder with 6.000 ± 0.06 g of a 49.5% lithium metaborate + 49.5% lithium tetraborate + 0.5% lithium iodide flux in a platinum crucible and fusing the mixture at 1065°C using a Claisse LeNeo Fusion Fluxer. The resulting glass disks were then loaded sequentially into the 10-position carousel of the PANalytical Epsilon3^{XLE} energy-dispersive XRF spectrometer in the Louisiana State University Shared Instrumentation Facility. Each sample was run in triplicate under a series of varying conditions which are ideal for different groups of elements of interest. The conditions employed for this analysis can be found in Appendix E. The current for each condition is automatically set by the instrument to maximize the intensity of the elements of interest while reducing artifacts. In addition, each sample is rotated during the analysis to maximize the interaction volume within the material.

Quantitation of the analyses was performed based on a set of standards from the Geophysical Survey of Japan (JA-3 Andesite, JB-2 Basalt, JG-2 Granite, JLk-1 Lake Sediment, JLs-1 Limestone, JP-1 Peridotite, JR-1 Rhyolite) and the United States Geological Survey (AGV-1 Andesite, BIR-1 Iceland Basalt, SCo-1 Cody Shale, W-2 Diabase, G-2 Granite, GSP-2 Granodiorite, SGR-1 Green River Shale, QLO-1 Quartz Latite, RGM-1 Rhyolite, SDC-1 Mica

Schist, STM-1 Syenite). The calibration curves were derived from the statistical means of ten repeat analyses of each standard. Three standards, USGS MAG-1 (Marine Sediment), GSJ JSd-1 (Stream Sediment), and GSJ JSl-1 (Slate) were analyzed in triplicate as unknowns at the beginning and end of each analytical session to check the accuracy of the calibration and to monitor for instrumental drift.

CHAPTER 4. RESULTS

4.1. OSL Dating

Seven successful OSL ages were collected and are shown in Table 2. The age spectra of the OSL dating ranges from 8.6 ka to 2.5 ka which spans over 1500 years and encompasses the Medieval Warm Period to the Roman Warm Period. Uncertainties were on the order of 100 to 300 years but provides confidence that the rough correlations with existing climate records might be possible.

Table 2. Optically Stimulated Luminescence Age Information. (1) Age analysis using the single-aliquot regenerative-dose procedure of (Murray and Wintle 2000) on 1-mm small-aliquots of quartz sand. Number of aliquots used in age calculation and number of aliquots analyzed in parentheses. (2) Equivalent dose (DE) calculated using the Minimum Age Model (MAM) of Galbraith and Roberts (Galbraith and Roberts 2012)

Sample num.	USU num.	Depth (m)	Num. of aliquots[1]	Dose rate (Gy/kyr)	Equivalent Dose[2] ± 2s (Gy)	OSL age ± 1s (ka)	Distance to next dated site (m)	Rate of migration (m/y)
B3-2	USU-3553	3	25 (32)	2.82 ± 0.11	2.44 ± 0.48	0.86 ± 0.16	538	0.96
B1-2	USU-3552	3	20 (23)	2.34 ± 0.09	2.35 ± 0.40	1.01 ± 0.14	522	3.48
W10-2	USU-3555	3	16 (23)	2.87 ± 0.11	4.31 ± 0.69	1.50 ± 0.23	2504	5.11
W9-2	USU-3554	3	17 (23)	2.77 ± 0.11	4.68 ± 0.73	1.69 ± 0.18	407	2.14
J4-2	USU-3556	3	19 (20)	2.64 ± 0.10	5.88 ± 0.68	2.23 ± 0.23	1556	2.88
J7-2	USU-3557	3	19 (27)	2.61 ± 0.10	6.32 ± 0.84	2.42 ± 0.27	1332	7.01
J6-2	USU-3558	3	19 (26)	2.70 ± 0.10	6.65 ± 0.74	2.46 ± 0.28	824	20.60

4.2. Zircon U-Pb Dating

Eight tectonic provinces are represented throughout the nineteen samples analyzed (Fig. 5). Prominent populations include 0–100 Ma, 100–200 Ma, 900–1200 Ma, 1300–1500 Ma, and 1600–1800 Ma. Smaller populations are also noted between 350–650 Ma as well as around 2,500–2700 Ma. Many of these populations correlate with the basement ages summarized above.

Starting with zircons associated with the Superior Province (>2.5 Ga; (Hoffman 1988, Corfu, Krogh et al. 1989)), there are variations in the sample's populations amongst the False River and the modern samples, but there is no clear coherent trend in the data. The Trans-Hudson (1.8–2.3 Ga; (Dahl, Holm et al. 1999, Ross and Villeneuve 2003)) source is present in a few samples, some having more dominance than others. The Yavapai-Mazatzal Province (1.6–1.8 Ga; (Whitmeyer and Karlstrom 2007)) shows significant variation between the samples, but some samples are more dominant in Yavapai-Mazatzal zircons than other, as seen in 18020401, BL_BR, B1-2, W11-2, and W2-5. The Granite-Rhyolite Province (1.34–1.48 Ga; (Whitmeyer and Karlstrom 2007)) is similar throughout all samples mostly in the modern samples. Most samples show many grains that would be associated with the Grenville Province (1000–1250 Ma; (Blum and Pecha 2014)). The Peri-Gondwana Province (500–650 Ma; (Mueller, Heatherington et al. 1994)) shows a negligible amount of zircon grains present throughout the samples collected. The Taconic (380–500 Ma; (Drake Jr, Sinha et al. 1989, Park, Barbeau Jr et al. 2010)) is similar to the Peri-Gondwana, but there are slight variations between a few samples, for example the samples collected in 2017 shows a seven percent increase in Taconic grains compared to Peri-Gondwana which is higher than most samples. Lastly, zircons from the Cordilleran Province (<300 Ma; (Constenius 1996)), which includes ages also found in the

Rocky Mountain foreland, are quite common in all samples, both in the modern Mississippi and the False River point bar.

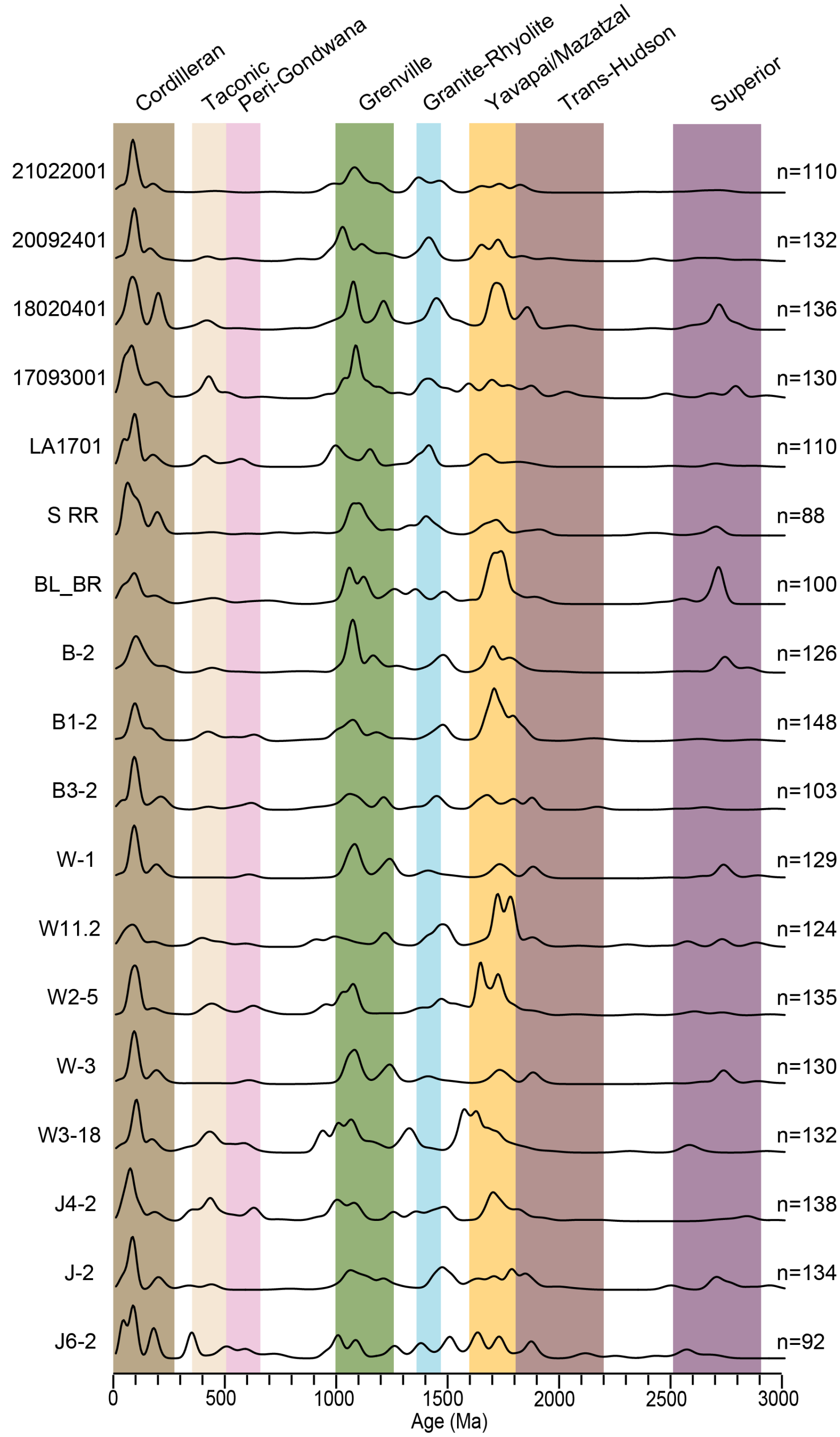

Figure 5. Kernel Density Estimate (KDE) diagram showing the relative frequency of zircons of a given age (Vermeesch 2018) taken from the False River point bar and modern samples from Reserve, Louisiana. Colored vertical bands show age populations that correspond to basement sources. See appendix for zircon spectra depicted as pie diagrams (Appendix A.2) and for Basement KDE (Appendix A.3).

4.3. Grain Size Analysis

The range of grain sizes measured is shown in Figure 6. The False River samples taken from deeper (>3 m) within the point bar complex are dominated by fine sand, with a minority of medium sand, while the shallow samples (<3 m) are dominated by silt and very fine sand. Samples taken from the modern Mississippi are dominantly composed of fine sand with some samples containing significant amounts of silt and very fine sand.

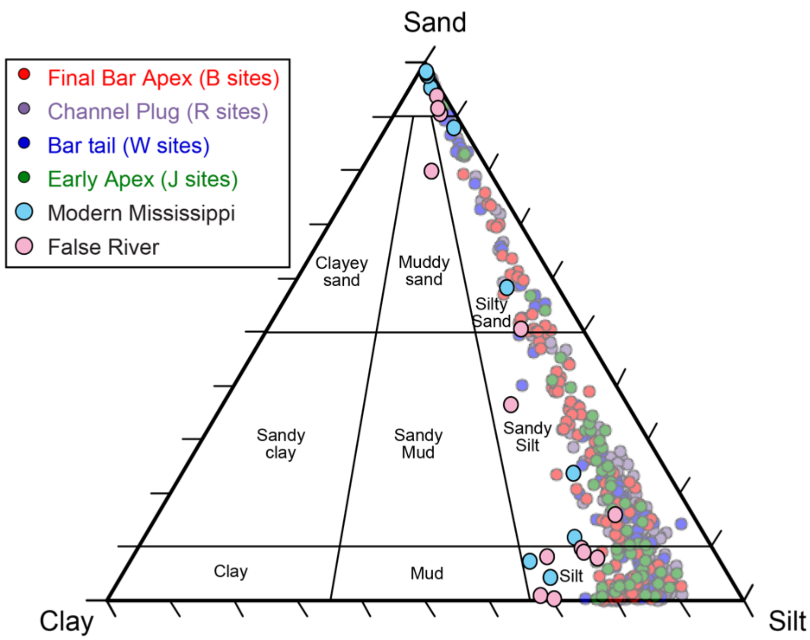

Figure 6. Folk plot showing the distinction between grain size and mineral composition in sedimentary samples (Folk 1954) collected from False River and modern samples from Reserve, Louisiana. Final bar apex, channel plug, bar tail, and early apex samples were collected in a previous study (Clift, Giosan et al. 2008), while the pink False River and blue modern Mississippi circles represent the samples collected for this study. Both the False River and the modern Mississippi samples cluster between silt and sand with few samples in between.

4.4. Geochemical Analysis

Sediments considered in this study span a wide range of major element compositions (Table 3). SiO_2 percentages range up to 86.8% and as low as 56.2%, while aluminium is as low as 3.5% and as high as 16.9%. Much of the variability can be attributed to grain size, with

muddier samples typically showing lower SiO_2. Loss on ignition (LOI) can be significant ranging up to 14.9%. Sediments with high LOIs typically show low SiO_2 reflecting their muddy lithology and generally more weathered state.

The triangular CN-A-K diagram (Fig. 7) can be used to understand the degree of chemical weathering (Fedo, Nesbitt et al. 1995). There is a wide range of compositions found in the lower Mississippi and the False River point bar. The sediments form a rough array trending towards the illite end member in the top right-hand part of this diagram, indicating progressive chemical weathering. The False River point bar sediments generally show higher degrees of alteration (Chemical Index of Alteration) than sediments in the modern Mississippi and major tributaries except for the Ohio which, show more chemical weathering than other contributors.

The overall character of the sediment can be revealed through a discrimination diagram based on SiO_2, K_2O, Fe_2O_3 and Al_2O_3 contents (Fig. 8) (Herron 1988). Again, the sediments show an array, with more sediments from the point bar plotting within the general field of litharenite and subarkose, while many of the sediments in the modern river are defined as being subarkose. Only two sediments qualify as quartz arenites, the most compositional mature variety.

Table 3. XRF Elemental analysis data. See appendix for continued sheet. (Appendix E)

Sample ID	SiO_2 (wt.%)	TiO_2	Al_2O_3	Fe_2O_3	MnO	MgO	CaO	Na_2O	K_2O	P_2O_5	LOI	Total
B3-2	56.171	0.7	16.884	5.995	0.087	1.805	1.038	0.336	2.555	0.188	14.1	99.859
B2	56.966	0.668	15.336	5.902	0.226	1.615	1.068	0.432	2.451	0.185	14.93	99.779
LA1701	59.321	0.422	19.044	3.833	0.067	0.632	6.559	3.049	1.724	0.189	4.94	99.78
W9-2	60.132	0.744	15.856	5.403	0.044	1.501	0.826	0.433	2.568	0.184	12.19	99.881
W10-2	61.561	0.626	15.199	4.565	0.022	1.242	0.982	0.44	2.492	0.074	12.62	99.823
J5-1	66.777	0.585	12.963	4.602	0.059	0.872	0.986	0.899	2.42	0.195	9.49	99.848
J6-2	69.087	0.654	9.906	4.63	0.084	1.054	0.988	0.923	2.579	0.194	9.82	99.919
21022001	71.223	0.595	10.619	3.509	0.103	0.978	1.752	0.82	2.149	0.198	7.98	99.926
J4-2	72.837	0.595	11.456	3.342	0.043	0.821	0.917	1.215	2.363	0.178	6.18	99.947
W11-2	73.027	0.595	11.45	3.388	0.04	0.831	0.965	1.075	2.328	0.188	6.01	99.897
B1-2	75.038	0.499	10.776	3.059	0.049	0.72	1.006	1.164	2.39	0.151	5.05	99.902
W2-5	79.855	0.442	6.05	2.535	0.03	0.802	1.672	1.375	2.308	0.163	4.65	99.882
21012501	79.957	0.378	8.207	2.108	0.053	0.721	1.65	1.095	2.006	0.148	3.53	99.853
10600112	81.564	0.459	7.847	2.206	0.074	0.559	1.433	1.141	1.847	0.17	2.57	99.87
20121501	81.906	0.284	7.859	1.899	0.052	0.48	1.364	1.026	1.859	0.11	3.05	99.889
W3-10	82.699	0.246	7.674	1.545	0.02	0.584	1.383	1.167	1.964	0	2.33	99.612
W3-18	82.81	0.233	7.785	1.483	0.017	0.434	1.408	1.393	2.034	0.016	2.05	99.663
J2-11	83.397	0.212	7.456	1.484	0.022	0.532	1.38	1.221	1.916	0	1.99	99.61
W1-18	84.233	0.209	7.275	1.303	0.013	0.304	1.257	1.194	1.893	0	1.93	99.611
17082402	85.217	0.109	7.279	0.98	0.015	0.366	1.04	1.3	1.832	0	1.44	99.578
20110101	85.641	0.29	4.124	1.953	0.032	0.434	1.433	1.256	2.075	0.094	2.52	99.852
17093001	86.345	0.094	6.798	0.835	0.01	0.215	0.877	1.093	1.756	0	1.46	99.483
20092401	86.615	0.636	3.529	2.545	0.04	0.438	1.397	1.221	1.711	0.14	1.55	99.822
18020401	86.63	0.178	6.87	1.2	0.018	0.143	1.062	0.95	1.871	0.005	1.27	100.197
BLBR21	86.844	0.173	6.448	1.133	0.015	0.287	1.034	1.041	1.69	0	1.01	99.675

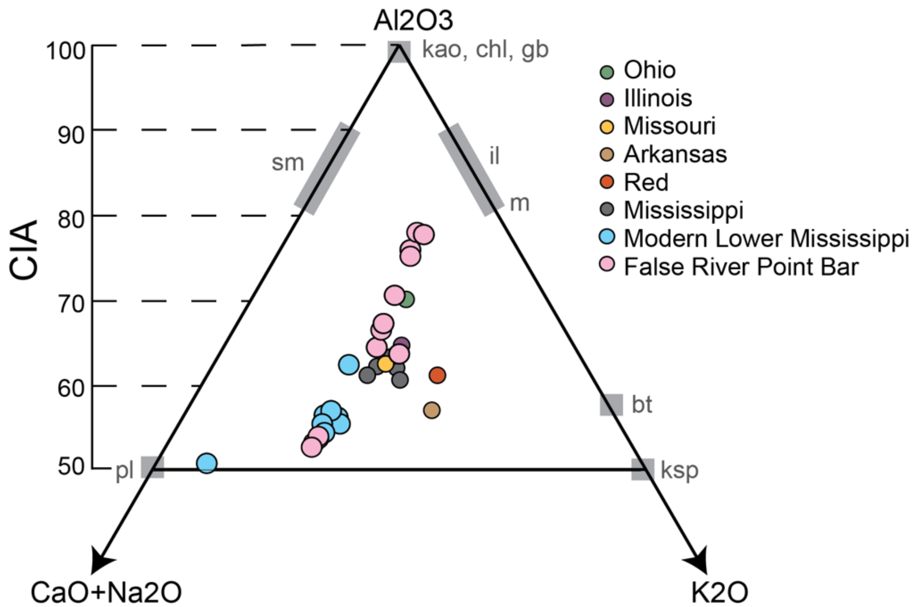

Figure 7. Geochemical signature of the analyzed samples illustrated by a CN-A-K ternary diagram (Fedo, Wayne Nesbitt et al. 1995). Modern tributary details from (Gregory, Herrmann et al. 2022) (Ohio, Illinois, Missouri, Arkansas, Red, and Mississippi). Samples closer to Al_2O_3 are rich in kaolinite, chlorite and/or gibbsite (representing by kao, chl and gib). CIA values are also calculated and shown on the left side, with its values are correlated with the CN-A-K. Abbreviations: sm (smectite), pl (plagioclase), ksp (K-feldspar), il (illite), m (muscovite).

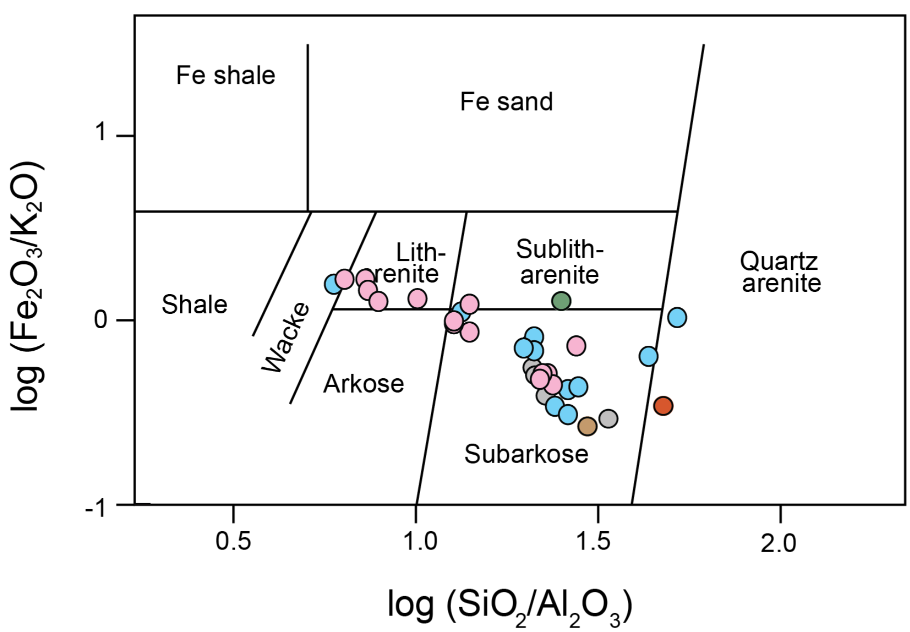

Figure 8. Geochemical classification of sediments from this study following the scheme of (Herron 1988). Most sediment from the point bar plot within the litharenite and subarkose sections, while the modern river samples are defined as subarkose.

CHAPTER 5. DISCUSSION

5.1. Geochemical Analysis

The major element analysis acquired using XRF is not very useful for defining provenance because it is dependent on grain size and chemical weathering, which can vary both temporarily and laterally over quite short distances, independent of source. However, a discrimination diagram can be used to understand how the different sediments have been affected by transport (Singh, Sharma et al. 2005) (Fig. 9). All sediments are displaced towards lower values of Al_2O_3/SiO_2 and Fe_2O_3/SiO_2 compared to the upper continental crust (UCC) average that might be expected to be derived from erosion of wide areas of the continental crust. The sediments are all displaced towards a quartz-rich end member indicating preferential loss of clay and micas as well as an enrichment in quartz during transport. Although some sediments indicate more quartz enrichment, this is not diagnostic of provenance but simply reflects hydrodynamic sorting during transport.

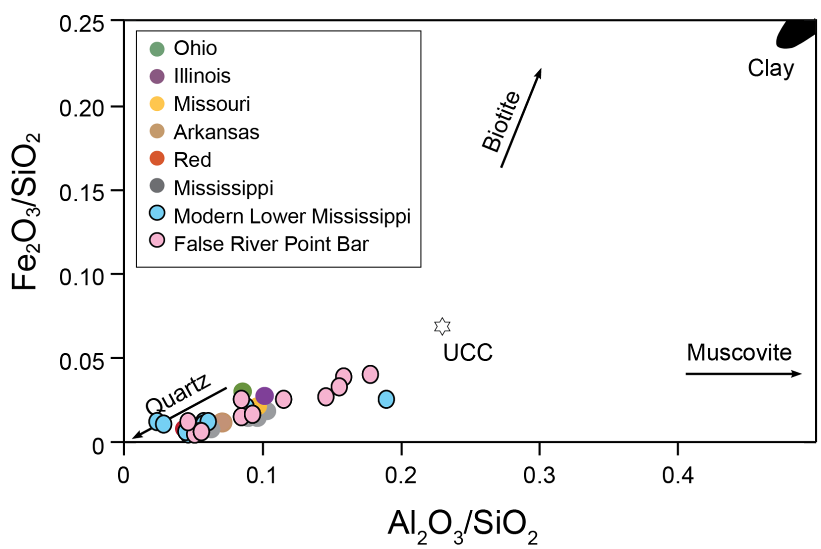

Figure 9. Plot of Al_2O_3/SiO_2 versus Fe_2O_3/SiO_2 for sediments from the Mississippi River after (Singh, Sharma et al. 2005). Lower ratios indicate increase of the quartz proportion and depletion of phyllosilicates. Linear trend corresponds to mineralogical sorting of these sediments during fluvial transport. Star corresponds to average Upper Continental Crust (UCC) (Taylor and McLennan 1995).

5.2. Zircon U-Pb Dating

As seen in the KDE diagrams (Fig. 5), there are significant variations amongst the populations that are derived from the various basement sources, and this reflects changing erosional patterns over different time scales. Even though variation is present within the data, there is no clear temporal evolution visible based on this type of analysis.

Using a 3D multi-dimensional scalar (MDS) diagram, made with the "R" software of Vermeesch (Vermeesch 2013), sediments can be assessed to relate the different tributaries. This type of analysis compares the different spectra of the DZ ages using a Kuiper statistical test and plots them as dimensionless factors that have no direct physical meaning (Fig. 10). Sediments with similar DZ age spectra plot close together on the diagram. There is a general clustering of the sediments in the False River point bar that overlaps with some sediments from lower reaches of the modern river. Two of the modern river samples plot on their own, away from all the other sediments and appear to be relatively unique (LA1701 and 18020401). These two samples plot closer to the Arkansas and Red River samples compared to other modern samples. Sediments from the LGM in the Gulf of Mexico, analyzed by Fildani, McKay (Fildani, McKay et al. 2016), plot separately from other Mississippi sediments, but very close to the modern Missouri River. The Ohio River appears to be the least similar to any of the lower reach samples, implying that this tributary contributes very little to the total zircon budget, which agrees with recent data. The Missouri appears to be closest to all the mixed sediments, consistent with earlier models that imply this to be the dominant supplier of material to the mainstem. Nonetheless, the distribution requires input from all the major tributaries to account for the variability seen in the MDS. In general, the 3D MDS diagram suggests that there are differences between sediments deposited at

different times spanning from the LGM to the Holocene and the recent, indicating a variable discharge of sediment.

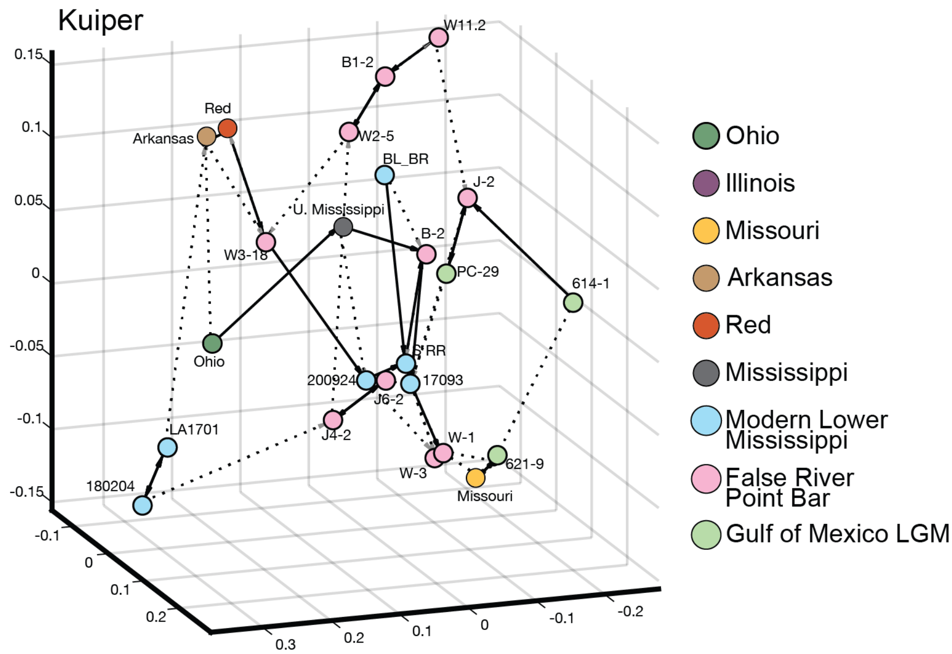

Figure 10. Three-dimensional multidimensional scalar diagram (MDS) comparing the age spectra of the detrital zircon from different samples considered in the study. Note that two of the modern samples are quite distinct from the other recent deposits and that the modern samples cluster separately from most samples taken from the False River Point Bar. See appendix for regular MDS plot (Appendix A. 1).

I further compare the sediments with modern tributaries and potential source terrains using a Kuiper statistical test that compares the age spectra using the software *DZStats* program (Sundell and Saylor 2017). The results from this test are used to generate a heat map (Fig. 11). Sediments whose age spectra are most similar are colored a dark blue, while dissimilar spectra are colored dark red. It is apparent that the sediments from the lower reaches and the False River point bar are generally quite similar to one another with a few notable exceptions. Sample 18020401 is somewhat different to many of the other sediments, while one of the sediments in the False River Point Bar, W11-2, stands out as being the most anomalous of any of the Holocene and modern sediments. The analysis underlines the fact that these sediments are

relatively similar, but not identical. When these sediments are compared with the major tributaries, there is a general similarity especially with the Arkansas and Red rivers, as well as to a lesser extent the Missouri and upper Mississippi. This statistical analysis confirms the results from the 3D MDS diagram (Fig. 10), indicating that the Ohio is the least similar to any of the modern Mississippi River deposits. The Rocky Mountain foreland is uniformly the most similar to the modern Mississippi River sediments, as well as several of the western tributaries. It is apparent that the Appalachians, Superior, Trans-Hudson, and Cordillera Provinces are the least similar, while there is some association between the sediments with the Grenville, Yavapai-Mazatzal and Peri-Gondwana Provinces.

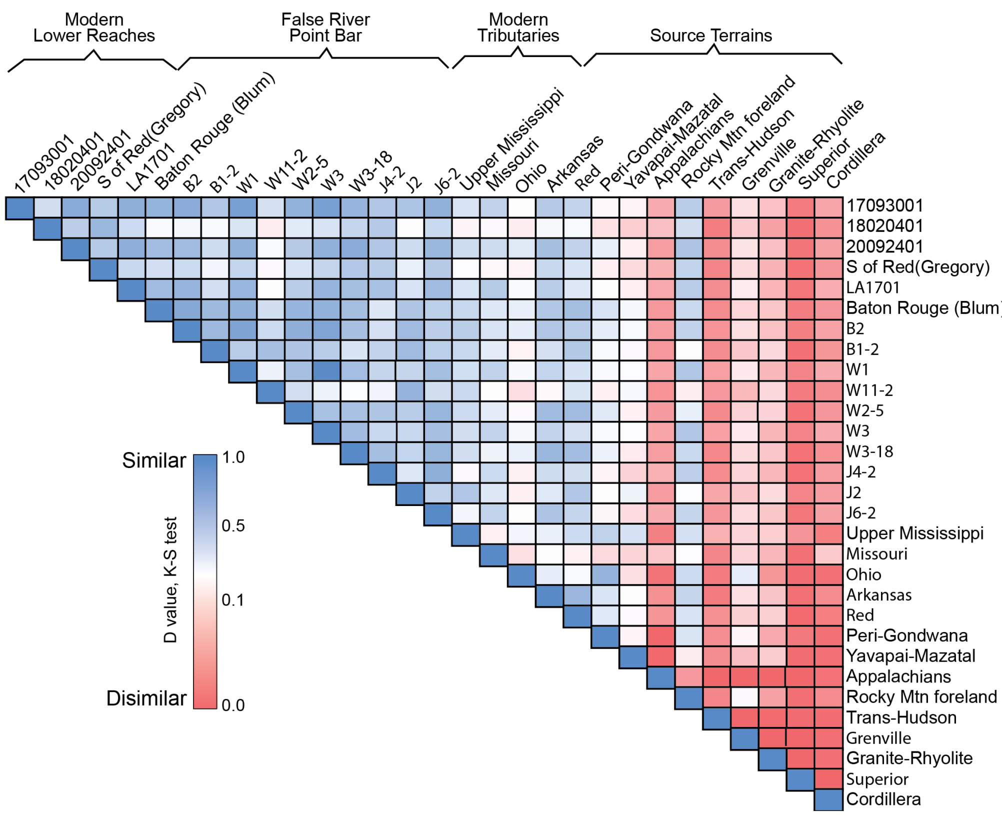

Figure 11. A heat map (Sundell and Saylor 2017) comparison of the zircon age spectra for the different detrital sediment samples compared with modern major tributaries (Gregory, Herrmann et al. 2022). and basement compilation from the various terrains for the source regions to the Mississippi River. Note the dissimilarity of most of the sediments with the Appalachian, Trans-Hudson and Superior Provinces, but the strong similarity of many samples with the Rocky Mountain foreland.

The Monte Carlo-based statistical method uses the varying sediment contributions from different source terrains to create a more quantitative estimate (Sundell and Saylor 2017). The sources used in this analytical method were the eight basement terrains listed in the introduction. In each case, 10,000 attempts were made to replicate a particular DZ age spectrum through varying the contributions from the source terrains to match the observed DZ age spectrum with the best 1% selected. This type of mixing can only be as good as the definition of the source areas, although in the case of the Mississippi, many of the sources are characterized by many hundreds if not thousands of data points. Furthermore, the complexity of this method may increase due to the potential reworking of older sediment due to not knowing a definitive way to remove the recycling effect, which was expected to influence all our samples. Instead, major systematic changes in DZ populations were used to quantify changes in provenance with the understanding that even unique peaks might be recycled through older sedimentary deposits. Although the unmixing method appears to be quite quantitative, it does not consider differences in DZ abundance within different source units or influences of recycling and grain size due to hydrodynamic sorting and so it is best used in a general fashion to look at overall trends in the DZ age spectra.

The results of the unmixing calculations are presented in Appendix F. The results are derived using three statistical tests one the Kuiper, the K-S test and the cross-correlation method (Sundell and Saylor 2017). Some statistical questions have been raised about the reliability of cross-correlation and as a result the Kuiper test was selected due to being widely accepted within the community. Using modern tributary DZ data resulted in relatively poor matches between models and the observed sediment (Appendices G and H), while major source terrains provided better matches amongst the data (Appendices G and H). This suggests that either the modern

tributaries are not well defined or that they are variable over short time periods, so that single grab samples are not suitable as long-term proxies for their influence on the system. The relative contributions from the major source terrains are shown as pie diagrams (Fig. 12) and are arranged in age order to demonstrate the temporal evolution. There is significant variability in the sediments, although the Rocky Mountain foreland and Yavapai-Mazatzal sources are the greatest contributors to many of the sediments. There is a major contribution to LGM sediments from the Superior Province and this continues throughout the section at a reduced rate in younger sediments. Many of the minor sources such as the Peri-Gondwana, Granite-Rhyolite and Grenville Province have a consistent but rather small contribution to the overall sediment budget. This analysis may be considered relatively robust since there are similar results when the K-S test is employed instead (Fig. 11).

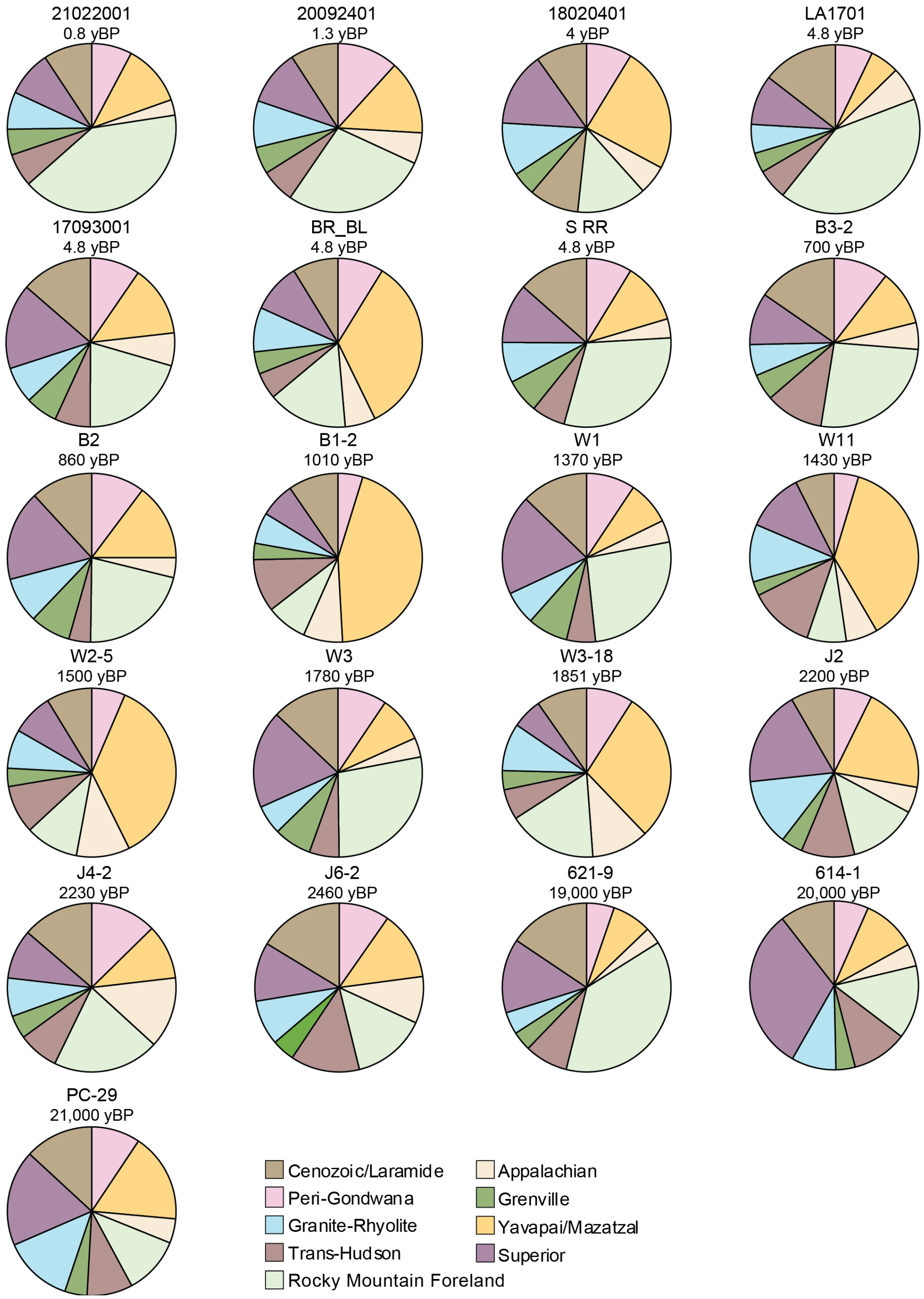

Figure 12. Unmixing calculations from (Sundell and Saylor 2017) using basement sources to correlate any similarities from the DZ spectra. The statistical test used was the Kuiper test from (Sundell and Saylor 2017).

5.3. Grain Size Analysis

Grain size analysis from the False River point bar as well as the modern samples collected from Reserve, Louisiana, both show a dominance of fine sand or silt (Table 1). The False River point bar generally shows very fine sand or silt, while the modern samples show a dominance of fine sand. Grain size was important to determine in order to potentially separate sediments deposited as bedload (coarse) versus suspended (fine). Suspended sediment will have faster transport times compared to bedload. Long transport times (>10^6 y) (Fildani, McKay et al. 2016) for bedload sediment would result in significant lags between changes in erosion of the upper reaches of the Mississippi River, compared to the sedimentation time in the lower Mississippi. The floodplain in the Lower Mississippi Valley is represented by five Holocene meander belts and the False River point bar is classified as meander belt one (Fig. 13) (Saucier and Snead 1989). Meander belt one soils are weakly developed and consist of bioturbated clay and silt (Aslan and Autin 1998), which is consistent with my grain size analysis of the point bar from the shallow samples. The modern samples were collected on the inner bend of meander loops at the edge of the river, and this sediment has a dominant content of fine sand. If the samples had been collected near the thalweg of the channel, the sediment would be coarser in grain size. When comparing the sediment from the False River to the modern samples collected, there is slight variation in grain size but is relatively similar overall. Since both grain size plots show relatively similar trends amongst the data, it can be determined that the samples collected for this study are most likely suspended sediments rather than bedload.

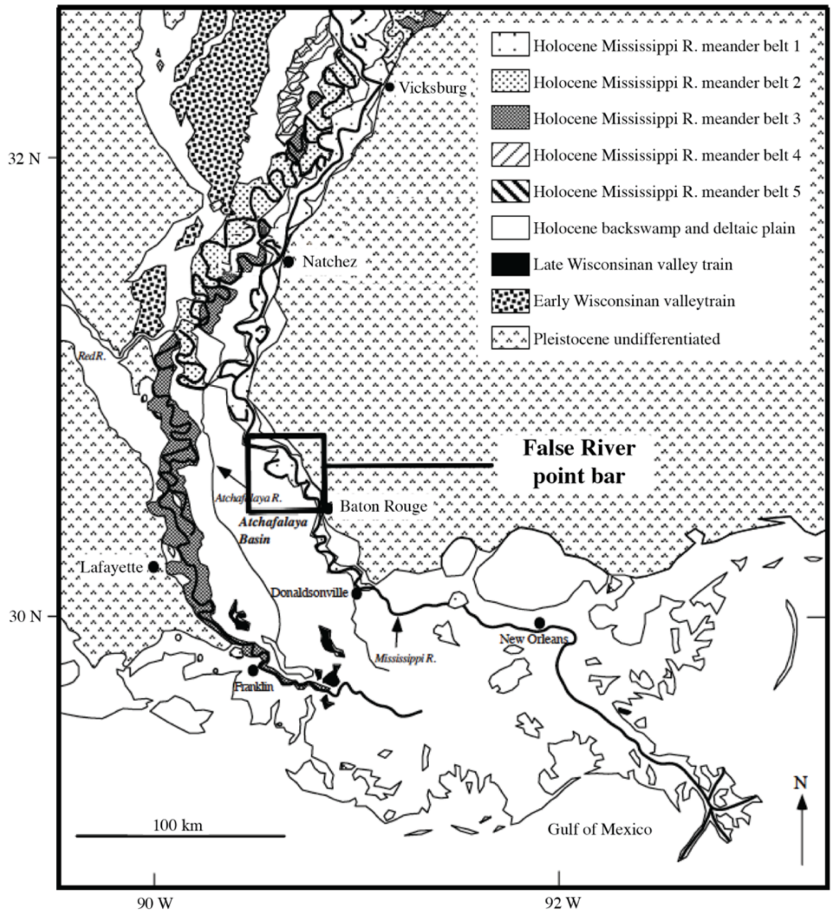

Figure 13. Geologic map of the Lower Mississippi Valley showing the distribution of Holocene meander belts. The False River point bar is indicated in the black box and consists of Holocene meander belt 1and backswamp/deltaic plain sediment. Image modified from (Saucier and Snead 1989)

When looking at the False River point bar in closer detail, I can see that the samples collected in this study (i.e., B1-2, B2-2, B3-2, W9-2, W10-2, W11-2, J4-2, J5-2, J6-2, and J7-2) all show a dominance in silt grains (Fig. 14). The samples used from previous research (i.e., B2-14;16, J2-11;10, W1-17;18, W2-5, and W3-10;11;18) were collected deeper in the Holocene section (>3 m) and exhibit coarser grains ranging from fine sand to medium sand. This was expected due to the depth taken in the core (>3 m) reflecting the depth in the channel during point bar accretion (Labrecque, Jensen et al. 2011, Durkin, Hubbard et al. 2015). Figure 14 shows a well-developed peak for each sample with only a few samples not showing a relatively

high degree of kurtosis indicating mostly good sorting. Many of the sediments show a positive skew with a long tail of coarser material.

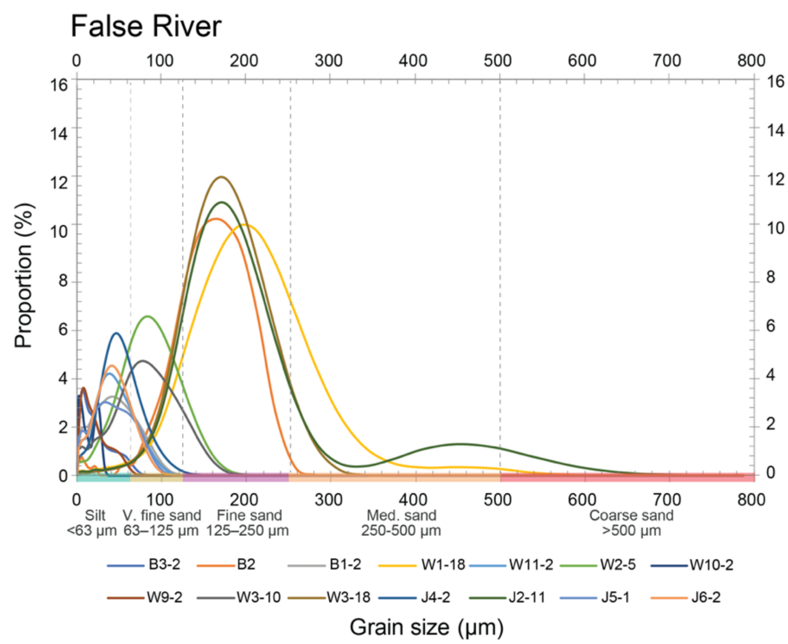

Figure 14. Grain size spectra of the False River point bar comparing proportion (%) to grain size (µm). Shallower samples are finer grained, while samples collected deeper within the point bar indicate a coarser grained material.

The Mississippi River sediments collected in Reserve, Louisiana, are dominated by fine sand, but a few samples contain high amounts of silt (Fig. 15). This is expected due to the location along the edge of the riverbank where velocities are lower than in the thalweg. Similar to the False River point bar samples (Fig. 14), most samples show a well-developed peak showing a relatively high degree of kurtosis indicating good sorting. Many of the sediments also show a positive skew with a long tail of coarser material.

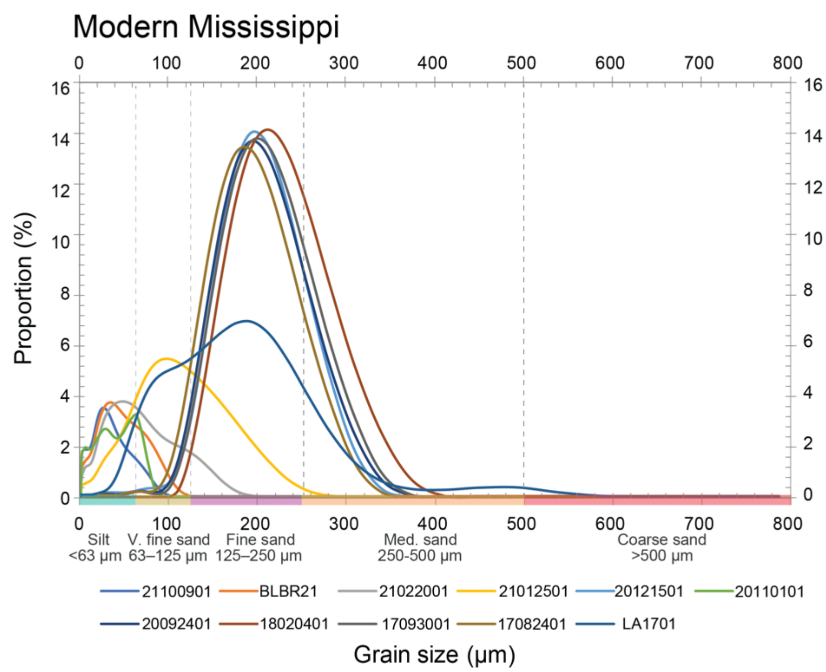

Figure 15. Grain size spectra of the modern river comparing proportion (%) to grain size (µm). Most samples are dominated by fine sand, but some samples indicate finer material present such as silt and very fine sand.

5.4. OSL Dating

The ages collected from the False River point bar show accretion of the point bar between 8.6 and 2.5 ka, which started in the Roman Warm Period and ends in the Medieval Warm Period. From previous findings/estimations of growth from literature, the expected time of migration of the channel was around 500 years, but the results indicate a life span of ~ 1.5 k.y. which means that the previous estimations were inaccurate, or that the point bar has not migrated much between 7.9 and 2.3 ka. The ages of the seven samples sent to the USU Laboratory are shown in Table 2 and imprinted on Figure 16 which shows the migration of the scroll bars through time. The final cutoff of the river had to have occurred after 8.6 ka, while the initial growth of the bend must have occurred before 2.5 ka.

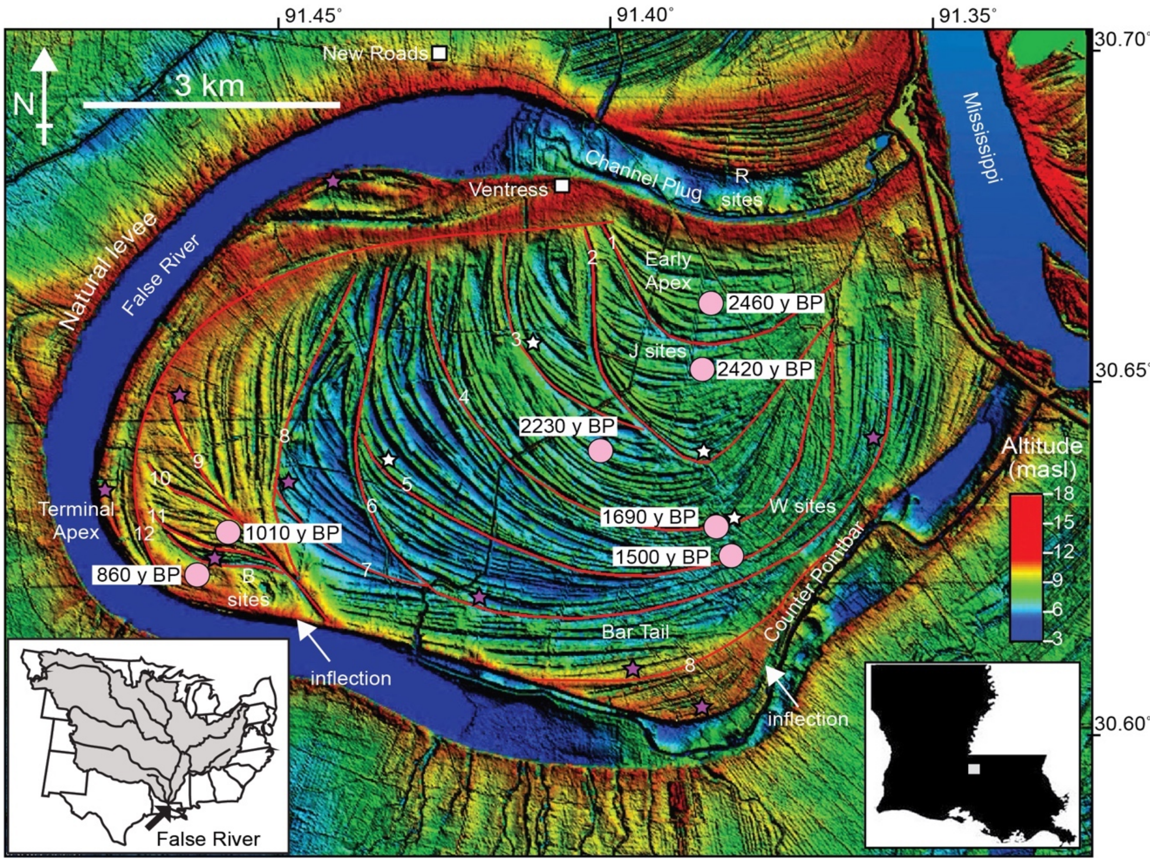

Figure 16. Lidar topography image of the region around False River and associated point bar showing the optically stimulated luminescence ages collected from various samples. The red lines show the major depositional units as defined by Clift and Olson (Clift, Olson et al.). The white stars indicate the apex of each bend through the migrational history of the point bar.

By using the OSL depositional ages, I can reconstruct the temporal evolution of sediment supply into the lower reaches of the Mississippi River. We also consider the Mississippi Fan LGM sediments (Fildani, McKay et al. 2016) and assign them an approximate depositional age of around 2 ka. Using the Monte Carlo unmixing zircon data (Appendix F), I plotted age (y BP) against the relative contribution from the Kuiper V statistical values and created a temporal diagram (Fig. 17) that shows how the supply of sediment from different critical source terrains, those selected showing consistent and significant variability, has changed with time. The analysis shows that the Superior Province was a much more dominant source of sediment at the LGM and has largely decreased since that time. In contrast, the Rocky Mountain foreland shows the

reverse with a general increase in flux between the LGM and the late Holocene and especially recently with significant variability. Supply from the Appalachians and Yavapai-Mazatzal was highly variable in the early/late Holocene. Age control is not sufficient to correlate these accurately with shorter climatic cycles, such as the Roman and Mediaeval Warm Periods, although the highest values of erosion from the Appalachians appear to have occurred during the Roman Warm Period (2.5 ka–1.6 ka; Campbell et al. 1998). I can also consider how the provenance of the sediment has varied with land use within the catchment. Prior to about 2000 years ago, most human societies in North America adopted hunter-gatherer economies but during the Woodland Period there was a transition to agriculture with the development of settled communities (Williams and Thomas 1982). It has been documented elsewhere that ploughing of the soil and removal of forests have resulted in enhanced soil erosion, which increases the total amount of sediment in the river (Southgate and Whitaker 1992, Anselmetti, Hodell et al. 2007). It is possible that the increase in sediment production from the Appalachians and Yavapai-Mazatzal during the late Holocene broadly correlates with the Woodland Period (1000 BC–AD 1000) and may partly reflect this transition in land use across wide areas of the Mississippi catchment. Since then, there has been a decrease in erosion from the Appalachians and an increase from the Rocky Mountain foreland (Fig. 17). The exact transition between those two periods is unknown because of a lack of samples, but it is possible that the spread of European settlement across the Great Plains would have increased the amount of erosion from the foreland. In more recent years, forests have largely regrown through much of the Appalachians, which in turn would have fostered the development of new soils, reducing the amount of flux into the river from that province (Leopold, Parker et al. 1985).

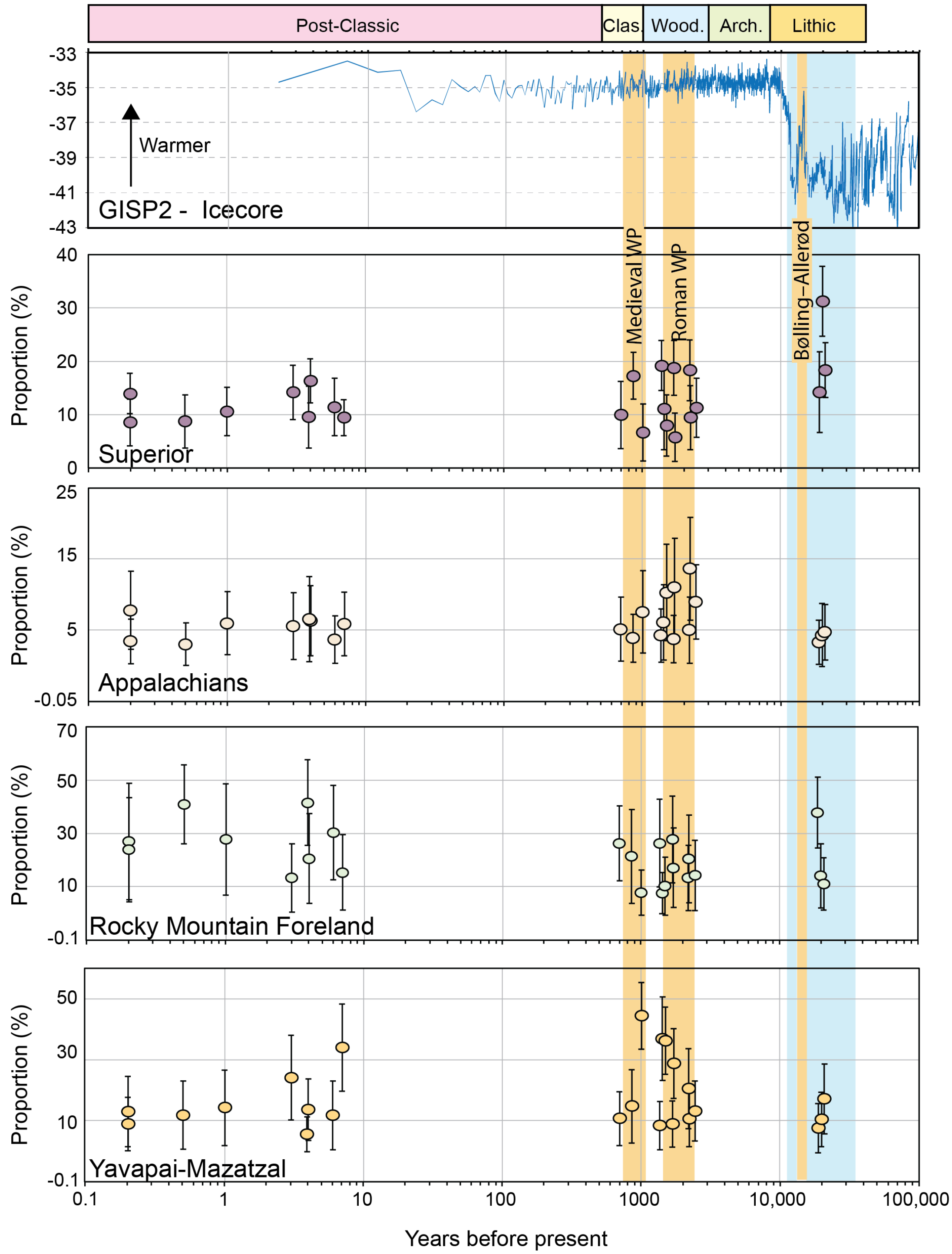

Figure 17. Summary of the unmixing calculations as plotted against depositional age showing the varying contribution from three contrasting source terrains of the Superior Province, Appalachian Mountains, and Rocky Mountain foreland. We compare the erosion history with climate variability as shown by the Greenland ice core (GISP2) (Grootes and Stuiver 1997). Clas= Classic, Woodld= Woodland., Arch=Archaic (Data from Appendix F).

5.5. Sediment Buffering

Modelling of rivers with large floodplains indicates that the composition of the river should be buffered over at significant periods of time because of storage and recycling (Mayer and Gloss 1980, Clift and Giosan 2014). However, the evidence from the Mississippi spanning the time since the LGM suggest that this is not so important. Figure 17 shows that there are coherent differences between the source of sediment at the LGM compared to the late Holocene and subsequently with the composition of the river in the last 10 years. The river is highly variable over the last 10 years, indicating that the river has not been buffered on a seasonal or annual basis, assuming the number of grains analyzed in this study is statistically robust. It is apparent that there are significant differences in provenance over short time periods, presumably related to the supply of sediment from upstream, and in turn potentially reflecting the effect of weather events in the upper reaches of the river enhancing or reducing sediment supply from individual source areas. The fact that the river is not strongly buffered in the present day may reflect its highly engineered state with the construction of levees. There is some scatter of compositions in the older samples as well, so it is not clear that even before installation of the levees that the river was fully buffered at that time either.

5.6. Efficiency of Zircon as a Provenance Method

The evidence collected during this study suggests that DZ provenance methodology is an effective tool for tracing sediment provenance, considering the number of grains analyzed. There is significant variability of the sediment flux from the modern river, so if a geologist wished to compare the composition of modern rivers with ancient deposits, then the sampling procedure must consist of multiple collections to generate a robust average composition. Since it predates the levees and dam constructions, the False River sediments likely make a better average

composition of the lower Mississippi. Also, the significant differences between sediment sampled in different years and seasons needs to be recognized when comparing modern samples with ancient sediments. In particular, the sediment deposited only a few thousand years ago is different from the modern river, potentially reflecting anthropogenic impacts on the patterns of erosion across the Mississippi basin in the recent past. Differences between sediments in the LGM, Holocene, and in recent times shows that erosion patterns are sensitive to climate change, indicating that the approach taken in this study yielded statistically robust results that can resolve changes of that magnitude.

The influence of grain size to the DZ provenance method has been questioned, since it might be expected that old grains that have experienced many cycles of reworking could be finer grained than younger grains. Figure 18 shows that there is a slight tendency of higher Zr concentrations (a proxy for zircon concentrations in the sediment) in finer grained sediments, (<100 μm) compared to coarser material, although there is significant scatter. On the other hand, I can determine if potential bias is introduced by comparing median grain size and provenance of age populations. Figure 19 shows that this is not likely the case. There is no clear relationship between the abundance of grains of any given age population being closely correlated with its median grain size. This gives confidence that sediment with a range of grain sizes is equally representative of the material being transported in the river at the time of its deposition.

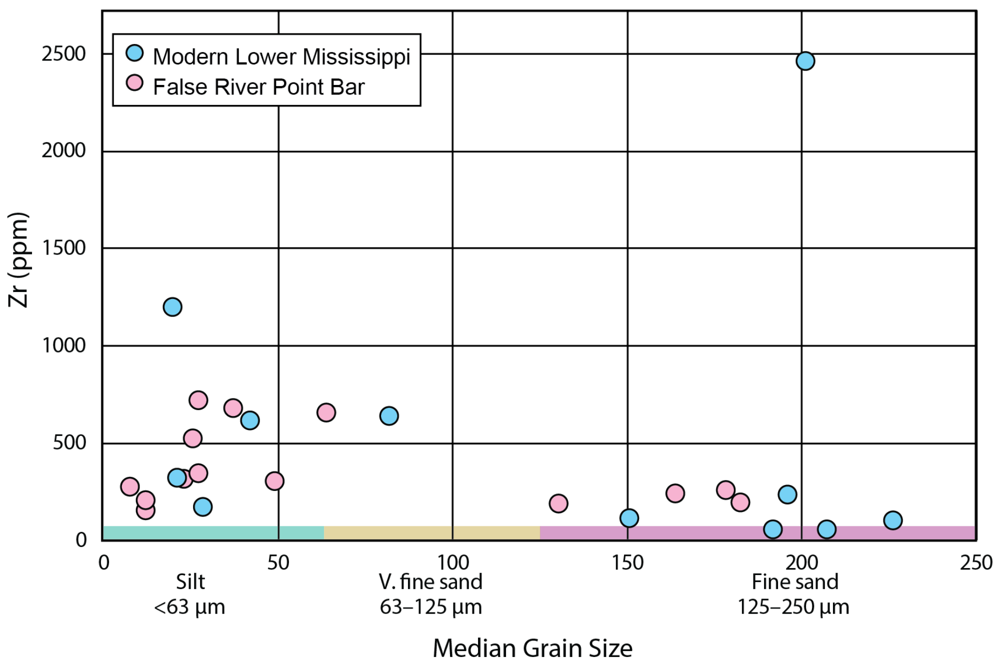

Figure 18. Cross plot of zirconium concentration (ppm)compared to medium grain size (µm). Higher zircon concentrations tend to have a smaller median grain size, although there is significant scatter.

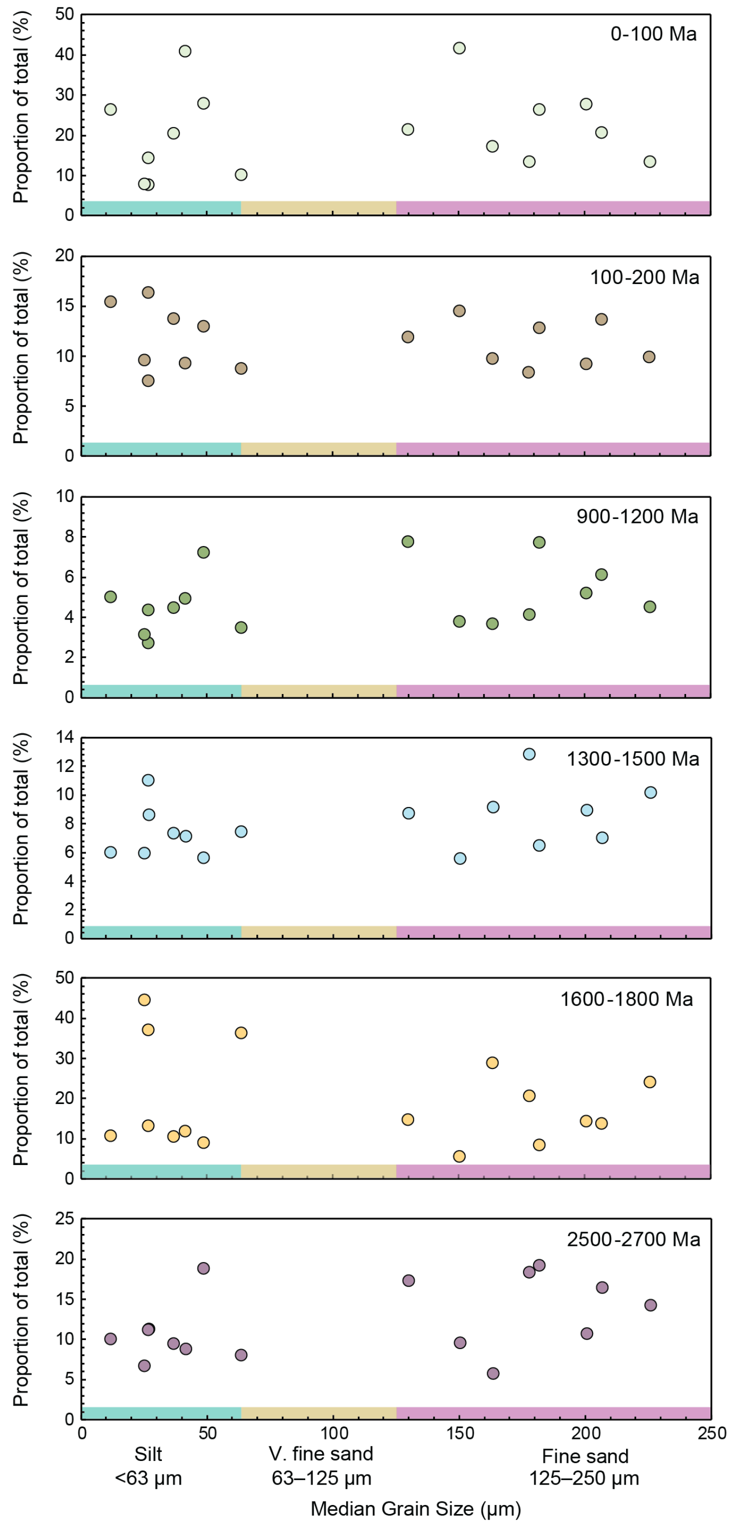

Figure 19. Plots showing the relationship between provenance-sensitive population groups and median grain size for the samples. The plot shows no clear relationship between grain size and zircon age spectra.

5.7. Future Research Recommendations

While the OSL ages obtained in this study give an overview of the accretionary history of the False River point bar (2.5–8.6 ka), gaps are still present in the coverage which if filled they would help determine the true migration rate of the point bar at a higher resolution. Additionally, more monthly samples from the modern river would provide a more robust analysis of for seasonal/centennial changes. Future work of Nd isotopic data is starting to be processed and will help provide more constraint on the Mississippi River erosional history from the LGM that can act as a cross-check to the DZ data presented here.

CHAPTER 6. CONCLUSION

Repeated analysis of detrital zircons in the Lower Mississippi Valley proves that the DZ provenance method is an accurate tool in identifying changing sediment flux from different source terrains in large river systems. This study confirmed earlier work that much of the sediment is being derived from the Rocky Mountain Foreland, although there are significant changes in sources since the LGM. Specifically, during glacial periods, the Superior Province generated higher relative amounts of sediment compared to the Holocene and that further changes in the dominant sources between 1000 years ago and the immediate past can be identified. In general, the river has not been strongly buffered in its composition over the last ten years which can be related to short-term changes in erosion in the headwaters and a reduced degree of recycling of sediment in the floodplains as a result of the construction of levees. The lack of buffering in the river implies that caution should be used when comparing modern rivers as proxies to ancient deposits. Overall, the changes in erosion patterns from the source terrains during the Late Holocene can be a result of human settlement, but this is not clear due to not having sufficient samples preceding and post-dating those time periods. The sediment in the modern Mississippi River supports the idea that grain size is not a limiting factor in the influence on provenance methodology, at least in North America.

APPENDIX A. SUPPLEMENTARY FIGURES

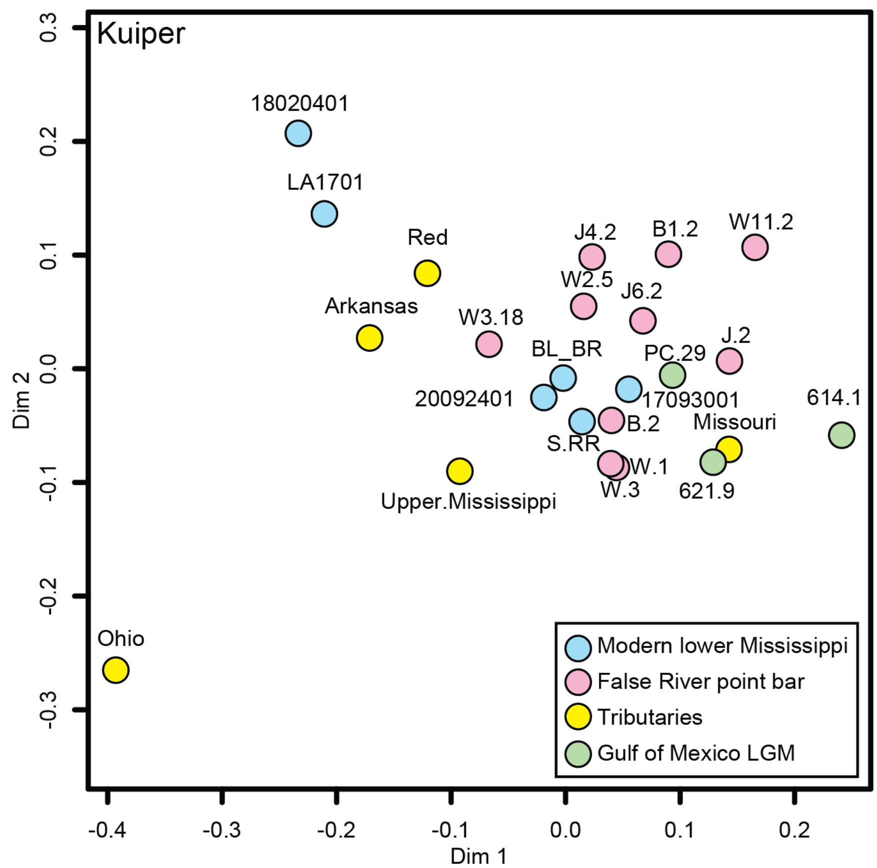

Appendix A. 1. Multidimensional scalar diagram (MDS) comparing the age spectra of the detrital zircon from different samples considered in the study. Note that two of the modern samples are quite distinct from the other recent deposits and that the modern samples cluster separately from most samples taken from the False River Point Bar.

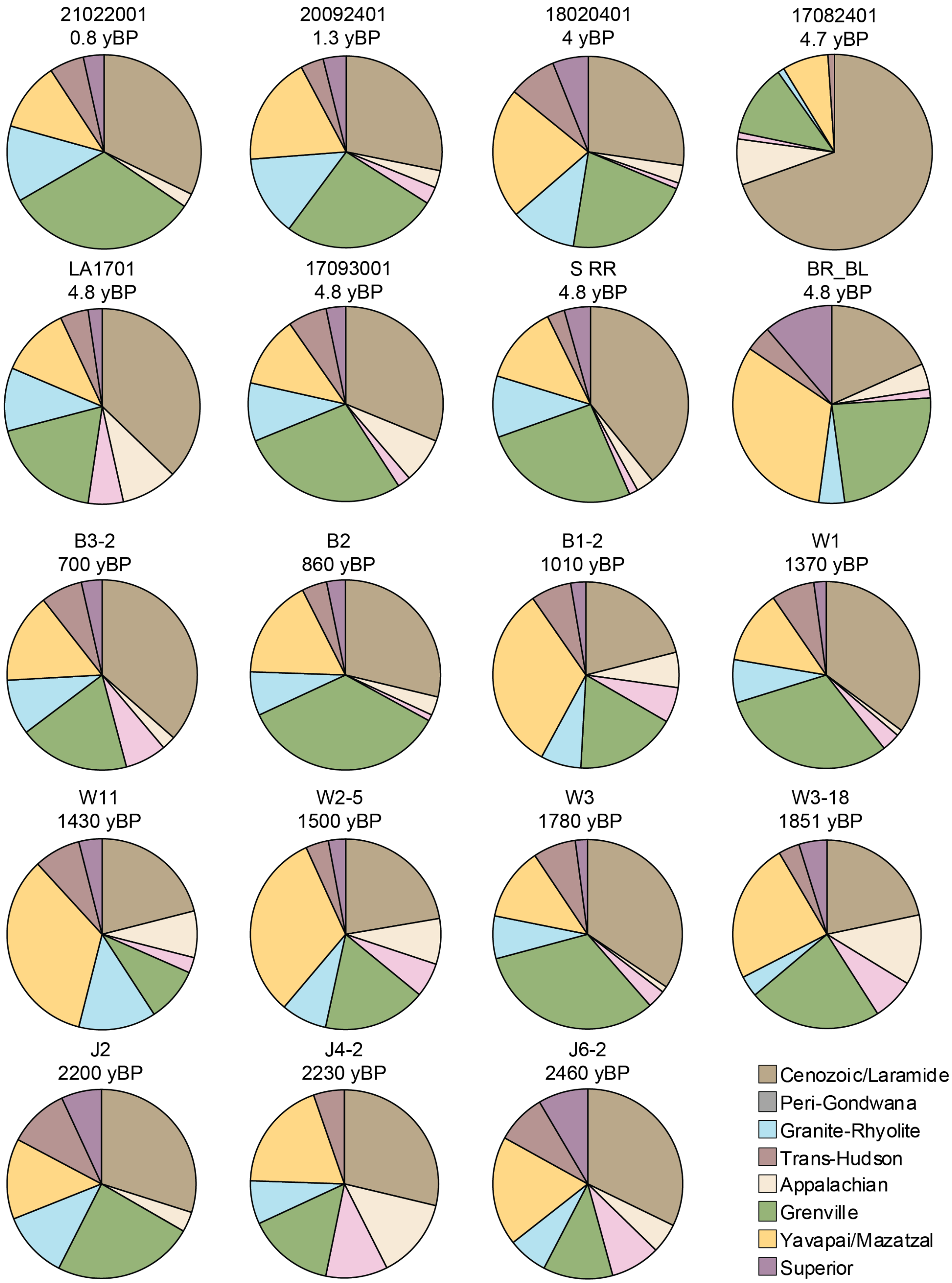

Appendix A. 2. Zircon Age Pies correlated with the basement sources used in this study. Also, pies are in chronological order to create a temporal evolution.

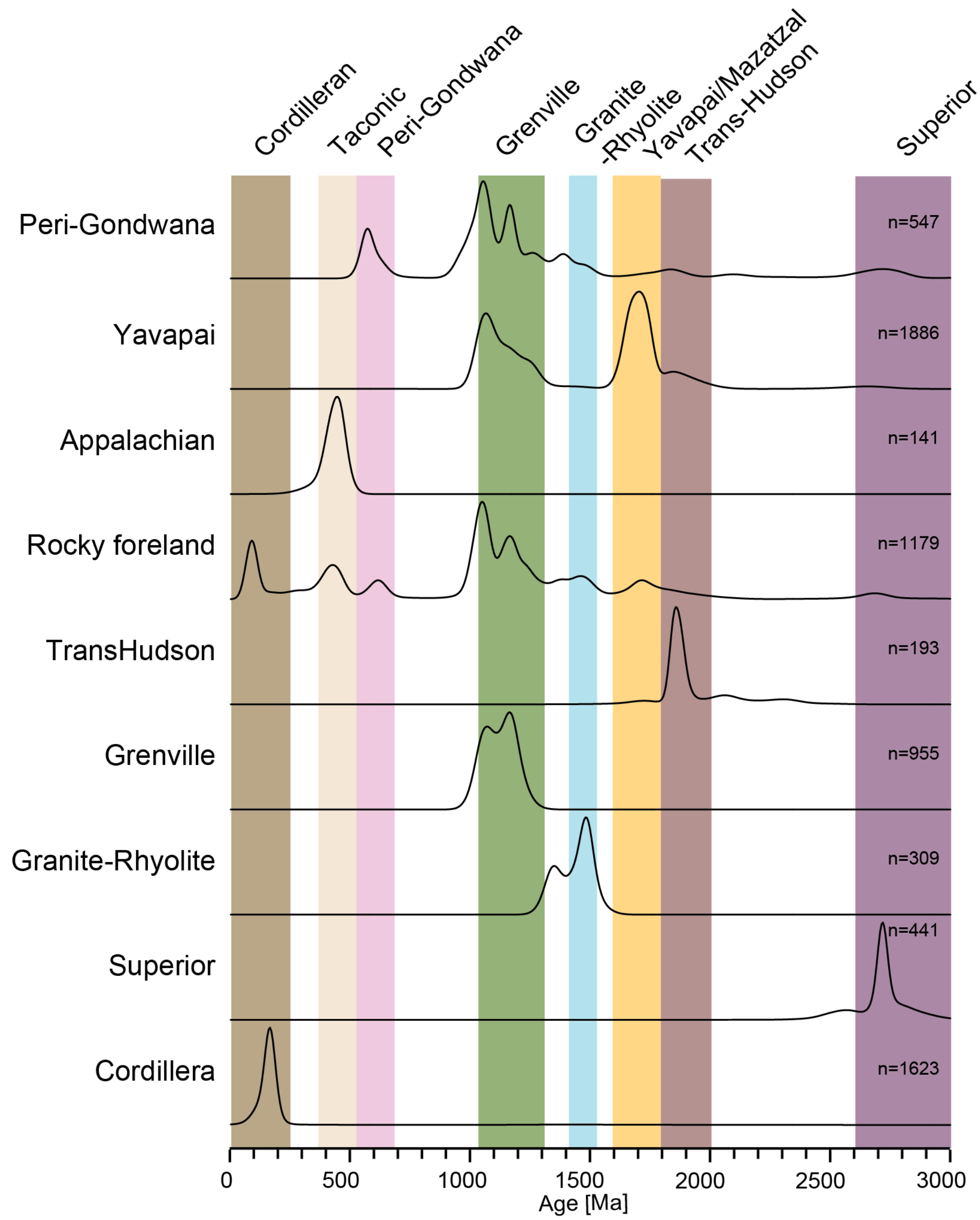

Appendix A. 3. Basement terrain KDE diagram.

APPENDIX B. ANALYTICAL DATA FOR GRAIN SIZE

Size (microns)	21100901	BLBR21	21022001	21012501	20121501	20110101	20092401	18020401	17093001	17082401	LA1701	B3-2
0.375124	0.0400	0.0452	0.0316	0.0185	0.0036	0.0522	0.0000	0.0000	0.0000	0.0000	0.0046	0.0240
0.411798	0.0710	0.0801	0.0560	0.0329	0.0070	0.0926	0.0000	0.0000	0.0000	0.0000	0.0088	0.0426
0.452057	0.1094	0.1209	0.0844	0.0495	0.0121	0.1422	0.0000	0.0000	0.0000	0.0000	0.0151	0.0667
0.496252	0.1694	0.1806	0.1256	0.0736	0.0173	0.2180	0.0003	0.0000	0.0003	0.0003	0.0215	0.1058
0.544768	0.2381	0.2421	0.1675	0.0981	0.0228	0.3024	0.0040	0.0000	0.0037	0.0036	0.0280	0.1541
0.598027	0.3173	0.3073	0.2114	0.1237	0.0286	0.3972	0.0122	0.0000	0.0113	0.0111	0.0348	0.2131
0.656493	0.4087	0.3777	0.2587	0.1512	0.0346	0.5042	0.0203	0.0000	0.0188	0.0184	0.0417	0.2845
0.720675	0.5149	0.4563	0.3112	0.1818	0.0409	0.6264	0.0275	0.0000	0.0255	0.0249	0.0487	0.3704
0.791132	0.6345	0.5406	0.3674	0.2144	0.0471	0.7613	0.0338	0.0000	0.0315	0.0306	0.0555	0.4713
0.868477	0.7647	0.6279	0.4256	0.2479	0.0533	0.9045	0.0391	0.0000	0.0365	0.0353	0.0620	0.5867
0.953383	0.9021	0.7162	0.4845	0.2817	0.0590	1.0514	0.0432	0.0000	0.0405	0.0389	0.0679	0.7156
1.04659	1.0420	0.8028	0.5430	0.3148	0.0641	1.1961	0.0459	0.0000	0.0433	0.0412	0.0729	0.8560
1.14891	1.1798	0.8860	0.6001	0.3468	0.0683	1.3336	0.0473	0.0000	0.0449	0.0422	0.0767	1.0052
1.26123	1.3097	0.9620	0.6534	0.3760	0.0713	1.4571	0.0476	0.0000	0.0455	0.0422	0.0793	1.1599
1.38454	1.4269	1.0283	0.7016	0.4014	0.0731	1.5615	0.0467	0.0000	0.0450	0.0411	0.0804	1.3171
1.5199	1.5272	1.0829	0.7438	0.4224	0.0737	1.6436	0.0450	0.0000	0.0437	0.0391	0.0802	1.4744
1.66849	1.6088	1.1261	0.7804	0.4390	0.0732	1.7028	0.0427	0.0000	0.0418	0.0365	0.0787	1.6305
1.83161	1.6715	1.1585	0.8119	0.4513	0.0717	1.7403	0.0399	0.0000	0.0394	0.0334	0.0762	1.7848
2.01068	1.7162	1.1814	0.8392	0.4597	0.0695	1.7593	0.0369	0.0000	0.0368	0.0301	0.0731	1.9380
2.20725	1.7455	1.1970	0.8636	0.4648	0.0670	1.7648	0.0341	0.0000	0.0341	0.0268	0.0699	2.0907
2.42304	1.7629	1.2080	0.8868	0.4676	0.0646	1.7630	0.0315	0.0000	0.0316	0.0238	0.0669	2.2439
2.65993	1.7730	1.2179	0.9108	0.4694	0.0626	1.7611	0.0293	0.0000	0.0295	0.0212	0.0646	2.3983
2.91998	1.7799	1.2293	0.9367	0.4713	0.0614	1.7640	0.0278	0.0000	0.0277	0.0190	0.0634	2.5541
3.20545	1.7869	1.2442	0.9654	0.4741	0.0610	1.7749	0.0269	0.0000	0.0265	0.0175	0.0632	2.7097
3.51883	1.7952	1.2629	0.9963	0.4781	0.0615	1.7940	0.0267	0.0000	0.0258	0.0166	0.0641	2.8622
3.86284	1.8050	1.2852	1.0289	0.4836	0.0629	1.8199	0.0270	0.0000	0.0256	0.0162	0.0658	3.0070
4.24049	1.8150	1.3099	1.0615	0.4905	0.0650	1.8492	0.0278	0.0000	0.0257	0.0163	0.0679	3.1383
4.65506	1.8239	1.3355	1.0926	0.4987	0.0675	1.8769	0.0290	0.0000	0.0261	0.0168	0.0700	3.2499
5.11017	1.8297	1.3605	1.1205	0.5075	0.0703	1.8975	0.0304	0.0000	0.0267	0.0175	0.0718	3.3364

Size (microns)	21100901	BLBR21	21022001	21012501	20121501	20110101	20092401	18020401	17093001	17082401	LA1701	B3-2
5.60976	1.8313	1.3838	1.1440	0.5166	0.0729	1.9074	0.0318	0.0000	0.0272	0.0183	0.0729	3.3944
6.1582	1.8293	1.4055	1.1629	0.5258	0.0754	1.9072	0.0333	0.0000	0.0278	0.0191	0.0733	3.4217
6.76025	1.8258	1.4265	1.1777	0.5352	0.0777	1.9003	0.0346	0.0000	0.0282	0.0198	0.0731	3.4183
7.42117	1.8241	1.4488	1.1896	0.5457	0.0796	1.8900	0.0357	0.0000	0.0284	0.0204	0.0723	3.3845
8.14669	1.8270	1.4744	1.2000	0.5571	0.0811	1.8763	0.0366	0.0000	0.0283	0.0207	0.0709	3.3201
8.94315	1.8366	1.5058	1.2112	0.5703	0.0825	1.8581	0.0373	0.0000	0.0280	0.0207	0.0693	3.2244
9.81748	1.8561	1.5457	1.2263	0.5853	0.0838	1.8371	0.0378	0.0000	0.0275	0.0204	0.0677	3.0988
10.7773	1.8931	1.5993	1.2515	0.6050	0.0854	1.8231	0.0384	0.0000	0.0268	0.0201	0.0666	2.9516
11.8309	1.9603	1.6755	1.2950	0.6317	0.0879	1.8312	0.0393	0.0000	0.0264	0.0199	0.0667	2.7990
12.9876	2.0722	1.7854	1.3677	0.6693	0.0920	1.8702	0.0409	0.0000	0.0266	0.0202	0.0692	2.6629
14.2573	2.2375	1.9384	1.4789	0.7201	0.0985	1.9406	0.0437	0.0000	0.0277	0.0217	0.0748	2.5595
15.6512	2.4530	2.1357	1.6339	0.7856	0.1076	2.0300	0.0481	0.0000	0.0303	0.0246	0.0841	2.4897
17.1813	2.7004	2.3687	1.8314	0.8676	0.1192	2.1281	0.0542	0.0000	0.0344	0.0294	0.0975	2.4345
18.861	2.9511	2.6196	2.0619	0.9652	0.1322	2.2317	0.0618	0.0000	0.0401	0.0359	0.1147	2.3607
20.705	3.1730	2.8683	2.3127	1.0785	0.1446	2.3414	0.0700	0.0000	0.0465	0.0431	0.1346	2.2389
22.7292	3.3383	3.0981	2.5682	1.2033	0.1546	2.4570	0.0777	0.0000	0.0529	0.0497	0.1563	2.0578
24.9513	3.4266	3.2978	2.8150	1.3347	0.1607	2.5616	0.0836	0.0000	0.0580	0.0541	0.1805	1.8313
27.3906	3.4248	3.4587	3.0420	1.4672	0.1643	2.6221	0.0869	0.0000	0.0613	0.0554	0.2145	1.5921
30.0685	3.3276	3.5714	3.2398	1.5975	0.1674	2.6082	0.0876	0.0000	0.0623	0.0537	0.2705	1.3735
33.0081	3.1413	3.6239	3.4028	1.7289	0.1703	2.5100	0.0849	0.0000	0.0608	0.0500	0.3639	1.2003
36.2352	2.8846	3.6059	3.5281	1.8705	0.1715	2.3713	0.0794	0.0000	0.0574	0.0472	0.5109	1.0806
39.7777	2.5921	3.5160	3.6165	2.0397	0.1687	2.2723	0.0735	0.0000	0.0542	0.0491	0.7292	1.0071
43.6665	2.3017	3.3668	3.6697	2.2574	0.1640	2.2865	0.0729	0.0000	0.0566	0.0615	1.0384	0.9631
47.9356	2.0424	3.1872	3.6864	2.5435	0.1633	2.4557	0.0849	0.0000	0.0713	0.0887	1.4482	0.9232
52.622	1.8251	3.0083	3.6590	2.9099	0.1716	2.7472	0.1130	0.0000	0.1016	0.1287	1.9452	0.8589
57.7666	1.6324	2.8479	3.5754	3.3520	0.1951	3.0347	0.1530	0.0000	0.1434	0.1687	2.5013	0.7491
63.4141	1.4289	2.6987	3.4222	3.8450	0.2376	3.1412	0.1888	0.0000	0.1802	0.1895	3.0829	0.5090
69.6138	1.1808	2.5183	3.1932	4.3424	0.2891	2.4273	0.1966	0.0000	0.1861	0.1815	3.6447	0.2440
76.4196	0.8711	2.2458	2.9064	4.7851	0.3263	1.2852	0.1679	0.0000	0.1458	0.1706	4.1303	0.0545
83.8907	0.5017	1.8409	2.6003	5.1151	0.3411	0.3041	0.1459	0.0000	0.0956	0.2330	4.4949	0.0053
92.0923	0.1988	1.3132	2.3261	5.2924	0.3846	0.0314	0.2255	0.0000	0.1207	0.5094	4.7341	0.0000
101.096	0.0389	0.7218	2.1169	5.3046	0.5958	0.0000	0.5850	0.0164	0.3734	1.2189	4.8926	0.0000

Size (microns)	21100901	BLBR21	21022001	21012501	20121501	20110101	20092401	18020401	17093001	17082401	LA1701	B3-2
110.979	0.0031	0.2705	1.9489	5.1664	1.2193	0.0000	1.4908	0.3046	1.1292	2.5614	5.0454	0.0000
121.829	0.0000	0.0505	1.7585	4.9044	2.5485	0.0000	3.1274	1.3850	2.5937	4.5895	5.2624	0.0000
133.74	0.0000	0.0038	1.4672	4.5397	4.7334	0.0000	5.4811	3.3304	4.7990	7.1401	5.5773	0.0000
146.815	0.0000	0.0000	1.0483	4.0763	7.5991	0.0000	8.2774	5.9702	7.5385	9.8192	5.9745	0.0000
161.168	0.0000	0.0000	0.5658	3.5050	10.6168	0.0000	10.9926	8.9670	10.3527	12.0710	6.3921	0.0000
176.925	0.0000	0.0000	0.2006	2.8292	13.0345	0.0000	12.9990	11.7219	12.6280	13.3654	6.7084	0.0000
194.222	0.0000	0.0000	0.0354	2.0816	14.1107	0.0000	13.7568	13.6168	13.7889	13.3284	6.7262	0.0000
213.21	0.0000	0.0000	0.0023	1.3313	13.4612	0.0000	13.0192	14.1807	13.4844	11.9294	6.2481	0.0000
234.054	0.0000	0.0000	0.0000	0.6610	11.1849	0.0000	10.9379	13.2487	11.7512	9.4493	5.2338	0.0000
256.936	0.0000	0.0000	0.0000	0.2250	7.9167	0.0000	8.0075	11.0422	8.9864	6.4384	3.8675	0.0000
282.056	0.0000	0.0000	0.0000	0.0388	4.5410	0.0000	4.9389	8.0691	5.8462	3.5815	2.4557	0.0000
309.631	0.0000	0.0000	0.0000	0.0026	1.7440	0.0000	2.3461	5.0026	3.0257	1.2482	1.2960	0.0000
339.902	0.0000	0.0000	0.0000	0.0000	0.2976	0.0000	0.6128	2.4331	0.8893	0.1518	0.5828	0.0000
373.132	0.0000	0.0000	0.0000	0.0000	0.0108	0.0000	0.0392	0.6662	0.0636	0.0022	0.2927	0.0000
409.611	0.0000	0.0000	0.0000	0.0000	0.0000	0.0000	0.0000	0.0449	0.0000	0.0000	0.2600	0.0000
449.657	0.0000	0.0000	0.0000	0.0000	0.0000	0.0000	0.0000	0.0000	0.0000	0.0000	0.3433	0.0000
493.617	0.0000	0.0000	0.0000	0.0000	0.0000	0.0000	0.0000	0.0000	0.0000	0.0000	0.3508	0.0000
541.876	0.0000	0.0000	0.0000	0.0000	0.0000	0.0000	0.0000	0.0000	0.0000	0.0000	0.1510	0.0000
594.852	0.0000	0.0000	0.0000	0.0000	0.0000	0.0000	0.0000	0.0000	0.0000	0.0000	0.0126	0.0000
653.008	0.0000	0.0000	0.0000	0.0000	0.0000	0.0000	0.0000	0.0000	0.0000	0.0000	0.0000	0.0000
716.849	0.0000	0.0000	0.0000	0.0000	0.0000	0.0000	0.0000	0.0000	0.0000	0.0000	0.0000	0.0000
786.932	0.0000	0.0000	0.0000	0.0000	0.0000	0.0000	0.0000	0.0000	0.0000	0.0000	0.0000	0.0000
863.866	0.0000	0.0000	0.0000	0.0000	0.0000	0.0000	0.0000	0.0000	0.0000	0.0000	0.0000	0.0000
948.322	0.0000	0.0000	0.0000	0.0000	0.0000	0.0000	0.0000	0.0000	0.0000	0.0000	0.0000	0.0000
1041.03	0.0000	0.0000	0.0000	0.0000	0.0000	0.0000	0.0000	0.0000	0.0000	0.0000	0.0000	0.0000
1142.81	0.0000	0.0000	0.0000	0.0000	0.0000	0.0000	0.0000	0.0000	0.0000	0.0000	0.0000	0.0000
1254.54	0.0000	0.0000	0.0000	0.0000	0.0000	0.0000	0.0000	0.0000	0.0000	0.0000	0.0000	0.0000
1377.19	0.0000	0.0000	0.0000	0.0000	0.0000	0.0000	0.0000	0.0000	0.0000	0.0000	0.0000	0.0000
1511.83	0.0000	0.0000	0.0000	0.0000	0.0000	0.0000	0.0000	0.0000	0.0000	0.0000	0.0000	0.0000
1659.63	0.0000	0.0000	0.0000	0.0000	0.0000	0.0000	0.0000	0.0000	0.0000	0.0000	0.0000	0.0000
1821.88	0.0000	0.0000	0.0000	0.0000	0.0000	0.0000	0.0000	0.0000	0.0000	0.0000	0.0000	0.0000

Size (microns)	B2	B1-2	W1-18	W11-2	W2-5	W10-2	W9-2	W3-10	W3-18	J4-2	J2-11	J5-1	J6-2
0.375124	0.0072	0.0320	0.0035	0.0449	0.0263	0.0821	0.0320	0.0356	0.0034	0.0349	0.0037	0.0588	0.0458
0.411798	0.0145	0.0567	0.0070	0.0795	0.0465	0.1457	0.0568	0.0632	0.0067	0.0619	0.0074	0.1042	0.0812
0.452057	0.0272	0.0859	0.0129	0.1202	0.0702	0.2248	0.0871	0.0968	0.0119	0.0926	0.0135	0.1579	0.1221
0.496252	0.0433	0.1295	0.0198	0.1802	0.1048	0.3485	0.1339	0.1481	0.0174	0.1359	0.0207	0.2375	0.1813
0.544768	0.0642	0.1759	0.0282	0.2426	0.1401	0.4910	0.1869	0.2046	0.0237	0.1775	0.0293	0.3212	0.2411
0.598027	0.0911	0.2268	0.0384	0.3092	0.1771	0.6554	0.2479	0.2676	0.0307	0.2193	0.0396	0.4109	0.3033
0.656493	0.1248	0.2838	0.0503	0.3818	0.2168	0.8441	0.3188	0.3382	0.0384	0.2626	0.0516	0.5089	0.3698
0.720675	0.1656	0.3491	0.0638	0.4630	0.2606	1.0614	0.4018	0.4184	0.0468	0.3095	0.0651	0.6185	0.4432
0.791132	0.2135	0.4217	0.0787	0.5505	0.3071	1.3042	0.4966	0.5063	0.0556	0.3580	0.0798	0.7367	0.5212
0.868477	0.2674	0.5005	0.0944	0.6416	0.3543	1.5668	0.6022	0.5988	0.0646	0.4064	0.0953	0.8591	0.6012
0.953383	0.3255	0.5844	0.1102	0.7340	0.4009	1.8402	0.7176	0.6927	0.0734	0.4542	0.1107	0.9822	0.6815
1.04659	0.3851	0.6721	0.1252	0.8248	0.4452	2.1126	0.8411	0.7840	0.0815	0.5006	0.1251	1.1016	0.7600
1.14891	0.4425	0.7623	0.1387	0.9120	0.4861	2.3725	0.9708	0.8692	0.0885	0.5454	0.1378	1.2141	0.8356
1.26123	0.4935	0.8524	0.1498	0.9917	0.5212	2.6091	1.1037	0.9442	0.0940	0.5863	0.1479	1.3143	0.9047
1.38454	0.5346	0.9403	0.1581	1.0611	0.5492	2.8141	1.2376	1.0058	0.0977	0.6224	0.1550	1.3984	0.9654
1.5199	0.5628	1.0243	0.1632	1.1182	0.5690	2.9794	1.3708	1.0517	0.0996	0.6530	0.1587	1.4639	1.0162
1.66849	0.5767	1.1041	0.1652	1.1633	0.5809	3.1008	1.5032	1.0819	0.0997	0.6788	0.1593	1.5114	1.0577
1.83161	0.5771	1.1795	0.1646	1.1970	0.5853	3.1770	1.6351	1.0976	0.0982	0.6996	0.1570	1.5426	1.0905
2.01068	0.5672	1.2508	0.1620	1.2207	0.5832	3.2163	1.7679	1.1014	0.0956	0.7158	0.1527	1.5604	1.1158
2.20725	0.5531	1.3189	0.1586	1.2370	0.5762	3.2276	1.9033	1.0968	0.0923	0.7282	0.1474	1.5689	1.1358
2.42304	0.5421	1.3848	0.1552	1.2487	0.5660	3.2220	2.0431	1.0884	0.0889	0.7381	0.1422	1.5734	1.1527
2.65993	0.5420	1.4498	0.1529	1.2594	0.5552	3.2050	2.1891	1.0808	0.0860	0.7470	0.1381	1.5795	1.1697
2.91998	0.5581	1.5149	0.1524	1.2719	0.5455	3.1827	2.3419	1.0778	0.0839	0.7558	0.1359	1.5916	1.1889
3.20545	0.5920	1.5804	0.1540	1.2880	0.5383	3.1616	2.5011	1.0814	0.0829	0.7653	0.1360	1.6119	1.2120
3.51883	0.6394	1.6454	0.1576	1.3079	0.5340	3.1441	2.6642	1.0917	0.0831	0.7759	0.1383	1.6401	1.2389
3.86284	0.6914	1.7087	0.1625	1.3308	0.5330	3.1281	2.8274	1.1074	0.0844	0.7882	0.1422	1.6739	1.2693
4.24049	0.7358	1.7678	0.1680	1.3550	0.5345	3.0938	2.9849	1.1254	0.0864	0.8020	0.1471	1.7096	1.3015
4.65506	0.7614	1.8208	0.1730	1.3784	0.5382	3.0289	3.1307	1.1422	0.0887	0.8167	0.1519	1.7430	1.3338
5.11017	0.7616	1.8659	0.1768	1.3990	0.5427	2.9241	3.2588	1.1539	0.0910	0.8319	0.1560	1.7693	1.3644
5.60976	0.7374	1.9021	0.1790	1.4152	0.5471	2.7921	3.3645	1.1579	0.0929	0.8476	0.1587	1.7855	1.3923
6.1582	0.6969	1.9291	0.1795	1.4270	0.5511	2.6453	3.4447	1.1542	0.0943	0.8643	0.1600	1.7911	1.4169
6.76025	0.6506	1.9474	0.1784	1.4354	0.5548	2.4855	3.4971	1.1441	0.0951	0.8823	0.1600	1.7883	1.4386

Size (microns)	B2	B1-2	W1-18	W11-2	W2-5	W10-2	W9-2	W3-10	W3-18	J4-2	J2-11	J5-1	J6-2
7.42117	0.6074	1.9583	0.1761	1.4425	0.5593	2.3112	3.5197	1.1300	0.0952	0.9022	0.1588	1.7805	1.4586
8.14669	0.5692	1.9629	0.1729	1.4506	0.5647	2.1142	3.5093	1.1123	0.0946	0.9250	0.1566	1.7694	1.4786
8.94315	0.5316	1.9627	0.1688	1.4619	0.5715	1.9449	3.4628	1.0917	0.0936	0.9533	0.1534	1.7557	1.5010
9.81748	0.4867	1.9592	0.1645	1.4791	0.5795	1.8123	3.3781	1.0691	0.0924	0.9904	0.1497	1.7412	1.5282
10.7773	0.4318	1.9564	0.1608	1.5080	0.5925	1.7326	3.2581	1.0510	0.0916	1.0404	0.1462	1.7338	1.5647
11.8309	0.3731	1.9631	0.1591	1.5586	0.6136	1.6506	3.1142	1.0459	0.0923	1.1078	0.1445	1.7479	1.6182
12.9876	0.3213	1.9926	0.1610	1.6440	0.6478	1.4785	2.9636	1.0641	0.0955	1.1998	0.1461	1.8001	1.7010
14.2573	0.2905	2.0567	0.1680	1.7750	0.6981	1.2893	2.8249	1.1101	0.1022	1.3261	0.1531	1.8993	1.8244
15.6512	0.2833	2.1586	0.1804	1.9546	0.7656	1.1459	2.7045	1.1807	0.1128	1.4966	0.1658	2.0408	1.9935
17.1813	0.2959	2.2887	0.1972	2.1756	0.8517	1.2317	2.5933	1.2660	0.1268	1.7170	0.1835	2.2061	2.2028
18.861	0.3339	2.4264	0.2162	2.4245	0.9547	1.5852	2.4692	1.3500	0.1427	1.9872	0.2035	2.3720	2.4390
20.705	0.3655	2.5520	0.2336	2.6892	1.0754	2.1509	2.3062	1.4217	0.1576	2.3044	0.2200	2.5221	2.6901
22.7292	0.3009	2.6564	0.2445	2.9623	1.2120	2.7243	2.0965	1.4759	0.1688	2.6660	0.2263	2.6508	2.9509
24.9513	0.1172	2.7457	0.2485	3.2402	1.3649	2.9069	1.8520	1.5179	0.1752	3.0740	0.2197	2.7610	3.2257
27.3906	0.0096	2.8339	0.2540	3.5149	1.5357	2.2566	1.6060	1.5616	0.1807	3.5305	0.2097	2.8527	3.5174
30.0685	0.0000	2.9309	0.2702	3.7674	1.7279	1.1700	1.3969	1.6226	0.1910	4.0288	0.2098	2.9178	3.8165
33.0081	0.0000	3.0338	0.2945	3.9684	1.9503	0.2788	1.2445	1.7193	0.2076	4.5465	0.2238	2.9443	4.0975
36.2352	0.0000	3.1258	0.3149	4.0852	2.2155	0.0295	1.1518	1.8689	0.2276	5.0393	0.2450	2.9235	4.3180
39.7777	0.0000	3.1822	0.3262	4.0926	2.5413	0.0000	1.0987	2.0878	0.2473	5.4450	0.2661	2.8629	4.4327
43.6665	0.0143	3.1820	0.3416	3.9815	2.9466	0.0000	1.0443	2.3904	0.2692	5.6941	0.2916	2.7848	4.4062
47.9356	0.1743	3.1172	0.3775	3.7615	3.4449	0.0000	0.9520	2.7795	0.3018	5.7259	0.3275	2.7095	4.2185
52.622	0.4138	2.9891	0.4315	3.4530	4.0345	0.0000	0.7901	3.2386	0.3522	5.5074	0.3667	2.6424	3.8734
57.7666	0.4223	2.8052	0.4927	3.0796	4.6878	0.0000	0.5125	3.7250	0.4299	5.0451	0.4117	2.5580	3.3919
63.4141	0.3976	2.5680	0.5649	2.6598	5.3437	0.0000	0.2327	4.1676	0.5512	4.3872	0.4940	2.3995	2.8004
69.6138	0.6285	2.2640	0.6684	2.1985	5.9121	0.0000	0.0506	4.4854	0.7348	3.6115	0.6507	2.1128	2.1447
76.4196	1.1884	1.8816	0.8360	1.7048	6.2977	0.0000	0.0047	4.6207	1.0082	2.8071	0.9032	1.6753	1.4793
83.8907	1.8678	1.4235	1.1161	1.1998	6.4208	0.0000	0.0000	4.5515	1.4296	2.0507	1.2798	1.1215	0.8630
92.0923	2.5765	0.9221	1.5727	0.7225	6.2384	0.0000	0.0000	4.3076	2.1029	1.3950	1.8622	0.5666	0.3839
101.096	3.5367	0.4570	2.2695	0.3346	5.7438	0.0000	0.0000	3.9329	3.1591	0.8688	2.7880	0.1867	0.1103
110.979	4.9796	0.1497	3.2400	0.1029	4.9508	0.0000	0.0000	3.4313	4.6911	0.4785	4.1714	0.0308	0.0161
121.829	6.8534	0.0248	4.4557	0.0162	3.9206	0.0000	0.0000	2.8080	6.6506	0.2119	5.9814	0.0018	0.0007
133.74	8.6978	0.0015	5.8192	0.0009	2.7703	0.0000	0.0000	2.0645	8.7919	0.0668	7.9716	0.0000	0.0000

Size (microns)	B2	B1-2	W1-18	W11-2	W2-5	W10-2	W9-2	W3-10	W3-18	J4-2	J2-11	J5-1	J6-2
146.815	9.9286	0.0000	7.2024	0.0000	1.6663	0.0000	0.0000	1.2408	10.6899	0.0111	9.7276	0.0000	0.0000
161.168	10.3462	0.0000	8.4921	0.0000	0.7732	0.0000	0.0000	0.5453	11.8617	0.0007	10.8170	0.0000	0.0000
176.925	10.1387	0.0000	9.5502	0.0000	0.2437	0.0000	0.0000	0.1389	11.9601	0.0000	10.9329	0.0000	0.0000
194.222	9.1311	0.0000	10.1105	0.0000	0.0396	0.0000	0.0000	0.0172	10.8371	0.0000	9.9468	0.0000	0.0000
213.21	6.4762	0.0000	9.8328	0.0000	0.0024	0.0000	0.0000	0.0004	8.6647	0.0000	7.9798	0.0000	0.0000
234.054	2.5948	0.0000	8.5847	0.0000	0.0000	0.0000	0.0000	0.0000	5.9089	0.0000	5.4771	0.0000	0.0000
256.936	0.3622	0.0000	6.6103	0.0000	0.0000	0.0000	0.0000	0.0000	3.1829	0.0000	3.0699	0.0000	0.0000
282.056	0.0078	0.0000	4.3890	0.0000	0.0000	0.0000	0.0000	0.0000	1.1969	0.0000	1.3090	0.0000	0.0000
309.631	0.0000	0.0000	2.4419	0.0000	0.0000	0.0000	0.0000	0.0000	0.2396	0.0000	0.4831	0.0000	0.0000
339.902	0.0000	0.0000	1.1282	0.0000	0.0000	0.0000	0.0000	0.0000	0.0125	0.0000	0.3632	0.0000	0.0000
373.132	0.0000	0.0000	0.4850	0.0000	0.0000	0.0000	0.0000	0.0000	0.0000	0.0000	0.6442	0.0000	0.0000
409.611	0.0000	0.0000	0.3061	0.0000	0.0000	0.0000	0.0000	0.0000	0.0000	0.0000	1.0546	0.0000	0.0000
449.657	0.0000	0.0000	0.3242	0.0000	0.0000	0.0000	0.0000	0.0000	0.0000	0.0000	1.2520	0.0000	0.0000
493.617	0.0000	0.0000	0.2685	0.0000	0.0000	0.0000	0.0000	0.0000	0.0000	0.0000	1.1153	0.0000	0.0000
541.876	0.0000	0.0000	0.0893	0.0000	0.0000	0.0000	0.0000	0.0000	0.0000	0.0000	0.7170	0.0000	0.0000
594.852	0.0000	0.0000	0.0059	0.0000	0.0000	0.0000	0.0000	0.0000	0.0000	0.0000	0.3175	0.0000	0.0000
653.008	0.0000	0.0000	0.0000	0.0000	0.0000	0.0000	0.0000	0.0000	0.0000	0.0000	0.0816	0.0000	0.0000
716.849	0.0000	0.0000	0.0000	0.0000	0.0000	0.0000	0.0000	0.0000	0.0000	0.0000	0.0057	0.0000	0.0000
786.932	0.0000	0.0000	0.0000	0.0000	0.0000	0.0000	0.0000	0.0000	0.0000	0.0000	0.0000	0.0000	0.0000
863.866	0.0000	0.0000	0.0000	0.0000	0.0000	0.0000	0.0000	0.0000	0.0000	0.0000	0.0000	0.0000	0.0000
948.322	0.0000	0.0000	0.0000	0.0000	0.0000	0.0000	0.0000	0.0000	0.0000	0.0000	0.0000	0.0000	0.0000
1041.03	0.0000	0.0000	0.0000	0.0000	0.0000	0.0000	0.0000	0.0000	0.0000	0.0000	0.0000	0.0000	0.0000
1142.81	0.0000	0.0000	0.0000	0.0000	0.0000	0.0000	0.0000	0.0000	0.0000	0.0000	0.0000	0.0000	0.0000
1254.54	0.0000	0.0000	0.0000	0.0000	0.0000	0.0000	0.0000	0.0000	0.0000	0.0000	0.0000	0.0000	0.0000
1377.19	0.0000	0.0000	0.0000	0.0000	0.0000	0.0000	0.0000	0.0000	0.0000	0.0000	0.0000	0.0000	0.0000
1511.83	0.0000	0.0000	0.0000	0.0000	0.0000	0.0000	0.0000	0.0000	0.0000	0.0000	0.0000	0.0000	0.0000
1659.63	0.0000	0.0000	0.0000	0.0000	0.0000	0.0000	0.0000	0.0000	0.0000	0.0000	0.0000	0.0000	0.0000
1821.88	0.0000	0.0000	0.0000	0.0000	0.0000	0.0000	0.0000	0.0000	0.0000	0.0000	0.0000	0.0000	0.0000

APPENDIX C. OSL GEOCHEMISTRY DATA

	ME-MS61	ME-MS61	ME-MS61	ME-MS61	ME-MS61	ME-MS61	ME-MS61	ME-MS61	ME-MS61	ME-MS61	ME-MS61
Element	Silver	Aluminium	Arsenic	Barium	Beryllium	Bismuth	Calcium	Cadmium	Cerium	Cobalt	Chromium
Atomic number	47	13	33	56	4	83	20	48	58	27	24
SAMPLE	Ag	Al	As	Ba	Be	Bi	Ca	Cd	Ce	Co	Cr
DESCRIPTION	ppm	%	ppm	ppm	ppm	ppm	%	ppm	ppm	ppm	ppm
USU-3552A	0.09	5.05	5.1	750	1.2	0.1	0.82	0.17	54.5	7.5	43
USU-3552B	0.06	3.82	3.8	610	0.89	0.08	1.17	0.06	52.6	5.2	46
USU-3553A	0.09	5.07	7.9	710	1.34	0.13	0.77	0.15	55	8.7	48
USU-3553B	0.14	6.7	9.1	810	1.85	0.25	0.78	0.43	71.4	14.9	60
USU-3554A	0.13	6.15	5.4	750	1.61	0.19	0.67	0.23	63.2	10.5	59
USU-3554B	0.12	5.59	6.9	750	1.57	0.18	0.65	0.3	55	11.6	47
USU-3555A	0.1	5.44	6	740	1.43	0.14	0.74	0.18	59.7	12	48
USU-3555B	0.13	6.76	8.1	790	1.94	0.25	0.71	0.35	75.3	16.8	63
USU-3556A	0.09	5.15	8.1	770	1.31	0.12	0.7	0.1	48	8.9	38
USU-3556B	0.12	5.54	5.2	780	1.47	0.15	0.73	0.18	60.1	9.2	48
USU-3557A	0.13	5.45	6.4	750	1.4	0.17	0.7	0.14	60	7.5	61
USU-3557B	0.1	5.2	12.7	740	1.36	0.15	0.7	0.16	53.9	7.5	49
USU-3558A	0.13	5.78	6.9	790	1.63	0.19	0.71	0.26	61.8	9.5	53
USU-3558B	0.11	5.32	9.4	780	1.37	0.13	0.74	0.12	52.3	6.9	40

	ME-MS61	ME-MS61	ME-MS61	ME-MS61	ME-MS61	ME-MS61	ME-MS61	ME-MS61	ME-MS61	ME-MS61	ME-MS61
Element	Caesium	Copper	Iron	Gallium	Germanium	Hafnium	Indium	Potassium	Lanthanum	Lithium	Magnesium
Atomic number	55	29	26	31	32	72	49	19	57	3	12
SAMPLE	Cs	Cu	Fe	Ga	Ge	Hf	In	K	La	Li	Mg
DESCRIPTION	ppm	ppm	%	ppm	ppm	ppm	ppm	%	ppm	ppm	%
USU-3552A	2.37	8.2	2.46	11.35	0.2	2.9	0.024	1.96	29.5	17	0.37
USU-3552B	1.3	7.8	2.31	8.67	0.18	2.9	0.019	1.51	28.5	10.8	0.46
USU-3553A	2.76	19.1	2.88	11.4	0.2	2.9	0.03	1.83	29.1	19.9	0.43
USU-3553B	5.23	29.2	3.26	15.6	0.22	3.7	0.051	1.99	37	33.9	0.71
USU-3554A	4.42	38.3	3.56	14.35	0.19	3.4	0.041	2	32.8	29.9	0.61
USU-3554B	3.74	28.4	2.87	13.1	0.18	3	0.037	1.92	29.5	25.5	0.51
USU-3555A	3.12	17.4	2.24	12.6	0.2	3.2	0.03	1.96	31.7	22.1	0.46
USU-3555B	5.23	20.7	3.29	16.05	0.23	4	0.052	2.07	39	34.3	0.7
USU-3556A	2.69	13.1	2.53	11.5	0.18	2.2	0.027	1.98	25.9	19.1	0.38
USU-3556B	3.32	20.3	2.43	12.5	0.19	3.3	0.029	1.97	32	21.9	0.46
USU-3557A	3.48	46.2	3.86	12.9	0.22	3.7	0.034	1.94	32.1	22.4	0.46
USU-3557B	3.01	31.6	3.39	12	0.21	2.7	0.032	1.83	28.8	20.1	0.43
USU-3558A	3.95	20.8	2.7	13.55	0.24	3.2	0.036	1.95	33	25.8	0.54
USU-3558B	2.9	17.6	2.38	11.95	0.19	2.6	0.03	1.96	28.2	20.3	0.42

	ME-MS61	ME-MS61	ME-MS61	ME-MS61	ME-MS61	ME-MS61	ME-MS61	ME-MS61	ME-MS61	ME-MS61	ME-MS61
Element	Manganese	Molybdenum	Sodium	Niobium	Nickel	Phosphorus	Lead	Rubidium	Rhenium	Sulfur	Antimony
Atomic number	25	42	11	60	28	15	82	37	75	16	51
SAMPLE	Mn	Mo	Na	Nb	Ni	P	Pb	Rb	Re	S	Sb
DESCRIPTION	ppm	ppm	%	ppm	ppm	ppm	ppm	ppm	ppm	%	ppm
USU-3552A	403	0.58	1.19	8.9	18.3	510	13.9	73.6	<0.002	0.01	0.63
USU-3552B	287	1.01	1.07	8.1	12.6	420	10.2	51.8	<0.002	0.02	0.45
USU-3553A	380	1.28	1.05	9.3	21.1	590	14.8	71	<0.002	0.01	0.83
USU-3553B	1080	1.24	0.84	12.9	33.5	690	18.6	98.4	<0.002	0.02	0.96
USU-3554A	387	1.29	0.92	11.6	27.7	710	17.7	91	<0.002	0.01	0.92
USU-3554B	268	1.07	0.96	10	25.5	560	17.2	83.8	0.002	0.04	0.82
USU-3555A	204	0.96	1.11	10.2	29.3	450	15.2	78.9	<0.002	0.09	0.74
USU-3555B	271	0.88	0.9	14.3	36.6	660	18.6	99.4	<0.002	0.02	0.95
USU-3556A	330	1.15	1.14	8.2	22	510	14.3	75.9	<0.002	0.01	0.73
USU-3556B	318	0.78	1.09	10.4	21.5	560	16.1	81.4	<0.002	0.01	0.72
USU-3557A	382	2	1.03	10.6	22.9	570	17	81.9	<0.002	0.01	0.81
USU-3557B	412	1.31	1.03	9.1	22.3	550	16.9	75.3	<0.002	0.01	0.73
USU-3558A	359	1.15	1	10.9	25.1	610	16.8	86.3	<0.002	0.01	0.82
USU-3558B	304	0.96	1.13	8.8	20.8	560	15.8	76.9	<0.002	0.01	0.74

	ME-MS61	ME-MS61	ME-MS61	ME-MS61	ME-MS61	ME-MS61	ME-MS61	ME-MS61	ME-MS61	ME-MS61	ME-MS61
Element	Scandium	Selenium	Tin	Strontium	Tantalum	Tellurium	Thorium	Titanium	Thallium	Uranium	Vanadium
Atomic number	21	34	50	38	73	52	90	22	81	92	23
SAMPLE	Sc	Se	Sn	Sr	Ta	Te	Th	Ti	Tl	U	V
DESCRIPTION	ppm	ppm	ppm	ppm	ppm	ppm	ppm	%	ppm	ppm	ppm
USU-3552A	5.1	<1	1.3	225	0.61	<0.05	7.75	0.223	0.45	2	49
USU-3552B	3.7	<1	1	204	0.57	<0.05	6.63	0.223	0.32	1.6	34
USU-3553A	5.9	<1	1.9	194.5	0.6	<0.05	8	0.242	0.46	2.3	58
USU-3553B	9.7	1	2.2	165	0.9	0.05	11.2	0.346	0.63	3.3	91
USU-3554A	8.4	<1	4.2	166.5	0.8	<0.05	9.86	0.315	0.61	2.6	79
USU-3554B	7.1	<1	1.6	172	0.7	<0.05	8.63	0.259	0.55	2.2	68
USU-3555A	6.5	<1	2.8	196	0.67	<0.05	8.68	0.266	0.5	2.1	60
USU-3555B	9.6	<1	3.7	163.5	0.96	<0.05	11.45	0.374	0.65	2.8	94
USU-3556A	5.4	<1	2.7	208	0.55	<0.05	7.01	0.206	0.48	1.8	52
USU-3556B	6.7	<1	2.2	201	0.71	<0.05	9.11	0.275	0.52	2.3	62
USU-3557A	6.9	<1	2.7	192.5	0.75	<0.05	9.21	0.281	0.55	2.3	62
USU-3557B	6.1	<1	1.7	195	0.6	<0.05	7.73	0.233	0.48	2	58
USU-3558A	7.5	<1	2	185	0.73	<0.05	9.66	0.289	0.58	2.6	71
USU-3558B	5.8	<1	1.6	209	0.6	<0.05	7.57	0.221	0.47	2	56

	ME-MS61	ME-MS61	ME-MS61	ME-MS61		WEI-21	WEI-21	WEI-21	
Element	Tungsten	Yttrium	Zinc	Zirconium					
Atomic number	74	39	30	40					
SAMPLE	W	Y	Zn	Zr		Recvd Wt.	Recvd Wt.	Recvd Wt.	Y:Th
DESCRIPTION	ppm	ppm	ppm	ppm		kg	kg	kg	
USU-3552A	4	17.5	42	116		0.04			
USU-3552B	0.7	14.4	28	102.5		0.06			
USU-3553A	2	18.2	53	106.5		0.04			
USU-3553B	1.6	23.6	91	128.5		0.06			
USU-3554A	2	21.5	84	118		0.04			
USU-3554B	1.2	19.2	68	106.5		0.06			
USU-3555A	1.7	19.5	57	111.5		0.06			
USU-3555B	1.6	25.9	93	150.5		0.04			
USU-3556A	1.8	16.7	48	81.3		0.06			
USU-3556B	1.2	19.8	62	113		0.06			
USU-3557A	4.2	20.6	82	121.5		0.02			
USU-3557B	1.1	19.1	68	99		0.04			
USU-3558A	1.7	21	69	114		0.06			
USU-3558B	1	17.8	58	88.6		0.06			

APPENDIX D. ANALYTICAL DATA FOR ZIRCON U-PB DATING

				RATIO						AGES									
Grain	U [ppm]	Th [ppm]	Th/U	207/ 235	± s.e.	206/ 238	± s.e.	207/ 206	± s.e.	207/ 235	± 2s	206/ 238	± 2s	207/ 206	± 2s	%disc (5/8)	%disc (7/6)	Best Age [Ma]	± 2s
Sample 18020401																			
G120	1008	671	1	0	0	0	0	0	0	26	2	25	1	182	215	7	86	25	1
G99	961	1017	1	0	0	0	0	0	0	27	3	26	1	159	263	5	84	26	1
G30	735	184	0	0	0	0	0	0	0	31	4	31	1	0	314	-2	-31000	31	1
G32	1270	703	1	0	0	0	0	0	0	50	4	52	2	0	139	-3	-51700	52	2
G70	231	91	0	0	0	0	0	0	0	65	14	61	3	217	490	6	72	61	3
G44	1554	744	0	0	0	0	0	0	0	64	4	62	2	129	140	3	52	62	2
G26	1378	318	0	0	0	0	0	0	0	64	4	63	2	118	152	2	47	63	2
G48	547	299	1	0	0	0	0	0	0	58	7	64	2	0	0	-9	-63900	64	2
G114	784	150	0	0	0	0	0	0	0	68	5	66	2	147	163	3	55	66	2
G97	663	474	1	0	0	0	0	0	0	67	6	68	2	36	209	-1	-89	68	2
G2	468	259	1	0	0	0	0	0	0	74	11	73	3	127	335	2	43	73	3
G133	432	255	1	0	0	0	0	0	0	85	7	86	3	68	194	-1	-27	86	3
G118	784	240	0	0	0	0	0	0	0	90	5	89	3	133	140	2	33	89	3
G95	238	101	0	0	0	0	0	0	0	89	11	92	3	29	307	-3	-215	92	3
G74	627	244	0	0	0	0	0	0	0	94	8	92	3	155	196	2	41	92	3
G124	654	330	1	0	0	0	0	0	0	92	6	92	3	89	155	0	-3	92	3
G21	464	204	0	0	0	0	0	0	0	99	8	98	3	118	196	1	16	98	3
G149	819	165	0	0	0	0	0	0	0	103	6	102	3	136	136	1	25	102	3
G91	253	119	0	0	0	0	0	0	0	110	12	107	4	186	258	3	42	107	4
G126	605	387	1	0	0	0	0	0	0	162	8	160	4	198	119	1	19	160	4
G89	156	57	0	0	0	0	0	0	0	177	18	180	6	152	255	-1	-18	180	6
G147	503	499	1	0	0	0	0	0	0	184	9	182	5	215	121	1	16	182	5
G128	440	213	0	0	0	0	0	0	0	193	10	189	5	247	126	2	24	189	5
G63	449	168	0	0	0	0	0	0	0	198	12	191	6	290	147	4	34	191	6
G151	506	201	0	0	0	0	0	0	0	191	10	191	5	196	126	0	2	191	5
G9	375	163	0	0	0	0	0	0	0	190	12	192	6	173	155	-1	-11	192	6
G19	399	278	1	0	0	0	0	0	0	196	11	196	6	209	142	0	6	196	6
G40	480	202	0	0	0	0	0	0	0	194	11	199	6	138	146	-3	-44	199	6
G38	422	210	0	0	0	0	0	0	0	216	13	218	6	203	146	-1	-7	218	6
G125	350	306	1	0	0	0	0	0	0	337	14	334	9	367	107	1	9	334	9
G94	482	312	1	0	0	0	0	0	0	391	15	372	10	505	99	5	26	372	10
G127	262	186	1	0	0	0	0	0	0	409	17	409	11	412	106	0	1	409	11

Grain	U [ppm]	Th [ppm]	Th/U	RATIO 207/ 235	± s.e.	206/ 238	± s.e.	207/ 206	± s.e.	AGES 207/ 235	± 2s	206/ 238	± 2s	207/ 206	± 2s	%disc (5/8)	%disc (7/6)	Best Age [Ma]	± 2s
G79	431	587	1	1	0	0	0	0	0	423	18	411	11	493	113	3	17	411	11
G55	1159	577	0	1	0	0	0	0	0	446	13	427	11	551	72	4	23	427	11
G28	427	302	1	1	0	0	0	0	0	537	18	543	14	517	90	-1	-5	543	14
G49	117	121	1	1	0	0	0	0	0	852	30	817	22	952	103	4	14	817	22
G113	41	20	0	2	0	0	0	0	0	945	45	929	28	986	144	2	6	929	28
G143	866	91	0	2	0	0	0	0	0	975	21	949	23	1039	58	3	9	949	23
G52	105	30	0	2	0	0	0	0	0	976	32	974	26	985	99	0	1	974	26
G45	46	44	1	2	0	0	0	0	0	1021	47	1001	30	1067	142	2	6	1001	30
G116	138	54	0	2	0	0	0	0	0	1005	27	1002	25	1017	80	0	1	1002	25
G106	486	370	1	2	0	0	0	0	0	1068	23	1029	25	1154	62	4	11	1029	25
G61	404	177	0	2	0	0	0	0	0	1033	24	1032	25	1040	66	0	1	1032	25
G86	231	128	1	2	0	0	0	0	0	1059	27	1051	26	1080	75	1	3	1051	26
G109	619	45	0	2	0	0	0	0	0	1057	22	1053	26	1071	60	0	2	1053	26
G83	204	54	0	2	0	0	0	0	0	1067	28	1061	27	1083	78	1	2	1061	27
G132	254	113	0	2	0	0	0	0	0	1070	24	1064	26	1088	67	1	2	1064	26
G73	154	132	1	2	0	0	0	0	0	1081	31	1065	27	1118	86	2	5	1065	27
G88	722	658	1	2	0	0	0	0	0	1094	23	1066	26	1154	59	3	8	1066	26
G121	59	36	1	2	0	0	0	0	0	1083	35	1070	28	1114	100	1	4	1070	28
G130	88	62	1	2	0	0	0	0	0	1079	33	1072	28	1097	95	1	2	1072	28
G7	126	50	0	2	0	0	0	0	0	1088	29	1075	27	1120	82	1	4	1075	27
G141	428	107	0	2	0	0	0	0	0	1104	23	1075	26	1164	61	3	8	1075	26
G75	651	125	0	2	0	0	0	0	0	1100	23	1094	27	1115	59	0	2	1094	27
G80	151	103	1	2	0	0	0	0	0	1118	31	1114	28	1132	85	0	2	1132	85
G11	232	101	0	2	0	0	0	0	0	1145	25	1148	28	1143	67	0	0	1143	67
G62	266	134	1	2	0	0	0	0	0	1142	26	1131	28	1168	69	1	3	1168	69
G42	371	117	0	2	0	0	0	0	0	1170	24	1167	28	1181	62	0	1	1181	62
G142	99	91	1	2	0	0	0	0	0	1137	31	1110	28	1194	84	2	7	1194	84
G43	51	18	0	2	0	0	0	0	0	1176	43	1165	33	1200	119	1	3	1200	119
G35	94	35	0	2	0	0	0	0	0	1210	44	1217	34	1202	118	-1	-1	1202	118
G66	110	56	1	2	0	0	0	0	0	1226	34	1241	32	1204	89	-1	-3	1204	89
G4	37	19	1	2	0	0	0	0	0	1168	45	1148	33	1210	123	2	5	1210	123
G29	266	117	0	2	0	0	0	0	0	1197	26	1192	29	1211	65	0	2	1211	65
G136	127	55	0	2	0	0	0	0	0	1207	29	1188	30	1246	74	2	5	1246	74

				RATIO						AGES										
Grain	U [ppm]	Th [ppm]	Th/U	207/ 235	± s.e.	206/ 238	± s.e.	207/ 206	± s.e.	207/ 235	± 2s	206/ 238	± 2s	207/ 206	± 2s	%disc (5/8)	%disc (7/6)	Best Age [Ma]	± 2s
G57	392	157	0	2	0	0	0	0	0	1225	26	1207	29	1261	63	2	4	1261	63
G41	91	49	1	2	0	0	0	0	0	1262	35	1257	33	1275	91	0	1	1275	91
G123	55	52	1	3	0	0	0	0	0	1301	36	1287	33	1329	90	1	3	1329	90
G122	300	224	1	3	0	0	0	0	0	1329	27	1321	32	1346	65	1	2	1346	65
G117	643	206	0	3	0	0	0	0	0	1371	27	1375	33	1368	61	0	0	1368	61
G107	595	259	0	3	0	0	0	0	0	1333	24	1302	31	1387	55	2	6	1387	55
G105	2470	269	0	3	0	0	0	0	0	1339	23	1299	31	1408	50	3	8	1408	50
G27	75	44	1	3	0	0	0	0	0	1379	37	1358	35	1415	88	2	4	1415	88
G129	67	22	0	3	0	0	0	0	0	1404	34	1397	35	1419	80	1	2	1419	80
G34	201	108	1	3	0	0	0	0	0	1418	29	1416	34	1427	66	0	1	1427	66
G46	217	129	1	3	0	0	0	0	0	1436	29	1440	35	1434	64	0	0	1434	64
G76	392	225	1	3	0	0	0	0	0	1432	26	1433	34	1436	57	0	0	1436	57
G6	179	108	1	3	0	0	0	0	0	1459	28	1472	35	1444	61	-1	-2	1444	61
G60	469	479	1	3	0	0	0	0	0	1446	26	1443	34	1454	55	0	1	1454	55
G98	184	114	1	3	0	0	0	0	0	1456	28	1456	35	1460	63	0	0	1460	63
G16	452	176	0	3	0	0	0	0	0	1446	25	1436	34	1465	53	1	2	1465	53
G20	350	83	0	3	0	0	0	0	0	1482	26	1492	35	1473	54	-1	-1	1473	54
G13	234	134	1	3	0	0	0	0	0	1497	27	1510	36	1483	59	-1	-2	1483	59
G39	258	185	1	3	0	0	0	0	0	1484	27	1474	35	1503	59	1	2	1503	59
G1	175	97	1	3	0	0	0	0	0	1517	28	1513	36	1527	59	0	1	1527	59
G146	127	74	1	3	0	0	0	0	0	1525	30	1516	36	1540	64	1	2	1540	64
G150	254	140	1	4	0	0	0	0	0	1575	28	1591	37	1559	58	-1	-2	1559	58
G110	966	348	0	4	0	0	0	0	0	1584	26	1568	37	1610	52	1	3	1610	52
G139	159	123	1	4	0	0	0	0	0	1621	29	1605	38	1646	59	1	3	1646	59
G148	217	94	0	4	0	0	0	0	0	1666	28	1665	39	1671	57	0	0	1671	57
G31	255	213	1	4	0	0	0	0	0	1650	28	1632	38	1678	55	1	3	1678	55
G33	238	113	0	4	0	0	0	0	0	1678	28	1678	40	1682	56	0	0	1682	56
G104	136	112	1	4	0	0	0	0	0	1695	31	1707	41	1684	63	-1	-1	1684	63
G53	235	171	1	4	0	0	0	0	0	1651	28	1624	38	1690	56	2	4	1690	56
G72	618	151	0	4	0	0	0	0	0	1721	27	1750	40	1691	52	-2	-3	1691	52
G101	372	114	0	4	0	0	0	0	0	1679	27	1670	39	1693	53	1	1	1693	53
G131	90	104	1	4	0	0	0	0	0	1648	32	1609	39	1701	66	2	5	1701	66
G71	296	122	0	4	0	0	0	0	0	1702	28	1702	40	1706	55	0	0	1706	55

				RATIO						AGES									
																		Best	
	U	Th		207/		206/		207/		207/		206/		207/		%disc	%disc	Age	
Grain	**[ppm]**	**[ppm]**	**Th/U**	**235**	**± s.e.**	**238**	**± s.e.**	**206**	**± s.e.**	**235**	**± 2s**	**238**	**± 2s**	**206**	**± 2s**	**(5/8)**	**(7/6)**	**[Ma]**	**± 2s**
G119	357	133	0	4	0	0	0	0	0	1682	27	1662	39	1710	52	1	3	1710	52
G81	610	214	0	4	0	0	0	0	0	1712	26	1712	39	1717	50	0	0	1717	50
G85	62	60	1	4	0	0	0	0	0	1686	43	1663	44	1719	94	1	3	1719	94
G65	111	31	0	5	0	0	0	0	0	1747	33	1767	43	1727	67	-1	-2	1727	67
G78	241	237	1	4	0	0	0	0	0	1712	29	1702	40	1728	57	1	2	1728	57
G67	187	199	1	5	0	0	0	0	0	1732	30	1735	41	1733	60	0	0	1733	60
G15	196	98	1	4	0	0	0	0	0	1724	28	1716	40	1738	55	0	1	1738	55
G14	190	119	1	5	0	0	0	0	0	1760	29	1779	42	1741	55	-1	-2	1741	55
G56	153	89	1	4	0	0	0	0	0	1714	30	1690	40	1747	60	1	3	1747	60
G10	421	209	0	5	0	0	0	0	0	1758	26	1765	41	1753	49	0	-1	1753	49
G68	336	201	1	4	0	0	0	0	0	1690	28	1640	39	1756	54	3	7	1756	54
G154	354	145	0	5	0	0	0	0	0	1779	29	1772	41	1791	56	0	1	1791	56
G145	303	70	0	5	0	0	0	0	0	1799	28	1795	41	1808	52	0	1	1808	52
G111	113	73	1	5	0	0	0	0	0	1761	32	1722	41	1812	64	2	5	1812	64
G58	22	32	1	5	0	0	0	0	0	1822	55	1818	53	1831	116	0	1	1831	116
G93	141	180	1	5	0	0	0	0	0	1828	31	1818	43	1844	59	1	1	1844	59
G90	150	180	1	5	0	0	0	0	0	1831	30	1818	43	1850	59	1	2	1850	59
G36	65	30	0	5	0	0	0	0	0	1856	37	1860	46	1856	74	0	0	1856	74
G137	250	120	0	5	0	0	0	0	0	1855	28	1857	43	1857	52	0	0	1857	52
G92	276	114	0	5	0	0	0	0	0	1864	28	1871	43	1861	52	0	-1	1861	52
G23	305	194	1	6	0	0	0	0	0	1969	28	1970	45	1972	49	0	0	1972	49
G24	40	32	1	6	0	0	0	0	0	2038	40	2044	51	2036	76	0	0	2036	76
G102	218	207	1	6	0	0	0	0	0	1959	32	1865	44	2064	58	5	10	2064	58
G82	109	35	0	9	0	0	0	0	0	2370	32	2331	53	2408	53	2	3	2408	53
G87	147	73	0	11	0	0	0	0	0	2565	30	2550	56	2580	48	1	1	2580	48
G64	28	35	1	12	0	0	0	0	0	2593	42	2599	65	2593	72	0	0	2593	72
G37	405	210	1	13	0	1	0	0	0	2648	29	2644	57	2655	43	0	0	2655	43
G134	234	116	0	12	0	0	0	0	0	2629	30	2594	56	2660	45	1	2	2660	45
G108	273	140	1	13	0	1	0	0	0	2700	30	2719	58	2690	45	-1	-1	2690	45
G84	42	48	1	13	0	1	0	0	0	2685	36	2676	63	2697	59	0	1	2697	59
G50	145	150	1	13	0	1	0	0	0	2680	30	2656	58	2702	45	1	2	2702	45
G77	96	100	1	13	0	1	0	0	0	2680	32	2648	59	2708	51	1	2	2708	51
G59	477	93	0	13	0	1	0	0	0	2707	29	2704	58	2713	42	0	0	2713	42

Grain	U [ppm]	Th [ppm]	Th/U	RATIO 207/235	± s.e.	RATIO 206/238	± s.e.	RATIO 207/206	± s.e.	AGES 207/235	± 2s	AGES 206/238	± 2s	AGES 207/206	± 2s	%disc (5/8)	%disc (7/6)	Best Age [Ma]	± 2s
G135	124	82	1	13	0	1	0	0	0	2698	31	2682	58	2713	47	1	1	2713	47
G152	147	61	0	14	0	1	0	0	0	2734	32	2738	60	2734	49	0	0	2734	49
G96	122	115	1	14	0	1	0	0	0	2738	31	2719	60	2755	48	1	1	2755	48
G8	309	35	0	15	0	1	0	0	0	2804	29	2838	61	2784	42	-1	-2	2784	42
G153	85	29	0	15	0	1	0	0	0	2797	34	2808	63	2792	53	0	-1	2792	53
Sample 17113001																			
GG1	234	256	1	0	0	0	0	0	0	186	12	188	5	168	158	-1	-12	188	5
GG2	144	67	0	4	0	0	0	0	0	1693	29	1708	40	1677	58	-1	-2	1677	58
GG4	195	127	1	0	0	0	0	0	0	73	9	71	3	143	277	3	51	71	3
GG5	150	257	2	1	0	0	0	0	0	716	31	669	19	873	122	7	23	669	19
GG6	1027	353	0	14	0	1	0	0	0	2727	30	2678	57	2767	44	2	3	2767	44
GG7	1335	401	0	0	0	0	0	0	0	54	3	53	2	81	138	1	35	53	2
GG8	49	24	0	3	0	0	0	0	0	1380	36	1373	35	1393	86	0	1	1393	86
GG9	705	641	1	3	0	0	0	0	0	1366	24	1342	32	1407	54	2	5	1407	54
GG10	197	97	0	0	0	0	0	0	0	160	12	156	5	227	188	3	32	156	5
GG11	145	93	1	5	0	0	0	0	0	1828	30	1810	42	1853	57	1	2	1853	57
GG13	616	404	1	0	0	0	0	0	0	192	9	182	5	317	108	5	42	182	5
GG14	430	70	0	0	0	0	0	0	0	79	6	83	2	0	156	-4	-82500	83	2
GG15	65	41	1	3	0	0	0	0	0	1326	34	1302	33	1370	83	2	5	1370	83
GG16	163	264	2	0	0	0	0	0	0	172	14	164	5	301	196	5	46	164	5
GG17	76	58	1	2	0	0	0	0	0	1074	32	1077	28	1072	92	0	0	1077	28
GG18	188	251	1	5	0	0	0	0	0	1862	29	1882	43	1843	55	-1	-2	1843	55
GG19	419	173	0	4	0	0	0	0	0	1717	27	1707	39	1734	53	1	2	1734	53
GG20	428	147	0	5	0	0	0	0	0	1748	27	1722	40	1783	52	2	3	1783	52
GG21	266	84	0	3	0	0	0	0	0	1443	27	1453	34	1433	59	-1	-1	1433	59
GG22	2137	2590	1	0	0	0	0	0	0	157	6	155	4	195	82	1	20	155	4
GG23	289	80	0	4	0	0	0	0	0	1710	28	1697	39	1731	55	1	2	1731	55
GG24	86	53	1	2	0	0	0	0	0	1175	31	1156	29	1215	82	2	5	1215	82
GG25	159	65	0	2	0	0	0	0	0	1174	27	1172	29	1182	70	0	1	1182	70
GG26	77	28	0	2	0	0	0	0	0	1122	31	1130	29	1112	87	-1	-2	1112	87
GG27	120	106	1	4	0	0	0	0	0	1663	30	1642	39	1692	62	1	3	1692	62
GG28	675	100	0	17	0	1	0	0	0	2932	31	2912	61	2950	45	1	1	2950	45

				RATIO						AGES									
	U	Th		207/		206/		207/		207/		206/		207/		%disc	%disc	Best Age	
Grain	[ppm]	[ppm]	Th/U	235	± s.e.	238	± s.e.	206	± s.e.	235	± 2s	238	± 2s	206	± 2s	(5/8)	(7/6)	[Ma]	± 2s
GG29	216	147	1	3	0	0	0	0	0	1384	27	1376	33	1400	62	1	2	1400	62
GG30	363	119	0	3	0	0	0	0	0	1382	26	1376	33	1396	58	0	1	1396	58
GG31	44	36	1	2	0	0	0	0	0	1081	38	1057	29	1134	110	2	7	1057	29
GG32	639	90	0	4	0	0	0	0	0	1632	27	1593	37	1686	53	2	6	1686	53
GG33	210	128	1	1	0	0	0	0	0	653	21	650	17	666	89	0	2	650	17
GG34	618	337	1	12	0	0	0	0	0	2627	30	2577	55	2670	46	2	3	2670	46
GG35	188	138	1	14	0	1	0	0	0	2734	31	2726	59	2744	48	0	1	2744	48
GG36	112	59	1	3	0	0	0	0	0	1440	30	1436	35	1449	70	0	1	1449	70
GG37	190	145	1	2	0	0	0	0	0	1008	25	1008	25	1013	74	0	1	1008	25
GG38	150	70	0	2	0	0	0	0	0	1029	27	1032	26	1028	79	0	0	1032	26
GG40	181	275	2	14	0	1	0	0	0	2716	31	2727	59	2712	48	0	-1	2712	48
GG41	541	88	0	4	0	0	0	0	0	1691	28	1649	38	1748	56	3	6	1748	56
GG44	141	166	1	14	0	1	0	0	0	2715	32	2728	59	2710	49	0	-1	2710	49
GG45	58	28	0	2	0	0	0	0	0	1067	35	1066	28	1072	103	0	1	1066	28
GG46	338	308	1	0	0	0	0	0	0	59	6	60	2	20	248	-2	-200	60	2
GG47	335	98	0	2	0	0	0	0	0	1079	24	1071	26	1099	66	1	3	1071	26
GG48	357	165	0	3	0	0	0	0	0	1447	27	1446	34	1454	58	0	1	1454	58
GG49	263	207	1	5	0	0	0	0	0	1740	29	1714	40	1775	56	1	3	1775	56
GG50	150	150	1	3	0	0	0	0	0	1513	32	1469	36	1580	71	3	7	1580	71
GG51	91	31	0	13	0	0	0	0	0	2668	33	2602	57	2722	51	3	4	2722	51
GG54	470	260	1	5	0	0	0	0	0	1761	28	1741	40	1790	54	1	3	1790	54
GG55	100	71	1	2	0	0	0	0	0	1081	30	1083	28	1083	86	0	0	1083	28
GG56	289	155	1	2	0	0	0	0	0	1013	24	1014	25	1015	70	0	0	1014	25
GG58	255	168	1	1	0	0	0	0	0	510	21	472	13	687	106	8	31	472	13
GG59	241	181	1	3	0	0	0	0	0	1492	28	1503	35	1482	61	-1	-1	1482	61
GG60	261	241	1	0	0	0	0	0	0	51	6	50	2	112	288	2	55	50	2
GG61	238	121	1	4	0	0	0	0	0	1694	29	1697	39	1694	58	0	0	1694	58
GG62	431	248	1	0	0	0	0	0	0	98	7	95	3	157	168	2	39	95	3
GG63	330	403	1	11	0	0	0	0	0	2559	31	2548	55	2571	49	0	1	2571	49
GG64	157	170	1	14	0	1	0	0	0	2730	32	2746	59	2721	50	-1	-1	2721	50
GG66	3873	2538	1	0	0	0	0	0	0	33	2	32	1	56	123	1	42	32	1
GG67	133	76	1	3	0	0	0	0	0	1315	30	1316	32	1317	73	0	0	1317	73
GG68	68	70	1	2	0	0	0	0	0	1067	34	1051	28	1104	99	2	5	1051	28

Grain	U [ppm]	Th [ppm]	Th/U	RATIO 207/235	± s.e.	206/238	± s.e.	207/206	± s.e.	AGES 207/235	± 2s	206/238	± 2s	207/206	± 2s	%disc (5/8)	%disc (7/6)	Best Age [Ma]	± 2s
GG69	569	151	0	2	0	0	0	0	0	1055	23	1059	26	1051	63	0	-1	1059	26
GG70	677	484	1	3	0	0	0	0	0	1283	25	1249	30	1344	59	3	7	1344	59
GG71	314	202	1	5	0	0	0	0	0	1773	29	1786	41	1762	56	-1	-1	1762	56
GG72	118	63	1	3	0	0	0	0	0	1327	31	1338	33	1314	75	-1	-2	1314	75
GG73	177	95	1	2	0	0	0	0	0	1054	27	1063	26	1040	77	-1	-2	1063	26
GG74	261	99	0	2	0	0	0	0	0	1152	26	1152	28	1155	69	0	0	1155	69
GG75	121	88	1	2	0	0	0	0	0	1165	30	1159	29	1179	79	0	2	1179	79
GG76	503	304	1	11	0	0	0	0	0	2513	31	2423	53	2590	49	4	6	2590	49
GG77	675	307	0	4	0	0	0	0	0	1687	28	1677	39	1702	56	1	1	1702	56
GG78	156	116	1	2	0	0	0	0	0	1094	28	1099	27	1088	79	0	-1	1099	27
GG80	414	408	1	5	0	0	0	0	0	1896	29	1896	43	1900	55	0	0	1900	55
GG81	133	64	0	2	0	0	0	0	0	963	28	928	24	1050	86	4	12	928	24
GG82	58	36	1	2	0	0	0	0	0	1062	36	1065	28	1060	106	0	0	1065	28
GG83	837	881	1	0	0	0	0	0	0	76	5	71	2	241	146	7	70	71	2
GG84	82	37	0	0	0	0	0	0	0	222	22	216	7	291	240	3	26	216	7
GG85	250	6	0	3	0	0	0	0	0	1437	28	1417	34	1471	64	1	4	1471	64
GG86	366	203	1	3	0	0	0	0	0	1458	28	1465	35	1451	61	0	-1	1451	61
GG87	362	302	1	13	0	1	0	0	0	2670	32	2719	58	2638	50	-2	-3	2638	50
GG88	249	79	0	2	0	0	0	0	0	1184	28	1180	29	1195	75	0	1	1195	75
GG89	185	258	1	13	0	1	0	0	0	2706	33	2735	59	2688	51	-1	-2	2688	51
GG90	1250	560	0	0	0	0	0	0	0	43	3	43	1	33	164	-1	-30	43	1
GG91	667	294	0	0	0	0	0	0	0	26	3	25	1	153	266	5	84	25	1
GG92	28	10	0	2	0	0	0	0	0	1040	51	1026	31	1073	154	1	4	1026	31
GG93	193	179	1	7	0	0	0	0	0	2114	32	2086	47	2146	56	1	3	2146	56
GG94	526	357	1	0	0	0	0	0	0	101	7	99	3	159	158	2	38	99	3
GG95	129	85	1	2	0	0	0	0	0	1081	29	1091	27	1065	83	-1	-2	1091	27
GG96	214	125	1	2	0	0	0	0	0	1154	27	1145	28	1177	73	1	3	1177	73
GG97	195	67	0	2	0	0	0	0	0	1129	27	1144	28	1106	74	-1	-3	1106	74
GG98	579	244	0	3	0	0	0	0	0	1393	27	1376	33	1424	61	1	3	1424	61
GG99	126	112	1	2	0	0	0	0	0	1259	33	1249	31	1281	84	1	2	1281	84
GG100	132	55	0	0	0	0	0	0	0	222	18	224	7	201	203	-1	-12	224	7
GG105	977	183	0	2	0	0	0	0	0	1016	23	961	23	1141	63	6	16	961	23
GG106	140	103	1	10	0	0	0	0	0	2477	33	2448	54	2504	55	1	2	2504	55

				RATIO						AGES									
Grain	U [ppm]	Th [ppm]	Th/U	207/ 235	± s.e.	206/ 238	± s.e.	207/ 206	± s.e.	207/ 235	± 2s	206/ 238	± 2s	207/ 206	± 2s	%disc (5/8)	%disc (7/6)	Best Age [Ma]	± 2s
GG107	126	123	1	2	0	0	0	0	0	1099	30	1113	28	1076	83	-1	-3	1076	83
GG108	190	163	1	0	0	0	0	0	0	168	13	164	5	234	194	3	30	164	5
GG109	172	86	1	2	0	0	0	0	0	1135	28	1131	28	1145	77	0	1	1145	77
GG110	110	44	0	2	0	0	0	0	0	1134	31	1135	29	1139	85	0	0	1139	85
GG111	180	92	1	2	0	0	0	0	0	1256	29	1252	31	1269	72	0	1	1269	72
GG112	195	160	1	4	0	0	0	0	0	1674	31	1672	39	1681	63	0	1	1681	63
GG113	144	98	1	2	0	0	0	0	0	1084	29	1082	27	1092	81	0	1	1082	27
GG115	365	88	0	4	0	0	0	0	0	1542	29	1542	36	1546	62	0	0	1546	62
GG116	355	177	0	6	0	0	0	0	0	2002	31	1997	45	2011	57	0	1	2011	57
GG117	121	51	0	3	0	0	0	0	0	1320	31	1311	32	1340	76	1	2	1340	76
GG118	251	98	0	2	0	0	0	0	0	1039	26	1045	26	1029	75	-1	-2	1045	26
GG119	485	227	0	4	0	0	0	0	0	1684	29	1684	39	1689	59	0	0	1689	59
GG120	232	154	1	4	0	0	0	0	0	1696	30	1689	39	1709	62	0	1	1709	62
GG122	535	295	1	0	0	0	0	0	0	357	13	357	9	362	94	0	1	357	9
GG123	246	77	0	0	0	0	0	0	0	174	12	166	5	278	171	4	40	166	5
GG124	114	68	1	5	0	0	0	0	0	1856	34	1848	43	1868	66	0	1	1868	66
GG125	108	90	1	3	0	0	0	0	0	1446	33	1433	35	1468	75	1	2	1468	75
GG126	203	117	1	5	0	0	0	0	0	1734	31	1715	40	1760	62	1	3	1760	62
GG127	375	251	1	4	0	0	0	0	0	1727	30	1694	39	1771	60	2	4	1771	60
GG128	238	93	0	3	0	0	0	0	0	1442	29	1438	34	1452	67	0	1	1452	67
GG129	144	53	0	0	0	0	0	0	0	117	13	111	4	257	258	6	57	111	4
GG130	387	89	0	2	0	0	0	0	0	1057	25	1054	26	1068	71	0	1	1054	26
GG131	67	49	1	4	0	0	0	0	0	1664	36	1667	41	1663	76	0	0	1663	76
GG132	741	340	0	0	0	0	0	0	0	177	8	176	5	203	113	1	13	176	5
GG133	95	56	1	3	0	0	0	0	0	1439	33	1432	35	1453	78	0	1	1453	78
GG134	189	79	0	2	0	0	0	0	0	1170	29	1160	29	1192	76	1	3	1192	76
GG135	1070	409	0	13	0	1	0	0	0	2697	33	2726	58	2679	53	-1	-2	2679	53
GG137	672	368	1	2	0	0	0	0	0	1014	24	1001	24	1045	68	1	4	1001	24
GG138	359	575	2	0	0	0	0	0	0	219	12	214	6	271	133	2	21	214	6
GG139	159	117	1	13	0	1	0	0	0	2690	34	2687	58	2696	54	0	0	2696	54
GG140	1695	830	0	0	0	0	0	0	0	27	2	25	1	222	167	8	89	25	1
GG142	807	259	0	4	0	0	0	0	0	1705	30	1676	39	1745	59	2	4	1745	59
GG144	62	44	1	2	0	0	0	0	0	1090	37	1081	29	1113	107	1	3	1081	29

				RATIO						AGES									
Grain	U [ppm]	Th [ppm]	Th/U	207/ 235	± s.e.	206/ 238	± s.e.	207/ 206	± s.e.	207/ 235	± 2s	206/ 238	± 2s	207/ 206	± 2s	%disc (5/8)	%disc (7/6)	Best Age [Ma]	± 2s
GG146	53	54	1	4	0	0	0	0	0	1601	37	1588	40	1622	82	1	2	1622	82
GG147	241	166	1	4	0	0	0	0	0	1725	31	1709	40	1748	63	1	2	1748	63
GG148	331	205	1	0	0	0	0	0	0	184	11	184	5	181	147	0	-2	184	5
GG149	451	182	0	2	0	0	0	0	0	1145	26	1153	28	1132	70	-1	-2	1132	70
GG150	475	236	0	0	0	0	0	0	0	74	6	76	2	39	194	-2	-95	76	2
GG151	1485	698	0	0	0	0	0	0	0	92	5	85	2	291	112	9	71	85	2
GG153	132	100	1	4	0	0	0	0	0	1682	33	1688	40	1678	69	0	-1	1678	69
GG154	73	72	1	2	0	0	0	0	0	1007	50	1008	31	1011	157	0	0	1008	31
GG156	26	15	1	3	0	0	0	0	0	1399	47	1412	39	1384	116	-1	-2	1384	116
GG157	66	52	1	2	0	0	0	0	0	1042	35	1053	28	1025	105	-1	-3	1053	28
GG158	197	73	0	5	0	0	0	0	0	1859	32	1825	42	1900	63	2	4	1900	63
GG159	90	30	0	0	0	0	0	0	0	151	18	151	5	163	291	0	7	151	5
GG160	307	99	0	2	0	0	0	0	0	1072	27	1071	26	1077	74	0	1	1071	26
GG161	144	113	1	5	0	0	0	0	0	1813	33	1806	42	1825	66	0	1	1825	66
GG162	103	43	0	13	0	1	0	0	0	2711	36	2723	60	2707	57	0	-1	2707	57
Sample J2																			
G27	607	243	0	0	0	0	0	0	0	27	3	27	1	42	282	0	35	27	1
G120	305	224	1	0	0	0	0	0	0	33	6	31	2	208	435	7	85	31	2
G142	557	450	1	0	0	0	0	0	0	32	4	31	1	139	268	4	78	31	1
G150	310	216	1	0	0	0	0	0	0	37	7	33	2	268	398	10	88	33	2
G64	367	276	1	0	0	0	0	0	0	48	7	45	2	211	336	7	79	45	2
G18	604	489	1	0	0	0	0	0	0	57	4	59	2	18	173	-2	-223	59	2
G108	1489	554	0	0	0	0	0	0	0	62	4	60	2	158	158	4	62	60	2
G25	764	350	0	0	0	0	0	0	0	65	4	66	2	49	155	-1	-34	66	2
G128	852	758	1	0	0	0	0	0	0	66	5	66	2	53	164	-1	-25	66	2
G33	270	106	0	0	0	0	0	0	0	68	7	67	2	121	254	2	45	67	2
G95	896	519	1	0	0	0	0	0	0	73	5	73	2	87	151	0	16	73	2
G106	395	178	0	0	0	0	0	0	0	75	8	73	3	142	253	3	48	73	3
G19	155	77	0	0	0	0	0	0	0	75	10	76	3	71	311	0	-6	76	3
G54	233	129	1	0	0	0	0	0	0	80	11	77	3	181	327	4	58	77	3
G145	295	210	1	0	0	0	0	0	0	78	8	79	3	58	258	-1	-37	79	3
G136	386	203	1	0	0	0	0	0	0	80	8	79	3	109	224	1	27	79	3

				RATIO						AGES									
Grain	U [ppm]	Th [ppm]	Th/U	207/ 235	± s.e.	206/ 238	± s.e.	207/ 206	± s.e.	207/ 235	± 2s	206/ 238	± 2s	207/ 206	± 2s	%disc (5/8)	%disc (7/6)	Best Age [Ma]	± 2s
G111	200	68	0	0	0	0	0	0	0	82	9	82	3	84	266	0	2	82	3
G32	117	121	1	0	0	0	0	0	0	86	12	86	3	92	340	0	6	86	3
G38	1648	166	0	0	0	0	0	0	0	93	5	86	2	280	118	8	69	86	2
G71	1382	663	0	0	0	0	0	0	0	88	4	89	2	72	114	-1	-24	89	2
G30	276	134	0	0	0	0	0	0	0	90	8	92	3	30	218	-3	-208	92	3
G89	371	309	1	0	0	0	0	0	0	194	11	182	5	343	131	6	47	182	5
G8	299	128	0	0	0	0	0	0	0	188	12	183	5	262	154	3	30	183	5
G141	712	407	1	0	0	0	0	0	0	186	9	186	5	195	111	0	5	186	5
G90	532	377	1	0	0	0	0	0	0	184	9	190	5	111	122	-3	-71	190	5
G114	345	46	0	0	0	0	0	0	0	210	12	207	6	242	135	1	14	207	6
G110	1367	515	0	0	0	0	0	0	0	216	8	212	6	260	84	2	18	212	6
G93	1078	654	1	0	0	0	0	0	0	317	12	299	8	452	88	6	34	299	8
G43	873	749	1	0	0	0	0	0	0	332	10	333	9	334	74	0	0	333	9
G52	1400	15	0	0	0	0	0	0	0	335	10	337	9	326	69	-1	-4	337	9
G15	283	174	1	1	0	0	0	0	0	439	15	423	11	524	86	4	19	423	11
G67	188	145	1	1	0	0	0	0	0	431	20	428	12	452	121	1	5	428	12
G2	809	42	0	1	0	0	0	0	0	439	12	438	11	450	63	0	3	438	11
G101	874	535	1	1	0	0	0	0	0	799	21	780	20	858	72	2	9	780	20
G13	1048	139	0	2	0	0	0	0	0	963	19	952	23	994	51	1	4	952	23
G75	157	54	0	2	0	0	0	0	0	977	25	986	25	961	75	-1	-3	986	25
G99	211	89	0	2	0	0	0	0	0	995	26	1006	26	974	74	-1	-3	1006	26
G31	74	38	1	2	0	0	0	0	0	1014	36	1015	28	1014	110	0	0	1015	28
G82	151	47	0	2	0	0	0	0	0	1023	26	1034	26	1006	75	-1	-3	1034	26
G12	313	134	0	2	0	0	0	0	0	1038	21	1039	26	1040	57	0	0	1039	26
G112	63	52	1	2	0	0	0	0	0	1080	37	1101	30	1042	106	-2	-6	1042	106
G29	344	174	1	2	0	0	0	0	0	1037	22	1046	26	1023	59	-1	-2	1046	26
G5	736	63	0	2	0	0	0	0	0	1055	20	1055	26	1061	51	0	1	1055	26
G137	360	133	0	2	0	0	0	0	0	1047	27	1069	27	1006	77	-2	-6	1069	27
G41	211	198	1	2	0	0	0	0	0	1078	27	1070	27	1098	75	1	3	1070	27
G127	126	65	1	2	0	0	0	0	0	1086	30	1073	28	1115	82	1	4	1073	28
G6	678	270	0	2	0	0	0	0	0	1090	20	1093	27	1088	51	0	0	1093	27
G7	460	287	1	2	0	0	0	0	0	1102	21	1106	27	1097	53	0	-1	1097	53
G81	130	91	1	2	0	0	0	0	0	1096	28	1099	28	1094	76	0	-1	1099	28

				RATIO						AGES									
Grain	U [ppm]	Th [ppm]	Th/U	207/ 235	± s.e.	206/ 238	± s.e.	207/ 206	± s.e.	207/ 235	± 2s	206/ 238	± 2s	207/ 206	± 2s	%disc (5/8)	%disc (7/6)	Best Age [Ma]	± 2s
G116	218	98	0	2	0	0	0	0	0	1106	27	1105	28	1113	71	0	1	1113	71
G60	300	116	0	2	0	0	0	0	0	1130	24	1134	28	1126	61	0	-1	1126	61
G94	145	57	0	2	0	0	0	0	0	1149	28	1157	30	1136	75	-1	-2	1136	75
G107	249	110	0	2	0	0	0	0	0	1155	26	1164	29	1143	68	-1	-2	1143	68
G34	132	71	1	2	0	0	0	0	0	1152	27	1158	29	1144	70	-1	-1	1144	70
G57	97	46	0	2	0	0	0	0	0	1221	29	1247	32	1180	74	-2	-6	1180	74
G86	36	15	0	2	0	0	0	0	0	1188	43	1190	34	1189	117	0	0	1189	117
G24	348	124	0	2	0	0	0	0	0	1200	23	1202	29	1201	54	0	0	1201	54
G144	286	132	0	2	0	0	0	0	0	1211	28	1218	31	1204	69	-1	-1	1204	69
G125	51	31	1	2	0	0	0	0	0	1239	36	1255	33	1216	95	-1	-3	1216	95
G138	699	363	1	2	0	0	0	0	0	1266	26	1279	32	1250	61	-1	-2	1250	61
G122	105	88	1	2	0	0	0	0	0	1200	31	1174	30	1251	80	2	6	1251	80
G48	438	199	0	3	0	0	0	0	0	1344	25	1377	33	1295	57	-2	-6	1295	57
G23	99	64	1	3	0	0	0	0	0	1367	28	1389	34	1337	66	-2	-4	1337	66
G44	74	40	1	3	0	0	0	0	0	1394	31	1390	35	1404	73	0	1	1404	73
G119	91	45	0	3	0	0	0	0	0	1413	33	1410	36	1422	75	0	1	1422	75
G87	285	278	1	3	0	0	0	0	0	1416	26	1413	34	1425	56	0	1	1425	56
G83	125	89	1	3	0	0	0	0	0	1393	30	1374	34	1427	68	1	4	1427	68
G40	364	244	1	3	0	0	0	0	0	1472	25	1501	36	1435	51	-2	-5	1435	51
G68	199	89	0	3	0	0	0	0	0	1464	27	1478	36	1447	59	-1	-2	1447	59
G11	348	234	1	3	0	0	0	0	0	1491	24	1518	36	1456	49	-2	-4	1456	49
G109	122	104	1	3	0	0	0	0	0	1495	31	1523	38	1460	69	-2	-4	1460	69
G134	224	85	0	3	0	0	0	0	0	1489	30	1511	37	1463	64	-1	-3	1463	64
G50	211	279	1	3	0	0	0	0	0	1498	27	1523	37	1469	56	-2	-4	1469	56
G135	88	63	1	4	0	0	0	0	0	1548	36	1604	41	1475	80	-4	-9	1475	80
G3	155	161	1	3	0	0	0	0	0	1515	26	1543	37	1480	53	-2	-4	1480	53
G28	479	145	0	3	0	0	0	0	0	1516	24	1536	36	1493	48	-1	-3	1493	48
G63	157	111	1	3	0	0	0	0	0	1517	28	1529	37	1503	59	-1	-2	1503	59
G117	319	109	0	3	0	0	0	0	0	1518	28	1532	37	1505	59	-1	-2	1505	59
G97	303	154	1	3	0	0	0	0	0	1513	27	1518	37	1511	57	0	0	1511	57
G98	145	181	1	3	0	0	0	0	0	1495	30	1475	37	1526	65	1	3	1526	65
G37	521	86	0	4	0	0	0	0	0	1566	25	1593	38	1534	49	-2	-4	1534	49
G115	153	56	0	4	0	0	0	0	0	1534	30	1503	37	1581	63	2	5	1581	63

				RATIO						AGES									
Grain	U [ppm]	Th [ppm]	Th/U	207/ 235	± s.e.	206/ 238	± s.e.	207/ 206	± s.e.	207/ 235	± 2s	206/ 238	± 2s	207/ 206	± 2s	%disc (5/8)	%disc (7/6)	Best Age [Ma]	± 2s
G92	596	401	1	4	0	0	0	0	0	1636	27	1676	40	1589	52	-2	-6	1589	52
G79	168	167	1	4	0	0	0	0	0	1541	28	1503	37	1597	58	3	6	1597	58
G1	107	95	1	4	0	0	0	0	0	1649	27	1679	40	1615	53	-2	-4	1615	53
G129	152	57	0	4	0	0	0	0	0	1661	32	1688	41	1631	64	-2	-3	1631	64
G133	90	80	1	4	0	0	0	0	0	1635	34	1638	41	1636	71	0	0	1636	71
G140	210	162	1	4	0	0	0	0	0	1656	31	1671	41	1642	62	-1	-2	1642	62
G61	154	96	1	4	0	0	0	0	0	1705	29	1734	41	1673	56	-2	-4	1673	56
G4	336	203	1	4	0	0	0	0	0	1685	25	1697	40	1675	46	-1	-1	1675	46
G96	114	80	1	4	0	0	0	0	0	1722	31	1751	42	1692	61	-2	-4	1692	61
G121	356	206	1	4	0	0	0	0	0	1712	29	1728	41	1697	56	-1	-2	1697	56
G123	178	110	1	4	0	0	0	0	0	1714	31	1724	42	1706	60	-1	-1	1706	60
G35	160	79	0	5	0	0	0	0	0	1741	28	1770	42	1710	53	-2	-3	1710	53
G10	229	189	1	5	0	0	0	0	0	1757	26	1784	42	1730	48	-1	-3	1730	48
G146	41	38	1	5	0	0	0	0	0	1737	45	1733	47	1746	96	0	1	1746	96
G131	334	154	0	5	0	0	0	0	0	1813	30	1858	44	1765	56	-2	-5	1765	56
G47	221	68	0	5	0	0	0	0	0	1816	27	1862	43	1768	50	-2	-5	1768	50
G84	372	153	0	5	0	0	0	0	0	1766	28	1765	42	1770	52	0	0	1770	52
G42	487	193	0	5	0	0	0	0	0	1815	26	1852	43	1777	47	-2	-4	1777	47
G62	278	169	1	5	0	0	0	0	0	1787	27	1798	42	1779	50	-1	-1	1779	50
G16	284	158	1	5	0	0	0	0	0	1820	26	1855	43	1784	47	-2	-4	1784	47
G139	242	127	1	5	0	0	0	0	0	1810	31	1830	44	1791	59	-1	-2	1791	59
G103	719	187	0	5	0	0	0	0	0	1785	28	1768	42	1810	51	1	2	1810	51
G100	85	62	1	5	0	0	0	0	0	1857	33	1885	46	1829	64	-2	-3	1829	64
G126	181	268	1	5	0	0	0	0	0	1870	31	1909	46	1831	59	-2	-4	1831	59
G22	165	176	1	5	0	0	0	0	0	1848	27	1865	43	1833	49	-1	-2	1833	49
G118	114	159	1	5	0	0	0	0	0	1839	32	1847	45	1834	61	0	-1	1834	61
G69	272	170	1	5	0	0	0	0	0	1887	28	1916	45	1859	50	-2	-3	1859	50
G20	358	120	0	5	0	0	0	0	0	1879	26	1899	44	1861	45	-1	-2	1861	45
G88	144	43	0	6	0	0	0	0	0	1910	31	1953	46	1867	56	-2	-5	1867	56
G14	271	344	1	6	0	0	0	0	0	1905	26	1925	44	1887	46	-1	-2	1887	46
G147	115	96	1	6	0	0	0	0	0	1933	34	1951	47	1917	64	-1	-2	1917	64
G132	252	125	0	6	0	0	0	0	0	1981	31	1994	47	1972	56	-1	-1	1972	56
G70	237	157	1	6	0	0	0	0	0	1991	28	1988	46	1998	49	0	0	1998	49

				RATIO						AGES									
	U	Th		207/		206/		207/		207/		206/		207/		%disc	%disc	Best Age	
Grain	[ppm]	[ppm]	Th/U	235	± s.e.	238	± s.e.	206	± s.e.	235	± 2s	238	± 2s	206	± 2s	(5/8)	(7/6)	[Ma]	± 2s
G26	152	81	1	7	0	0	0	0	0	2118	28	2178	50	2064	47	-3	-6	2064	47
G17	132	48	0	11	0	0	0	0	0	2500	29	2532	56	2478	44	-1	-2	2478	44
G73	200	123	1	10	0	0	0	0	0	2456	31	2421	55	2488	48	1	3	2488	48
G78	66	42	1	11	0	0	0	0	0	2506	34	2499	58	2515	55	0	1	2515	55
G102	71	42	1	12	0	0	0	0	0	2618	34	2560	59	2667	52	2	4	2667	52
G39	162	110	1	13	0	1	0	0	0	2679	29	2694	59	2672	44	-1	-1	2672	44
G74	121	12	0	13	0	1	0	0	0	2701	31	2732	61	2682	48	-1	-2	2682	48
G53	176	68	0	13	0	1	0	0	0	2710	29	2731	60	2698	43	-1	-1	2698	43
G113	619	144	0	13	0	1	0	0	0	2710	31	2730	60	2700	46	-1	-1	2700	46
G130	74	55	1	14	0	1	0	0	0	2721	34	2750	62	2704	53	-1	-2	2704	53
G36	80	44	1	14	0	1	0	0	0	2743	33	2763	63	2732	51	-1	-1	2732	51
G148	137	87	1	14	0	1	0	0	0	2765	35	2798	63	2744	53	-1	-2	2744	53
G59	156	238	2	13	0	0	0	0	0	2655	32	2518	57	2764	48	5	9	2764	48
G143	147	76	1	14	0	1	0	0	0	2764	34	2766	62	2767	52	0	0	2767	52
G85	230	238	1	15	0	1	0	0	0	2839	31	2847	62	2838	45	0	0	2838	45
G56	56	27	0	16	0	1	0	0	0	2882	34	2923	66	2857	51	-1	-2	2857	51
G45	161	112	1	17	0	1	0	0	0	2908	29	2884	62	2928	41	1	2	2928	41
G76	464	375	1	17	0	1	0	0	0	2931	30	2933	63	2934	42	0	0	2934	42
G104	165	289	2	17	0	1	0	0	0	2955	32	2939	65	2969	47	1	1	2969	47
Sample W1																			
G117	109	257	2	0	0	0	0	0	0	20	12	19	2	108	1216	4	82	19	2
G9	379	518	1	0	0	0	0	0	0	25	4	25	1	30	402	0	18	25	1
G5	283	177	1	0	0	0	0	0	0	33	5	32	1	122	358	4	73	32	1
G106	1868	1361	1	0	0	0	0	0	0	63	4	59	2	213	131	6	72	59	2
G129	468	103	0	0	0	0	0	0	0	62	6	67	2	0	38	-7	-66500	67	2
G105	521	295	1	0	0	0	0	0	0	70	7	68	2	162	232	4	58	68	2
G115	1509	388	0	0	0	0	0	0	0	70	4	70	2	75	141	0	7	70	2
G44	1108	687	1	0	0	0	0	0	0	73	4	72	2	111	135	1	35	72	2
G43	1020	270	0	0	0	0	0	0	0	72	4	72	2	68	148	0	-6	72	2
G84	1043	432	0	0	0	0	0	0	0	81	6	74	2	305	159	10	76	74	2
G93	380	201	1	0	0	0	0	0	0	75	9	75	3	97	298	1	23	75	3
G118	349	223	1	0	0	0	0	0	0	77	8	77	3	83	247	0	8	77	3

Grain	U [ppm]	Th [ppm]	Th/U	RATIO 207/235	± s.e.	206/238	± s.e.	207/206	± s.e.	AGES 207/235	± 2s	206/238	± 2s	207/206	± 2s	%disc (5/8)	%disc (7/6)	Best Age [Ma]	± 2s
G150	272	223	1	0	0	0	0	0	0	80	12	80	3	86	363	0	7	80	3
G40	368	226	1	0	0	0	0	0	0	82	8	81	3	105	232	1	22	81	3
G114	568	183	0	0	0	0	0	0	0	83	6	82	3	113	186	1	27	82	3
G58	210	66	0	0	0	0	0	0	0	86	11	86	3	96	308	0	11	86	3
G71	394	175	0	0	0	0	0	0	0	96	8	89	3	291	197	8	70	89	3
G74	899	369	0	0	0	0	0	0	0	91	5	92	3	91	145	0	-1	92	3
G116	1335	662	0	0	0	0	0	0	0	94	5	93	3	127	122	1	27	93	3
G94	2029	798	0	0	0	0	0	0	0	96	5	94	3	153	128	2	38	94	3
G38	919	513	1	0	0	0	0	0	0	95	5	94	3	115	129	1	18	94	3
G131	474	199	0	0	0	0	0	0	0	93	7	95	3	51	192	-2	-87	95	3
G57	409	316	1	0	0	0	0	0	0	105	8	100	3	232	191	5	57	100	3
G98	505	265	1	0	0	0	0	0	0	102	9	102	3	95	208	0	-7	102	3
G132	1423	764	1	0	0	0	0	0	0	106	5	107	3	85	115	-1	-27	107	3
G90	1189	299	0	0	0	0	0	0	0	125	7	120	3	227	137	4	47	120	3
G28	353	299	1	0	0	0	0	0	0	168	10	166	5	211	143	2	21	166	5
G146	585	361	1	0	0	0	0	0	0	170	10	166	5	235	143	3	30	166	5
G8	400	214	1	0	0	0	0	0	0	175	9	174	5	192	127	1	9	174	5
G45	74	105	1	0	0	0	0	0	0	171	23	175	7	127	328	-2	-38	175	7
G69	161	147	1	0	0	0	0	0	0	181	17	189	6	75	235	-4	-151	189	6
G124	426	256	1	0	0	0	0	0	0	187	11	190	5	156	141	-2	-22	190	5
G12	846	426	1	0	0	0	0	0	0	194	8	191	5	236	93	2	19	191	5
G119	381	126	0	0	0	0	0	0	0	212	12	211	6	236	142	1	11	211	6
G148	147	42	0	0	0	0	0	0	0	225	24	229	8	191	265	-2	-20	229	8
G51	676	69	0	0	0	0	0	0	0	339	12	336	9	362	85	1	7	336	9
G104	406	275	1	1	0	0	0	0	0	466	17	463	12	484	93	1	4	463	12
G59	391	297	1	1	0	0	0	0	0	592	18	587	15	618	81	1	5	587	15
G110	62	26	0	1	0	0	0	0	0	642	43	602	20	791	185	7	24	602	20
G143	433	1160	3	1	0	0	0	0	0	597	19	603	15	579	83	-1	-4	603	15
G125	120	51	0	2	0	0	0	0	0	990	33	961	26	1058	101	3	9	961	26
G39	48	34	1	2	0	0	0	0	0	1031	37	1013	28	1073	111	2	6	1013	28
G107	189	163	1	2	0	0	0	0	0	1014	26	1019	26	1007	77	-1	-1	1019	26
G41	490	254	1	2	0	0	0	0	0	1031	21	1035	25	1026	58	0	-1	1035	25
G7	123	114	1	2	0	0	0	0	0	1094	28	1036	26	1214	77	6	15	1036	26

				RATIO						AGES									
																		Best	
	U	Th		207/		206/		207/		207/		206/		207/		%disc	%disc	Age	
Grain	[ppm]	[ppm]	Th/U	235	± s.e.	238	± s.e.	206	± s.e.	235	± 2s	238	± 2s	206	± 2s	(5/8)	(7/6)	[Ma]	± 2s
G50	153	201	1	2	0	0	0	0	0	1024	26	1038	26	1001	76	-1	-4	1038	26
G34	108	63	1	2	0	0	0	0	0	1075	28	1042	27	1147	78	3	9	1042	27
G134	41	20	0	2	0	0	0	0	0	1033	45	1046	30	1011	136	-1	-3	1046	30
G120	189	58	0	2	0	0	0	0	0	1033	26	1047	26	1009	76	-1	-4	1047	26
G47	51	34	1	2	0	0	0	0	0	1082	38	1054	29	1143	109	3	8	1054	29
G75	130	88	1	2	0	0	0	0	0	1113	30	1145	29	1057	85	-3	-8	1057	85
G140	174	275	2	2	0	0	0	0	0	1048	28	1062	27	1023	81	-1	-4	1062	27
G130	33	23	1	2	0	0	0	0	0	1102	48	1066	32	1178	139	3	10	1066	32
G13	714	109	0	2	0	0	0	0	0	1077	21	1073	26	1089	54	0	1	1073	26
G37	310	743	2	2	0	0	0	0	0	1060	23	1074	26	1036	62	-1	-4	1074	26
G101	136	48	0	2	0	0	0	0	0	1091	28	1102	28	1074	79	-1	-3	1074	79
G85	212	116	1	2	0	0	0	0	0	1090	29	1101	28	1074	83	-1	-2	1074	83
G3	13	15	1	2	0	0	0	0	0	1128	61	1080	36	1226	174	4	12	1080	36
G151	38	29	1	2	0	0	0	0	0	1066	46	1083	31	1035	138	-2	-5	1083	31
G96	328	121	0	2	0	0	0	0	0	1087	24	1084	27	1096	65	0	1	1084	27
G92	68	109	2	2	0	0	0	0	0	1079	41	1088	30	1067	122	-1	-2	1088	30
G111	121	52	0	2	0	0	0	0	0	1094	30	1096	28	1094	84	0	0	1096	28
G89	463	88	0	2	0	0	0	0	0	1111	23	1116	27	1104	60	-1	-1	1104	60
G11	49	29	1	2	0	0	0	0	0	1137	38	1155	31	1108	106	-2	-4	1108	106
G14	350	80	0	2	0	0	0	0	0	1121	23	1130	28	1109	59	-1	-2	1109	59
G79	398	125	0	2	0	0	0	0	0	1177	26	1200	29	1138	66	-2	-5	1138	66
G20	76	27	0	2	0	0	0	0	0	1140	31	1124	29	1176	85	1	4	1176	85
G4	768	356	0	2	0	0	0	0	0	1156	21	1144	28	1184	52	1	3	1184	52
G42	132	58	0	2	0	0	0	0	0	1187	28	1188	30	1191	73	0	0	1191	73
G86	122	46	0	2	0	0	0	0	0	1207	36	1213	32	1201	95	0	-1	1201	95
G122	231	81	0	2	0	0	0	0	0	1201	26	1201	29	1205	67	0	0	1205	67
G49	394	157	0	2	0	0	0	0	0	1172	23	1150	28	1218	57	2	6	1218	57
G64	28	33	1	2	0	0	0	0	0	1217	49	1218	35	1220	133	0	0	1220	133
G126	201	92	0	2	0	0	0	0	0	1217	27	1211	30	1230	69	0	2	1230	69
G60	664	18	0	2	0	0	0	0	0	1226	24	1225	30	1232	58	0	1	1232	58
G19	204	141	1	2	0	0	0	0	0	1246	25	1255	30	1236	61	-1	-2	1236	61
G103	120	45	0	2	0	0	0	0	0	1270	30	1291	32	1238	75	-2	-4	1238	75
G138	67	42	1	2	0	0	0	0	0	1229	38	1223	32	1245	100	1	2	1245	100

				RATIO						AGES								Best	
	U	Th		207/		206/		207/		207/		206/		207/		%disc	%disc	Age	
Grain	[ppm]	[ppm]	Th/U	235	± s.e.	238	± s.e.	206	± s.e.	235	± 2s	238	± 2s	206	± 2s	(5/8)	(7/6)	[Ma]	± 2s
G21	76	25	0	2	0	0	0	0	0	1265	32	1275	32	1253	80	-1	-2	1253	80
G24	262	119	0	2	0	0	0	0	0	1268	25	1272	31	1266	58	0	-1	1266	58
G67	745	67	0	2	0	0	0	0	0	1250	24	1228	30	1292	57	2	5	1292	57
G139	136	94	1	3	0	0	0	0	0	1338	30	1338	33	1343	73	0	0	1343	73
G22	43	20	0	3	0	0	0	0	0	1378	37	1383	36	1376	90	0	-1	1376	90
G15	157	54	0	3	0	0	0	0	0	1402	27	1421	34	1377	62	-1	-3	1377	62
G55	232	526	2	3	0	0	0	0	0	1435	27	1461	35	1401	60	-2	-4	1401	60
G141	209	60	0	3	0	0	0	0	0	1419	28	1429	34	1410	64	-1	-1	1410	64
G6	218	100	0	3	0	0	0	0	0	1409	26	1409	34	1414	56	0	0	1414	56
G108	132	43	0	3	0	0	0	0	0	1409	31	1382	34	1453	71	2	5	1453	71
G135	323	119	0	3	0	0	0	0	0	1484	27	1502	35	1464	57	-1	-3	1464	57
G91	55	17	0	3	0	0	0	0	0	1507	40	1510	40	1507	93	0	0	1507	93
G17	136	142	1	3	0	0	0	0	0	1472	28	1436	35	1530	61	3	6	1530	61
G80	1604	748	0	4	0	0	0	0	0	1630	25	1629	38	1635	48	0	0	1635	48
G127	576	103	0	4	0	0	0	0	0	1698	26	1721	40	1675	51	-1	-3	1675	51
G144	222	71	0	4	0	0	0	0	0	1673	29	1669	39	1682	58	0	1	1682	58
G128	207	75	0	4	0	0	0	0	0	1726	29	1749	41	1701	58	-1	-3	1701	58
G123	284	123	0	4	0	0	0	0	0	1717	28	1730	40	1706	55	-1	-1	1706	55
G99	128	79	1	4	0	0	0	0	0	1702	30	1695	40	1714	61	0	1	1714	61
G142	202	103	1	4	0	0	0	0	0	1724	29	1731	40	1720	58	0	-1	1720	58
G109	317	161	1	5	0	0	0	0	0	1731	27	1742	40	1723	53	-1	-1	1723	53
G27	161	98	1	4	0	0	0	0	0	1729	28	1727	40	1736	54	0	1	1736	54
G46	353	282	1	5	0	0	0	0	0	1765	26	1779	41	1753	50	-1	-1	1753	50
G136	283	74	0	5	0	0	0	0	0	1779	29	1804	42	1754	56	-1	-3	1754	56
G145	416	57	0	5	0	0	0	0	0	1820	29	1879	43	1757	55	-3	-7	1757	55
G77	510	258	1	5	0	0	0	0	0	1783	27	1793	41	1775	50	-1	-1	1775	50
G35	743	56	0	5	0	0	0	0	0	1823	26	1801	41	1854	46	1	3	1854	46
G112	126	71	1	5	0	0	0	0	0	1848	32	1847	44	1854	63	0	0	1854	63
G18	24	33	1	5	0	0	0	0	0	1862	42	1864	48	1863	85	0	0	1863	85
G26	198	156	1	5	0	0	0	0	0	1868	28	1867	43	1872	51	0	0	1872	51
G52	298	169	1	5	0	0	0	0	0	1893	27	1912	44	1876	49	-1	-2	1876	49
G133	222	145	1	6	0	0	0	0	0	1905	29	1932	44	1880	54	-1	-3	1880	54
G95	107	60	1	6	0	0	0	0	0	1929	33	1959	46	1900	62	-2	-3	1900	62

Grain	U [ppm]	Th [ppm]	Th/U	RATIO 207/235	± s.e.	206/238	± s.e.	207/206	± s.e.	AGES 207/235	± 2s	206/238	± 2s	207/206	± 2s	%disc (5/8)	%disc (7/6)	Best Age [Ma]	± 2s
G82	213	127	1	6	0	0	0	0	0	1954	29	1997	46	1913	52	-2	-4	1913	52
G72	380	189	0	11	0	0	0	0	0	2512	29	2547	55	2488	44	-1	-2	2488	44
G10	948	435	0	12	0	0	0	0	0	2591	28	2546	55	2631	41	2	3	2631	41
G147	512	137	0	12	0	0	0	0	0	2619	29	2602	56	2636	45	1	1	2636	45
G83	96	74	1	13	0	1	0	0	0	2673	34	2639	60	2702	53	1	2	2702	53
G113	58	43	1	14	0	1	0	0	0	2749	33	2804	62	2713	52	-2	-3	2713	52
G121	96	88	1	14	0	1	0	0	0	2731	32	2757	61	2716	50	-1	-2	2716	50
G65	117	136	1	14	0	1	0	0	0	2726	31	2732	60	2725	46	0	0	2725	46
G63	406	344	1	15	0	1	0	0	0	2790	29	2884	61	2726	42	-3	-6	2726	42
G48	76	74	1	14	0	1	0	0	0	2747	31	2777	61	2728	47	-1	-2	2728	47
G73	157	212	1	14	0	1	0	0	0	2766	30	2791	60	2751	45	-1	-1	2751	45
G33	82	92	1	14	0	1	0	0	0	2759	30	2775	61	2752	46	-1	-1	2752	46
G32	550	357	1	14	0	1	0	0	0	2744	28	2727	58	2760	41	1	1	2760	41
G66	1494	531	0	15	0	1	0	0	0	2836	28	2806	59	2861	40	1	2	2861	40
G23	426	246	1	17	0	1	0	0	0	2954	29	3071	64	2878	40	-4	-7	2878	40
G70	603	88	0	17	0	1	0	0	0	2950	29	3014	63	2911	41	-2	-4	2911	41
G87	45	20	0	18	0	1	0	0	0	2990	40	2956	72	3016	63	1	2	3016	63
G137	206	94	0	28	0	1	0	0	0	3419	31	3371	69	3452	42	1	2	3452	42
Sample B2																			
G121	6494	10212	2	0	0	0	0	0	0	15	2	14	0	103	240	3	86	14	0
G131	1650	1112	1	0	0	0	0	0	0	23	3	22	1	91	339	3	76	22	1
G6	707	873	1	0	0	0	0	0	0	34	5	32	1	238	313	9	87	32	1
G146	562	209	0	0	0	0	0	0	0	58	8	58	2	59	325	0	1	58	2
G69	692	358	1	0	0	0	0	0	0	61	8	60	2	106	301	2	44	60	2
G112	970	337	0	0	0	0	0	0	0	59	8	62	2	0	234	-4	-61600	62	2
G138	420	215	1	0	0	0	0	0	0	76	13	73	3	171	400	4	57	73	3
G81	222	219	1	0	0	0	0	0	0	75	15	75	4	77	471	0	3	75	4
G9	140	76	1	0	0	0	0	0	0	84	21	77	5	297	543	9	74	77	5
G10	238	175	1	0	0	0	0	0	0	85	13	77	3	307	352	10	75	77	3
G35	378	120	0	0	0	0	0	0	0	93	11	86	3	281	283	8	69	86	3
G104	251	152	1	0	0	0	0	0	0	90	18	89	4	119	468	1	25	89	4
G73	1262	18	0	0	0	0	0	0	0	91	8	93	3	38	204	-2	-144	93	3

				RATIO						AGES									
Grain	U [ppm]	Th [ppm]	Th/U	207/ 235	± s.e.	206/ 238	± s.e.	207/ 206	± s.e.	207/ 235	± 2s	206/ 238	± 2s	207/ 206	± 2s	%disc (5/8)	%disc (7/6)	Best Age [Ma]	± 2s
G8	1344	373	0	0	0	0	0	0	0	98	7	96	3	146	174	2	34	96	3
G13	976	535	1	0	0	0	0	0	0	105	8	98	3	283	177	8	65	98	3
G68	98	75	1	0	0	0	0	0	0	103	27	99	6	209	594	4	53	99	6
G90	993	365	0	0	0	0	0	0	0	108	9	109	3	95	211	-1	-14	109	3
G74	295	207	1	0	0	0	0	0	0	112	15	113	4	94	317	-1	-20	113	4
G126	642	340	1	0	0	0	0	0	0	114	13	116	4	76	271	-2	-52	116	4
G50	390	208	1	0	0	0	0	0	0	124	13	123	4	143	255	1	14	123	4
G118	1484	780	1	0	0	0	0	0	0	143	12	130	4	359	198	9	64	130	4
G107	1902	2897	2	0	0	0	0	0	0	134	10	133	4	150	179	1	12	133	4
G142	131	64	0	0	0	0	0	0	0	155	25	146	7	286	387	6	49	146	7
G49	1266	1067	1	0	0	0	0	0	0	160	10	151	4	294	155	6	49	151	4
G31	1131	793	1	0	0	0	0	0	0	156	10	155	5	173	162	1	11	155	5
G30	756	458	1	0	0	0	0	0	0	199	13	197	6	226	167	1	13	197	6
G45	442	262	1	0	0	0	0	0	0	207	16	205	6	242	194	1	16	205	6
G123	607	423	1	0	0	0	0	0	0	216	18	223	7	148	218	-3	-51	223	7
G71	279	137	0	0	0	0	0	0	0	234	22	232	8	257	238	1	9	232	8
G79	163	55	0	0	0	0	0	0	0	408	33	420	14	349	217	-3	-20	420	14
G101	328	86	0	1	0	0	0	0	0	437	29	429	13	482	178	2	11	429	13
G7	282	355	1	1	0	0	0	0	0	455	27	443	13	520	156	3	15	443	13
G15	867	236	0	1	0	0	0	0	0	543	24	538	15	566	120	1	5	538	15
G24	204	125	1	1	0	0	0	0	0	798	37	790	22	824	136	1	4	790	22
G133	164	132	1	1	0	0	0	0	0	897	50	884	27	933	171	1	5	884	27
G93	98	78	1	2	0	0	0	0	0	1008	52	1006	30	1016	163	0	1	1006	30
G18	246	151	1	2	0	0	0	0	0	1013	39	1010	27	1024	119	0	1	1010	27
G33	461	180	0	2	0	0	0	0	0	1081	38	1012	27	1228	107	7	18	1012	27
G19	212	104	0	2	0	0	0	0	0	1060	40	1034	28	1118	118	3	7	1034	28
G85	110	58	1	2	0	0	0	0	0	1041	51	1038	31	1051	155	0	1	1038	31
G40	121	44	0	2	0	0	0	0	0	1051	46	1044	30	1070	139	1	2	1044	30
G114	211	207	1	2	0	0	0	0	0	1081	50	1101	32	1047	151	-2	-5	1047	151
G106	247	124	1	2	0	0	0	0	0	1064	47	1049	29	1101	140	1	5	1049	29
G32	344	108	0	2	0	0	0	0	0	1053	39	1051	28	1060	114	0	1	1051	28
G38	644	370	1	2	0	0	0	0	0	1044	37	1052	28	1030	109	-1	-2	1052	28
G59	256	127	0	2	0	0	0	0	0	1073	42	1057	29	1110	124	2	5	1057	29

				RATIO						AGES									
																		Best	
	U	Th		207/		206/		207/		207/		206/		207/		%disc	%disc	Age	
Grain	[ppm]	[ppm]	Th/U	235	± s.e.	238	± s.e.	206	± s.e.	235	± 2s	238	± 2s	206	± 2s	(5/8)	(7/6)	[Ma]	± 2s
G52	1473	1059	1	2	0	0	0	0	0	1036	38	1057	28	996	113	-2	-6	1057	28
G116	586	8	0	2	0	0	0	0	0	1051	45	1061	29	1036	137	-1	-2	1061	29
G22	268	221	1	2	0	0	0	0	0	1071	40	1064	29	1090	116	1	2	1064	29
G66	497	339	1	2	0	0	0	0	0	1058	42	1067	29	1046	125	-1	-2	1067	29
G43	629	295	0	2	0	0	0	0	0	1066	37	1069	28	1062	110	0	-1	1069	28
G150	122	51	0	2	0	0	0	0	0	1111	56	1071	32	1197	163	4	11	1071	32
G70	56	81	1	2	0	0	0	0	0	1106	61	1125	36	1074	178	-2	-5	1074	178
G109	135	60	0	2	0	0	0	0	0	1068	52	1075	32	1058	157	-1	-2	1075	32
G56	1177	536	0	2	0	0	0	0	0	1085	38	1076	28	1105	109	1	3	1076	28
G99	102	48	0	2	0	0	0	0	0	1085	53	1079	32	1101	157	1	2	1079	32
G98	261	159	1	2	0	0	0	0	0	1083	45	1083	30	1088	134	0	0	1083	30
G61	82	38	0	2	0	0	0	0	0	1090	54	1085	33	1103	157	0	2	1085	33
G28	156	90	1	2	0	0	0	0	0	1117	44	1127	31	1101	125	-1	-2	1101	125
G47	224	195	1	2	0	0	0	0	0	1164	43	1184	32	1130	118	-2	-5	1130	118
G5	136	93	1	2	0	0	0	0	0	1120	43	1111	31	1140	122	1	3	1140	122
G83	1325	156	0	2	0	0	0	0	0	1119	41	1108	29	1146	115	1	3	1146	115
G63	208	128	1	2	0	0	0	0	0	1140	45	1138	31	1148	126	0	1	1148	126
G2	28	24	1	2	0	0	0	0	0	1148	70	1145	39	1156	197	0	1	1156	197
G88	44	26	1	2	0	0	0	0	0	1203	67	1231	40	1158	186	-2	-6	1158	186
G102	77	37	0	2	0	0	0	0	0	1190	58	1199	36	1178	161	-1	-2	1178	161
G113	523	178	0	2	0	0	0	0	0	1141	47	1123	31	1179	132	2	5	1179	132
G17	60	33	1	2	0	0	0	0	0	1183	54	1182	35	1190	149	0	1	1190	149
G128	242	129	1	2	0	0	0	0	0	1263	54	1281	36	1235	144	-1	-4	1235	144
G86	211	66	0	2	0	0	0	0	0	1207	48	1190	33	1242	129	1	4	1242	129
G11	87	74	1	2	0	0	0	0	0	1270	49	1278	36	1261	128	-1	-1	1261	128
G14	65	59	1	3	0	0	0	0	0	1301	53	1311	38	1289	137	-1	-2	1289	137
G103	195	107	1	3	0	0	0	0	0	1322	52	1342	37	1293	134	-2	-4	1293	134
G105	649	300	0	3	0	0	0	0	0	1400	49	1428	37	1362	122	-2	-5	1362	122
G147	927	231	0	3	0	0	0	0	0	1375	54	1370	37	1388	135	0	1	1388	135
G48	308	156	1	3	0	0	0	0	0	1405	44	1408	37	1405	108	0	0	1405	108
G137	438	210	0	3	0	0	0	0	0	1363	53	1327	36	1423	135	3	7	1423	135
G92	361	96	0	3	0	0	0	0	0	1485	49	1521	40	1438	117	-2	-6	1438	117
G91	177	83	0	3	0	0	0	0	0	1462	52	1474	40	1448	124	-1	-2	1448	124

				RATIO						AGES									
Grain	**U [ppm]**	**Th [ppm]**	**Th/U**	**207/ 235**	**± s.e.**	**206/ 238**	**± s.e.**	**207/ 206**	**± s.e.**	**207/ 235**	**± 2s**	**206/ 238**	**± 2s**	**207/ 206**	**± 2s**	**%disc (5/8)**	**%disc (7/6)**	**Best Age [Ma]**	**± 2s**
G145	364	250	1	3	0	0	0	0	0	1486	56	1516	41	1449	137	-2	-5	1449	137
G58	382	150	0	3	0	0	0	0	0	1420	45	1397	36	1459	109	2	4	1459	109
G140	338	123	0	3	0	0	0	0	0	1426	55	1397	38	1473	136	2	5	1473	136
G117	192	121	1	3	0	0	0	0	0	1481	56	1485	41	1479	135	0	0	1479	135
G76	112	46	0	3	0	0	0	0	0	1485	53	1491	41	1481	127	0	-1	1481	127
G36	149	80	1	3	0	0	0	0	0	1479	48	1475	39	1487	113	0	1	1487	113
G75	440	187	0	3	0	0	0	0	0	1480	47	1470	38	1498	110	1	2	1498	110
G39	358	183	1	3	0	0	0	0	0	1483	44	1466	38	1513	103	1	3	1513	103
G141	530	247	0	4	0	0	0	0	0	1671	58	1702	45	1636	130	-2	-4	1636	130
G54	496	270	1	4	0	0	0	0	0	1614	46	1591	40	1649	101	1	3	1649	101
G139	380	93	0	4	0	0	0	0	0	1693	58	1720	45	1665	130	-2	-3	1665	130
G115	276	165	1	4	0	0	0	0	0	1680	56	1686	45	1676	124	0	-1	1676	124
G89	486	243	0	4	0	0	0	0	0	1681	50	1688	43	1678	110	0	-1	1678	110
G135	262	124	0	4	0	0	0	0	0	1635	58	1599	43	1686	130	2	5	1686	130
G144	195	81	0	4	0	0	0	0	0	1731	61	1768	47	1690	134	-2	-5	1690	134
G42	89	106	1	4	0	0	0	0	0	1693	53	1697	46	1693	115	0	0	1693	115
G26	274	104	0	5	0	0	0	0	0	1745	46	1788	45	1698	98	-2	-5	1698	98
G96	457	342	1	4	0	0	0	0	0	1700	51	1704	44	1700	112	0	0	1700	112
G151	375	227	1	4	0	0	0	0	0	1730	60	1759	47	1700	133	-2	-3	1700	133
G110	528	199	0	5	0	0	0	0	0	1740	54	1773	46	1705	118	-2	-4	1705	118
G29	314	114	0	5	0	0	0	0	0	1751	46	1765	44	1737	96	-1	-2	1737	96
G148	260	129	0	5	0	0	0	0	0	1735	61	1736	46	1737	133	0	0	1737	133
G60	343	203	1	5	0	0	0	0	0	1732	48	1720	43	1750	103	1	2	1750	103
G97	294	114	0	5	0	0	0	0	0	1740	53	1735	45	1751	113	0	1	1751	113
G124	225	304	1	5	0	0	0	0	0	1784	59	1802	48	1768	127	-1	-2	1768	127
G51	237	111	0	5	0	0	0	0	0	1797	48	1815	46	1779	101	-1	-2	1779	101
G149	253	80	0	5	0	0	0	0	0	1748	62	1723	47	1782	135	1	3	1782	135
G82	513	130	0	5	0	0	0	0	0	1789	50	1793	45	1789	106	0	0	1789	106
G120	344	137	0	4	0	0	0	0	0	1712	57	1637	44	1809	123	5	10	1809	123
G34	255	246	1	5	0	0	0	0	0	1816	47	1818	45	1818	97	0	0	1818	97
G132	278	92	0	5	0	0	0	0	0	1857	60	1873	49	1842	126	-1	-2	1842	126
G129	450	168	0	5	0	0	0	0	0	1872	59	1860	48	1889	122	1	2	1889	122
G122	164	214	1	6	0	0	0	0	0	1955	61	1928	51	1988	124	1	3	1988	124

				RATIO						AGES									
Grain	U [ppm]	Th [ppm]	Th/U	207/ 235	± s.e.	206/ 238	± s.e.	207/ 206	± s.e.	207/ 235	± 2s	206/ 238	± 2s	207/ 206	± 2s	%disc (5/8)	%disc (7/6)	Best Age [Ma]	± 2s
G78	352	166	0	11	0	0	0	0	0	2516	54	2526	60	2512	95	0	-1	2512	95
G25	434	476	1	11	0	0	0	0	0	2506	49	2382	56	2610	84	5	9	2610	84
G119	217	133	1	14	0	1	0	0	0	2722	63	2759	67	2699	108	-1	-2	2699	108
G77	255	168	1	13	0	1	0	0	0	2700	55	2696	64	2706	94	0	0	2706	94
G20	1181	876	1	15	0	1	0	0	0	2786	50	2873	65	2726	81	-3	-5	2726	81
G100	246	262	1	14	0	1	0	0	0	2764	59	2821	67	2727	100	-2	-3	2727	100
G95	110	93	1	13	0	1	0	0	0	2703	59	2673	65	2730	101	1	2	2730	101
G108	211	158	1	14	0	1	0	0	0	2776	61	2838	68	2736	104	-2	-4	2736	104
G65	493	230	0	13	0	1	0	0	0	2710	53	2660	62	2751	89	2	3	2751	89
G80	126	60	0	14	0	1	0	0	0	2732	57	2706	65	2754	96	1	2	2754	96
G16	90	57	1	15	0	1	0	0	0	2789	52	2808	67	2778	86	-1	-1	2778	86
G130	191	159	1	16	1	1	0	0	0	2862	65	2920	71	2825	110	-2	-3	2825	110
G67	242	58	0	15	0	1	0	0	0	2818	54	2784	65	2846	90	1	2	2846	90
G125	130	152	1	17	1	1	0	0	0	2919	65	3031	74	2846	110	-4	-6	2846	110
Sample W3																			
G117	328	3225	10	0	0	0	0	0	0	20	12	19	2	108	1216	4	82	19	2
G9	123	628	5	0	0	0	0	0	0	25	4	25	1	30	402	0	18	25	1
G5	13	96	8	0	0	0	0	0	0	33	5	32	1	122	358	4	73	32	1
G106	212	105	0	0	0	0	0	0	0	63	4	59	2	213	131	6	72	59	2
G129	132	23	0	0	0	0	0	0	0	62	6	67	2	0	38	-7	-66500	67	2
G105	1043	172	0	0	0	0	0	0	0	70	7	68	2	162	232	4	58	68	2
G115	2029	382	0	0	0	0	0	0	0	70	4	70	2	75	141	0	7	70	2
G44	453	1022	2	0	0	0	0	0	0	73	4	72	2	111	135	1	35	72	2
G43	743	138	0	0	0	0	0	0	0	72	4	72	2	68	148	0	-6	72	2
G84	745	27	0	0	0	0	0	0	0	81	6	74	2	305	159	10	76	74	2
G93	130	151	1	0	0	0	0	0	0	75	9	75	3	97	298	1	23	75	3
G118	328	127	0	0	0	0	0	0	0	77	8	77	3	83	247	0	8	77	3
G150	207	120	1	0	0	0	0	0	0	80	12	80	3	86	363	0	7	80	3
G40	550	81	0	0	0	0	0	0	0	82	8	81	3	105	232	1	22	81	3
G114	380	80	0	0	0	0	0	0	0	83	6	82	3	113	186	1	27	82	3
G58	51	441	9	0	0	0	0	0	0	86	11	86	3	96	308	0	11	86	3
G71	409	162	0	0	0	0	0	0	0	96	8	89	3	291	197	8	70	89	3

Grain	U [ppm]	Th [ppm]	Th/U	RATIO						AGES						%disc (5/8)	%disc (7/6)	Best Age [Ma]	± 2s
				207/ 235	± s.e.	206/ 238	± s.e.	207/ 206	± s.e.	207/ 235	± 2s	206/ 238	± 2s	207/ 206	± 2s				
G74	664	112	0	0	0	0	0	0	0	91	5	92	3	91	145	0	-1	92	3
G116	107	61	1	0	0	0	0	0	0	94	5	93	3	127	122	1	27	93	3
G94	86	57	1	0	0	0	0	0	0	96	5	94	3	153	128	2	38	94	3
G38	335	65	0	0	0	0	0	0	0	95	5	94	3	115	129	1	18	94	3
G131	62	21	0	0	0	0	0	0	0	93	7	95	3	51	192	-2	-87	95	3
G57	353	163	0	0	0	0	0	0	0	105	8	100	3	232	191	5	57	100	3
G98	398	313	1	0	0	0	0	0	0	102	9	102	3	95	208	0	-7	102	3
G132	121	97	1	0	0	0	0	0	0	106	5	107	3	85	115	-1	-27	107	3
G90	380	94	0	0	0	0	0	0	0	125	7	120	3	227	137	4	47	120	3
G28	262	129	0	0	0	0	0	0	0	168	10	166	5	211	143	2	21	166	5
G146	120	129	1	0	0	0	0	0	0	170	10	166	5	235	143	3	30	166	5
G8	218	362	2	0	0	0	0	0	0	175	9	174	5	192	127	1	9	174	5
G45	310	231	1	0	0	0	0	0	0	171	23	175	7	127	328	-2	-38	175	7
G69	232	254	1	0	0	0	0	0	0	181	17	189	6	75	235	-4	-151	189	6
G124	120	191	2	0	0	0	0	0	0	187	11	190	5	156	141	-2	-22	190	5
G12	948	175	0	0	0	0	0	0	0	194	8	191	5	236	93	2	19	191	5
G119	505	21	0	0	0	0	0	0	0	212	12	211	6	236	142	1	11	211	6
G148	576	158	0	0	0	0	0	0	0	225	24	229	8	191	265	-2	-20	229	8
G51	1020	16	0	0	0	0	0	0	0	339	12	336	9	362	85	1	7	336	9
G104	96	78	1	1	0	0	0	0	0	466	17	463	12	484	93	1	4	463	12
G59	76	134	2	1	0	0	0	0	0	592	18	587	15	618	81	1	5	587	15
G110	463	30	0	1	0	0	0	0	0	642	43	602	20	791	185	7	24	602	20
G143	231	965	4	1	0	0	0	0	0	597	19	603	15	579	83	-1	-4	603	15
G125	406	48	0	2	0	0	0	0	0	990	33	961	26	1058	101	3	9	961	26
G39	676	189	0	2	0	0	0	0	0	1031	37	1013	28	1073	111	2	6	1013	28
G107	122	182	1	2	0	0	0	0	0	1014	26	1019	26	1007	77	-1	-1	1019	26
GG1	33	76	2	2	0	0	0	0	0	1042	30	1031	26	1071	86	1	4	1031	26
G41	82	83	1	2	0	0	0	0	0	1031	21	1035	25	1026	58	0	-1	1035	25
G7	283	680	2	2	0	0	0	0	0	1094	28	1036	26	1214	77	6	15	1036	26
G50	132	97	1	2	0	0	0	0	0	1024	26	1038	26	1001	76	-1	-4	1038	26
G34	161	201	1	2	0	0	0	0	0	1075	28	1042	27	1147	78	3	9	1042	27
G134	58	412	7	2	0	0	0	0	0	1033	45	1046	30	1011	136	-1	-3	1046	30
G120	128	189	1	2	0	0	0	0	0	1033	26	1047	26	1009	76	-1	-4	1047	26

				RATIO						AGES								Best	
Grain	U [ppm]	Th [ppm]	Th/U	207/ 235	± s.e.	206/ 238	± s.e.	207/ 206	± s.e.	207/ 235	± 2s	206/ 238	± 2s	207/ 206	± 2s	%disc (5/8)	%disc (7/6)	Age [Ma]	± 2s
G47	48	142	3	2	0	0	0	0	0	1082	38	1054	29	1143	109	3	8	1054	29
G75	904	160	0	2	0	0	0	0	0	1113	30	1145	29	1057	85	-3	-8	1057	85
G140	381	354	1	2	0	0	0	0	0	1048	28	1062	27	1023	81	-1	-4	1062	27
G130	317	125	0	2	0	0	0	0	0	1102	48	1066	32	1178	139	3	10	1066	32
G13	49	48	1	2	0	0	0	0	0	1077	21	1073	26	1089	54	0	1	1073	26
G37	627	176	0	2	0	0	0	0	0	1060	23	1074	26	1036	62	-1	-4	1074	26
G101	773	51	0	2	0	0	0	0	0	1091	28	1102	28	1074	79	-1	-3	1074	79
G85	1697	92	0	2	0	0	0	0	0	1090	29	1101	28	1074	83	-1	-2	1074	83
G3	199	126	1	2	0	0	0	0	0	1128	61	1080	36	1226	174	4	12	1080	36
G151	468	219	0	2	0	0	0	0	0	1066	46	1083	31	1035	138	-2	-5	1083	31
G96	265	197	1	2	0	0	0	0	0	1087	24	1084	27	1096	65	0	1	1084	27
G92	899	58	0	2	0	0	0	0	0	1079	41	1088	30	1067	122	-1	-2	1088	30
G111	1189	309	0	2	0	0	0	0	0	1094	30	1096	28	1094	84	0	0	1096	28
G89	394	24	0	2	0	0	0	0	0	1111	23	1116	27	1104	60	-1	-1	1104	60
G11	379	137	0	2	0	0	0	0	0	1137	38	1155	31	1108	106	-2	-4	1108	106
G14	846	240	0	2	0	0	0	0	0	1121	23	1130	28	1109	59	-1	-2	1109	59
G79	406	63	0	2	0	0	0	0	0	1177	26	1200	29	1138	66	-2	-5	1138	66
G20	136	216	2	2	0	0	0	0	0	1140	31	1124	29	1176	85	1	4	1176	85
G4	1	375	653	2	0	0	0	0	0	1156	21	1144	28	1184	52	1	3	1184	52
G42	108	35	0	2	0	0	0	0	0	1187	28	1188	30	1191	73	0	0	1191	73
G86	161	49	0	2	0	0	0	0	0	1207	36	1213	32	1201	95	0	-1	1201	95
G122	136	53	0	2	0	0	0	0	0	1201	26	1201	29	1205	67	0	0	1205	67
G49	490	347	1	2	0	0	0	0	0	1172	23	1150	28	1218	57	2	6	1218	57
G64	676	112	0	2	0	0	0	0	0	1217	49	1218	35	1220	133	0	0	1220	133
G126	521	42	0	2	0	0	0	0	0	1217	27	1211	30	1230	69	0	2	1230	69
G60	394	6	0	2	0	0	0	0	0	1226	24	1225	30	1232	58	0	1	1232	58
G19	1062	92	0	2	0	0	0	0	0	1246	25	1255	30	1236	61	-1	-2	1236	61
G103	213	337	2	2	0	0	0	0	0	1270	30	1291	32	1238	75	-2	-4	1238	75
G138	109	157	1	2	0	0	0	0	0	1229	38	1223	32	1245	100	1	2	1245	100
G21	24	51	2	2	0	0	0	0	0	1265	32	1275	32	1253	80	-1	-2	1253	80
G24	76	45	1	2	0	0	0	0	0	1268	25	1272	31	1266	58	0	-1	1266	58
G67	2530	14	0	2	0	0	0	0	0	1250	24	1228	30	1292	57	2	5	1292	57
G139	349	62	0	3	0	0	0	0	0	1338	30	1338	33	1343	73	0	0	1343	73

Grain	U [ppm]	Th [ppm]	Th/U	RATIO 207/ 235	± s.e.	206/ 238	± s.e.	207/ 206	± s.e.	AGES 207/ 235	± 2s	206/ 238	± 2s	207/ 206	± 2s	%disc (5/8)	%disc (7/6)	Best Age [Ma]	± 2s
G22	204	169	1	3	0	0	0	0	0	1378	37	1383	36	1376	90	0	-1	1376	90
G15	714	93	0	3	0	0	0	0	0	1402	27	1421	34	1377	62	-1	-3	1377	62
G55	74	994	14	3	0	0	0	0	0	1435	27	1461	35	1401	60	-2	-4	1401	60
G141	189	25	0	3	0	0	0	0	0	1419	28	1429	34	1410	64	-1	-1	1410	64
G6	768	154	0	3	0	0	0	0	0	1409	26	1409	34	1414	56	0	0	1414	56
G108	45	28	1	3	0	0	0	0	0	1409	31	1382	34	1453	71	2	5	1453	71
G135	568	56	0	3	0	0	0	0	0	1484	27	1502	35	1464	57	-1	-3	1464	57
G91	157	72	0	3	0	0	0	0	0	1507	40	1510	40	1507	93	0	0	1507	93
G17	350	296	1	3	0	0	0	0	0	1472	28	1436	35	1530	61	3	6	1530	61
G80	28	56	2	4	0	0	0	0	0	1630	25	1629	38	1635	48	0	0	1635	48
G127	1868	54	0	4	0	0	0	0	0	1698	26	1721	40	1675	51	-1	-3	1675	51
G144	284	222	1	4	0	0	0	0	0	1673	29	1669	39	1682	58	0	1	1682	58
G128	189	128	1	4	0	0	0	0	0	1726	29	1749	41	1701	58	-1	-3	1701	58
G123	6	95	15	4	0	0	0	0	0	1717	28	1730	40	1706	55	-1	-1	1706	55
G99	1604	665	0	4	0	0	0	0	0	1702	30	1695	40	1714	61	0	1	1714	61
G142	96	196	2	4	0	0	0	0	0	1724	29	1731	40	1720	58	0	-1	1720	58
G109	667	444	1	5	0	0	0	0	0	1731	27	1742	40	1723	53	-1	-1	1723	53
G27	426	465	1	4	0	0	0	0	0	1729	28	1727	40	1736	54	0	1	1736	54
G46	919	290	0	5	0	0	0	0	0	1765	26	1779	41	1753	50	-1	-1	1753	50
G136	1509	19	0	5	0	0	0	0	0	1779	29	1804	42	1754	56	-1	-3	1754	56
G145	426	33	0	5	0	0	0	0	0	1820	29	1879	43	1757	55	-3	-7	1757	55
G77	155	701	5	5	0	0	0	0	0	1783	27	1793	41	1775	50	-1	-1	1775	50
G35	353	21	0	5	0	0	0	0	0	1823	26	1801	41	1854	46	1	3	1854	46
G112	55	93	2	5	0	0	0	0	0	1848	32	1847	44	1854	63	0	0	1854	63
G18	157	383	2	5	0	0	0	0	0	1862	42	1864	48	1863	85	0	0	1863	85
G26	43	273	6	5	0	0	0	0	0	1868	28	1867	43	1872	51	0	0	1872	51
G52	1108	126	0	5	0	0	0	0	0	1893	27	1912	44	1876	49	-1	-2	1876	49
G133	126	82	1	6	0	0	0	0	0	1905	29	1932	44	1880	54	-1	-3	1880	54
G95	510	207	0	6	0	0	0	0	0	1929	33	1959	46	1900	62	-2	-3	1900	62
G82	117	94	1	6	0	0	0	0	0	1954	29	1997	46	1913	52	-2	-4	1913	52
G72	210	93	0	11	0	0	0	0	0	2512	29	2547	55	2488	44	-1	-2	2488	44
G10	400	137	0	12	0	0	0	0	0	2591	28	2546	55	2631	41	2	3	2631	41
G147	201	191	1	12	0	0	0	0	0	2619	29	2602	56	2636	45	1	1	2636	45

Grain	U [ppm]	Th [ppm]	Th/U	RATIO 207/235	± s.e.	206/238	± s.e.	207/206	± s.e.	AGES 207/235	± 2s	206/238	± 2s	207/206	± 2s	%disc (5/8)	%disc (7/6)	Best Age [Ma]	± 2s
G83	1494	358	0	13	0	1	0	0	0	2673	34	2639	60	2702	53	1	2	2702	53
G113	68	290	4	14	0	1	0	0	0	2749	33	2804	62	2713	52	-2	-3	2713	52
G121	1288	316	0	14	0	1	0	0	0	2731	32	2757	61	2716	50	-1	-2	2716	50
G65	298	181	1	14	0	1	0	0	0	2726	31	2732	60	2725	46	0	0	2725	46
G63	153	48	0	15	0	1	0	0	0	2790	29	2884	61	2726	42	-3	-6	2726	42
G48	368	478	1	14	0	1	0	0	0	2747	31	2777	61	2728	47	-1	-2	2728	47
G73	391	268	1	14	0	1	0	0	0	2766	30	2791	60	2751	45	-1	-1	2751	45
G33	198	534	3	14	0	1	0	0	0	2759	30	2775	61	2752	46	-1	-1	2752	46
G32	332	393	1	14	0	1	0	0	0	2744	28	2727	58	2760	41	1	1	2760	41
G66	384	107	0	15	0	1	0	0	0	2836	28	2806	59	2861	40	1	2	2861	40
G23	76	95	1	17	0	1	0	0	0	2954	29	3071	64	2878	40	-4	-7	2878	40
G70	2037	23	0	17	0	1	0	0	0	2950	29	3014	63	2911	41	-2	-4	2911	41
G87	603	65	0	18	0	1	0	0	0	2990	40	2956	72	3016	63	1	2	3016	63
G137	1335	153	0	28	0	1	0	0	0	3419	31	3371	69	3452	42	1	2	3452	42
Sample W11-2																			
G1	1239	883	1	0	0	0	0	0	0	101	5	93	2	319	119	9	71	93	2
G2	386	135	0	5	0	0	0	0	0	1816	23	1748	31	1906	50	4	8	1906	50
G3	426	192	0	4	0	0	0	0	0	1626	22	1561	28	1722	51	4	9	1722	51
G4	292	122	0	4	0	0	0	0	0	1683	23	1618	29	1774	52	4	9	1774	52
G5	281	46	0	2	0	0	0	0	0	933	20	919	18	977	67	2	6	919	18
G6	71	22	0	2	0	0	0	0	0	1168	30	1094	22	1318	85	7	17	1094	22
G7	367	162	0	4	0	0	0	0	0	1720	23	1672	30	1789	52	3	7	1789	52
G8	292	85	0	4	0	0	0	0	0	1689	23	1645	30	1753	52	3	6	1753	52
G9	175	78	0	4	0	0	0	0	0	1675	24	1619	30	1756	55	3	8	1756	55
G10	720	219	0	4	0	0	0	0	0	1689	22	1622	29	1782	50	4	9	1782	50
G11	407	149	0	4	0	0	0	0	0	1635	22	1567	28	1732	51	4	10	1732	51
G12	351	114	0	2	0	0	0	0	0	1101	20	1017	19	1278	60	8	20	1017	19
G13	389	240	1	4	0	0	0	0	0	1683	23	1623	29	1768	52	4	8	1768	52
G14	368	246	1	2	0	0	0	0	0	957	20	898	17	1104	64	7	19	898	17
G15	208	154	1	3	0	0	0	0	0	1427	23	1381	26	1507	58	3	8	1507	58
G16	25	31	1	13	0	0	0	0	0	2675	39	2604	55	2738	70	3	5	2738	70
G17	352	210	1	3	0	0	0	0	0	1412	22	1375	25	1478	56	3	7	1478	56

				RATIO						AGES									
	U	Th		207/		206/		207/		207/		206/		207/		%disc	%disc	Best Age	
Grain	[ppm]	[ppm]	Th/U	235	± s.e.	238	± s.e.	206	± s.e.	235	± 2s	238	± 2s	206	± 2s	(5/8)	(7/6)	[Ma]	± 2s
G18	1170	437	0	0	0	0	0	0	0	103	5	98	2	243	128	6	60	98	2
G19	229	123	1	13	0	0	0	0	0	2646	26	2566	44	2716	47	3	6	2716	47
G20	425	204	0	5	0	0	0	0	0	1862	24	1858	33	1876	51	0	1	1876	51
G21	545	275	1	3	0	0	0	0	0	1380	21	1343	25	1446	54	3	7	1446	54
G22	238	99	0	4	0	0	0	0	0	1633	24	1581	29	1708	55	3	7	1708	55
G23	185	108	1	4	0	0	0	0	0	1694	25	1652	30	1755	56	3	6	1755	56
G24	173	76	0	4	0	0	0	0	0	1630	25	1580	29	1703	58	3	7	1703	58
G25	382	254	1	3	0	0	0	0	0	1422	22	1380	25	1494	56	3	8	1494	56
G26	887	804	1	5	0	0	0	0	0	1740	23	1671	30	1833	52	4	9	1833	52
G27	755	424	1	15	0	1	0	0	0	2813	26	2745	45	2870	45	2	4	2870	45
G28	255	341	1	2	0	0	0	0	0	981	21	892	17	1194	69	10	25	892	17
G29	1306	1200	1	4	0	0	0	0	0	1653	23	1587	28	1745	52	4	9	1745	52
G30	730	226	0	4	0	0	0	0	0	1633	24	1581	29	1710	56	3	8	1710	56
G31	651	951	1	1	0	0	0	0	0	418	13	392	8	577	83	7	32	392	8
G32	744	461	1	0	0	0	0	0	0	96	6	91	2	249	156	6	64	91	2
G33	219	164	1	3	0	0	0	0	0	1343	26	1308	25	1407	68	3	7	1407	68
G34	114	43	0	4	0	0	0	0	0	1619	32	1565	30	1697	74	3	8	1697	74
G35	170	80	0	2	0	0	0	0	0	1007	29	957	20	1123	91	5	15	957	20
G36	378	123	0	5	0	0	0	0	0	1794	29	1814	33	1777	64	-1	-2	1777	64
G37	740	170	0	3	0	0	0	0	0	1383	24	1350	25	1442	63	2	6	1442	63
G38	325	92	0	4	0	0	0	0	0	1692	27	1644	30	1759	62	3	7	1759	62
G39	203	166	1	5	0	0	0	0	0	1812	29	1759	32	1880	63	3	6	1880	63
G40	355	194	1	3	0	0	0	0	0	1413	26	1367	26	1490	66	3	8	1490	66
G41	1958	1178	1	0	0	0	0	0	0	89	4	85	2	193	111	4	56	85	2
G42	442	202	0	11	0	0	0	0	0	2492	30	2398	41	2576	56	4	7	2576	56
G43	321	239	1	0	0	0	0	0	0	187	12	174	4	362	162	7	52	174	4
G44	157	97	1	8	0	0	0	0	0	2266	32	2222	40	2313	63	2	4	2313	63
G45	600	282	0	0	0	0	0	0	0	187	9	175	4	344	120	7	49	175	4
G46	456	202	0	4	0	0	0	0	0	1637	28	1595	29	1697	65	3	6	1697	65
G47	696	282	0	2	0	0	0	0	0	1164	24	1079	21	1332	70	8	19	1079	21
G48	1707	2099	1	0	0	0	0	0	0	75	4	72	2	196	120	5	63	72	2
G49	423	721	2	11	0	0	0	0	0	2531	32	2495	43	2566	59	1	3	2566	59
G50	331	261	1	12	0	0	0	0	0	2599	33	2452	43	2722	60	6	10	2722	60

				RATIO						AGES									
Grain	**U [ppm]**	**Th [ppm]**	**Th/U**	**207/ 235**	**± s.e.**	**206/ 238**	**± s.e.**	**207/ 206**	**± s.e.**	**207/ 235**	**± 2s**	**206/ 238**	**± 2s**	**207/ 206**	**± 2s**	**%disc (5/8)**	**%disc (7/6)**	**Best Age [Ma]**	**± 2s**
G51	401	264	1	4	0	0	0	0	0	1680	29	1616	30	1767	67	4	9	1767	67
G52	473	179	0	4	0	0	0	0	0	1643	29	1597	29	1707	68	3	6	1707	68
G53	303	166	1	2	0	0	0	0	0	1177	27	1144	22	1243	76	3	8	1243	76
G54	659	328	0	4	0	0	0	0	0	1706	29	1648	30	1783	67	4	8	1783	67
G55	251	157	1	1	0	0	0	0	0	516	20	498	11	602	106	4	17	498	11
G56	453	181	0	4	0	0	0	0	0	1671	30	1599	29	1768	68	5	10	1768	68
G57	76	56	1	3	0	0	0	0	0	1441	35	1418	29	1481	87	2	4	1481	87
G58	705	660	1	3	0	0	0	0	0	1407	28	1381	26	1451	72	2	5	1451	72
G59	296	90	0	2	0	0	0	0	0	996	25	978	19	1041	83	2	6	978	19
G60	530	226	0	2	0	0	0	0	0	1004	24	983	19	1055	79	2	7	983	19
G61	1555	1042	1	0	0	0	0	0	0	159	6	149	3	309	102	6	52	149	3
G62	390	64	0	2	0	0	0	0	0	937	25	878	17	1086	83	7	19	878	17
G63	7421	3927	1	0	0	0	0	0	0	35	2	34	1	154	106	5	78	34	1
G64	637	202	0	4	0	0	0	0	0	1719	30	1666	30	1789	69	3	7	1789	69
G65	262	61	0	5	0	0	0	0	0	1813	32	1768	32	1869	70	3	5	1869	70
G66	598	476	1	1	0	0	0	0	0	595	19	579	12	659	91	3	12	579	12
G67	322	190	1	11	0	0	0	0	0	2539	34	2526	44	2554	64	1	1	2554	64
G68	366	209	1	1	0	0	0	0	0	413	17	394	8	529	111	5	26	394	8
G69	318	78	0	4	0	0	0	0	0	1668	31	1639	30	1709	73	2	4	1709	73
G70	417	173	0	2	0	0	0	0	0	1055	26	1029	20	1114	82	3	8	1029	20
G71	822	126	0	7	0	0	0	0	0	2169	34	2062	37	2277	67	5	9	2277	67
G72	490	315	1	4	0	0	0	0	0	1692	21	1668	30	1726	48	1	3	1726	48
G73	862	372	0	4	0	0	0	0	0	1697	21	1706	30	1690	47	-1	-1	1690	47
G74	268	217	1	13	0	0	0	0	0	2659	24	2603	44	2706	42	2	4	2706	42
G75	444	341	1	3	0	0	0	0	0	1454	21	1456	27	1456	51	0	0	1456	51
G76	684	286	0	0	0	0	0	0	0	36	4	33	1	200	269	7	83	33	1
G77	493	402	1	4	0	0	0	0	0	1637	21	1621	29	1661	49	1	2	1661	49
G78	323	145	0	4	0	0	0	0	0	1715	22	1670	30	1774	49	3	6	1774	49
G79	456	164	0	5	0	0	0	0	0	1740	22	1758	31	1724	48	-1	-2	1724	48
G80	680	439	1	0	0	0	0	0	0	37	4	35	1	191	267	6	82	35	1
G81	138	111	1	4	0	0	0	0	0	1677	25	1646	31	1720	57	2	4	1720	57
G82	346	258	1	2	0	0	0	0	0	1183	20	1173	22	1208	58	1	3	1208	58
G83	303	226	1	4	0	0	0	0	0	1637	22	1638	30	1640	51	0	0	1640	51

				RATIO						AGES									
Grain	U [ppm]	Th [ppm]	Th/U	207/ 235	± s.e.	206/ 238	± s.e.	207/ 206	± s.e.	207/ 235	± 2s	206/ 238	± 2s	207/ 206	± 2s	%disc (5/8)	%disc (7/6)	Best Age [Ma]	± 2s
G84	271	142	1	2	0	0	0	0	0	1031	21	974	19	1159	64	6	16	974	19
G85	75	41	1	4	0	0	0	0	0	1598	29	1625	32	1567	69	-2	-4	1567	69
G86	210	109	1	4	0	0	0	0	0	1672	24	1650	30	1704	54	1	3	1704	54
G87	668	124	0	1	0	0	0	0	0	452	12	454	9	443	73	-1	-3	454	9
G88	480	240	0	3	0	0	0	0	0	1405	21	1398	26	1419	54	0	1	1419	54
G89	466	69	0	4	0	0	0	0	0	1659	25	1592	30	1749	56	4	9	1749	56
G90	617	559	1	0	0	0	0	0	0	65	7	61	2	191	255	5	68	61	2
G91	229	322	1	2	0	0	0	0	0	1270	23	1257	24	1297	62	1	3	1297	62
G92	263	68	0	5	0	0	0	0	0	1777	24	1776	32	1782	52	0	0	1782	52
G93	930	403	0	0	0	0	0	0	0	96	5	95	2	106	128	0	10	95	2
G94	251	104	0	5	0	0	0	0	0	1743	25	1760	32	1727	57	-1	-2	1727	57
G95	134	63	0	4	0	0	0	0	0	1728	26	1743	32	1715	59	-1	-2	1715	59
G96	204	212	1	3	0	0	0	0	0	1390	24	1392	26	1392	62	0	0	1392	62
G97	176	79	0	3	0	0	0	0	0	1445	25	1445	27	1449	62	0	0	1449	62
G98	208	137	1	3	0	0	0	0	0	1481	25	1470	28	1500	61	1	2	1500	61
G99	130	110	1	1	0	0	0	0	0	476	29	472	12	504	170	1	6	472	12
G100	293	118	0	3	0	0	0	0	0	1368	25	1349	26	1403	63	1	4	1403	63
G101	233	145	1	15	0	1	0	0	0	2800	28	2720	47	2861	48	3	5	2861	48
G102	150	77	1	2	0	0	0	0	0	1054	25	1036	21	1096	78	2	5	1036	21
G103	492	87	0	0	0	0	0	0	0	362	13	366	8	346	94	-1	-6	366	8
G104	410	203	0	5	0	0	0	0	0	1775	25	1756	32	1801	54	1	3	1801	54
G105	1004	1483	1	0	0	0	0	0	0	58	4	56	1	161	176	4	65	56	1
G106	353	158	0	2	0	0	0	0	0	1272	24	1314	25	1206	66	-3	-9	1206	66
G107	301	248	1	2	0	0	0	0	0	1179	25	1166	23	1209	71	1	4	1209	71
G108	300	76	0	17	0	1	0	0	0	2915	29	2935	50	2905	49	-1	-1	2905	49
G109	1256	1172	1	0	0	0	0	0	0	32	3	33	1	14	215	-1	-140	33	1
G110	434	174	0	0	0	0	0	0	0	300	12	296	6	332	109	1	11	296	6
G111	763	99	0	2	0	0	0	0	0	1160	21	1163	22	1160	62	0	0	1160	62
G112	191	64	0	5	0	0	0	0	0	1840	28	1845	34	1838	61	0	0	1838	61
G113	337	436	1	1	0	0	0	0	0	633	19	591	12	794	84	7	26	591	12
G114	160	78	0	1	0	0	0	0	0	419	22	419	10	422	139	0	1	419	10
G115	613	369	1	4	0	0	0	0	0	1603	25	1592	29	1623	58	1	2	1623	58
G116	376	344	1	0	0	0	0	0	0	356	15	365	8	304	111	-2	-20	365	8

Grain	U [ppm]	Th [ppm]	Th/U	RATIO 207/235	± s.e.	206/238	± s.e.	207/206	± s.e.	AGES 207/235	± 2s	206/238	± 2s	207/206	± 2s	%disc (5/8)	%disc (7/6)	Best Age [Ma]	± 2s
G117	92	15	0	3	0	0	0	0	0	1404	31	1363	28	1471	79	3	7	1471	79
G118	122	68	1	7	0	0	0	0	0	2166	33	2267	43	2077	65	-4	-9	2077	65
G119	404	166	0	4	0	0	0	0	0	1678	27	1685	31	1674	60	0	-1	1674	60
G120	157	119	1	2	0	0	0	0	0	1189	29	1191	24	1190	82	0	0	1190	82
G121	528	336	1	3	0	0	0	0	0	1360	25	1349	26	1382	64	1	2	1382	64
G122	230	49	0	2	0	0	0	0	0	1207	26	1206	24	1214	73	0	1	1214	73
G123	370	165	0	10	0	0	0	0	0	2472	30	2491	43	2460	55	-1	-1	2460	55
G124	841	552	1	0	0	0	0	0	0	64	5	64	2	36	183	-1	-81	64	2
Sample B1-2																			
G1	407	240	1	3	0	0	0	0	0	1490	20	1436	27	1570	49	4	9	1570	49
G2	315	153	0	6	0	0	0	0	0	2038	22	2000	35	2080	44	2	4	2080	44
G3	613	338	1	6	0	0	0	0	0	1913	21	1936	34	1893	44	-1	-2	1893	44
G4	516	448	1	4	0	0	0	0	0	1678	21	1667	30	1695	46	1	2	1695	46
G5	400	131	0	0	0	0	0	0	0	173	9	169	4	233	135	2	27	169	4
G6	1156	771	1	0	0	0	0	0	0	77	4	76	2	122	126	2	38	76	2
G7	304	131	0	3	0	0	0	0	0	1509	21	1511	28	1510	50	0	0	1510	50
G8	249	109	0	2	0	0	0	0	0	1102	21	1026	20	1261	61	7	19	1026	20
G9	160	45	0	2	0	0	0	0	0	1186	23	1203	23	1159	66	-1	-4	1159	66
G10	279	109	0	4	0	0	0	0	0	1702	22	1695	31	1716	48	0	1	1716	48
G11	207	184	1	4	0	0	0	0	0	1649	22	1635	30	1670	51	1	2	1670	51
G12	121	58	0	4	0	0	0	0	0	1681	24	1668	31	1702	55	1	2	1702	55
G13	155	298	2	3	0	0	0	0	0	1345	23	1305	25	1412	60	3	8	1412	60
G14	335	192	1	3	0	0	0	0	0	1466	21	1485	28	1443	51	-1	-3	1443	51
G15	363	255	1	4	0	0	0	0	0	1679	21	1671	30	1693	48	0	1	1693	48
G16	116	54	0	4	0	0	0	0	0	1702	25	1682	32	1730	56	1	3	1730	56
G17	273	86	0	2	0	0	0	0	0	995	20	991	19	1007	63	0	2	991	19
G18	840	173	0	5	0	0	0	0	0	1768	21	1760	32	1781	45	0	1	1781	45
G19	246	104	0	4	0	0	0	0	0	1695	22	1702	31	1689	50	0	-1	1689	50
G20	724	586	1	0	0	0	0	0	0	93	5	92	2	139	142	2	34	92	2
G21	317	158	0	2	0	0	0	0	0	1234	20	1211	23	1277	56	2	5	1277	56
G22	147	57	0	15	0	1	0	0	0	2791	24	2740	47	2830	42	2	3	2830	42
G23	650	661	1	0	0	0	0	0	0	164	7	156	3	284	112	5	45	156	3

				RATIO						AGES									
Grain	**U [ppm]**	**Th [ppm]**	**Th/U**	**207/ 235**	**± s.e.**	**206/ 238**	**± s.e.**	**207/ 206**	**± s.e.**	**207/ 235**	**± 2s**	**206/ 238**	**± 2s**	**207/ 206**	**± 2s**	**%disc (5/8)**	**%disc (7/6)**	**Best Age [Ma]**	**± 2s**
G24	257	93	0	3	0	0	0	0	0	1398	23	1374	26	1439	59	2	4	1439	59
G25	208	74	0	3	0	0	0	0	0	1386	22	1333	25	1473	57	4	10	1473	57
G26	292	124	0	5	0	0	0	0	0	1801	22	1776	32	1834	48	1	3	1834	48
G27	1338	1310	1	0	0	0	0	0	0	161	6	159	3	199	89	1	20	159	3
G28	349	105	0	4	0	0	0	0	0	1697	22	1701	31	1696	49	0	0	1696	49
G29	445	168	0	0	0	0	0	0	0	366	13	362	8	400	89	1	10	362	8
G30	999	495	0	0	0	0	0	0	0	175	6	169	4	256	93	3	34	169	4
G31	230	102	0	1	0	0	0	0	0	426	22	407	10	538	138	5	24	407	10
G32	100	50	1	4	0	0	0	0	0	1574	29	1522	30	1648	68	3	8	1648	68
G33	823	518	1	0	0	0	0	0	0	166	7	162	4	230	113	3	29	162	4
G34	298	234	1	3	0	0	0	0	0	1436	22	1420	27	1463	54	1	3	1463	54
G35	579	157	0	2	0	0	0	0	0	1008	19	991	19	1051	60	2	6	991	19
G36	572	328	1	4	0	0	0	0	0	1667	21	1607	29	1748	48	4	8	1748	48
G37	295	82	0	4	0	0	0	0	0	1714	23	1704	31	1731	50	1	2	1731	50
G38	110	60	1	1	0	0	0	0	0	689	26	632	14	882	109	9	28	632	14
G39	283	64	0	4	0	0	0	0	0	1643	23	1638	30	1652	52	0	1	1652	52
G40	616	99	0	2	0	0	0	0	0	1022	18	993	19	1089	57	3	9	993	19
G41	364	244	1	7	0	0	0	0	0	2082	23	2009	36	2159	46	4	7	2159	46
G42	832	321	0	0	0	0	0	0	0	101	7	94	2	278	162	8	66	94	2
G43	666	34	0	4	0	0	0	0	0	1722	22	1726	31	1721	49	0	0	1721	49
G44	510	103	0	4	0	0	0	0	0	1646	22	1664	31	1628	51	-1	-2	1628	51
G45	359	157	0	0	0	0	0	0	0	105	9	105	3	121	207	0	14	105	3
G46	139	95	1	12	0	1	0	0	0	2637	26	2629	46	2647	47	0	1	2647	47
G47	394	190	0	0	0	0	0	0	0	79	10	78	2	113	290	1	31	78	2
G48	523	227	0	2	0	0	0	0	0	1066	21	1046	20	1111	64	2	6	1046	20
G49	274	338	1	0	0	0	0	0	0	410	17	397	9	486	112	3	18	397	9
G50	436	163	0	1	0	0	0	0	0	923	19	905	18	970	64	2	7	905	18
G51	812	409	1	2	0	0	0	0	0	1085	19	1070	20	1119	56	1	4	1070	20
G52	520	558	1	0	0	0	0	0	0	237	11	232	5	289	118	2	20	232	5
G53	153	121	1	4	0	0	0	0	0	1699	26	1701	32	1701	59	0	0	1701	59
G54	228	63	0	2	0	0	0	0	0	1168	23	1165	23	1180	66	0	1	1180	66
G55	745	176	0	4	0	0	0	0	0	1683	23	1620	30	1765	52	4	8	1765	52
G56	433	152	0	4	0	0	0	0	0	1671	24	1618	30	1742	55	3	7	1742	55

Grain	U [ppm]	Th [ppm]	Th/U	RATIO						AGES						%disc (5/8)	%disc (7/6)	Best Age [Ma]	± 2s
				207/ 235	± s.e.	206/ 238	± s.e.	207/ 206	± s.e.	207/ 235	± 2s	206/ 238	± 2s	207/ 206	± 2s				
G57	330	80	0	0	0	0	0	0	0	121	11	116	3	219	212	4	47	116	3
G58	91	78	1	2	0	0	0	0	0	1089	30	1076	23	1120	90	1	4	1076	23
G59	411	138	0	2	0	0	0	0	0	1158	21	1167	22	1146	62	-1	-2	1146	62
G60	216	114	1	5	0	0	0	0	0	1778	25	1752	33	1813	55	1	3	1813	55
G61	238	126	1	4	0	0	0	0	0	1645	26	1625	31	1675	60	1	3	1675	60
G62	123	92	1	24	0	1	0	0	0	3287	28	3260	54	3307	45	1	1	3307	45
G63	294	324	1	5	0	0	0	0	0	1810	25	1788	33	1839	54	1	3	1839	54
G64	295	126	0	0	0	0	0	0	0	140	12	130	3	330	201	8	61	130	3
G65	166	58	0	1	0	0	0	0	0	914	25	835	18	1115	83	9	25	835	18
G66	387	454	1	16	0	1	0	0	0	2876	28	2859	49	2892	47	1	1	2892	47
G67	655	298	0	2	0	0	0	0	0	1145	21	1073	21	1290	59	7	17	1073	21
G68	35	50	1	2	0	0	0	0	0	999	54	951	25	1110	167	5	14	951	25
G69	1108	320	0	2	0	0	0	0	0	1053	20	1041	20	1081	62	1	4	1041	20
G70	382	133	0	4	0	0	0	0	0	1691	25	1664	31	1729	56	2	4	1729	56
G71	201	81	0	2	0	0	0	0	0	1055	26	1030	21	1111	79	2	7	1030	21
G72	202	130	1	1	0	0	0	0	0	427	20	420	10	468	127	2	10	420	10
G73	205	160	1	4	0	0	0	0	0	1694	28	1690	33	1703	64	0	1	1703	64
G74	330	216	1	5	0	0	0	0	0	1792	26	1798	33	1788	56	0	-1	1788	56
G75	193	193	1	3	0	0	0	0	0	1450	26	1462	28	1437	65	-1	-2	1437	65
G76	263	121	0	4	0	0	0	0	0	1651	27	1608	31	1710	62	3	6	1710	62
G77	160	59	0	2	0	0	0	0	0	1181	28	1179	24	1188	80	0	1	1188	80
G78	740	503	1	0	0	0	0	0	0	90	6	86	2	186	170	4	54	86	2
G79	390	612	2	1	0	0	0	0	0	629	18	626	13	646	83	1	3	626	13
G80	254	98	0	3	0	0	0	0	0	1477	27	1470	28	1492	65	0	1	1492	65
G81	72	38	1	3	0	0	0	0	0	1315	34	1311	28	1327	91	0	1	1327	91
G82	225	129	1	4	0	0	0	0	0	1719	27	1743	33	1694	61	-1	-3	1694	61
G83	682	494	1	5	0	0	0	0	0	1781	26	1745	32	1827	56	2	4	1827	56
G84	705	364	1	5	0	0	0	0	0	1741	26	1757	32	1725	57	-1	-2	1725	57
G85	147	86	1	4	0	0	0	0	0	1674	29	1687	33	1663	67	-1	-1	1663	67
G86	735	452	1	2	0	0	0	0	0	1142	24	1121	22	1188	70	2	6	1188	70
G87	514	474	1	2	0	0	0	0	0	1087	28	1054	22	1156	83	3	9	1054	22
G88	694	450	1	4	0	0	0	0	0	1563	26	1506	28	1645	60	4	8	1645	60
G89	3139	859	0	0	0	0	0	0	0	91	4	89	2	134	105	2	34	89	2

				RATIO						AGES									
Grain	U [ppm]	Th [ppm]	Th/U	207/ 235	± s.e.	206/ 238	± s.e.	207/ 206	± s.e.	207/ 235	± 2s	206/ 238	± 2s	207/ 206	± 2s	%disc (5/8)	%disc (7/6)	Best Age [Ma]	± 2s
G90	170	50	0	1	0	0	0	0	0	631	27	625	14	657	121	1	5	625	14
G91	403	247	1	4	0	0	0	0	0	1634	29	1617	31	1660	66	1	3	1660	66
G92	1932	2373	1	0	0	0	0	0	0	68	4	63	1	225	137	7	72	63	1
G93	244	78	0	5	0	0	0	0	0	1775	31	1773	34	1782	68	0	1	1782	68
G94	328	145	0	11	0	0	0	0	0	2528	31	2426	43	2615	56	4	7	2615	56
G95	672	854	1	3	0	0	0	0	0	1437	27	1413	27	1476	66	2	4	1476	66
G96	197	95	0	7	0	0	0	0	0	2151	32	2092	39	2212	62	3	5	2212	62
G97	888	486	1	5	0	0	0	0	0	1735	29	1682	32	1803	64	3	7	1803	64
G98	233	121	1	4	0	0	0	0	0	1643	31	1625	31	1670	70	1	3	1670	70
G99	358	140	0	12	0	1	0	0	0	2588	33	2645	47	2547	59	-2	-4	2547	59
G100	194	161	1	3	0	0	0	0	0	1421	31	1387	28	1477	76	2	6	1477	76
G101	152	118	1	1	0	0	0	0	0	538	26	526	12	594	134	2	11	526	12
G102	835	518	1	2	0	0	0	0	0	1107	26	1081	22	1164	76	2	7	1081	22
G103	448	465	1	6	0	0	0	0	0	2026	33	1929	36	2130	65	5	9	2130	65
G104	6	2	0	4	0	0	0	0	0	1705	30	1710	33	1703	69	0	0	1703	69
G105	11	11	1	2	0	0	0	0	0	1069	26	1050	21	1113	80	2	6	1050	21
G106	20	9	0	3	0	0	0	0	0	1366	23	1352	25	1393	60	1	3	1393	60
G107	96	27	0	0	0	0	0	0	0	72	4	67	2	230	142	7	71	67	2
G108	22	7	0	1	0	0	0	0	0	412	18	389	9	553	117	6	30	389	9
G109	82	40	0	0	0	0	0	0	0	106	6	105	2	129	129	1	18	105	2
G110	27	7	0	1	0	0	0	0	0	451	16	434	9	541	97	4	20	434	9
G111	20	14	1	0	0	0	0	0	0	70	13	68	2	172	407	4	61	68	2
G112	34	13	0	5	0	0	0	0	0	1782	23	1774	32	1796	51	0	1	1796	51
G113	8	6	1	4	0	0	0	0	0	1681	34	1629	33	1752	76	3	7	1752	76
G114	49	30	1	4	0	0	0	0	0	1666	22	1618	29	1731	51	3	7	1731	51
G115	3	2	0	2	0	0	0	0	0	1129	42	1095	26	1199	122	3	9	1095	26
G116	42	35	1	0	0	0	0	0	0	10	4	11	1	0	651	-5	-10900	11	1
G117	44	22	1	1	0	0	0	0	0	571	15	561	11	612	77	2	8	561	11
G118	16	6	0	5	0	0	0	0	0	1747	28	1686	32	1826	61	4	8	1826	61
G119	8	9	1	3	0	0	0	0	0	1351	30	1320	26	1404	77	2	6	1404	77
G120	36	24	1	0	0	0	0	0	0	87	8	84	2	167	222	3	50	84	2
G121	62	13	0	4	0	0	0	0	0	1683	23	1702	30	1663	52	-1	-2	1663	52
G122	18	10	1	4	0	0	0	0	0	1690	25	1687	31	1698	58	0	1	1698	58

Grain	U [ppm]	Th [ppm]	Th/U	RATIO 207/235	± s.e.	206/238	± s.e.	207/206	± s.e.	AGES 207/235	± 2s	206/238	± 2s	207/206	± 2s	%disc (5/8)	%disc (7/6)	Best Age [Ma]	± 2s
G123	29	22	1	2	0	0	0	0	0	1140	22	1138	22	1149	65	0	1	1149	65
G124	86	43	0	0	0	0	0	0	0	96	6	89	2	298	137	9	70	89	2
G125	27	9	0	4	0	0	0	0	0	1680	25	1656	30	1715	56	1	3	1715	56
G126	75	16	0	4	0	0	0	0	0	1712	24	1691	30	1741	53	1	3	1741	53
G127	84	9	0	1	0	0	0	0	0	573	14	522	10	787	69	10	34	522	10
G128	26	47	2	2	0	0	0	0	0	1232	24	1220	23	1257	66	1	3	1257	66
G129	26	18	1	0	0	0	0	0	0	67	10	72	2	0	119	-8	-72300	72	2
G130	26	10	0	5	0	0	0	0	0	1803	28	1820	33	1788	61	-1	-2	1788	61
G131	59	21	0	5	0	0	0	0	0	1749	24	1742	31	1761	54	0	1	1761	54
G132	31	15	0	0	0	0	0	0	0	91	9	88	2	201	240	4	56	88	2
G133	21	10	0	3	0	0	0	0	0	1427	25	1402	26	1470	64	2	5	1470	64
G134	7	3	0	2	0	0	0	0	0	1103	32	1092	23	1130	97	1	3	1092	23
G135	19	10	1	4	0	0	0	0	0	1624	27	1582	29	1683	62	3	6	1683	62
G136	24	16	1	2	0	0	0	0	0	1022	28	1016	21	1039	89	1	2	1016	21
G137	22	7	0	2	0	0	0	0	0	1007	24	991	19	1048	75	2	5	991	19
G138	151	201	1	0	0	0	0	0	0	29	2	28	1	149	184	5	82	28	1
G139	10	1	0	1	0	0	0	0	0	610	27	603	14	641	128	1	6	603	14
G140	22	23	1	1	0	0	0	0	0	518	20	474	10	722	103	9	34	474	10
G141	9	6	1	2	0	0	0	0	0	1076	30	1071	22	1090	91	0	2	1071	22
G142	3	1	0	6	0	0	0	0	0	1901	49	1953	46	1849	104	-3	-6	1849	104
G143	20	13	1	5	0	0	0	0	0	1793	28	1805	33	1782	63	-1	-1	1782	63
G144	19	8	0	0	0	0	0	0	0	139	18	132	4	263	310	5	50	132	4
G145	14	10	1	1	0	0	0	0	0	437	21	441	10	421	134	-1	-5	441	10
G146	18	18	1	5	0	0	0	0	0	1758	29	1748	32	1774	65	1	1	1774	65
G147	13	11	1	4	0	0	0	0	0	1660	30	1642	31	1686	69	1	3	1686	69
G148	30	12	0	4	0	0	0	0	0	1692	28	1705	31	1679	64	-1	-2	1679	64
Sample 20092401																			
G1	298	156	1	0	0	0	0	0	0	236	12	235	5	191	132	1	-23	235	5
G2	288	146	1	1	0	0	0	0	0	420	15	416	9	384	98	1	-8	416	9
G3	152	41	0	2	0	0	0	0	0	1122	23	1103	21	1109	68	2	1	1109	68
G4	130	148	1	10	0	0	0	0	0	2414	24	2367	40	2410	44	2	2	2410	44
G5	173	79	0	3	0	0	0	0	0	1417	22	1403	26	1390	56	1	-1	1390	56

				RATIO						AGES									
Grain	U [ppm]	Th [ppm]	Th/U	207/ 235	± s.e.	206/ 238	± s.e.	207/ 206	± s.e.	207/ 235	± 2s	206/ 238	± 2s	207/ 206	± 2s	%disc (5/8)	%disc (7/6)	Best Age [Ma]	± 2s
G6	426	489	1	0	0	0	0	0	0	96	9	91	3	147	223	5	38	91	3
G7	212	118	1	16	0	1	0	0	0	2898	23	2864	46	2880	39	1	1	2880	39
G8	139	106	1	1	0	0	0	0	0	544	21	536	11	524	112	2	-2	536	11
G9	390	238	1	3	0	0	0	0	0	1354	21	1292	24	1406	55	5	8	1406	55
G10	120	55	0	2	0	0	0	0	0	1238	28	1197	24	1261	78	3	5	1261	78
G11	539	532	1	0	0	0	0	0	0	173	8	170	4	165	117	2	-3	170	4
G12	376	141	0	4	0	0	0	0	0	1693	22	1696	30	1644	49	0	-3	1644	49
G13	314	101	0	2	0	0	0	0	0	977	22	958	19	969	73	2	1	958	19
G14	985	437	0	0	0	0	0	0	0	91	5	91	2	18	124	-1	-402	91	2
G15	198	88	0	3	0	0	0	0	0	1386	22	1371	25	1362	56	1	-1	1362	56
G16	249	88	0	2	0	0	0	0	0	1146	20	1125	21	1139	59	2	1	1139	59
G17	728	28	0	10	0	0	0	0	0	2420	21	2377	39	2416	40	2	2	2416	40
G18	67	30	0	12	0	0	0	0	0	2624	26	2558	44	2636	46	3	3	2636	46
G19	21	10	0	2	0	0	0	0	0	999	54	967	26	1023	170	3	6	967	26
G20	219	87	0	3	0	0	0	0	0	1358	21	1310	24	1389	55	4	6	1389	55
G21	268	91	0	2	0	0	0	0	0	1123	23	1117	21	1088	67	1	-3	1088	67
G22	105	39	0	2	0	0	0	0	0	1003	25	1000	20	962	81	0	-4	1000	20
G23	69	38	1	5	0	0	0	0	0	1860	27	1819	34	1864	58	2	2	1864	58
G24	581	326	1	0	0	0	0	0	0	69	5	70	2	0	170	-1	-69800	70	2
G25	47	25	1	2	0	0	0	0	0	1121	34	1109	24	1100	102	1	-1	1100	102
G26	87	51	1	2	0	0	0	0	0	1010	26	975	20	1040	84	4	6	975	20
G27	1283	758	1	0	0	0	0	0	0	77	5	73	2	131	151	5	44	73	2
G28	523	185	0	4	0	0	0	0	0	1596	20	1541	27	1629	46	4	5	1629	46
G29	651	603	1	2	0	0	0	0	0	993	17	915	17	1125	53	9	19	915	17
G30	323	99	0	4	0	0	0	0	0	1713	21	1668	29	1728	47	3	3	1728	47
G31	971	471	0	0	0	0	0	0	0	35	4	33	1	110	271	5	70	33	1
G32	192	153	1	4	0	0	0	0	0	1696	22	1646	29	1718	50	3	4	1718	50
G33	84	24	0	2	0	0	0	0	0	978	27	964	20	963	88	1	0	964	20
G34	468	372	1	5	0	0	0	0	0	1742	21	1708	30	1743	46	2	2	1743	46
G35	203	48	0	2	0	0	0	0	0	1079	21	1064	20	1066	64	1	0	1064	20
G36	186	38	0	2	0	0	0	0	0	1125	21	1116	21	1099	63	1	-2	1099	63
G37	148	63	0	4	0	0	0	0	0	1641	23	1574	29	1689	53	4	7	1689	53
G38	113	59	1	2	0	0	0	0	0	1007	25	1010	20	957	80	0	-6	1010	20

				RATIO						AGES									
Grain	U [ppm]	Th [ppm]	Th/U	207/ 235	± s.e.	206/ 238	± s.e.	207/ 206	± s.e.	207/ 235	± 2s	206/ 238	± 2s	207/ 206	± 2s	%disc (5/8)	%disc (7/6)	Best Age [Ma]	± 2s
G39	135	109	1	2	0	0	0	0	0	1014	23	993	19	1017	73	2	2	993	19
G40	43	27	1	2	0	0	0	0	0	1033	38	992	23	1081	119	4	8	992	23
G41	22	11	0	14	0	1	0	0	0	2766	32	2663	51	2808	56	4	5	2808	56
G42	131	106	1	3	0	0	0	0	0	1375	24	1346	25	1380	62	2	2	1380	62
G43	359	96	0	3	0	0	0	0	0	1416	20	1398	25	1402	51	1	0	1402	51
G44	443	252	1	0	0	0	0	0	0	95	7	89	2	223	168	8	60	89	2
G45	357	206	1	0	0	0	0	0	0	91	8	94	2	0	166	-3	-93500	94	2
G46	622	267	0	0	0	0	0	0	0	98	6	94	2	142	144	4	34	94	2
G47	199	35	0	2	0	0	0	0	0	1041	21	1010	19	1066	65	3	5	1010	19
G48	253	142	1	2	0	0	0	0	0	1048	20	1033	19	1039	62	1	1	1033	19
G49	129	46	0	5	0	0	0	0	0	1739	28	1725	32	1721	63	1	0	1721	63
G50	236	89	0	2	0	0	0	0	0	1033	20	1015	19	1033	63	2	2	1015	19
G51	446	335	1	5	0	0	0	0	0	1738	21	1705	30	1742	47	2	2	1742	47
G52	36	11	0	2	0	0	0	0	0	970	40	946	22	988	131	3	4	946	22
G53	166	58	0	3	0	0	0	0	0	1403	23	1365	25	1426	58	3	4	1426	58
G54	53	41	1	2	0	0	0	0	0	1074	33	1025	22	1136	99	5	10	1025	22
G55	296	159	1	2	0	0	0	0	0	1203	23	1177	22	1213	66	2	3	1213	66
G56	830	307	0	0	0	0	0	0	0	74	4	69	2	208	137	8	67	69	2
G57	134	59	0	4	0	0	0	0	0	1633	24	1591	29	1652	56	3	4	1652	56
G58	381	276	1	3	0	0	0	0	0	1370	20	1344	24	1375	53	2	2	1375	53
G59	252	108	0	2	0	0	0	0	0	1120	20	1112	21	1100	60	1	-1	1100	60
G60	1302	438	0	0	0	0	0	0	0	85	4	84	2	55	112	1	-53	84	2
G61	83	51	1	2	0	0	0	0	0	1045	27	1025	20	1051	83	2	2	1025	20
G62	489	72	0	3	0	0	0	0	0	1324	20	1294	23	1340	52	2	3	1340	52
G63	153	155	1	0	0	0	0	0	0	148	14	141	4	217	233	5	35	141	4
G64	316	191	1	3	0	0	0	0	0	1462	25	1453	27	1444	62	1	-1	1444	62
G65	491	374	1	1	0	0	0	0	0	601	14	574	11	667	68	5	14	574	11
G66	48	31	1	13	0	1	0	0	0	2687	28	2623	46	2707	49	2	3	2707	49
G67	172	91	1	5	0	0	0	0	0	1761	24	1699	30	1805	52	4	6	1805	52
G68	92	53	1	4	0	0	0	0	0	1620	26	1565	29	1662	61	4	6	1662	61
G69	30	19	1	2	0	0	0	0	0	1136	43	1114	26	1146	124	2	3	1146	124
G70	119	58	0	2	0	0	0	0	0	1067	24	1047	20	1076	73	2	3	1047	20
G71	90	78	1	2	0	0	0	0	0	1034	28	1021	21	1028	87	1	1	1021	21

				RATIO						AGES									
Grain	U [ppm]	Th [ppm]	Th/U	207/ 235	± s.e.	206/ 238	± s.e.	207/ 206	± s.e.	207/ 235	± 2s	206/ 238	± 2s	207/ 206	± 2s	%disc (5/8)	%disc (7/6)	Best Age [Ma]	± 2s
G72	130	110	1	0	0	0	0	0	0	159	16	148	4	285	246	7	48	148	4
G73	556	268	0	2	0	0	0	0	0	1261	19	1244	22	1259	53	1	1	1259	53
G74	455	151	0	1	0	0	0	0	0	429	12	407	8	518	79	6	21	407	8
G75	81	49	1	4	0	0	0	0	0	1624	27	1595	30	1632	63	2	2	1632	63
G76	352	306	1	5	0	0	0	0	0	1810	22	1776	31	1822	49	2	3	1822	49
G77	170	54	0	4	0	0	0	0	0	1685	24	1643	29	1709	54	3	4	1709	54
G78	122	55	0	3	0	0	0	0	0	1425	25	1411	26	1418	63	1	1	1418	63
G79	311	122	0	0	0	0	0	0	0	69	8	70	2	12	277	-1	-488	70	2
G80	53	70	1	1	0	0	0	0	0	522	35	513	13	530	186	2	3	513	13
G81	916	324	0	3	0	0	0	0	0	1328	20	1310	23	1329	53	1	1	1329	53
G82	385	111	0	0	0	0	0	0	0	61	7	63	2	0	212	-3	-62600	63	2
G83	210	136	1	0	0	0	0	0	0	11	8	11	1	0	1330	0	-10700	11	1
G84	439	56	0	4	0	0	0	0	0	1710	23	1698	30	1698	52	1	0	1698	52
G85	915	275	0	0	0	0	0	0	0	105	5	101	2	161	126	4	37	101	2
G86	113	174	2	12	0	0	0	0	0	2572	26	2495	42	2610	47	3	4	2610	47
G87	212	122	1	6	0	0	0	0	0	1969	24	1893	33	2026	50	4	7	2026	50
G88	148	95	1	2	0	0	0	0	0	1143	23	1100	21	1199	68	4	8	1199	68
G89	171	54	0	3	0	0	0	0	0	1509	24	1435	26	1589	59	5	10	1589	59
G90	139	103	1	0	0	0	0	0	0	91	14	89	3	112	369	2	21	89	3
G91	205	124	1	2	0	0	0	0	0	1072	22	1030	19	1131	66	4	9	1030	19
G92	442	228	1	0	0	0	0	0	0	66	6	67	2	0	190	-2	-67000	67	2
G93	667	1597	2	0	0	0	0	0	0	30	4	31	1	0	174	-3	-30600	31	1
G94	312	295	1	13	0	1	0	0	0	2709	25	2700	44	2696	45	0	0	2696	45
G95	331	118	0	0	0	0	0	0	0	84	7	86	2	17	200	-2	-418	86	2
G96	1389	158	0	0	0	0	0	0	0	82	4	80	2	108	135	2	26	80	2
G97	1100	756	1	0	0	0	0	0	0	88	4	86	2	106	123	2	19	86	2
G98	131	55	0	4	0	0	0	0	0	1608	25	1574	29	1631	60	2	3	1631	60
G99	172	225	1	2	0	0	0	0	0	1021	22	1013	19	1014	71	1	0	1013	19
G100	76	40	1	4	0	0	0	0	0	1642	34	1583	32	1697	78	4	7	1697	78
G101	268	157	1	0	0	0	0	0	0	411	14	405	8	417	95	1	3	405	8
G102	24	13	1	3	0	0	0	0	0	1391	41	1352	30	1429	105	3	5	1429	105
G103	91	20	0	2	0	0	0	0	0	1130	29	1121	22	1126	85	1	0	1126	85
G104	156	65	0	2	0	0	0	0	0	1182	23	1165	22	1192	68	1	2	1192	68

Grain	U [ppm]	Th [ppm]	Th/U	RATIO 207/235	± s.e.	206/238	± s.e.	207/206	± s.e.	AGES 207/235	± 2s	206/238	± 2s	207/206	± 2s	%disc (5/8)	%disc (7/6)	Best Age [Ma]	± 2s
G105	286	222	1	2	0	0	0	0	0	1068	23	1006	19	1176	71	6	14	1006	19
G106	165	99	1	3	0	0	0	0	0	1400	24	1380	25	1410	62	1	2	1410	62
G107	76	28	0	0	0	0	0	0	0	212	22	194	6	388	248	9	50	194	6
G108	118	45	0	0	0	0	0	0	0	159	18	154	5	203	278	3	24	154	5
G109	29	38	1	6	0	0	0	0	0	1923	45	1886	43	1944	95	2	3	1944	95
G110	107	54	1	1	0	0	0	0	0	828	24	814	16	845	90	2	4	814	16
G111	115	27	0	1	0	0	0	0	0	902	24	834	17	1052	82	8	21	834	17
G112	340	40	0	2	0	0	0	0	0	1118	21	1095	20	1145	62	2	4	1095	20
G113	217	126	1	2	0	0	0	0	0	1055	24	1050	20	1046	75	1	0	1050	20
G114	135	108	1	4	0	0	0	0	0	1633	26	1603	29	1653	60	2	3	1653	60
G115	333	119	0	2	0	0	0	0	0	1049	21	1038	19	1053	65	1	1	1038	19
G116	131	59	0	2	0	0	0	0	0	1200	25	1173	22	1231	70	2	5	1231	70
G117	84	61	1	5	0	0	0	0	0	1790	28	1747	32	1823	62	2	4	1823	62
G118	81	93	1	3	0	0	0	0	0	1391	28	1358	26	1425	72	2	5	1425	72
G119	266	96	0	2	0	0	0	0	0	1152	23	1149	22	1139	69	0	-1	1139	69
G120	244	118	0	0	0	0	0	0	0	92	9	86	2	240	227	7	64	86	2
G121	205	111	1	3	0	0	0	0	0	1385	24	1368	25	1396	62	1	2	1396	62
G122	101	74	1	4	0	0	0	0	0	1633	28	1560	29	1712	64	5	9	1712	64
G123	26	20	1	2	0	0	0	0	0	1150	52	1129	29	1174	151	2	4	1174	151
G124	350	276	1	0	0	0	0	0	0	146	9	144	3	159	148	1	9	144	3
G125	119	131	1	3	0	0	0	0	0	1329	27	1307	25	1349	71	2	3	1349	71
G126	197	234	1	0	0	0	0	0	0	73	11	70	2	163	339	5	57	70	2
G127	186	99	1	0	0	0	0	0	0	170	14	161	4	277	202	5	42	161	4
G128	2933	740	0	11	0	0	0	0	0	2560	27	2517	41	2581	49	2	2	2581	49
G129	15291	2	0	6	0	0	0	0	0	2002	46	2035	45	1955	95	-2	-4	1955	95
G130	124	58	0	4	0	0	0	0	0	1703	29	1679	31	1719	66	1	2	1719	66
G131	130	144	1	4	0	0	0	0	0	1600	27	1571	29	1625	64	2	3	1625	64
G132	173	53	0	3	0	0	0	0	0	1416	26	1376	25	1463	65	3	6	1463	65
Sample W3-18																			
G1	197	114	1	2	0	0	0	0	0	1010	20	928	18	1040	63	9	11	928	18
G2	199	87	0	4	0	0	0	0	0	1710	22	1705	30	1576	48	0	-8	1576	48
G3	216	95	0	10	0	0	0	0	0	2449	22	2467	40	2306	39	-1	-7	2306	39

				RATIO						AGES									
Grain	U [ppm]	Th [ppm]	Th/U	207/ 235	± s.e.	206/ 238	± s.e.	207/ 206	± s.e.	207/ 235	± 2s	206/ 238	± 2s	207/ 206	± 2s	%disc (5/8)	%disc (7/6)	Best Age [Ma]	± 2s
G4	903	789	1	0	0	0	0	0	0	93	6	93	2	0	0	0	-93100	93	2
G5	73	75	1	4	0	0	0	0	0	1678	27	1642	31	1585	60	2	-4	1585	60
G6	477	289	1	5	0	0	0	0	0	1830	20	1692	29	1857	41	8	9	1857	41
G7	98	48	0	2	0	0	0	0	0	1057	25	1008	20	1011	76	5	0	1008	20
G8	90	35	0	1	0	0	0	0	0	914	26	917	19	752	90	0	-22	917	19
G9	47	91	2	6	0	0	0	0	0	1979	29	1995	37	1828	59	-1	-9	1828	59
G10	248	119	0	3	0	0	0	0	0	1402	20	1395	25	1270	50	1	-10	1270	50
G11	103	62	1	13	0	1	0	0	0	2691	23	2720	45	2546	40	-1	-7	2546	40
G12	48	34	1	5	0	0	0	0	0	1766	30	1770	34	1624	66	0	-9	1624	66
G13	425	338	1	1	0	0	0	0	0	420	12	383	8	471	79	10	19	383	8
G14	35	72	2	5	0	0	0	0	0	1806	33	1786	35	1696	72	1	-5	1696	72
G15	615	944	2	0	0	0	0	0	0	30	4	30	1	0	105	1	-29800	30	1
G16	354	212	1	0	0	0	0	0	0	93	8	92	2	0	77	1	-91900	92	2
G17	972	623	1	0	0	0	0	0	0	102	5	102	2	0	0	-1	-102100	102	2
G18	73	38	1	1	0	0	0	0	0	515	29	512	12	366	158	0	-40	512	12
G19	258	146	1	2	0	0	0	0	0	1052	19	1042	19	929	59	1	-12	1042	19
G20	232	46	0	4	0	0	0	0	0	1643	22	1605	29	1560	51	2	-3	1560	51
G21	92	79	1	1	0	0	0	0	0	586	26	577	13	466	127	2	-24	577	13
G22	457	464	1	0	0	0	0	0	0	159	9	161	4	0	52	-1	-160800	161	4
G23	1404	167	0	0	0	0	0	0	0	344	8	328	6	296	63	5	-11	328	6
G24	186	214	1	5	0	0	0	0	0	1733	23	1715	31	1628	51	1	-5	1628	51
G25	62	80	1	0	0	0	0	0	0	144	31	143	5	0	503	1	-143100	143	5
G26	272	89	0	2	0	0	0	0	0	1009	19	994	19	900	59	1	-10	994	19
G27	98	41	0	3	0	0	0	0	0	1444	31	1431	29	1332	78	1	-7	1332	78
G28	363	101	0	4	0	0	0	0	0	1603	22	1548	28	1549	50	4	0	1549	50
G29	43	28	1	2	0	0	0	0	0	1060	35	1047	23	949	109	1	-10	1047	23
G30	590	174	0	3	0	0	0	0	0	1384	19	1362	24	1286	47	2	-6	1286	47
G31	290	51	0	2	0	0	0	0	0	982	18	907	17	1019	58	8	11	907	17
G32	155	70	0	5	0	0	0	0	0	1874	23	1866	33	1761	47	0	-6	1761	47
G33	577	232	0	2	0	0	0	0	0	1032	17	1029	19	901	54	0	-14	1029	19
G34	456	156	0	2	0	0	0	0	0	1188	18	1138	21	1147	49	4	1	1147	49
G35	218	73	0	4	0	0	0	0	0	1569	25	1494	28	1547	58	5	3	1547	58
G36	336	89	0	4	0	0	0	0	0	1612	20	1546	27	1576	46	4	2	1576	46

				RATIO						AGES									
Grain	U [ppm]	Th [ppm]	Th/U	207/ 235	± s.e.	206/ 238	± s.e.	207/ 206	± s.e.	207/ 235	± 2s	206/ 238	± 2s	207/ 206	± 2s	%disc (5/8)	%disc (7/6)	Best Age [Ma]	± 2s
G37	146	68	0	3	0	0	0	0	0	1405	23	1372	25	1327	57	2	-3	1327	57
G38	354	229	1	0	0	0	0	0	0	188	10	192	4	0	88	-2	-192300	192	4
G39	282	187	1	23	0	1	0	0	0	3220	23	3255	50	3095	36	-1	-5	3095	36
G40	92	58	1	3	0	0	0	0	0	1373	27	1289	25	1383	68	7	7	1383	68
G41	1112	372	0	0	0	0	0	0	0	91	4	93	2	0	0	-2	-92500	93	2
G42	127	102	1	3	0	0	0	0	0	1430	24	1432	27	1303	60	0	-10	1303	60
G43	297	169	1	3	0	0	0	0	0	1521	21	1479	27	1460	49	3	-1	1460	49
G44	96	191	2	2	0	0	0	0	0	956	26	935	19	876	85	2	-7	935	19
G45	118	72	1	4	0	0	0	0	0	1701	28	1668	32	1627	63	2	-3	1627	63
G46	1651	1682	1	0	0	0	0	0	0	71	4	71	2	0	0	-1	-71000	71	2
G47	237	84	0	5	0	0	0	0	0	1760	22	1758	31	1649	48	0	-7	1649	48
G48	78	30	0	2	0	0	0	0	0	1016	28	996	21	936	91	2	-6	996	21
G49	308	156	1	3	0	0	0	0	0	1442	21	1436	26	1334	51	0	-8	1334	51
G50	148	72	0	3	0	0	0	0	0	1315	24	1304	25	1216	62	1	-7	1216	62
G51	282	167	1	4	0	0	0	0	0	1637	22	1627	29	1537	49	1	-6	1537	49
G52	332	162	0	5	0	0	0	0	0	1867	22	1853	32	1773	46	1	-4	1773	46
G53	360	196	1	0	0	0	0	0	0	78	11	75	3	33	327	4	-130	75	3
G54	317	303	1	4	0	0	0	0	0	1587	23	1496	27	1601	53	6	7	1601	53
G55	317	151	0	4	0	0	0	0	0	1720	22	1711	30	1621	48	0	-6	1621	48
G56	540	649	1	1	0	0	0	0	0	430	12	428	9	309	79	0	-38	428	9
G57	199	312	2	12	0	0	0	0	0	2619	24	2559	43	2569	41	2	0	2569	41
G58	698	396	1	2	0	0	0	0	0	949	18	914	17	913	59	4	0	914	17
G59	1515	1222	1	0	0	0	0	0	0	90	4	88	2	15	100	3	-477	88	2
G60	128	60	0	4	0	0	0	0	0	1652	25	1635	30	1567	55	1	-4	1567	55
G61	99	70	1	6	0	0	0	0	0	2028	26	2013	36	1942	51	1	-4	1942	51
G62	334	55	0	5	0	0	0	0	0	1749	22	1725	30	1675	47	1	-3	1675	47
G63	476	113	0	3	0	0	0	0	0	1506	22	1423	26	1519	53	6	6	1519	53
G64	198	95	0	1	0	0	0	0	0	447	17	451	10	296	109	-1	-52	451	10
G65	223	70	0	2	0	0	0	0	0	1115	26	1070	21	1094	77	4	2	1070	21
G66	331	188	1	0	0	0	0	0	0	400	15	400	8	276	99	0	-45	400	8
G67	782	576	1	0	0	0	0	0	0	102	5	96	2	95	133	5	-1	96	2
G68	246	55	0	5	0	0	0	0	0	1807	23	1800	32	1716	48	0	-5	1716	48
G69	366	759	2	1	0	0	0	0	0	615	16	621	12	472	75	-1	-32	621	12

				RATIO						AGES									
	U	Th		207/		206/		207/		207/		206/		207/		%disc	%disc	Best Age	
Grain	[ppm]	[ppm]	Th/U	235	± s.e.	238	± s.e.	206	± s.e.	235	± 2s	238	± 2s	206	± 2s	(5/8)	(7/6)	[Ma]	± 2s
G70	146	74	1	4	0	0	0	0	0	1623	24	1597	29	1556	55	2	-3	1556	55
G71	48	26	1	4	0	0	0	0	0	1690	32	1628	32	1669	71	4	2	1669	71
G72	214	206	1	0	0	0	0	0	0	171	16	164	5	143	238	4	-15	164	5
G73	57	19	0	2	0	0	0	0	0	1125	32	1105	23	1060	94	2	-4	1060	94
G74	259	171	1	2	0	0	0	0	0	1101	23	1082	21	1033	69	2	-5	1082	21
G75	92	40	0	2	0	0	0	0	0	1114	27	1108	22	1021	80	1	-8	1021	80
G76	310	113	0	4	0	0	0	0	0	1633	23	1572	29	1616	52	4	3	1616	52
G77	100	41	0	2	0	0	0	0	0	1109	27	1082	22	1060	78	3	-2	1082	22
G78	273	212	1	3	0	0	0	0	0	1336	22	1292	24	1307	56	3	1	1307	56
G79	648	446	1	0	0	0	0	0	0	301	10	297	6	214	85	1	-38	297	6
G80	94	34	0	3	0	0	0	0	0	1384	28	1391	27	1275	72	0	-9	1275	72
G81	249	103	0	2	0	0	0	0	0	1180	22	1170	22	1097	60	1	-7	1097	60
G82	531	269	1	0	0	0	0	0	0	96	6	97	2	0	99	0	-96600	97	2
G83	115	124	1	12	0	0	0	0	0	2641	27	2612	45	2580	46	1	-1	2580	46
G84	388	170	0	0	0	0	0	0	0	80	7	79	2	0	156	1	-79300	79	2
G85	314	91	0	5	0	0	0	0	0	1759	23	1727	31	1706	50	2	-1	1706	50
G86	292	83	0	4	0	0	0	0	0	1656	23	1633	29	1596	52	1	-2	1596	52
G87	1372	1524	1	0	0	0	0	0	0	101	4	99	2	34	104	2	-192	99	2
G88	272	87	0	4	0	0	0	0	0	1581	24	1505	28	1595	54	5	6	1595	54
G89	179	148	1	5	0	0	0	0	0	1808	25	1787	32	1745	53	1	-2	1745	53
G90	253	115	0	3	0	0	0	0	0	1435	24	1397	26	1402	57	3	0	1402	57
G91	218	71	0	2	0	0	0	0	0	1222	23	1197	23	1174	62	2	-2	1174	62
G92	140	75	1	2	0	0	0	0	0	959	24	947	19	890	79	1	-6	947	19
G93	93	34	0	2	0	0	0	0	0	1202	28	1193	24	1128	77	1	-6	1128	77
G94	207	137	1	18	0	1	0	0	0	2964	27	2922	48	2919	44	1	0	2919	44
G95	139	125	1	13	0	1	0	0	0	2663	27	2625	45	2616	46	1	0	2616	46
G96	148	72	0	4	0	0	0	0	0	1663	26	1639	30	1609	58	1	-2	1609	58
G97	193	110	1	1	0	0	0	0	0	582	19	585	12	473	96	0	-24	585	12
G98	324	187	1	0	0	0	0	0	0	354	14	349	7	291	102	2	-20	349	7
G99	198	90	0	4	0	0	0	0	0	1725	25	1707	31	1667	55	1	-2	1667	55
G100	805	175	0	5	0	0	0	0	0	1749	24	1706	30	1722	50	3	1	1722	50
G101	1178	502	0	2	0	0	0	0	0	1154	20	1122	21	1127	55	3	0	1127	55
G102	544	359	1	0	0	0	0	0	0	399	12	399	8	302	83	0	-32	399	8

Grain	U [ppm]	Th [ppm]	Th/U	RATIO 207/235	± s.e.	206/238	± s.e.	207/206	± s.e.	AGES 207/235	± 2s	206/238	± 2s	207/206	± 2s	%disc (5/8)	%disc (7/6)	Best Age [Ma]	± 2s
G103	83	34	0	3	0	0	0	0	0	1362	29	1323	26	1342	75	3	1	1342	75
G104	404	205	1	4	0	0	0	0	0	1631	24	1580	29	1618	53	3	2	1618	53
G105	729	216	0	2	0	0	0	0	0	1002	19	936	18	1067	59	7	12	936	18
G106	183	52	0	4	0	0	0	0	0	1685	26	1653	30	1647	57	2	0	1647	57
G107	54	24	0	2	0	0	0	0	0	1010	36	976	22	1000	112	3	2	976	22
G108	394	107	0	5	0	0	0	0	0	1823	25	1775	32	1805	52	3	2	1805	52
G109	70	88	1	1	0	0	0	0	0	441	31	441	11	352	194	0	-25	441	11
G110	327	146	0	4	0	0	0	0	0	1706	25	1675	30	1669	54	2	0	1669	54
G111	117	104	1	4	0	0	0	0	0	1615	28	1602	30	1557	63	1	-3	1557	63
G112	227	184	1	2	0	0	0	0	0	1004	22	990	19	954	71	1	-4	990	19
G113	204	146	1	1	0	0	0	0	0	455	18	453	10	378	110	0	-20	453	10
G114	79	51	1	2	0	0	0	0	0	1085	33	1043	22	1095	97	4	5	1043	22
G115	140	65	0	2	0	0	0	0	0	1088	26	1063	21	1062	76	2	0	1063	21
G116	364	285	1	1	0	0	0	0	0	579	17	567	12	540	83	2	-5	567	12
G117	393	616	2	1	0	0	0	0	0	432	15	407	9	484	91	6	16	407	9
G118	2264	813	0	4	0	0	0	0	0	1584	23	1547	28	1564	53	2	1	1564	53
G119	41	31	1	2	0	0	0	0	0	1183	39	1143	26	1183	111	3	3	1183	111
G120	708	38	0	1	0	0	0	0	0	469	17	426	9	603	98	10	29	426	9
G121	139	111	1	4	0	0	0	0	0	1724	28	1683	31	1708	60	2	1	1708	60
G122	499	626	1	1	0	0	0	0	0	500	15	497	10	432	81	1	-15	497	10
G123	626	347	1	1	0	0	0	0	0	549	18	516	11	614	90	6	16	516	11
G124	385	223	1	2	0	0	0	0	0	1019	22	1002	19	983	67	2	-2	1002	19
G125	157	41	0	2	0	0	0	0	0	1012	25	988	20	992	79	2	0	988	20
G126	293	183	1	2	0	0	0	0	0	1071	26	1058	21	1025	80	1	-3	1058	21
G127	294	217	1	0	0	0	0	0	0	43	7	40	1	122	398	7	67	40	1
G128	119	62	1	0	0	0	0	0	0	170	19	164	5	164	275	3	-1	164	5
G129	73	32	0	3	0	0	0	0	0	1339	32	1315	27	1311	83	2	0	1311	83
G130	626	261	0	3	0	0	0	0	0	1498	25	1437	27	1524	59	4	6	1524	59
G131	796	1649	2	0	0	0	0	0	0	26	3	25	1	28	283	4	9	25	1
G132	1190	227	0	0	0	0	0	0	0	98	5	97	2	50	118	1	-95	97	2
Sample J6-2																			
G1	7119	2481	0	0	0	0	0	0	0	28	1	28	1	27	89	2	-2	28	1

				RATIO						AGES								Best	
Grain	U [ppm]	Th [ppm]	Th/U	207/ 235	± s.e.	206/ 238	± s.e.	207/ 206	± s.e.	207/ 235	± 2s	206/ 238	± 2s	207/ 206	± 2s	%disc (5/8)	%disc (7/6)	Age [Ma]	± 2s
G2	347	120	0	4	0	0	0	0	0	1656	22	1581	28	1722	50	5	8	1722	50
G3	48	22	0	2	0	0	0	0	0	1211	47	1168	29	1258	129	4	7	1258	129
G4	994	1382	1	3	0	0	0	0	0	1326	20	1285	23	1362	51	3	6	1362	51
G5	471	673	1	3	0	0	0	0	0	1500	21	1452	26	1538	50	3	6	1538	50
G6	106	61	1	11	0	0	0	0	0	2518	33	2421	47	2572	60	4	6	2572	60
G7	216	178	1	4	0	0	0	0	0	1530	23	1476	27	1578	55	4	6	1578	55
G8	331	318	1	3	0	0	0	0	0	1334	21	1323	24	1323	55	1	0	1323	55
G9	259	127	0	0	0	0	0	0	0	175	12	171	4	199	169	2	14	171	4
G10	788	326	0	5	0	0	0	0	0	1754	22	1677	30	1822	48	5	8	1822	48
G11	283	154	1	11	0	0	0	0	0	2526	25	2457	41	2558	45	3	4	2558	45
G12	376	158	0	2	0	0	0	0	0	1022	21	997	19	1047	65	2	5	997	19
G13	601	368	1	0	0	0	0	0	0	167	8	161	3	221	117	4	27	161	3
G14	303	491	2	1	0	0	0	0	0	719	18	691	14	778	74	4	11	691	14
G15	560	165	0	0	0	0	0	0	0	74	7	71	2	146	231	5	51	71	2
G16	212	93	0	4	0	0	0	0	0	1665	24	1670	30	1633	55	0	-2	1633	55
G17	665	63	0	0	0	0	0	0	0	330	11	332	7	286	93	-1	-16	332	7
G18	206	191	1	3	0	0	0	0	0	1312	23	1269	24	1359	62	3	7	1359	62
G19	210	152	1	1	0	0	0	0	0	634	19	623	13	647	87	2	4	623	13
G20	530	22	0	0	0	0	0	0	0	371	12	345	7	510	87	8	32	345	7
G21	99	37	0	5	0	0	0	0	0	1849	27	1819	33	1859	58	2	2	1859	58
G22	430	292	1	8	0	0	0	0	0	2250	25	2237	38	2242	48	1	0	2242	48
G23	73	88	1	4	0	0	0	0	0	1583	32	1554	31	1600	75	2	3	1600	75
G24	149	69	0	2	0	0	0	0	0	1101	24	1083	21	1113	73	2	3	1083	21
G25	294	233	1	2	0	0	0	0	0	1136	22	1148	22	1091	64	-1	-5	1091	64
G26	1531	957	1	0	0	0	0	0	0	79	4	79	2	68	114	1	-15	79	2
G27	87	109	1	3	0	0	0	0	0	1435	30	1413	28	1446	74	2	2	1446	74
G28	115	115	1	4	0	0	0	0	0	1557	28	1488	28	1631	65	5	9	1631	65
G29	923	339	0	4	0	0	0	0	0	1645	24	1567	28	1727	53	5	9	1727	53
G30	429	326	1	0	0	0	0	0	0	179	9	172	4	248	130	4	30	172	4
G31	752	137	0	2	0	0	0	0	0	1007	19	993	19	1016	62	1	2	993	19
G32	992	910	1	10	0	0	0	0	0	2428	27	2415	41	2422	49	1	0	2422	49
G33	161	60	0	2	0	0	0	0	0	991	24	951	19	1060	77	4	10	951	19
G34	2745	8717	3	0	0	0	0	0	0	30	2	28	1	196	138	9	86	28	1

				RATIO						AGES								Best	
Grain	U [ppm]	Th [ppm]	Th/U	207/ 235	± s.e.	206/ 238	± s.e.	207/ 206	± s.e.	207/ 235	± 2s	206/ 238	± 2s	207/ 206	± 2s	%disc (5/8)	%disc (7/6)	Age [Ma]	± 2s
G35	46	22	0	2	0	0	0	0	0	1101	48	1036	26	1215	142	6	15	1036	26
G36	172	132	1	1	0	0	0	0	0	440	19	408	9	590	115	8	31	408	9
G37	964	42	0	4	0	0	0	0	0	1655	24	1598	28	1710	55	4	7	1710	55
G38	226	70	0	7	0	0	0	0	0	2068	27	2031	36	2089	55	2	3	2089	55
G39	1199	1067	1	0	0	0	0	0	0	31	3	32	1	0	121	-3	-31500	32	1
G40	1057	610	1	0	0	0	0	0	0	35	3	33	1	178	215	7	82	33	1
G41	742	75	0	0	0	0	0	0	0	329	12	338	7	249	102	-3	-36	338	7
G42	135	68	0	5	0	0	0	0	0	1772	30	1681	32	1865	65	5	10	1865	65
G43	762	77	0	0	0	0	0	0	0	343	12	338	7	358	91	2	6	338	7
G44	202	65	0	3	0	0	0	0	0	1411	30	1409	28	1398	76	0	-1	1398	76
G45	581	469	1	4	0	0	0	0	0	1614	26	1557	28	1673	59	4	7	1673	59
G46	365	269	1	5	0	0	0	0	0	1742	27	1732	31	1738	59	1	0	1738	59
G47	167	186	1	1	0	0	0	0	0	610	26	580	13	703	121	5	17	580	13
G48	197	107	1	1	0	0	0	0	0	634	26	579	13	817	117	9	29	579	13
G49	632	323	1	2	0	0	0	0	0	1139	25	1072	21	1252	73	6	14	1072	21
G50	363	149	0	2	0	0	0	0	0	1265	27	1263	24	1253	74	0	-1	1253	74
G51	1321	625	0	0	0	0	0	0	0	89	4	89	2	87	122	1	-2	89	2
G52	619	506	1	0	0	0	0	0	0	72	5	68	2	210	181	7	68	68	2
G53	237	479	2	3	0	0	0	0	0	1360	27	1339	25	1380	70	2	3	1380	70
G54	441	480	1	1	0	0	0	0	0	498	17	473	10	598	92	5	21	473	10
G55	361	305	1	0	0	0	0	0	0	41	8	40	2	129	425	4	69	40	2
G56	97	24	0	2	0	0	0	0	0	1226	36	1212	26	1239	100	1	2	1239	100
G57	83	78	1	5	0	0	0	0	0	1858	36	1842	36	1866	78	1	1	1866	78
G58	145	115	1	1	0	0	0	0	0	540	25	529	12	578	131	2	8	529	12
G59	522	187	0	2	0	0	0	0	0	1097	25	1068	21	1144	75	3	7	1068	21
G60	2701	891	0	4	0	0	0	0	0	1580	28	1526	28	1643	65	4	7	1643	65
G61	731	73	0	0	0	0	0	0	0	349	15	348	8	351	119	1	1	348	8
G62	1328	81	0	2	0	0	0	0	0	1026	16	998	20	1092	48	3	9	998	20
G63	534	78	0	5	0	0	0	0	0	1754	20	1803	33	1701	44	-3	-6	1701	44
G64	2614	1056	0	0	0	0	0	0	0	36	2	34	1	226	116	8	85	34	1
G65	127	87	1	3	0	0	0	0	0	1448	28	1435	29	1470	68	1	2	1470	68
G66	40	33	1	14	0	1	0	0	0	2741	29	2811	53	2693	49	-2	-4	2693	49
G67	174	54	0	3	0	0	0	0	0	1518	23	1525	30	1511	54	0	-1	1511	54

				RATIO						AGES									
Grain	U [ppm]	Th [ppm]	Th/U	207/ 235	± s.e.	206/ 238	± s.e.	207/ 206	± s.e.	207/ 235	± 2s	206/ 238	± 2s	207/ 206	± 2s	%disc (5/8)	%disc (7/6)	Best Age [Ma]	± 2s
G68	474	149	0	0	0	0	0	0	0	78	9	75	2	165	266	3	55	75	2
G69	1403	764	1	2	0	0	0	0	0	1184	17	1185	23	1187	47	0	0	1187	47
G70	289	255	1	12	0	0	0	0	0	2568	23	2493	45	2632	41	3	5	2632	41
G71	126	101	1	2	0	0	0	0	0	960	29	953	21	981	95	1	3	953	21
G72	517	212	0	0	0	0	0	0	0	175	12	160	4	391	165	10	59	160	4
G73	364	192	1	1	0	0	0	0	0	519	16	508	11	573	87	2	11	508	11
G74	426	22	0	4	0	0	0	0	0	1614	22	1621	31	1610	50	0	-1	1610	50
G75	20	96	5	2	0	0	0	0	0	1035	68	1001	30	1112	207	3	10	1001	30
G76	254	100	0	6	0	0	0	0	0	1918	22	1942	36	1895	46	-1	-2	1895	46
G77	593	623	1	0	0	0	0	0	0	175	9	172	4	217	123	2	21	172	4
G78	701	237	0	10	0	0	0	0	0	2446	23	2358	42	2523	40	4	7	2523	40
G79	346	209	1	3	0	0	0	0	0	1507	21	1528	29	1483	50	-1	-3	1483	50
G80	246	104	0	35	4	1	0	0	0	3650	249	3661	442	3647	373	0	0	3647	373
G81	352	132	0	1	0	0	0	0	0	525	18	487	11	695	96	8	30	487	11
G82	302	220	1	5	0	0	0	0	0	1777	24	1771	34	1787	52	0	1	1787	52
G83	5031	695	0	0	0	0	0	0	0	183	20	187	4	139	270	-2	-35	187	4
G84	240	72	0	0	0	0	0	0	0	85	12	88	3	22	327	-3	-297	88	3
G85	53	60	1	3	0	0	0	0	0	1519	33	1535	32	1500	79	-1	-2	1500	79
G86	444	113	0	3	0	0	0	0	0	1415	23	1360	26	1503	57	4	10	1503	57
G87	367	123	0	0	0	0	0	0	0	71	7	67	2	207	246	6	68	67	2
G88	854	127	0	7	0	0	0	0	0	2100	22	2080	37	2123	44	1	2	2123	44
G89	199	63	0	4	0	0	0	0	0	1585	25	1563	30	1617	59	1	3	1617	59
G90	1961	631	0	0	0	0	0	0	0	96	4	93	2	183	102	4	50	93	2
G91	367	71	0	1	0	0	0	0	0	772	21	736	15	884	80	5	17	736	15
G92	2063	1046	1	0	0	0	0	0	0	89	5	84	2	230	135	6	63	84	2
Sample J4-2																			
G1	132	148	1	3	0	0	0	0	0	1458	20	1461	27	1459	51	0	0	1459	51
G2	60	46	1	2	0	0	0	0	0	1238	21	1236	23	1245	59	0	1	1245	59
G3	35	40	1	13	0	1	0	0	0	2693	25	2685	45	2703	44	0	1	2703	44
G4	57	17	0	2	0	0	0	0	0	1076	21	1071	21	1091	64	0	2	1071	21
G5	8	5	1	6	0	0	0	0	0	1998	34	1936	39	2067	70	3	6	2067	70
G6	53	27	1	5	0	0	0	0	0	1732	23	1744	31	1721	52	-1	-1	1721	52

				RATIO						AGES									
Grain	U [ppm]	Th [ppm]	Th/U	207/ 235	± s.e.	206/ 238	± s.e.	207/ 206	± s.e.	207/ 235	± 2s	206/ 238	± 2s	207/ 206	± 2s	%disc (5/8)	%disc (7/6)	Best Age [Ma]	± 2s
G7	13	11	1	5	0	0	0	0	0	1818	30	1808	35	1834	66	1	1	1834	66
G8	613	224	0	0	0	0	0	0	0	112	4	107	2	225	82	5	52	107	2
G9	214	170	1	3	0	0	0	0	0	1420	20	1383	25	1480	49	3	6	1480	49
G10	18	9	0	3	0	0	0	0	0	1299	29	1277	26	1341	78	2	5	1341	78
G11	302	42	0	2	0	0	0	0	0	1036	17	974	18	1174	52	6	17	974	18
G12	21	20	1	5	0	0	0	0	0	1874	27	1851	34	1904	57	1	3	1904	57
G13	389	402	1	0	0	0	0	0	0	47	3	46	1	112	138	2	59	46	1
G14	123	75	1	0	0	0	0	0	0	78	6	78	2	86	200	0	10	78	2
G15	34	17	1	2	0	0	0	0	0	1000	23	991	20	1025	75	1	3	991	20
G16	25	17	1	1	0	0	0	0	0	654	26	632	14	737	113	4	14	632	14
G17	45	54	1	4	0	0	0	0	0	1714	24	1685	31	1753	53	2	4	1753	53
G18	149	129	1	0	0	0	0	0	0	70	6	67	2	187	217	5	64	67	2
G19	123	104	1	0	0	0	0	0	0	36	5	35	1	96	326	3	64	35	1
G20	14	9	1	2	0	0	0	0	0	1149	32	1152	24	1147	93	0	0	1147	93
G21	214	231	1	0	0	0	0	0	0	169	7	170	4	152	102	-1	-12	170	4
G22	32	19	1	6	0	0	0	0	0	1954	25	1985	36	1927	53	-2	-3	1927	53
G23	98	53	1	1	0	0	0	0	0	425	13	421	9	454	86	1	7	421	9
G24	188	31	0	5	0	0	0	0	0	1774	21	1737	31	1822	47	2	5	1822	47
G25	102	37	0	2	0	0	0	0	0	1008	19	1010	19	1006	60	0	0	1010	19
G26	47	13	0	2	0	0	0	0	0	1090	26	1093	22	1087	80	0	-1	1093	22
G27	121	46	0	5	0	0	0	0	0	1810	22	1817	32	1806	48	0	-1	1806	48
G28	60	34	1	1	0	0	0	0	0	637	18	632	13	660	82	1	4	632	13
G29	44	75	2	4	0	0	0	0	0	1645	26	1603	30	1703	59	3	6	1703	59
G30	63	54	1	1	0	0	0	0	0	424	15	421	9	446	99	1	6	421	9
G31	84	36	0	2	0	0	0	0	0	1232	20	1225	23	1250	56	1	2	1250	56
G32	89	24	0	0	0	0	0	0	0	66	7	62	2	200	246	6	69	62	2
G33	84	41	0	4	0	0	0	0	0	1723	22	1720	31	1730	50	0	1	1730	50
G34	151	94	1	2	0	0	0	0	0	1079	18	1074	20	1093	56	0	2	1074	20
G35	143	140	1	1	0	0	0	0	0	517	13	513	10	543	72	1	6	513	10
G36	27	17	1	2	0	0	0	0	0	1016	26	1023	21	1005	82	-1	-2	1023	21
G37	94	25	0	5	0	0	0	0	0	1744	22	1747	31	1745	50	0	0	1745	50
G38	75	91	1	1	0	0	0	0	0	618	18	615	12	636	82	1	3	615	12
G39	97	16	0	2	0	0	0	0	0	1001	19	990	19	1029	60	1	4	990	19

				RATIO						AGES									
	U	Th		207/		206/		207/		207/		206/		207/		%disc	%disc	Best Age	
Grain	[ppm]	[ppm]	Th/U	235	± s.e.	238	± s.e.	206	± s.e.	235	± 2s	238	± 2s	206	± 2s	(5/8)	(7/6)	[Ma]	± 2s
G40	47	48	1	4	0	0	0	0	0	1637	25	1622	30	1662	58	1	2	1662	58
G41	106	55	1	2	0	0	0	0	0	1089	21	1067	20	1140	63	2	6	1067	20
G42	173	42	0	0	0	0	0	0	0	386	11	380	8	427	76	2	11	380	8
G43	297	129	0	0	0	0	0	0	0	99	5	97	2	157	113	2	38	97	2
G44	207	20	0	0	0	0	0	0	0	331	10	331	7	336	78	0	1	331	7
G45	60	28	0	2	0	0	0	0	0	950	21	886	17	1106	68	7	20	886	17
G46	139	163	1	1	0	0	0	0	0	465	13	436	9	621	76	7	30	436	9
G47	32	30	1	4	0	0	0	0	0	1633	26	1620	30	1655	59	1	2	1655	59
G48	234	140	1	0	0	0	0	0	0	98	5	96	2	166	123	3	42	96	2
G49	247	144	1	0	0	0	0	0	0	49	3	48	1	90	168	1	46	48	1
G50	42	18	0	1	0	0	0	0	0	525	20	510	11	595	106	3	14	510	11
G51	176	148	1	1	0	0	0	0	0	762	16	758	15	778	62	1	3	758	15
G52	112	41	0	3	0	0	0	0	0	1365	22	1377	26	1351	58	-1	-2	1351	58
G53	186	122	1	0	0	0	0	0	0	62	4	60	1	179	169	5	67	60	1
G54	112	99	1	0	0	0	0	0	0	159	9	159	4	169	148	0	6	159	4
G55	72	54	1	0	0	0	0	0	0	69	10	71	2	21	352	-2	-245	71	2
G56	18	11	1	15	0	1	0	0	0	2792	27	2776	48	2808	48	1	1	2808	48
G57	52	92	2	4	0	0	0	0	0	1731	24	1778	32	1678	55	-3	-6	1678	55
G58	75	44	1	0	0	0	0	0	0	220	12	203	5	406	134	8	50	203	5
G59	52	29	1	2	0	0	0	0	0	981	22	978	19	994	71	0	2	978	19
G60	59	36	1	5	0	0	0	0	0	1851	26	1843	33	1864	56	0	1	1864	56
G61	50	84	2	1	0	0	0	0	0	591	19	593	12	590	93	0	-1	593	12
G62	34	38	1	1	0	0	0	0	0	632	22	628	13	654	102	1	4	628	13
G63	172	80	0	0	0	0	0	0	0	80	5	77	2	171	153	4	55	77	2
G64	139	211	2	0	0	0	0	0	0	36	6	36	1	57	373	1	37	36	1
G65	103	49	0	4	0	0	0	0	0	1708	23	1715	31	1703	52	0	-1	1703	52
G66	49	41	1	15	0	1	0	0	0	2811	26	2892	48	2758	46	-3	-5	2758	46
G67	162	125	1	0	0	0	0	0	0	165	8	167	4	135	127	-1	-23	167	4
G68	138	70	1	2	0	0	0	0	0	1231	20	1229	23	1240	57	0	1	1240	57
G69	89	43	0	1	0	0	0	0	0	463	15	459	9	489	89	1	6	459	9
G70	69	59	1	0	0	0	0	0	0	56	10	55	2	116	425	2	52	55	2
G71	16	13	1	1	0	0	0	0	0	456	36	425	12	624	206	7	32	425	12
G72	234	45	0	4	0	0	0	0	0	1626	22	1590	28	1676	51	2	5	1676	51

				RATIO						AGES									
Grain	U [ppm]	Th [ppm]	Th/U	207/ 235	± s.e.	206/ 238	± s.e.	207/ 206	± s.e.	207/ 235	± 2s	206/ 238	± 2s	207/ 206	± 2s	%disc (5/8)	%disc (7/6)	Best Age [Ma]	± 2s
G73	230	66	0	4	0	0	0	0	0	1634	22	1597	28	1686	51	2	5	1686	51
G74	190	140	1	0	0	0	0	0	0	29	4	31	1	0	171	-5	-30400	31	1
G75	62	67	1	3	0	0	0	0	0	1423	25	1383	26	1487	62	3	7	1487	62
G76	48	36	1	1	0	0	0	0	0	486	19	469	10	571	105	4	18	469	10
G77	38	17	0	2	0	0	0	0	0	1025	28	1041	21	997	88	-1	-4	1041	21
G78	76	49	1	1	0	0	0	0	0	568	17	564	11	591	84	1	5	564	11
G79	5	5	1	2	0	0	0	0	0	1036	56	1010	27	1097	172	3	8	1010	27
G80	151	37	0	0	0	0	0	0	0	65	5	65	2	87	192	1	26	65	2
G81	24	33	1	1	0	0	0	0	0	542	26	536	12	574	135	1	7	536	12
G82	62	29	0	4	0	0	0	0	0	1651	26	1624	30	1689	60	2	4	1689	60
G83	94	86	1	1	0	0	0	0	0	415	14	404	8	484	91	3	17	404	8
G84	134	38	0	0	0	0	0	0	0	402	14	399	8	425	91	1	6	399	8
G85	251	54	0	5	0	0	0	0	0	1775	23	1761	31	1795	52	1	2	1795	52
G86	145	112	1	2	0	0	0	0	0	1095	20	1091	20	1110	61	0	2	1091	20
G87	46	24	1	1	0	0	0	0	0	431	18	424	9	474	117	2	10	424	9
G88	58	34	1	0	0	0	0	0	0	103	11	103	3	108	259	0	5	103	3
G89	145	210	1	0	0	0	0	0	0	197	8	191	4	276	108	3	31	191	4
G90	44	26	1	1	0	0	0	0	0	472	19	468	10	496	115	1	6	468	10
G91	54	22	0	0	0	0	0	0	0	52	10	50	2	136	457	3	63	50	2
G92	158	67	0	4	0	0	0	0	0	1647	23	1612	29	1697	54	2	5	1697	54
G93	133	72	1	3	0	0	0	0	0	1427	23	1421	26	1441	57	0	1	1441	57
G94	25	8	0	1	0	0	0	0	0	922	32	913	20	949	110	1	4	913	20
G95	32	17	1	2	0	0	0	0	0	1062	28	1054	22	1085	88	1	3	1054	22
G96	150	104	1	1	0	0	0	0	0	443	14	436	9	486	88	2	10	436	9
G97	29	15	1	2	0	0	0	0	0	978	26	964	20	1014	86	1	5	964	20
G98	18	11	1	5	0	0	0	0	0	1785	35	1771	36	1805	76	1	2	1805	76
G99	103	115	1	0	0	0	0	0	0	325	12	324	7	339	101	0	4	324	7
G100	342	363	1	0	0	0	0	0	0	25	2	24	1	46	210	1	47	24	1
G101	190	21	0	2	0	0	0	0	0	1015	20	1009	19	1034	63	1	2	1009	19
G102	12	10	1	0	0	0	0	0	0	350	40	362	11	281	296	-3	-29	362	11
G103	115	22	0	5	0	0	0	0	0	1766	25	1774	32	1761	55	0	-1	1761	55
G104	30	24	1	3	0	0	0	0	0	1415	27	1405	27	1434	69	1	2	1434	69
G105	186	18	0	0	0	0	0	0	0	341	11	339	7	364	87	1	7	339	7

Grain	U [ppm]	Th [ppm]	Th/U	RATIO 207/235	± s.e.	206/238	± s.e.	207/206	± s.e.	AGES 207/235	± 2s	206/238	± 2s	207/206	± 2s	%disc (5/8)	%disc (7/6)	Best Age [Ma]	± 2s
G106	53	49	1	0	0	0	0	0	0	111	12	103	3	274	255	7	62	103	3
G107	60	28	0	2	0	0	0	0	0	1054	23	1047	20	1073	71	1	2	1047	20
G108	36	26	1	3	0	0	0	0	0	1368	29	1342	26	1413	76	2	5	1413	76
G109	90	38	0	0	0	0	0	0	0	74	9	70	2	212	282	6	67	70	2
G110	83	30	0	5	0	0	0	0	0	1732	26	1705	31	1769	58	2	4	1769	58
G111	18	16	1	18	0	1	0	0	0	2980	30	3015	51	2960	52	-1	-2	2960	52
G112	65	30	0	4	0	0	0	0	0	1703	26	1692	31	1721	60	1	2	1721	60
G113	218	2	0	3	0	0	0	0	0	1278	23	1259	23	1315	61	2	4	1315	61
G114	45	10	0	3	0	0	0	0	0	1399	26	1404	26	1396	68	0	-1	1396	68
G115	19	10	1	16	0	1	0	0	0	2858	31	2888	50	2841	54	-1	-2	2841	54
G116	219	50	0	2	0	0	0	0	0	961	20	932	18	1033	65	3	10	932	18
G117	84	47	1	4	0	0	0	0	0	1580	28	1525	29	1659	65	4	8	1659	65
G118	112	46	0	3	0	0	0	0	0	1341	24	1329	25	1365	63	1	3	1365	63
G119	42	11	0	3	0	0	0	0	0	1327	27	1326	25	1334	71	0	1	1334	71
G120	35	25	1	15	0	1	0	0	0	2838	30	2840	48	2841	52	0	0	2841	52
G121	60	34	1	3	0	0	0	0	0	1365	25	1337	25	1412	66	2	5	1412	66
G122	309	38	0	0	0	0	0	0	0	71	6	71	2	92	199	1	23	71	2
G123	83	61	1	2	0	0	0	0	0	990	22	978	19	1021	72	1	4	978	19
G124	61	69	1	3	0	0	0	0	0	1465	27	1449	27	1493	67	1	3	1493	67
G125	44	42	1	4	0	0	0	0	0	1680	31	1677	32	1689	71	0	1	1689	71
G126	65	39	1	0	0	0	0	0	0	69	10	67	2	141	342	3	52	67	2
G127	58	96	2	3	0	0	0	0	0	1450	26	1443	27	1465	67	0	1	1465	67
G128	43	47	1	0	0	0	0	0	0	26	12	27	1	0	927	-2	-26500	27	1
G129	21	10	0	3	0	0	0	0	0	1412	40	1360	30	1495	102	4	9	1495	102
G130	39	20	1	2	0	0	0	0	0	1094	26	1095	22	1095	80	0	0	1095	22
G131	93	65	1	3	0	0	0	0	0	1514	28	1453	27	1604	67	4	9	1604	67
G132	20	11	1	7	0	0	0	0	0	2147	32	2122	39	2174	64	1	2	2174	64
G133	182	186	1	1	0	0	0	0	0	686	18	696	14	660	78	-1	-5	696	14
G134	26	21	1	1	0	0	0	0	0	595	27	608	14	552	131	-2	-10	608	14
G135	228	26	0	2	0	0	0	0	0	1222	23	1211	23	1246	64	1	3	1246	64
G136	84	25	0	5	0	0	0	0	0	1801	28	1873	33	1724	62	-4	-9	1724	62
G137	183	291	2	0	0	0	0	0	0	378	12	382	8	354	90	-1	-8	382	8
G138	192	19	0	0	0	0	0	0	0	335	11	337	7	324	92	-1	-4	337	7

				RATIO						AGES									
																		Best	
	U	Th		207/		206/		207/		207/		206/		207/		%disc	%disc	Age	
Grain	[ppm]	[ppm]	Th/U	235	± s.e.	238	± s.e.	206	± s.e.	235	± 2s	238	± 2s	206	± 2s	(5/8)	(7/6)	[Ma]	± 2s
Sample W2-5																			
G1	694	204	0	5	0	0	0	0	0	1822	21	1819	32	1830	45	0	1	1830	45
G2	538	778	1	1	0	0	0	0	0	422	13	412	8	479	82	2	14	412	8
G3	758	312	0	4	0	0	0	0	0	1663	21	1659	30	1672	47	0	1	1672	47
G4	395	198	0	2	0	0	0	0	0	1063	20	1062	20	1070	60	0	1	1062	20
G5	956	706	1	0	0	0	0	0	0	104	5	99	2	223	124	5	56	99	2
G6	563	84	0	5	0	0	0	0	0	1761	21	1748	31	1780	46	1	2	1780	46
G7	80	40	1	4	0	0	0	0	0	1593	29	1564	31	1636	67	2	4	1636	67
G8	2136	567	0	0	0	0	0	0	0	74	3	71	2	175	101	4	59	71	2
G9	125	116	1	4	0	0	0	0	0	1639	26	1644	31	1638	59	0	0	1638	59
G10	385	81	0	5	0	0	0	0	0	1733	22	1658	30	1829	48	5	9	1829	48
G11	169	111	1	4	0	0	0	0	0	1677	26	1747	33	1594	59	-4	-10	1594	59
G12	183	65	0	4	0	0	0	0	0	1713	24	1730	32	1696	53	-1	-2	1696	53
G13	175	64	0	1	0	0	0	0	0	674	21	679	14	665	93	-1	-2	679	14
G14	355	208	1	0	0	0	0	0	0	159	10	153	4	253	157	4	39	153	4
G15	185	197	1	3	0	0	0	0	0	1505	24	1497	28	1520	57	1	2	1520	57
G16	622	470	1	0	0	0	0	0	0	34	4	35	1	7	308	-1	-423	35	1
G17	382	120	0	1	0	0	0	0	0	479	15	461	9	570	84	4	19	461	9
G18	413	194	0	2	0	0	0	0	0	1180	20	1198	22	1153	56	-1	-4	1153	56
G19	1571	621	0	3	0	0	0	0	0	1276	18	1270	23	1291	49	0	2	1291	49
G20	538	246	0	5	0	0	0	0	0	1769	21	1762	31	1782	47	0	1	1782	47
G21	192	142	1	0	0	0	0	0	0	288	27	281	8	349	235	2	20	281	8
G22	651	181	0	2	0	0	0	0	0	1050	18	1050	20	1055	56	0	0	1050	20
G23	271	83	0	5	0	0	0	0	0	1747	23	1775	32	1717	51	-2	-3	1717	51
G24	58	66	1	2	0	0	0	0	0	1062	35	1077	24	1038	107	-1	-4	1077	24
G25	309	37	0	2	0	0	0	0	0	944	20	934	18	972	67	1	4	934	18
G26	147	85	1	2	0	0	0	0	0	1080	24	1071	21	1104	74	1	3	1071	21
G27	1448	845	1	0	0	0	0	0	0	68	3	67	1	104	125	1	35	67	1
G28	87	29	0	2	0	0	0	0	0	1013	31	1024	22	996	98	-1	-3	1024	22
G29	1878	518	0	4	0	0	0	0	0	1661	20	1616	29	1723	46	3	6	1723	46
G30	379	131	0	4	0	0	0	0	0	1562	25	1553	29	1578	59	1	2	1578	59
G31	87	61	1	4	0	0	0	0	0	1664	28	1688	32	1638	65	-1	-3	1638	65
G32	225	75	0	0	0	0	0	0	0	398	17	392	9	434	116	1	10	392	9

				RATIO						AGES									
Grain	**U [ppm]**	**Th [ppm]**	**Th/U**	**207/ 235**	**± s.e.**	**206/ 238**	**± s.e.**	**207/ 206**	**± s.e.**	**207/ 235**	**± 2s**	**206/ 238**	**± 2s**	**207/ 206**	**± 2s**	**%disc (5/8)**	**%disc (7/6)**	**Best Age [Ma]**	**± 2s**
G33	190	118	1	4	0	0	0	0	0	1655	24	1679	31	1629	55	-1	-3	1629	55
G34	298	148	0	1	0	0	0	0	0	637	21	619	13	706	96	3	12	619	13
G35	448	344	1	1	0	0	0	0	0	445	14	449	9	432	84	-1	-4	449	9
G36	632	122	0	0	0	0	0	0	0	179	9	166	4	356	122	8	53	166	4
G37	465	158	0	4	0	0	0	0	0	1598	23	1583	29	1622	54	1	2	1622	54
G38	211	285	1	4	0	0	0	0	0	1620	24	1613	30	1633	55	0	1	1633	55
G39	292	149	1	2	0	0	0	0	0	1070	21	1069	20	1076	64	0	1	1069	20
G40	130	71	1	2	0	0	0	0	0	970	26	962	20	993	86	1	3	962	20
G41	361	101	0	2	0	0	0	0	0	1035	20	1011	19	1090	63	2	7	1011	19
G42	304	74	0	13	0	0	0	0	0	2665	24	2611	44	2711	43	2	4	2711	43
G43	92	62	1	3	0	0	0	0	0	1397	29	1387	27	1418	73	1	2	1418	73
G44	422	151	0	3	0	0	0	0	0	1522	21	1522	28	1527	52	0	0	1527	52
G45	323	101	0	3	0	0	0	0	0	1359	22	1354	25	1371	56	0	1	1371	56
G46	122	99	1	1	0	0	0	0	0	623	27	617	14	650	123	1	5	617	14
G47	865	311	0	2	0	0	0	0	0	1036	18	1007	19	1101	55	3	9	1007	19
G48	293	84	0	0	0	0	0	0	0	105	10	103	3	164	233	2	37	103	3
G49	539	235	0	0	0	0	0	0	0	95	7	94	2	129	182	1	27	94	2
G50	282	116	0	4	0	0	0	0	0	1612	24	1566	29	1676	56	3	7	1676	56
G51	126	57	0	4	0	0	0	0	0	1702	27	1701	32	1708	60	0	0	1708	60
G52	222	134	1	2	0	0	0	0	0	1066	22	1064	21	1076	68	0	1	1064	21
G53	470	146	0	2	0	0	0	0	0	1012	19	999	19	1047	61	1	5	999	19
G54	296	231	1	4	0	0	0	0	0	1669	25	1642	30	1709	56	2	4	1709	56
G55	1543	610	0	0	0	0	0	0	0	69	4	66	1	191	124	5	66	66	1
G56	984	725	1	3	0	0	0	0	0	1441	20	1476	27	1394	51	-2	-6	1394	51
G57	704	674	1	1	0	0	0	0	0	514	13	497	10	597	73	3	17	497	10
G58	201	99	0	3	0	0	0	0	0	1400	30	1355	27	1473	76	3	8	1473	76
G59	112	81	1	4	0	0	0	0	0	1662	27	1665	31	1662	63	0	0	1662	63
G60	194	102	1	1	0	0	0	0	0	557	28	512	12	747	140	9	31	512	12
G61	65	21	0	2	0	0	0	0	0	937	35	920	21	982	116	2	6	920	21
G62	78	68	1	2	0	0	0	0	0	967	34	946	21	1022	111	2	7	946	21
G63	914	1537	2	3	0	0	0	0	0	1527	22	1511	27	1553	53	1	3	1553	53
G64	1248	390	0	0	0	0	0	0	0	63	4	66	2	0	41	-5	-66300	66	2
G65	611	4	0	1	0	0	0	0	0	803	17	787	15	851	65	2	8	787	15

				RATIO						AGES									
Grain	U [ppm]	Th [ppm]	Th/U	207/ 235	± s.e.	206/ 238	± s.e.	207/ 206	± s.e.	207/ 235	± 2s	206/ 238	± 2s	207/ 206	± 2s	%disc (5/8)	%disc (7/6)	Best Age [Ma]	± 2s
G66	954	73	0	4	0	0	0	0	0	1647	22	1602	29	1710	51	3	6	1710	51
G67	175	55	0	2	0	0	0	0	0	982	29	953	20	1051	93	3	9	953	20
G68	325	190	1	10	0	0	0	0	0	2446	26	2336	41	2543	49	5	8	2543	49
G69	125	35	0	0	0	0	0	0	0	213	25	202	7	347	291	6	42	202	7
G70	73	46	1	2	0	0	0	0	0	1126	38	1100	25	1183	111	2	7	1100	25
G71	409	158	0	2	0	0	0	0	0	1174	21	1153	22	1217	61	2	5	1217	61
G72	602	289	0	1	0	0	0	0	0	438	14	425	9	513	88	3	17	425	9
G73	208	83	0	4	0	0	0	0	0	1729	26	1728	32	1734	59	0	0	1734	59
G74	401	127	0	4	0	0	0	0	0	1682	24	1684	30	1682	54	0	0	1682	54
G75	143	69	0	3	0	0	0	0	0	1302	26	1281	25	1341	70	2	4	1341	70
G76	563	137	0	2	0	0	0	0	0	1053	20	1046	20	1070	61	1	2	1046	20
G77	914	478	1	4	0	0	0	0	0	1704	23	1703	30	1710	51	0	0	1710	51
G78	264	153	1	4	0	0	0	0	0	1677	28	1715	32	1633	63	-2	-5	1633	63
G79	143	44	0	0	0	0	0	0	0	70	17	73	3	0	480	-5	-73000	73	3
G80	166	71	0	4	0	0	0	0	0	1725	27	1743	32	1707	61	-1	-2	1707	61
G81	1516	1106	1	0	0	0	0	0	0	101	4	98	2	177	106	3	45	98	2
G82	252	10	0	2	0	0	0	0	0	1023	22	1019	20	1034	70	0	1	1019	20
G83	390	148	0	2	0	0	0	0	0	1119	21	1139	21	1083	63	-2	-5	1083	63
G84	385	471	1	0	0	0	0	0	0	104	8	100	3	211	194	4	53	100	3
G85	157	360	2	3	0	0	0	0	0	1463	26	1438	27	1504	65	2	4	1504	65
G86	246	194	1	4	0	0	0	0	0	1601	27	1568	29	1648	63	2	5	1648	63
G87	216	76	0	5	0	0	0	0	0	1753	26	1737	31	1778	57	1	2	1778	57
G88	796	198	0	3	0	0	0	0	0	1437	24	1491	27	1362	60	-4	-9	1362	60
G89	176	138	1	17	0	1	0	0	0	2917	27	2897	48	2934	47	1	1	2934	47
G90	183	42	0	8	0	0	0	0	0	2246	27	2141	38	2347	52	5	9	2347	52
G91	637	46	0	4	0	0	0	0	0	1600	24	1582	28	1628	56	1	3	1628	56
G92	735	279	0	3	0	0	0	0	0	1377	24	1324	25	1464	62	4	10	1464	62
G93	718	389	1	12	0	0	0	0	0	2611	27	2466	41	2730	48	6	10	2730	48
G94	1345	841	1	0	0	0	0	0	0	67	5	61	2	289	172	10	79	61	2
G95	506	177	0	0	0	0	0	0	0	104	7	97	2	256	169	6	62	97	2
G96	103	21	0	2	0	0	0	0	0	1099	29	1125	23	1053	88	-2	-7	1053	88
G97	325	110	0	1	0	0	0	0	0	651	19	631	13	725	83	3	13	631	13
G98	869	613	1	0	0	0	0	0	0	102	6	98	2	193	132	4	49	98	2

				RATIO						AGES									
Grain	U [ppm]	Th [ppm]	Th/U	207/235	± s.e.	206/238	± s.e.	207/206	± s.e.	207/235	± 2s	206/238	± 2s	207/206	± 2s	%disc (5/8)	%disc (7/6)	Best Age [Ma]	± 2s
G99	538	289	1	0	0	0	0	0	0	77	6	74	2	178	193	4	58	74	2
G100	318	116	0	4	0	0	0	0	0	1639	25	1643	30	1638	59	0	0	1638	59
G101	764	393	1	0	0	0	0	0	0	94	7	93	2	121	172	1	23	93	2
G102	690	242	0	1	0	0	0	0	0	589	16	581	12	625	78	1	7	581	12
G103	132	121	1	5	0	0	0	0	0	1875	29	1868	34	1887	62	0	1	1887	62
G104	327	261	1	0	0	0	0	0	0	76	9	72	2	224	268	6	68	72	2
G105	270	172	1	7	0	0	0	0	0	2140	30	2221	40	2066	61	-4	-8	2066	61
G106	633	384	1	1	0	0	0	0	0	684	17	681	13	702	74	1	3	681	13
G107	533	233	0	2	0	0	0	0	0	1032	22	1022	19	1056	70	1	3	1022	19
G108	678	369	1	0	0	0	0	0	0	77	6	76	2	118	176	1	35	76	2
G109	207	230	1	4	0	0	0	0	0	1717	27	1719	31	1720	62	0	0	1720	62
G110	190	141	1	3	0	0	0	0	0	1363	28	1320	25	1435	72	3	8	1435	72
G111	50	45	1	12	0	0	0	0	0	2567	33	2530	46	2599	60	1	3	2599	60
G112	227	33	0	5	0	0	0	0	0	1806	28	1742	32	1885	62	4	8	1885	62
G113	467	160	0	1	0	0	0	0	0	596	17	592	12	616	82	1	4	592	12
G114	451	218	0	0	0	0	0	0	0	170	9	169	4	183	140	0	7	169	4
G115	305	126	0	4	0	0	0	0	0	1659	27	1610	29	1725	61	3	7	1725	61
G116	246	104	0	3	0	0	0	0	0	1480	26	1462	27	1510	65	1	3	1510	65
G117	241	35	0	3	0	0	0	0	0	1469	35	1407	30	1563	85	4	10	1563	85
G118	207	80	0	4	0	0	0	0	0	1647	24	1670	31	1621	56	-1	-3	1621	56
G119	446	234	1	0	0	0	0	0	0	98	13	95	3	188	323	4	50	95	3
G120	566	144	0	1	0	0	0	0	0	926	26	896	19	1002	89	3	11	896	19
G121	292	118	0	3	0	0	0	0	0	1443	24	1438	28	1454	60	0	1	1454	60
G122	429	104	0	5	0	0	0	0	0	1761	23	1783	33	1739	51	-1	-3	1739	51
G123	710	162	0	4	0	0	0	0	0	1669	23	1673	31	1668	52	0	0	1668	52
G124	546	55	0	3	0	0	0	0	0	1440	24	1425	28	1466	61	1	3	1466	61
G125	81	58	1	2	0	0	0	0	0	1092	32	1075	23	1130	95	2	5	1075	23
G126	163	65	0	2	0	0	0	0	0	1037	25	1009	21	1100	77	3	8	1009	21
G127	309	105	0	0	0	0	0	0	0	397	16	394	9	419	105	1	6	394	9
G128	347	144	0	4	0	0	0	0	0	1665	25	1594	30	1760	57	4	9	1760	57
G129	593	172	0	3	0	0	0	0	0	1372	22	1325	25	1450	55	4	9	1450	55
G130	1286	246	0	1	0	0	0	0	0	480	13	442	9	674	71	9	34	442	9
G131	638	225	0	4	0	0	0	0	0	1668	23	1667	31	1672	52	0	0	1672	52

Grain	U [ppm]	Th [ppm]	Th/U	RATIO 207/235	± s.e.	206/238	± s.e.	207/206	± s.e.	AGES 207/235	± 2s	206/238	± 2s	207/206	± 2s	%disc (5/8)	%disc (7/6)	Best Age [Ma]	± 2s
G132	435	106	0	4	0	0	0	0	0	1576	23	1530	29	1642	55	3	7	1642	55
G133	377	190	1	12	0	0	0	0	0	2594	26	2587	45	2604	46	0	1	2604	46
G134	132	30	0	4	0	0	0	0	0	1714	27	1694	32	1742	60	1	3	1742	60
G135	267	84	0	4	0	0	0	0	0	1587	26	1555	30	1635	60	2	5	1635	60
Sample LA1701																			
2293A2	481	352	1	0	0	0	0	0	0	28	7	26	1	174	348	5	85	26	1
2293A2	528	396	1	0	0	0	0	0	0	28	7	27	2	200	399	5	87	27	2
2293A2	521	192	3	0	0	0	0	0	0	40	6	34	2	282	381	13	88	34	2
2293A2	417	337	1	0	0	0	0	0	0	37	8	35	3	231	462	7	85	35	3
2293A2	575	216	3	0	0	0	0	0	0	40	7	35	2	298	431	13	88	35	2
2293A2	234	148	2	0	0	0	0	0	0	37	9	35	2	248	497	5	86	35	2
2293A2	257	166	2	0	0	0	0	0	0	39	10	35	2	343	685	9	90	35	2
2293A2	458	383	1	0	0	0	0	0	0	40	9	36	4	295	548	9	88	36	4
2293A2	440	161	3	0	0	0	0	0	0	58	7	56	2	162	314	3	65	56	2
2293A2	403	144	3	0	0	0	0	0	0	58	6	56	2	173	249	3	67	56	2
2293A2	956	752	1	0	0	0	0	0	0	71	7	70	5	172	222	2	59	70	5
2293A2	519	389	1	0	0	0	0	0	0	76	8	73	2	152	239	5	52	73	2
2293A2	468	343	1	0	0	0	0	0	0	76	7	73	2	137	208	4	47	73	2
2293A2	793	124	6	0	0	0	0	0	0	75	6	75	2	111	201	1	33	75	2
2293A2	727	112	6	0	0	0	0	0	0	76	5	75	2	115	170	1	35	75	2
2293A2	1551	180	9	0	0	0	0	0	0	79	5	78	4	155	157	1	49	78	4
2293A2	221	141	2	0	0	0	0	0	0	84	15	82	5	231	449	2	64	82	5
2293A2	640	368	2	0	0	0	0	0	0	86	7	86	3	156	184	1	45	86	3
2293A2	584	328	2	0	0	0	0	0	0	88	6	86	3	168	156	2	49	86	3
2293A2	466	260	2	0	0	0	0	0	0	91	9	90	6	196	259	2	54	90	6
2293A2	424	234	2	0	0	0	0	0	0	92	8	90	5	198	221	2	54	90	5
2293A2	329	101	3	0	0	0	0	0	0	95	10	95	3	161	260	0	41	95	3
2293A2	352	178	2	0	0	0	0	0	0	95	12	95	3	219	307	0	57	95	3
2293A2	303	91	3	0	0	0	0	0	0	97	9	96	3	169	225	1	44	96	3
2293A2	299	256	1	0	0	0	0	0	0	104	12	97	4	280	295	7	66	97	4
2293A2	271	226	1	0	0	0	0	0	0	105	11	97	3	252	268	7	61	97	3

				RATIO						AGES									
Grain	U [ppm]	Th [ppm]	Th/U	207/ 235	± s.e.	206/ 238	± s.e.	207/ 206	± s.e.	207/ 235	± 2s	206/ 238	± 2s	207/ 206	± 2s	%disc (5/8)	%disc (7/6)	Best Age [Ma]	± 2s
2293A2	2260	1958	1	0	0	0	0	0	0	101	7	98	6	198	150	3	51	98	6
2293A2	194	68	3	0	0	0	0	0	0	150	18	141	5	303	277	7	54	141	5
2293A2	306	157	2	0	0	0	0	0	0	164	13	160	5	258	196	3	38	160	5
2293A2	657	392	2	0	0	0	0	0	0	162	9	161	6	195	136	1	17	161	6
2293A2	684	517	1	0	0	0	0	0	0	170	9	169	4	170	123	0	1	169	4
2293A2	749	579	1	0	0	0	0	0	0	171	10	169	5	181	144	1	7	169	5
2293A2	282	58	5	0	0	0	0	0	0	205	18	195	13	299	225	5	35	195	13
2293A2	333	107	3	0	0	0	0	0	0	207	14	201	6	234	160	3	14	201	6
2293A2	1018	210	5	0	0	0	0	0	0	368	19	340	17	500	128	8	32	340	17
2293A2	738	262	3	0	0	0	0	0	0	384	16	384	13	383	102	0	0	384	13
2293A2	810	291	3	0	0	0	0	0	0	386	18	386	15	383	121	0	-1	386	15
2293A2	78	33	2	0	0	0	0	0	0	405	37	394	12	509	199	3	23	394	12
2293A2	428	148	3	0	0	0	0	0	0	405	19	407	10	374	106	0	-9	407	10
2293A2	276	30	9	0	0	0	0	0	0	416	22	410	12	388	112	1	-6	410	12
2293A2	847	557	2	1	0	0	0	0	0	446	18	433	10	524	101	3	17	433	10
2293A2	523	11	46	1	0	0	0	0	0	512	22	488	18	606	110	5	20	488	18
2293A2	575	168	3	1	0	0	0	0	0	499	28	496	28	539	138	1	8	496	28
2293A2	120	51	2	1	0	0	0	0	0	559	46	534	28	675	206	4	21	534	28
2293A2	96	77	1	1	0	0	0	0	0	558	31	563	12	575	119	-1	2	563	12
2293A2	424	176	2	1	0	0	0	0	0	574	24	565	17	595	93	2	5	565	17
2293A2	105	87	1	1	0	0	0	0	0	565	37	568	13	573	138	0	1	568	13
2293A2	625	590	1	1	0	0	0	0	0	605	27	602	27	668	116	0	10	602	27
2293A2	1215	303	4	2	0	0	0	0	0	943	23	920	23	1015	60	2	9	920	23
2293A2	553	185	3	2	0	0	0	0	0	988	34	954	35	1089	85	3	12	954	35
2293A2	116	31	4	2	0	0	0	0	0	962	47	959	45	1021	126	0	6	959	45
2293A2	653	166	4	2	0	0	0	0	0	1005	43	964	50	1073	121	4	10	964	50
2293A2	54	17	3	2	0	0	0	0	0	977	54	976	22	948	124	0	-3	976	22
2293A2	372	34	11	2	0	0	0	0	0	980	26	979	19	999	60	0	2	979	19
2293A2	122	25	5	2	0	0	0	0	0	950	43	981	46	984	114	-3	0	981	46
2293A2	421	40	11	2	0	0	0	0	0	1011	27	988	29	1032	70	2	4	988	29
2293A2	187	161	1	2	0	0	0	0	0	1001	39	995	30	1030	88	1	3	995	30
2293A2	110	28	4	2	0	0	0	0	0	1020	43	1004	36	1028	91	2	2	1004	36
2293A2	350	70	5	2	0	0	0	0	0	1036	45	1009	61	1099	133	3	8	1009	61

				RATIO						AGES									
																		Best	
	U	Th		207/		206/		207/		207/		206/		207/		%disc	%disc	Age	
Grain	[ppm]	[ppm]	Th/U	235	± s.e.	238	± s.e.	206	± s.e.	235	± 2s	238	± 2s	206	± 2s	(5/8)	(7/6)	[Ma]	± 2s
2293A2	165	49	3	2	0	0	0	0	0	1042	49	1015	55	1078	134	3	6	1015	55
2293A2	43	21	2	2	0	0	0	0	0	985	52	1025	33	1102	120	-4	7	1025	33
2293A2	501	261	2	2	0	0	0	0	0	1069	60	1045	40	1209	122	2	14	1045	40
2293A2	570	44	13	2	0	0	0	0	0	1072	27	1058	26	1072	62	1	1	1058	26
2293A2	45	31	1	2	0	0	0	0	0	1064	68	1061	29	1054	142	0	-1	1061	29
2293A2	266	144	2	2	0	0	0	0	0	1158	70	1089	87	1261	117	6	14	1089	87
2293A2	273	82	3	2	0	0	0	0	0	1099	29	1111	26	1104	68	-1	-1	1111	26
2293A2	621	319	2	2	0	0	0	0	0	1178	47	1128	61	1324	119	4	15	1128	61
2293A2	41	12	3	2	0	0	0	0	0	1094	65	1137	30	1182	103	-4	4	1137	30
2293A2	558	283	2	2	0	0	0	0	0	1179	40	1141	53	1301	101	3	12	1141	53
2293A2	1105	17	66	2	0	0	0	0	0	1118	35	1143	47	1101	101	-2	-4	1143	47
2293A2	145	69	2	2	0	0	0	0	0	1120	50	1143	65	1182	138	-2	3	1143	65
2293A2	209	97	2	2	0	0	0	0	0	1162	48	1148	72	1262	128	1	9	1148	72
2293A2	35	9	4	2	0	0	0	0	0	1172	72	1161	52	1206	132	1	4	1161	52
2293A2	20	12	2	3	0	0	0	0	0	1215	92	1256	42	1331	175	-3	6	1256	42
2293A2	230	81	3	3	0	0	0	0	0	1279	34	1282	25	1328	55	0	3	1282	25
2293A2	267	271	1	3	0	0	0	0	0	1330	31	1326	28	1370	57	0	3	1326	28
2293A2	1722	736	2	3	0	0	0	0	0	1362	25	1354	31	1399	54	1	3	1354	31
2293A2	109	34	3	3	0	0	0	0	0	1358	60	1357	76	1375	126	0	1	1357	76
2293A2	278	122	2	3	0	0	0	0	0	1393	39	1360	33	1407	64	2	3	1360	33
2293A2	194	92	2	3	0	0	0	0	0	1412	46	1361	68	1444	117	4	6	1361	68
2293A2	676	122	6	3	0	0	0	0	0	1406	61	1382	67	1521	122	2	9	1382	67
2293A2	402	451	1	3	0	0	0	0	0	1397	28	1398	29	1422	51	0	2	1398	29
2293A2	69	17	4	3	0	0	0	0	0	1399	51	1400	30	1460	76	0	4	1400	30
2293A2	449	20	22	3	0	0	0	0	0	1427	57	1403	79	1538	118	2	9	1403	79
2293A2	101	44	2	3	0	0	0	0	0	1419	57	1407	61	1460	104	1	4	1407	61
2293A2	54	58	1	3	0	0	0	0	0	1405	62	1414	32	1425	89	-1	1	1414	32
2293A2	875	385	2	3	0	0	0	0	0	1427	31	1415	40	1463	66	1	3	1415	40
2293A2	505	287	2	3	0	0	0	0	0	1423	32	1416	38	1461	63	1	3	1416	38
2293A2	420	97	4	3	0	0	0	0	0	1430	32	1432	29	1458	50	0	2	1432	29
2293A2	214	120	2	4	0	0	0	0	0	1538	39	1563	30	1552	57	-2	-1	1552	57
2293A2	189	34	6	4	0	0	0	0	0	1574	61	1595	84	1625	121	-1	2	1625	121
2293A2	74	36	2	4	0	0	0	0	0	1606	57	1547	35	1625	73	4	5	1625	73

				RATIO						AGES									
Grain	U [ppm]	Th [ppm]	Th/U	207/ 235	± s.e.	206/ 238	± s.e.	207/ 206	± s.e.	207/ 235	± 2s	206/ 238	± 2s	207/ 206	± 2s	%disc (5/8)	%disc (7/6)	Best Age [Ma]	± 2s
2293A	148	73	2	4	0	0	0	0	0	1622	37	1626	41	1633	62	0	0	1633	62
2293A	912	378	2	4	0	0	0	0	0	1586	46	1520	77	1639	102	4	7	1639	102
2293A	59	29	2	4	0	0	0	0	0	1675	61	1617	38	1667	80	3	3	1667	80
2293A	148	106	1	4	0	0	0	0	0	1624	55	1599	85	1669	102	2	4	1669	102
2293A	109	44	2	4	0	0	0	0	0	1680	46	1645	45	1672	70	2	2	1672	70
2293A	88	42	2	4	0	0	0	0	0	1648	51	1616	37	1678	68	2	4	1678	68
2293A	384	221	2	4	0	0	0	0	0	1671	48	1650	77	1716	98	1	4	1716	98
2293A	339	68	5	4	0	0	0	0	0	1641	61	1586	79	1744	127	3	9	1744	127
2293A	215	76	3	4	0	0	0	0	0	1643	54	1596	68	1768	90	3	10	1768	90
2293A	93	66	1	5	0	0	0	0	0	1737	56	1786	72	1805	96	-3	1	1805	96
2293A	204	85	2	5	0	0	0	0	0	1791	38	1781	36	1817	52	1	2	1817	52
2293A	195	96	2	5	0	0	0	0	0	1798	58	1812	83	1855	98	-1	2	1855	98
2293A	116	97	1	5	0	0	0	0	0	1846	49	1869	53	1881	64	-1	1	1881	64
2293A	184	41	4	10	1	0	0	0	0	2438	56	2452	97	2493	88	-1	2	2493	88
2293A	243	351	1	12	0	0	0	0	0	2587	42	2555	55	2684	50	1	5	2684	50
2293A	107	47	2	13	0	1	0	0	0	2683	47	2659	46	2688	45	1	1	2688	45
2293A	242	112	2	12	1	0	0	0	0	2564	82	2359	143	2751	115	8	14	2751	115
2293A	346	217	2	13	2	0	0	0	0	2590	167	2396	343	2870	238	7	16	2870	238
Sample 21022001																			
4972A_	257	120	2	0	0	0	0	0	0	23	4	22	1	65	130	3	65	22	1
4972A_	87	28	3	0	0	0	0	0	0	31	5	27	2	297	429	13	91	27	2
4972A_	88	29	3	0	0	0	0	0	0	32	6	29	2	267	441	12	89	29	2
4972A_	180	120	1	0	0	0	0	0	0	36	4	34	1	189	292	6	82	34	1
4972A_	48	21	2	0	0	0	0	0	0	68	11	67	4	10	19	0	-601	67	4
4972A_	142	56	3	0	0	0	0	0	0	71	10	67	2	111	221	5	39	67	2
4972A_	144	58	3	0	0	0	0	0	0	73	10	70	2	107	214	4	35	70	2
4972A_	122	47	3	0	0	0	0	0	0	70	8	72	3	62	124	-2	-16	72	3
4972A_	216	106	2	0	0	0	0	0	0	71	8	72	2	89	177	-2	18	72	2
4972A_	62	25	2	0	0	0	0	0	0	77	10	73	3	93	187	5	22	73	3
4972A_	134	80	2	0	0	0	0	0	0	71	11	73	3	10	20	-2	-631	73	3
4972A_	127	51	3	0	0	0	0	0	0	71	8	74	3	38	75	-3	-97	74	3
4972A_	135	82	2	0	0	0	0	0	0	72	11	75	3	5	10	-3	-1375	75	3

				RATIO						AGES									
Grain	U [ppm]	Th [ppm]	Th/U	207/ 235	± s.e.	206/ 238	± s.e.	207/ 206	± s.e.	207/ 235	± 2s	206/ 238	± 2s	207/ 206	± 2s	%disc (5/8)	%disc (7/6)	Best Age [Ma]	± 2s
4972A_	267	154	2	0	0	0	0	0	0	78	6	75	2	137	188	4	45	75	2
4972A_	67	46	1	0	0	0	0	0	0	81	11	75	2	112	225	7	33	75	2
4972A_	179	63	3	0	0	0	0	0	0	79	8	76	2	153	248	4	50	76	2
4972A_	150	74	2	0	0	0	0	0	0	83	8	77	3	213	207	8	64	77	3
4972A_	125	22	6	0	0	0	0	0	0	80	8	79	2	143	249	1	44	79	2
4972A_	145	36	4	0	0	0	0	0	0	94	11	91	4	193	295	3	53	91	4
4972A_	122	41	3	0	0	0	0	0	0	100	12	93	3	272	305	7	66	93	3
4972A_	151	52	3	0	0	0	0	0	0	99	9	94	2	174	231	5	46	94	2
4972A_	488	102	5	0	0	0	0	0	0	95	5	95	3	88	136	1	-7	95	3
4972A_	123	42	3	0	0	0	0	0	0	104	13	97	3	267	305	7	64	97	3
4972A_	124	31	4	0	0	0	0	0	0	109	9	99	2	199	173	9	50	99	2
4972A_	160	57	3	0	0	0	0	0	0	110	9	107	3	171	190	3	37	107	3
4972A_	114	113	1	0	0	0	0	0	0	173	16	163	4	251	235	6	35	163	4
4972A_	98	49	2	0	0	0	0	0	0	164	21	163	5	131	262	1	-24	163	5
4972A_	112	118	1	0	0	0	0	0	0	172	12	166	4	207	158	4	20	166	4
4972A_	115	115	1	0	0	0	0	0	0	180	17	168	4	267	235	6	37	168	4
4972A_	117	124	1	0	0	0	0	0	0	177	12	171	4	194	153	3	12	171	4
4972A_	52	30	2	0	0	0	0	0	0	265	23	250	7	329	192	6	24	250	7
4972A_	45	18	2	1	0	0	0	0	0	438	30	425	9	428	105	3	1	425	9
4972A_	42	26	2	1	0	0	0	0	0	483	30	464	8	513	141	4	9	464	8
4972A_	67	13	5	1	0	0	0	0	0	745	34	702	15	759	111	6	7	702	15
4972A_	25	5	5	2	0	0	0	0	0	946	51	939	18	884	117	1	-6	939	18
4972A_	8	4	2	2	0	0	0	0	0	1125	88	942	33	936	176	16	-1	942	33
4972A_	9	4	2	2	0	0	0	0	0	1149	85	965	33	952	168	16	-1	965	33
4972A_	37	42	1	2	0	0	0	0	0	973	46	966	17	961	91	1	-1	966	17
4972A_	48	13	4	2	0	0	0	0	0	1018	36	975	15	1000	70	4	3	975	15
4972A_	24	10	2	2	0	0	0	0	0	983	40	993	20	1000	84	-1	1	993	20
4972A_	29	10	3	2	0	0	0	0	0	1006	49	1008	19	1005	104	0	0	1008	19
4972A_	8	6	1	2	0	0	0	0	0	1017	87	1013	27	974	184	0	-4	1013	27
4972A_	47	10	5	2	0	0	0	0	0	1038	31	1030	13	1075	64	1	4	1030	13
4972A_	35	22	2	2	0	0	0	0	0	1031	57	1045	24	1057	133	-1	1	1045	24
4972A_	9	3	3	2	0	0	0	0	0	1115	77	1050	22	1012	154	6	-4	1050	22
4972A_	31	8	4	2	0	0	0	0	0	1034	36	1051	13	1016	59	-2	-3	1051	13

				RATIO						AGES									
Grain	U [ppm]	Th [ppm]	Th/U	207/ 235	± s.e.	206/ 238	± s.e.	207/ 206	± s.e.	207/ 235	± 2s	206/ 238	± 2s	207/ 206	± 2s	%disc (5/8)	%disc (7/6)	Best Age [Ma]	± 2s
4972A_	7	4	2	2	0	0	0	0	0	1124	116	1052	33	1049	195	6	0	1052	33
4972A_	27	21	1	2	0	0	0	0	0	1077	55	1053	15	1121	90	2	6	1053	15
4972A_	27	15	2	2	0	0	0	0	0	1039	51	1059	21	1024	98	-2	-3	1059	21
4972A_	28	24	1	2	0	0	0	0	0	1123	52	1069	15	1081	84	5	1	1069	15
4972A_	38	13	3	2	0	0	0	0	0	1076	34	1070	16	1057	65	1	-1	1070	16
4972A_	186	21	9	2	0	0	0	0	0	1100	23	1079	16	1114	45	2	3	1079	16
4972A_	13	7	2	2	0	0	0	0	0	1113	65	1079	19	1045	92	3	-3	1079	19
4972A_	33	18	2	2	0	0	0	0	0	1099	47	1084	17	1092	93	1	1	1084	17
4972A_	36	13	3	2	0	0	0	0	0	1052	44	1084	18	1037	74	-3	-5	1084	18
4972A_	51	10	5	2	0	0	0	0	0	1094	40	1089	21	1067	77	0	-2	1089	21
4972A_	17	37	0	2	0	0	0	0	0	1055	67	1102	20	1086	125	-4	-1	1102	20
4972A_	129	26	5	2	0	0	0	0	0	1147	24	1103	13	1156	45	4	5	1103	13
4972A_	129	25	5	2	0	0	0	0	0	1151	25	1110	13	1162	47	4	4	1110	13
4972A_	17	38	0	2	0	0	0	0	0	1088	69	1123	20	1117	124	-3	-1	1123	20
4972A_	9	4	2	2	0	0	0	0	0	1168	137	1130	45	1265	212	3	11	1130	45
4972A_	8	3	3	2	0	0	0	0	0	1210	158	1132	39	1162	144	6	3	1132	39
4972A_	29	18	2	2	0	0	0	0	0	1183	55	1148	31	1260	125	3	9	1148	31
4972A_	20	7	3	2	0	0	0	0	0	1128	58	1167	23	1167	88	-3	0	1167	23
4972A_	44	10	4	2	0	0	0	0	0	1141	51	1175	17	1168	71	-3	-1	1175	17
4972A_	8	4	2	2	0	0	0	0	0	1217	86	1188	28	1276	161	2	7	1188	28
4972A_	65	17	4	2	0	0	0	0	0	1223	37	1190	18	1161	60	3	-3	1190	18
4972A_	46	13	4	2	0	0	0	0	0	1235	44	1191	18	1188	64	4	0	1191	18
4972A_	42	19	2	3	0	0	0	0	0	1304	49	1330	21	1264	58	-2	-5	1330	21
4972A_	92	18	5	3	0	0	0	0	0	1357	30	1330	17	1328	48	2	0	1330	17
4972A_	35	4	8	3	0	0	0	0	0	1336	56	1340	20	1382	74	0	3	1340	20
4972A_	261	24	11	3	0	0	0	0	0	1354	29	1350	21	1401	52	0	4	1350	21
4972A_	24	7	3	3	0	0	0	0	0	1352	70	1354	29	1407	106	0	4	1354	29
4972A_	90	23	4	3	0	0	0	0	0	1391	34	1354	21	1359	43	3	0	1354	21
4972A_	86	17	5	3	0	0	0	0	0	1398	33	1364	18	1345	52	2	-1	1364	18
4972A_	31	18	2	3	0	0	0	0	0	1400	55	1373	19	1315	90	2	-4	1373	19
4972A_	65	25	3	3	0	0	0	0	0	1397	35	1382	21	1443	53	1	4	1382	21
4972A_	24	7	3	3	0	0	0	0	0	1389	68	1393	29	1414	102	0	1	1393	29
4972A_	30	9	3	3	0	0	0	0	0	1450	42	1402	21	1442	63	3	3	1402	21

				RATIO						AGES									
																		Best	
	U	Th		207/		206/		207/		207/		206/		207/		%disc	%disc	Age	
Grain	[ppm]	[ppm]	Th/U	235	± s.e.	238	± s.e.	206	± s.e.	235	± 2s	238	± 2s	206	± 2s	(5/8)	(7/6)	[Ma]	± 2s
4972A_	11	4	3	3	0	0	0	0	0	1501	88	1409	26	1467	105	6	4	1409	26
4972A_	130	43	3	3	0	0	0	0	0	1405	34	1431	29	1437	52	-2	0	1431	29
4972A_	55	26	2	3	0	0	0	0	0	1432	37	1438	31	1389	70	0	-4	1438	31
4972A_	191	46	4	3	0	0	0	0	0	1441	31	1444	19	1431	39	0	-1	1444	19
4972A_	38	18	2	3	0	0	0	0	0	1489	39	1457	25	1474	62	2	1	1457	25
4972A_	7	8	1	3	0	0	0	0	0	1478	61	1461	25	1547	100	1	6	1461	25
4972A_	67	12	6	3	0	0	0	0	0	1506	31	1467	29	1485	55	3	1	1467	29
4972A_	11	7	2	3	0	0	0	0	0	1491	114	1483	22	1477	90	1	0	1483	22
4972A_	66	12	5	4	0	0	0	0	0	1532	30	1485	29	1497	54	3	1	1485	29
4972A_	77	43	2	4	0	0	0	0	0	1665	31	1654	28	1627	48	1	-2	1627	48
4972A_	28	11	3	4	0	0	0	0	0	1634	53	1617	22	1635	55	1	1	1635	55
4972A_	45	27	2	4	0	0	0	0	0	1638	58	1587	25	1636	64	3	3	1636	64
4972A_	159	24	7	4	0	0	0	0	0	1648	28	1644	22	1651	41	0	0	1651	41
4972A_	53	36	1	4	0	0	0	0	0	1679	38	1680	21	1676	45	0	0	1676	45
4972A_	35	14	2	5	0	0	0	0	0	1803	58	1785	28	1709	86	1	-4	1709	86
4972A_	30	10	3	5	0	0	0	0	0	1734	44	1732	27	1721	43	0	-1	1721	43
4972A_	102	37	3	4	0	0	0	0	0	1730	33	1739	24	1722	44	0	-1	1722	44
4972A_	152	95	2	5	0	0	0	0	0	1767	32	1763	22	1729	38	0	-2	1729	38
4972A_	103	32	3	5	0	0	0	0	0	1743	29	1735	24	1730	35	0	0	1730	35
4972A_	100	59	2	5	0	0	0	0	0	1774	43	1727	27	1797	44	3	4	1797	44
4972A_	30	20	1	5	0	0	0	0	0	1798	51	1844	28	1805	43	-3	-2	1805	43
4972A_	65	29	2	5	0	0	0	0	0	1878	30	1843	28	1810	38	2	-2	1810	38
4972A_	20	7	3	5	0	0	0	0	0	1784	59	1843	35	1817	65	-3	-1	1817	65
4972A_	19	7	3	5	0	0	0	0	0	1798	64	1870	39	1834	70	-4	-2	1834	70
4972A_	32	19	2	5	0	0	0	0	0	1883	57	1850	25	1856	58	2	0	1856	58
4972A_	3	1	4	10	2	0	0	0	0	2399	176	2327	52	2362	92	3	1	2362	92
4972A_	21	13	2	11	1	0	0	0	0	2527	57	2542	40	2511	42	-1	-1	2511	42
4972A_	23	3	7	13	1	1	0	0	0	2667	56	2626	40	2622	46	2	0	2622	46
4972A_	130	86	2	13	1	1	0	0	0	2679	41	2692	42	2649	32	0	-2	2649	32
4972A_	35	16	2	13	1	1	0	0	0	2656	73	2662	37	2714	44	0	2	2714	44
4972A_	35	17	2	13	1	1	0	0	0	2697	69	2711	35	2733	42	-1	1	2733	42

Sample B3-2

				RATIO						AGES									
Grain	U [ppm]	Th [ppm]	Th/U	207/ 235	± s.e.	206/ 238	± s.e.	207/ 206	± s.e.	207/ 235	± 2s	206/ 238	± 2s	207/ 206	± 2s	%disc (5/8)	%disc (7/6)	Best Age [Ma]	± 2s
4752A_	295	142	2	0	0	0	0	0	0	26	4	25	1	38	76	2	34	25	1
4752A_	499	95	5	0	0	0	0	0	0	33	4	30	1	263	279	8	88	30	1
4752A_	501	97	5	0	0	0	0	0	0	35	4	32	1	274	272	8	88	32	1
4752A_	182	122	1	0	0	0	0	0	0	37	4	35	1	173	273	5	80	35	1
4752A_	48	21	2	0	0	0	0	0	0	72	12	71	4	21	42	1	-240	71	4
4752A_	104	54	2	0	0	0	0	0	0	75	11	72	4	259	361	4	72	72	4
4752A_	102	53	2	0	0	0	0	0	0	76	11	72	4	254	362	4	72	72	4
4752A_	105	62	2	0	0	0	0	0	0	88	14	74	3	455	390	16	84	74	3
4752A_	229	115	2	0	0	0	0	0	0	73	8	74	2	81	162	-2	9	74	2
4752A_	62	26	2	0	0	0	0	0	0	80	10	76	3	90	180	5	16	76	3
4752A_	177	63	3	0	0	0	0	0	0	80	8	77	2	174	247	5	56	77	2
4752A_	68	47	1	0	0	0	0	0	0	85	11	79	2	117	235	7	33	79	2
4752A_	107	63	2	0	0	0	0	0	0	94	15	79	3	455	390	16	83	79	3
4752A_	48	38	1	0	0	0	0	0	0	95	33	82	7	504	892	14	84	82	7
4752A_	83	27	3	0	0	0	0	0	0	109	21	92	10	527	499	16	83	92	10
4752A_	49	38	1	0	0	0	0	0	0	105	36	92	8	499	893	13	82	92	8
4752A_	147	36	4	0	0	0	0	0	0	99	12	94	4	201	296	4	53	94	4
4752A_	519	109	5	0	0	0	0	0	0	96	5	96	3	83	130	0	-15	96	3
4752A_	152	53	3	0	0	0	0	0	0	101	10	97	2	160	231	4	40	97	2
4752A_	298	105	3	0	0	0	0	0	0	106	14	98	4	347	321	7	72	98	4
4752A_	84	27	3	0	0	0	0	0	0	118	22	98	10	534	498	17	82	98	10
4752A_	302	107	3	0	0	0	0	0	0	111	15	105	4	336	321	6	69	105	4
4752A_	4	25	0	0	1	0	0	0	0	371	524	121	46	2215	4336	67	95	121	46
4752A_	25	14	2	0	0	0	0	0	0	218	113	160	24	811	1407	27	80	160	24
4752A_	99	50	2	0	0	0	0	0	0	171	22	169	5	132	264	1	-28	169	5
4752A_	58	53	1	0	0	0	0	0	0	193	41	186	12	305	491	4	39	186	12
4752A_	58	54	1	0	0	0	0	0	0	193	42	186	12	303	491	3	38	186	12
4752A_	21	0	50	0	0	0	0	0	0	227	78	205	18	625	826	10	67	205	18
4752A_	105	62	2	0	0	0	0	0	0	227	17	212	5	341	169	7	38	212	5
4752A_	22	0	50	0	0	0	0	0	0	242	83	221	19	627	826	9	65	221	19
4752A_	102	60	2	0	0	0	0	0	0	238	17	221	5	358	163	7	38	221	5
4752A_	52	31	2	0	0	0	0	0	0	269	23	254	7	324	192	5	21	254	7
4752A_	49	14	4	1	0	0	0	0	0	418	28	413	14	476	183	1	13	413	14

Grain	U [ppm]	Th [ppm]	Th/U	RATIO 207/ 235	± s.e.	206/ 238	± s.e.	207/ 206	± s.e.	AGES 207/ 235	± 2s	206/ 238	± 2s	207/ 206	± 2s	%disc (5/8)	%disc (7/6)	Best Age [Ma]	± 2s
4752A_	48	13	4	1	0	0	0	0	0	418	30	416	14	466	193	0	11	416	14
4752A_	71	44	2	1	0	0	0	0	0	533	17	524	19	583	98	2	10	524	19
4752A_	70	44	2	1	0	0	0	0	0	562	18	550	19	606	96	2	9	550	19
4752A_	30	42	1	1	0	0	0	0	0	623	37	581	14	658	143	7	12	581	14
4752A_	74	40	2	1	0	0	0	0	0	637	30	607	13	672	87	5	10	607	13
4752A_	73	39	2	1	0	0	0	0	0	651	30	619	13	690	87	5	10	619	13
4752A_	30	43	1	1	0	0	0	0	0	653	38	621	15	656	143	5	5	621	15
4752A_	114	61	2	1	0	0	0	0	0	902	30	877	23	1004	80	3	13	877	23
4752A_	114	62	2	2	0	0	0	0	0	948	30	911	23	1028	76	4	11	911	23
4752A_	24	5	5	2	0	0	0	0	0	952	57	954	20	891	128	0	-7	954	20
4752A_	37	43	1	2	0	0	0	0	0	977	46	978	18	949	90	0	-3	978	18
4752A_	49	13	4	2	0	0	0	0	0	1043	38	999	16	1011	73	4	1	999	16
4752A_	25	11	2	2	0	0	0	0	0	1006	42	1018	21	1010	88	-1	-1	1018	21
4752A_	29	10	3	2	0	0	0	0	0	1019	52	1025	19	1018	108	-1	-1	1025	19
4752A_	62	26	2	2	0	0	0	0	0	1063	39	1041	22	1139	81	2	9	1041	22
4752A_	25	12	2	2	0	0	0	0	0	1120	46	1041	17	1112	78	7	6	1041	17
4752A_	25	12	2	2	0	0	0	0	0	1123	44	1044	17	1128	75	7	8	1044	17
4752A_	9	3	3	2	0	0	0	0	0	1125	81	1059	23	1021	161	6	-4	1059	23
4752A_	32	8	4	2	0	0	0	0	0	1061	37	1071	14	1027	60	-1	-4	1071	14
4752A_	99	33	3	2	0	0	0	0	0	1055	33	1073	19	1151	60	-2	7	1073	19
4752A_	61	26	2	2	0	0	0	0	0	1094	39	1086	23	1145	79	1	5	1086	23
4752A_	29	11	3	2	0	0	0	0	0	1231	90	1099	32	1288	114	11	15	1099	32
4752A_	33	18	2	2	0	0	0	0	0	1108	47	1101	17	1094	92	1	-1	1101	17
4752A_	98	33	3	2	0	0	0	0	0	1087	32	1116	19	1154	57	-3	3	1116	19
4752A_	73	28	3	2	0	0	0	0	0	1224	34	1179	25	1258	79	4	6	1179	25
4752A_	72	27	3	2	0	0	0	0	0	1239	34	1199	26	1266	79	3	5	1199	26
4752A_	46	12	4	2	0	0	0	0	0	1165	48	1199	16	1181	65	-3	-1	1199	16
4752A_	66	17	4	2	0	0	0	0	0	1229	37	1201	18	1167	60	2	-3	1201	18
4752A_	30	27	1	2	0	0	0	0	0	1225	58	1206	27	1211	102	2	0	1206	27
4752A_	30	27	1	2	0	0	0	0	0	1229	56	1219	26	1231	98	1	1	1219	26
4752A_	140	164	1	3	0	0	0	0	0	1390	104	1335	95	1529	165	4	13	1335	95
4752A_	36	33	1	3	0	0	0	0	0	1419	93	1350	68	1566	148	5	14	1350	68
4752A_	43	39	1	3	0	0	0	0	0	1479	65	1405	50	1601	102	5	12	1405	50

Grain	U [ppm]	Th [ppm]	Th/U	RATIO 207/235	± s.e.	206/238	± s.e.	207/206	± s.e.	AGES 207/235	± 2s	206/238	± 2s	207/206	± 2s	%disc (5/8)	%disc (7/6)	Best Age [Ma]	± 2s
4752A_	37	28	1	3	0	0	0	0	0	1418	106	1415	73	1622	125	0	13	1415	73
4752A_	94	40	2	3	0	0	0	0	0	1486	55	1428	31	1517	67	4	6	1428	31
4752A_	29	9	3	3	0	0	0	0	0	1488	41	1436	21	1485	60	3	3	1436	21
4752A_	330	225	1	3	0	0	0	0	0	1509	52	1438	71	1605	108	5	10	1438	71
4752A_	97	40	2	3	0	0	0	0	0	1512	48	1453	28	1532	59	4	5	1453	28
4752A_	193	46	4	3	0	0	0	0	0	1449	33	1463	20	1441	42	-1	-2	1463	20
4752A_	10	6	2	4	1	0	0	0	0	1656	183	1468	50	1744	198	11	16	1468	50
4752A_	12	7	2	3	1	0	0	0	0	1515	118	1512	22	1488	91	0	-2	1512	22
4752A_	67	27	3	4	0	0	0	0	0	1669	37	1617	42	1613	67	3	0	1613	67
4752A_	90	27	3	4	0	0	0	0	0	1596	48	1665	73	1621	93	-4	-3	1621	93
4752A_	68	27	3	4	0	0	0	0	0	1705	39	1674	46	1630	70	2	-3	1630	70
4752A_	79	45	2	4	0	0	0	0	0	1671	31	1661	28	1634	48	1	-2	1634	48
4752A_	44	33	1	4	0	0	0	0	0	1611	56	1594	30	1659	64	1	4	1659	64
4752A_	28	11	3	4	0	0	0	0	0	1676	53	1650	22	1659	54	2	1	1659	54
4752A_	47	25	2	4	0	0	0	0	0	1711	40	1712	43	1672	56	0	-2	1672	56
4752A_	101	30	3	4	0	0	0	0	0	1662	40	1695	60	1673	76	-2	-1	1673	76
4752A_	47	25	2	5	0	0	0	0	0	1757	44	1783	49	1683	61	-1	-6	1683	61
4752A_	44	33	1	4	0	0	0	0	0	1655	53	1660	30	1692	60	0	2	1692	60
4752A_	12	9	1	4	1	0	0	0	0	1610	125	1525	34	1728	153	5	12	1728	153
4752A_	106	47	2	5	0	0	0	0	0	1752	73	1601	68	1730	84	9	7	1730	84
4752A_	101	42	2	4	0	0	0	0	0	1623	71	1564	54	1759	95	4	11	1759	95
4752A_	31	18	2	5	0	0	0	0	0	1824	65	1717	25	1781	54	6	4	1781	54
4752A_	101	60	2	5	0	0	0	0	0	1782	45	1757	29	1785	44	1	2	1785	44
4752A_	112	41	3	5	0	0	0	0	0	1753	40	1716	29	1787	56	2	4	1787	56
4752A_	33	18	2	5	0	0	0	0	0	1882	61	1841	25	1795	51	2	-3	1795	51
4752A_	132	21	6	5	0	0	0	0	0	1865	38	1809	38	1834	43	3	1	1834	43
4752A_	123	35	4	5	0	0	0	0	0	1794	45	1745	43	1858	57	3	6	1858	57
4752A_	7	5	1	4	1	0	0	0	0	1649	103	1586	141	1865	205	4	15	1865	205
4752A_	33	19	2	5	0	0	0	0	0	1888	58	1870	25	1869	58	1	0	1869	58
4752A_	139	22	6	5	0	0	0	0	0	1884	29	1823	30	1875	35	3	3	1875	35
4752A_	4	3	2	4	1	0	0	0	0	1594	173	1452	220	1876	353	9	23	1876	353
4752A_	4	13	0	6	1	0	0	0	0	2011	141	1919	70	2157	128	5	11	2157	128
4752A_	4	13	0	6	1	0	0	0	0	2012	147	1919	72	2162	132	5	11	2162	132

				RATIO						AGES									
Grain	U [ppm]	Th [ppm]	Th/U	207/ 235	± s.e.	206/ 238	± s.e.	207/ 206	± s.e.	207/ 235	± 2s	206/ 238	± 2s	207/ 206	± 2s	%disc (5/8)	%disc (7/6)	Best Age [Ma]	± 2s
4752A_	19	12	2	11	1	0	0	0	0	2538	64	2544	44	2523	47	0	-1	2523	47
4752A_	24	4	7	13	1	1	0	0	0	2682	60	2667	43	2629	49	1	-1	2629	49
4752A_	134	89	2	13	1	1	0	0	0	2697	40	2713	41	2655	31	-1	-2	2655	31
4752A_	4	21	0	21	4	1	0	0	0	3142	218	2839	149	2954	105	10	4	2954	105

APPENDIX E. XRF EXTENDED DATA

S (ppm)	V	Cr	Ni	Cu	Zn	Rb	Sr	Y	Zr	Nb	Ba	W	Pb	Th
12	137	78.2	53.5	33.5	135.8	163.1	106.9	33.8	159	0	394.9	0	32	0
18	136	60.2	46	29.1	111.8	138.3	117.4	29.3	191.6	0	380.9	218.4	12.2	0
11.7	76.5	2.8	7.1	218.4	63.3	82.9	263.5	20.4	118.9	3.9	236.6	4932.5	6.5	13.5
23.4	136.1	74.7	30	25	116.3	152.6	112.7	37	208.5	10.7	429.8	152.4	13	0
39.3	138.3	67.4	27.6	26.1	115.9	137.1	127.7	27.1	279.2	14.3	470.5	180.6	8.1	18.9
27.7	114.8	130.8	27.8	22.3	80.1	103.4	142.3	35.8	319.2	8.5	463.2	380.8	13.2	23.8
36.5	127.7	59.5	49.7	27.1	105.3	119.9	157.6	33.2	346.9	17.8	499.8	0	16.2	20.9
135.7	94.9	42.1	10.2	6.8	79.1	80	152.9	40.1	620.5	9.3	406.3	276.9	9.8	0
9.1	76.5	54.6	29.8	17.1	77.4	83.7	171.6	38.3	681.4	0	528.7	0	15.2	0
109.6	81.6	49.4	16	18.6	64.5	84.5	175.6	37.2	721.5	17.9	457.2	208.4	11.7	0
13.2	53.3	53.8	26.6	19.7	55.9	80	199.7	37	528.1	0	551.7	230.5	11.7	0
93.9	41.8	43.8	7.1	15.8	47.9	69.6	208.4	30.3	658.3	12.9	530.4	405.1	5.2	23.8
123	25	34.7	14	9.1	37.2	56.4	192.1	27.5	642.4	12.6	519.3	308.5	10.2	0
2.9	7.9	48	6.6	13.9	31	44.2	182	30.5	1203.9	0	477.1	480.7	7.7	0
6.2	9.2	69.1	64	14.8	62.6	50.3	175.1	16.8	238.3	8.8	470.4	0	9.7	0
35	0	27.7	19.7	12.2	33.4	46.6	185.2	19.5	309.5	5.7	411	1506.7	7.3	0
14.1	0	18.1	1.6	9.8	28.4	43.6	198.8	13.8	246	4.9	474.9	1284.7	5.8	17.1
29.9	0	18.6	10.5	10.3	25.1	45.7	191.5	15.3	260.1	0	412.4	777.1	7.3	0
3.6	0	8.1	12.2	8	25.7	38.9	186.9	12.7	199.4	4.5	39.9	1831.8	5.9	16.9
16.4	0	0	5.6	11.3	29.6	41	179.6	11	59.8	0	408.4	1625.7	5.8	0
11.8	5.7	29.6	6.2	6.6	33.8	47.8	203.7	26.1	323.2	7.6	487.3	425.8	10.8	0
22.2	0	3.2	20.6	17.5	23.2	40.3	172.6	6.1	56.2	0	428.6	2149	3.2	0
0	43.5	69.1	3.7	10.5	32.5	36.1	192.5	35.6	2466.3	0	515.6	523.2	7.1	0
9.5	0	4.6	19.1	16.3	21	39.8	176	9.7	106.4	15.7	634.7	589.3	7.4	14.1
14.8	0	9.2	14.7	11.4	19.4	34.7	174	10.7	172.6	0	424	737.9	4.1	0

Condition	kV	Filter	Medium	Time (s)	Elements
Omnian	50	Ag	Air	60	Ni-Nb, Tm-Am
Omnian1	50	Cu-500	Air	120	Mo-Ba
Omnian2	20	Al-200	Air	60	Cr-Co, Pr-Er
Omnian3	12	Al-50	Air	180	K-V, La-Ce
Omnian4	9	Ti	Helium	180	Al-Cl
Omnian5	5	none	Helium	180	Na-Mg

Appendix E. 1 XRD conditions employed during methodology.

APPENDIX F. MONTE CARLO ZIRCON U-PB UNMIXING DATA

	W11		B1-2		20092401		W3-18		J6-2		J4-2	
Cross-correlation												
Sample Names	Rel. Cont.	2σ	Rel. Cont.	2σ	Rel. Cont.	2σ	Rel. Cont.	2σ	Rel. Cont.	2σ	Rel. Cont.	2σ
Peri-Gondawa	0.021	0.029	0.026	0.034	0.031	0.039	0.036	0.047	0.048	0.057	0.026	0.036
Yavapai	0.704	0.166	0.675	0.164	0.055	0.079	0.066	0.086	0.097	0.105	0.083	0.095
Appalachian	0.031	0.037	0.032	0.035	0.011	0.012	0.024	0.031	0.030	0.027	0.043	0.049
Rocky foreland	0.070	0.088	0.115	0.134	0.790	0.111	0.777	0.131	0.466	0.175	0.738	0.155
TransHudson	0.025	0.032	0.022	0.028	0.015	0.018	0.020	0.023	0.044	0.044	0.022	0.028
Grenville	0.013	0.018	0.019	0.022	0.018	0.024	0.011	0.015	0.025	0.028	0.012	0.014
Granite-Rhyolite	0.081	0.087	0.048	0.051	0.032	0.036	0.022	0.031	0.079	0.074	0.032	0.041
Superior	0.031	0.038	0.017	0.021	0.021	0.024	0.017	0.021	0.023	0.025	0.015	0.019
Cordillera	0.024	0.030	0.046	0.041	0.027	0.029	0.027	0.031	0.189	0.063	0.028	0.031
Kuiper V value												
Sample Names	Rel. Cont.	2σ	Rel. Cont.	2σ	Rel. Cont.	2σ	Rel. Cont.	2σ	Rel. Cont.	2σ	Rel. Cont.	2σ
Peri-Gondawa	0.047	0.058	0.048	0.049	0.117	0.108	0.090	0.083	0.097	0.091	0.127	0.105
Yavapai	0.369	0.137	0.444	0.110	0.142	0.124	0.288	0.114	0.132	0.098	0.105	0.090
Appalachian	0.061	0.053	0.075	0.058	0.059	0.044	0.110	0.069	0.090	0.053	0.136	0.072
Rocky foreland	0.075	0.077	0.078	0.085	0.277	0.209	0.171	0.150	0.143	0.132	0.204	0.165
TransHudson	0.125	0.077	0.101	0.070	0.065	0.049	0.058	0.048	0.133	0.065	0.078	0.055
Grenville	0.027	0.025	0.031	0.031	0.052	0.052	0.037	0.035	0.044	0.038	0.045	0.036
Granite-Rhyolite	0.110	0.072	0.060	0.044	0.089	0.057	0.091	0.055	0.086	0.061	0.074	0.049
Superior	0.111	0.076	0.067	0.053	0.106	0.045	0.057	0.045	0.113	0.055	0.095	0.060
Cordillera	0.075	0.057	0.096	0.064	0.092	0.055	0.097	0.061	0.163	0.049	0.137	0.061
KS D value												
Sample Names	Rel. Cont.	2σ	Rel. Cont.	2σ	Rel. Cont.	2σ	Rel. Cont.	2σ	Rel. Cont.	2σ	Rel. Cont.	2σ
Peri-Gondawa	0.059	0.066	0.070	0.080	0.041	0.052	0.108	0.110	0.063	0.072	0.059	0.076
Yavapai	0.325	0.151	0.355	0.140	0.041	0.050	0.218	0.117	0.073	0.079	0.052	0.061
Appalachian	0.080	0.065	0.064	0.049	0.021	0.034	0.105	0.071	0.053	0.050	0.095	0.075

Rocky foreland	0.083	0.093	0.137	0.143	0.696	0.153	0.218	0.215	0.392	0.146	0.476	0.174
TransHudson	0.126	0.075	0.075	0.053	0.034	0.040	0.052	0.039	0.083	0.066	0.039	0.045
Grenville	0.032	0.032	0.037	0.034	0.027	0.039	0.048	0.047	0.035	0.039	0.033	0.040
Granite-Rhyolite	0.122	0.080	0.071	0.057	0.038	0.045	0.086	0.066	0.055	0.051	0.041	0.043
Superior	0.086	0.060	0.062	0.045	0.033	0.033	0.043	0.035	0.059	0.049	0.045	0.042
Cordillera	0.087	0.066	0.129	0.076	0.067	0.062	0.122	0.076	0.186	0.079	0.160	0.092

	W2-5		LA1701		17093001		18020401		B2		W1	
Cross-correlation												
Sample Names	Rel. Cont.	2σ	Rel. Cont.	2σ	Rel. Cont.	2σ	Rel. Cont.	2σ	Rel. Cont.	2σ	Rel. Cont.	2σ
Peri-Gondawa	0.025	0.034	0.028	0.039	0.023	0.029	0.036	0.044	0.040	0.049	0.038	0.048
Yavapai	0.152	0.173	0.028	0.043	0.072	0.083	0.352	0.156	0.113	0.136	0.047	0.067
Appalachian	0.023	0.026	0.021	0.023	0.019	0.023	0.019	0.021	0.012	0.014	0.013	0.013
Rocky foreland	0.705	0.208	0.789	0.105	0.767	0.131	0.377	0.198	0.718	0.173	0.783	0.122
TransHudson	0.018	0.023	0.024	0.029	0.025	0.029	0.036	0.036	0.018	0.021	0.023	0.027
Grenville	0.008	0.012	0.020	0.025	0.021	0.024	0.023	0.026	0.019	0.028	0.019	0.032
Granite-Rhyolite	0.028	0.036	0.032	0.037	0.031	0.039	0.068	0.062	0.027	0.033	0.017	0.024
Superior	0.021	0.027	0.022	0.027	0.017	0.022	0.054	0.050	0.028	0.033	0.035	0.042
Cordillera	0.020	0.024	0.036	0.046	0.026	0.028	0.034	0.028	0.025	0.027	0.026	0.029
Kuiper V value												
Sample Names	Rel. Cont.	2σ	Rel. Cont.	2σ	Rel. Cont.	2σ	Rel. Cont.	2σ	Rel. Cont.	2σ	Rel. Cont.	2σ
Peri-Gondawa	0.064	0.074	0.072	0.080	0.096	0.088	0.087	0.073	0.102	0.104	0.094	0.086
Yavapai	0.362	0.111	0.055	0.058	0.136	0.100	0.241	0.139	0.147	0.120	0.084	0.079
Appalachian	0.102	0.068	0.065	0.060	0.063	0.050	0.056	0.047	0.038	0.034	0.042	0.038
Rocky foreland	0.102	0.110	0.415	0.160	0.205	0.169	0.133	0.128	0.214	0.177	0.263	0.165
TransHudson	0.092	0.062	0.058	0.048	0.068	0.045	0.095	0.058	0.042	0.037	0.056	0.048
Grenville	0.035	0.036	0.038	0.045	0.061	0.057	0.045	0.043	0.078	0.063	0.077	0.067
Granite-Rhyolite	0.074	0.058	0.056	0.056	0.070	0.056	0.102	0.060	0.087	0.060	0.065	0.052
Superior	0.080	0.058	0.096	0.058	0.163	0.041	0.142	0.051	0.173	0.044	0.192	0.047
Cordillera	0.087	0.066	0.145	0.066	0.137	0.048	0.099	0.042	0.118	0.064	0.128	0.060
KS D value												

Sample Names	Rel. Cont.	2σ	Rel. Cont.	2σ	Rel. Cont.	2σ	Rel. Cont.	2σ	Rel. Cont.	2σ	Rel. Cont.	2σ
Peri-Gondawa	0.086	0.084	0.032	0.039	0.048	0.062	0.051	0.055	0.066	0.070	0.062	0.070
Yavapai	0.259	0.121	0.020	0.028	0.057	0.063	0.145	0.122	0.145	0.131	0.060	0.070
Appalachian	0.101	0.072	0.044	0.050	0.035	0.034	0.036	0.038	0.025	0.023	0.034	0.039
Rocky foreland	0.185	0.152	0.625	0.143	0.508	0.124	0.310	0.128	0.246	0.181	0.530	0.116
TransHudson	0.065	0.050	0.028	0.040	0.063	0.063	0.116	0.074	0.081	0.068	0.054	0.057
Grenville	0.044	0.040	0.029	0.043	0.038	0.040	0.044	0.048	0.055	0.050	0.039	0.052
Granite-Rhyolite	0.075	0.059	0.028	0.034	0.052	0.051	0.082	0.059	0.093	0.075	0.040	0.050
Superior	0.061	0.044	0.031	0.043	0.073	0.052	0.075	0.056	0.064	0.054	0.048	0.048
Cordillera	0.124	0.084	0.163	0.110	0.126	0.067	0.140	0.062	0.226	0.075	0.133	0.072

	W3		BR_BL		S_RR		621-9		614-1		PC-29	
Cross-correlation												
Sample Names	Rel. Cont.	2σ	Rel. Cont.	2σ	Rel. Cont.	2σ	Rel. Cont.	2σ	Rel. Cont.	2σ	Rel. Cont.	2σ
Peri-Gondawa	0.028	0.040	0.035	0.043	0.032	0.040	0.020	0.026	0.034	0.043	0.023	0.028
Yavapai	0.039	0.056	0.478	0.161	0.092	0.116	0.052	0.062	0.126	0.136	0.041	0.060
Appalachian	0.010	0.012	0.028	0.031	0.011	0.012	0.015	0.019	0.023	0.027	0.016	0.017
Rocky foreland	0.805	0.113	0.264	0.196	0.696	0.186	0.789	0.101	0.428	0.190	0.741	0.139
TransHudson	0.025	0.030	0.019	0.021	0.018	0.022	0.027	0.037	0.034	0.036	0.027	0.030
Grenville	0.019	0.024	0.023	0.027	0.033	0.044	0.019	0.023	0.021	0.024	0.017	0.021
Granite-Rhyolite	0.018	0.023	0.060	0.050	0.039	0.043	0.032	0.043	0.062	0.064	0.054	0.055
Superior	0.036	0.045	0.061	0.055	0.028	0.030	0.023	0.033	0.250	0.109	0.044	0.052
Cordillera	0.021	0.025	0.033	0.030	0.050	0.041	0.023	0.028	0.022	0.025	0.036	0.045
Kuiper V value												
Sample Names	Rel. Cont.	2σ	Rel. Cont.	2σ	Rel. Cont.	2σ	Rel. Cont.	2σ	Rel. Cont.	2σ	Rel. Cont.	2σ
Peri-Gondawa	0.094	0.083	0.088	0.081	0.087	0.086	0.053	0.063	0.066	0.064	0.094	0.083
Yavapai	0.088	0.076	0.340	0.143	0.117	0.113	0.076	0.081	0.104	0.090	0.171	0.115
Appalachian	0.037	0.034	0.058	0.045	0.037	0.033	0.032	0.031	0.043	0.044	0.047	0.039
Rocky foreland	0.278	0.162	0.153	0.141	0.303	0.177	0.378	0.133	0.141	0.120	0.110	0.098
TransHudson	0.057	0.048	0.051	0.039	0.064	0.057	0.083	0.078	0.106	0.073	0.087	0.064
Grenville	0.072	0.067	0.043	0.043	0.065	0.052	0.037	0.041	0.037	0.036	0.043	0.043
Granite-Rhyolite	0.056	0.046	0.085	0.063	0.078	0.054	0.043	0.040	0.086	0.070	0.133	0.070

Superior	0.187	0.051	0.095	0.034	0.114	0.054	0.142	0.075	0.312	0.066	0.184	0.051
Cordillera	0.129	0.057	0.088	0.051	0.135	0.062	0.156	0.072	0.105	0.064	0.131	0.052
KS D value												
Sample Names	Rel. Cont.	2σ	Rel. Cont.	2σ	Rel. Cont.	2σ	Rel. Cont.	2σ	Rel. Cont.	2σ	Rel. Cont.	2σ
Peri-Gondawa	0.063	0.064	0.057	0.072	0.039	0.044	0.029	0.041	0.037	0.048	0.059	0.061
Yavapai	0.063	0.069	0.180	0.141	0.039	0.047	0.028	0.035	0.051	0.066	0.096	0.109
Appalachian	0.028	0.031	0.034	0.037	0.027	0.034	0.031	0.044	0.031	0.038	0.035	0.042
Rocky foreland	0.538	0.132	0.432	0.169	0.606	0.138	0.594	0.137	0.527	0.111	0.331	0.117
TransHudson	0.054	0.058	0.051	0.047	0.040	0.054	0.030	0.049	0.107	0.089	0.105	0.081
Grenville	0.039	0.040	0.038	0.043	0.040	0.045	0.031	0.041	0.025	0.032	0.037	0.039
Granite-Rhyolite	0.033	0.039	0.073	0.061	0.041	0.049	0.030	0.037	0.046	0.047	0.074	0.066
Superior	0.048	0.048	0.057	0.046	0.029	0.038	0.037	0.044	0.105	0.094	0.088	0.066
Cordillera	0.134	0.069	0.079	0.064	0.139	0.080	0.190	0.131	0.071	0.075	0.174	0.080

	J2		B3-2		21022001	
Cross-correlation						
Sample Names	Rel. Cont.	2σ	Rel. Cont.	2σ	Rel. Cont.	2σ
Peri-Gondawa	0.021	0.029	0.023	0.032	0.024	0.035
Yavapai	0.103	0.120	0.039	0.063	0.045	0.049
Appalachian	0.013	0.014	0.017	0.020	0.012	0.016
Rocky foreland	0.677	0.188	0.799	0.091	0.781	0.109
TransHudson	0.048	0.049	0.034	0.047	0.019	0.024
Grenville	0.020	0.027	0.018	0.024	0.023	0.027
Granite-Rhyolite	0.072	0.066	0.032	0.039	0.040	0.053
Superior	0.037	0.041	0.018	0.024	0.021	0.029
Cordillera	0.011	0.013	0.019	0.028	0.035	0.041
Kuiper V value						
Sample Names	Rel. Cont.	2σ	Rel. Cont.	2σ	Rel. Cont.	2σ
Peri-Gondawa	0.073	0.069	0.105	0.096	0.078	0.084
Yavapai	0.205	0.131	0.107	0.088	0.118	0.112
Appalachian	0.050	0.047	0.051	0.045	0.030	0.030

Rocky foreland	0.133	0.123	0.262	0.141	0.409	0.148
TransHudson	0.102	0.071	0.111	0.068	0.063	0.053
Grenville	0.041	0.044	0.050	0.044	0.049	0.048
Granite-Rhyolite	0.129	0.069	0.060	0.049	0.072	0.057
Superior	0.183	0.057	0.100	0.063	0.088	0.050
Cordillera	0.084	0.042	0.154	0.052	0.093	0.049
KS D value						
Sample Names	Rel. Cont.	2σ	Rel. Cont.	2σ	Rel. Cont.	2σ
Peri-Gondawa	0.046	0.057	0.044	0.057	0.029	0.043
Yavapai	0.082	0.085	0.042	0.064	0.030	0.036
Appalachian	0.037	0.044	0.040	0.046	0.028	0.039
Rocky foreland	0.403	0.134	0.533	0.121	0.701	0.135
TransHudson	0.127	0.086	0.045	0.053	0.024	0.036
Grenville	0.035	0.041	0.032	0.040	0.031	0.040
Granite-Rhyolite	0.069	0.069	0.040	0.045	0.030	0.038
Superior	0.112	0.076	0.040	0.041	0.035	0.043
Cordillera	0.089	0.071	0.184	0.087	0.094	0.071

APPENDIX G. CUMULATIVE FREQUENCY PLOTS: K-S FORWAD MODELS

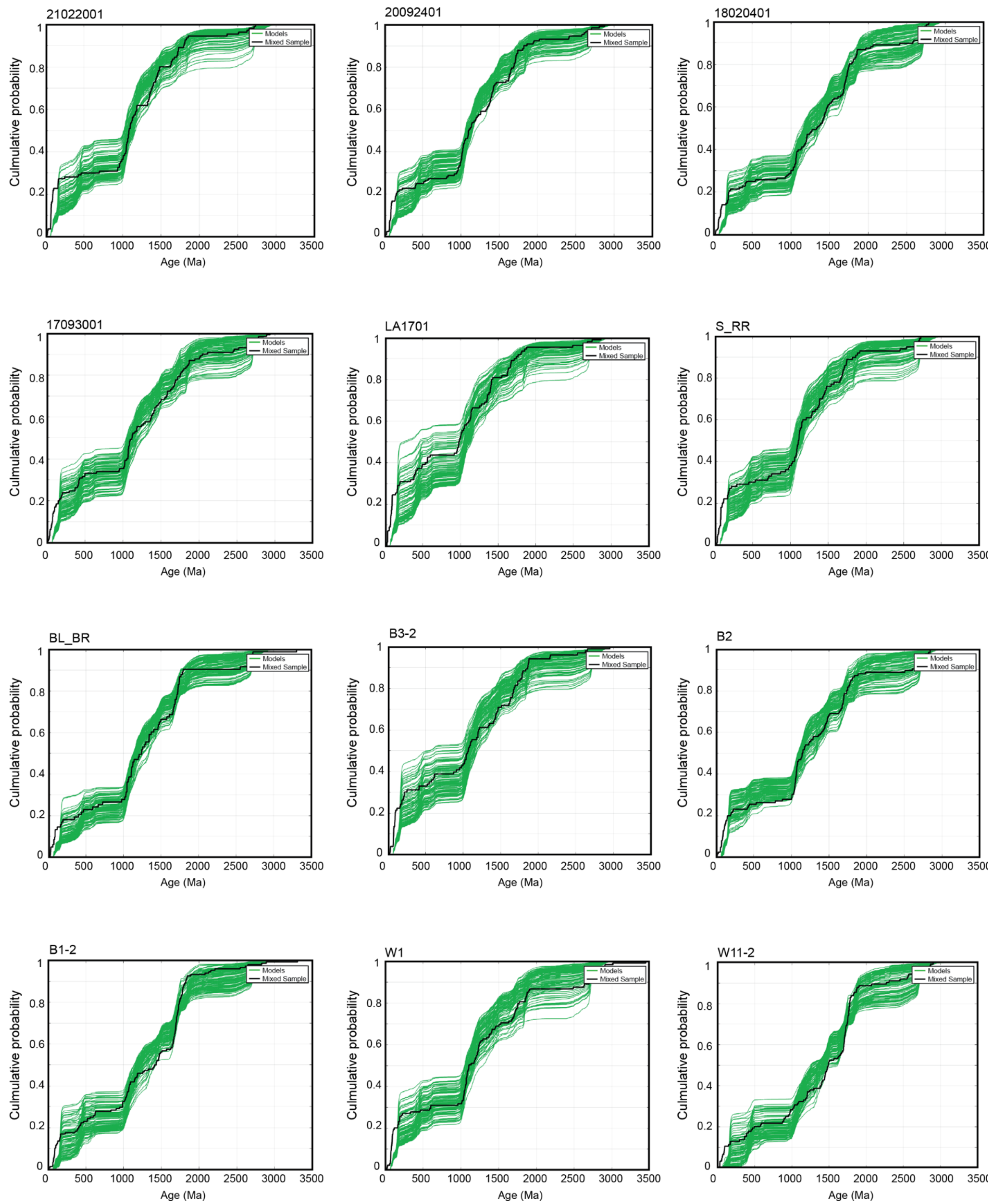

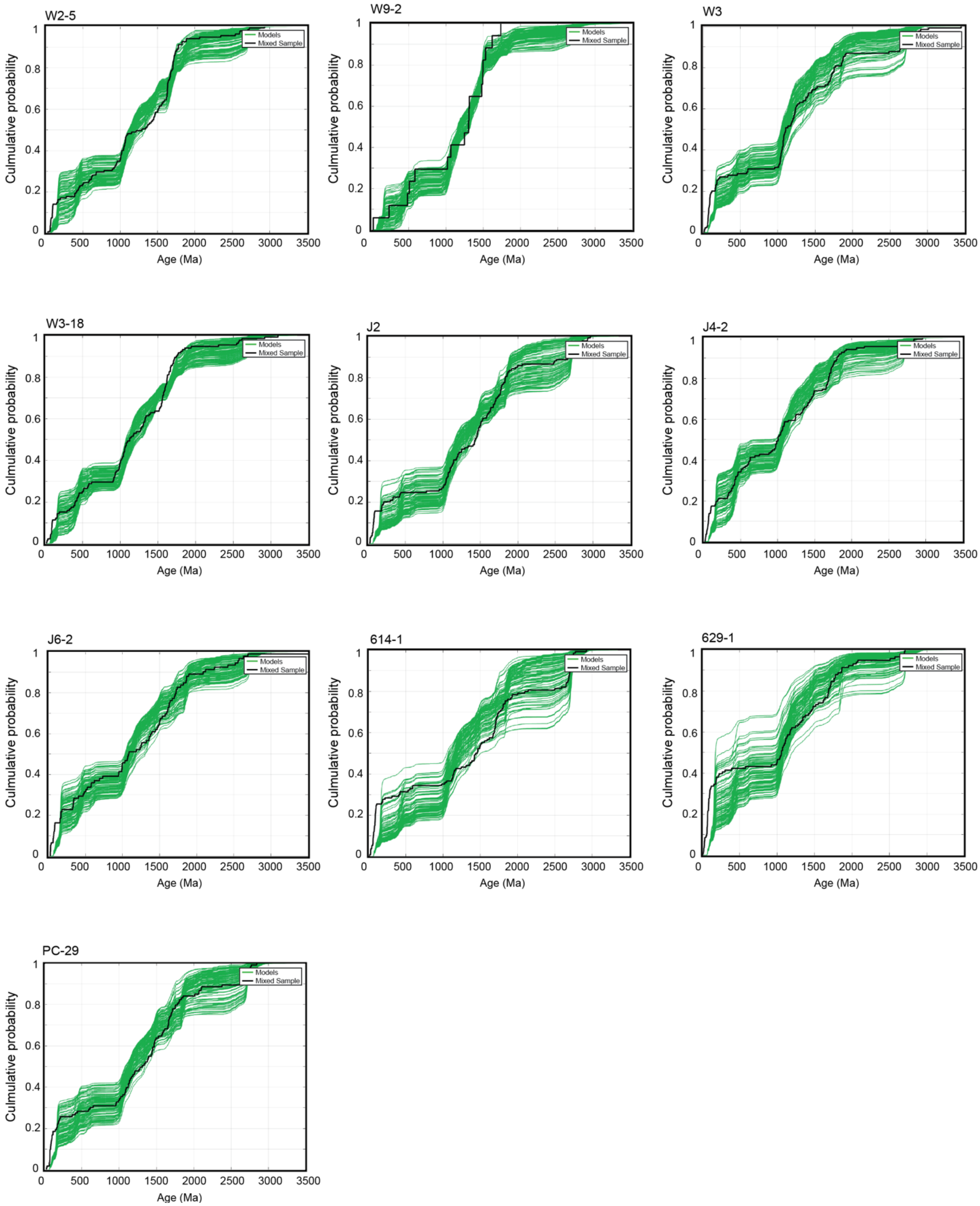
W2-5
W9-2
W3
W3-18
J2
J4-2
J6-2
614-1
629-1
PC-29
Culmulative probability
Age (Ma)
Models
Mixed Sample
0
0.2
0.4
0.6
0.8
1
0
500
1000
1500
2000
2500
3000
3500

APPENDIX H. CUMULATIVE FREQUENCY PLOTS: KUIPER FORWARD MODELS

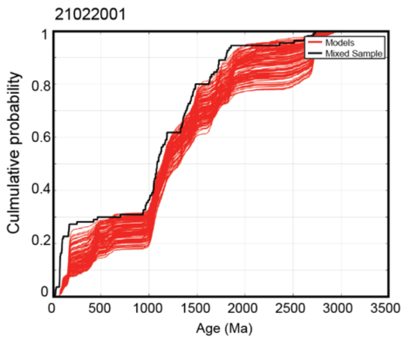

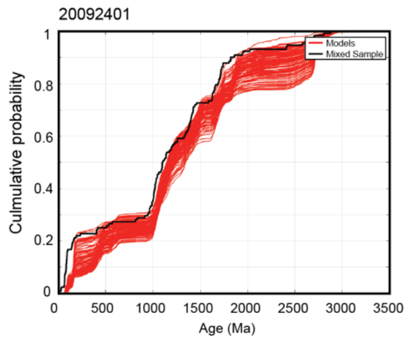

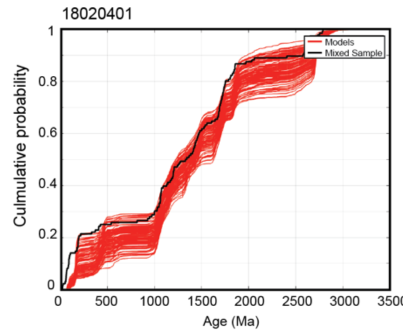

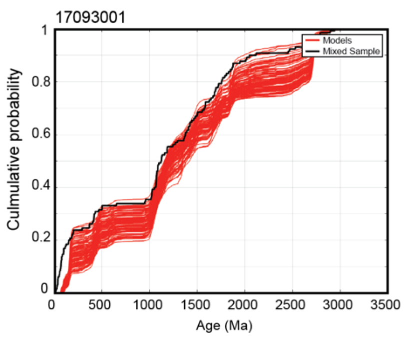

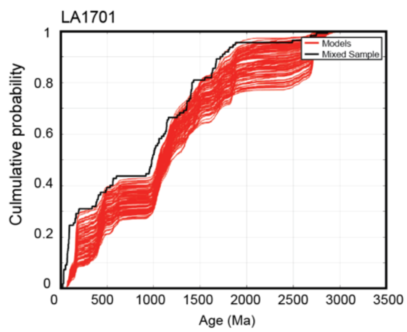

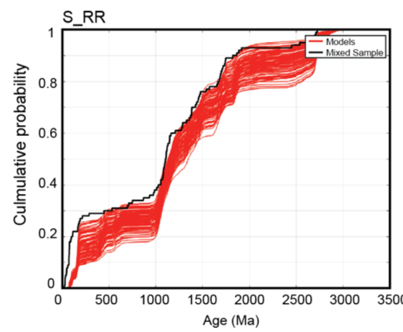

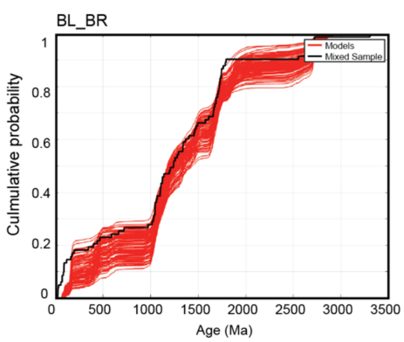

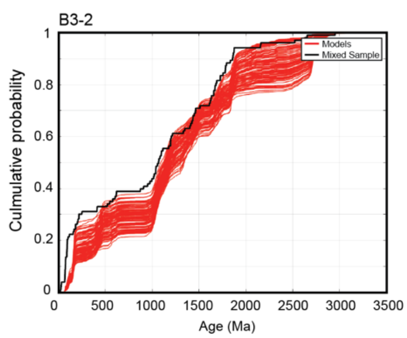

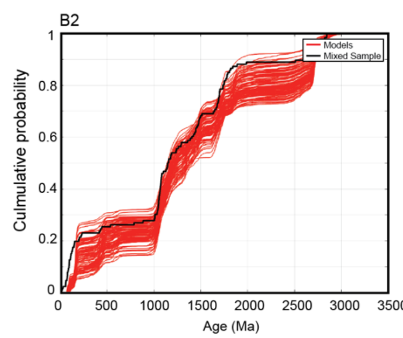

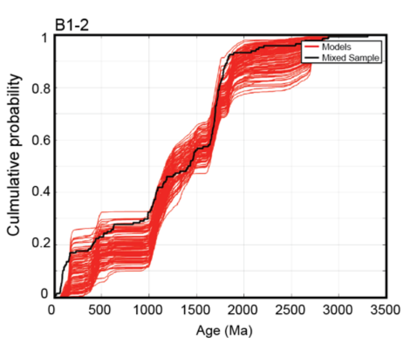

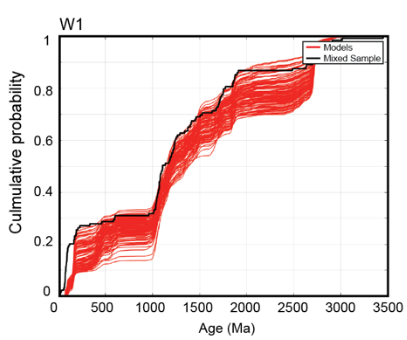

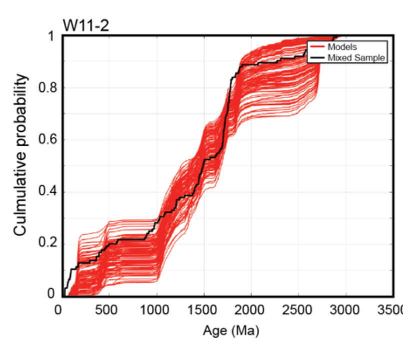

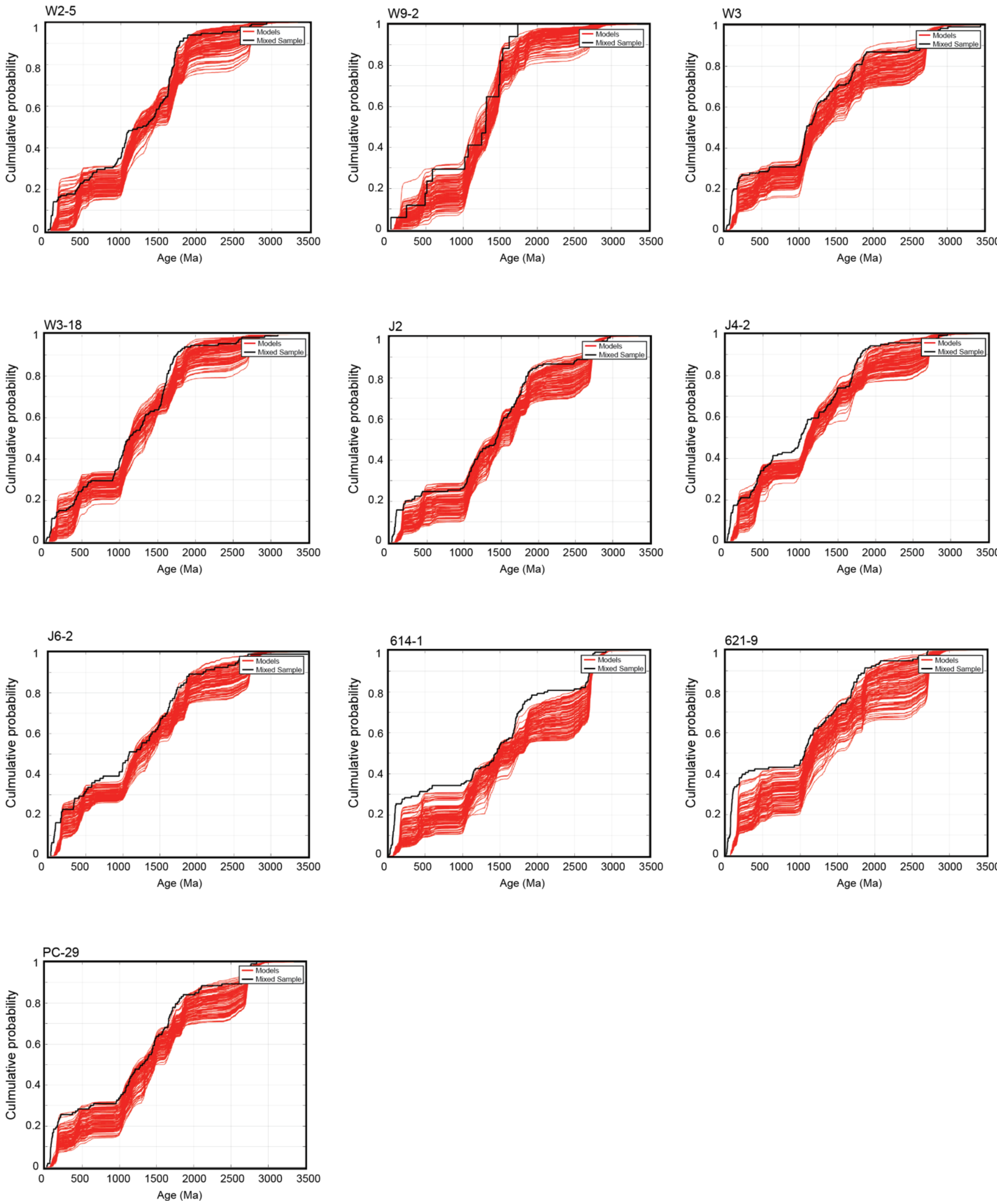
W2-5
W9-2
W3
W3-18
J2
J4-2
J6-2
614-1
621-9
PC-29
Culmulative probability
Age (Ma)
Models
Mixed Sample
0 0.2 0.4 0.6 0.8 1
0 500 1000 1500 2000 2500 3000 3500

REFERENCES

Aitken, M. and J. Xie (1990). "Moisture correction for annual gamma dose." Ancient TL 8(2): 6-9.

Aitken, M. J. (1998). Introduction to optical dating: the dating of Quaternary sediments by the use of photon-stimulated luminescence, Clarendon Press.

Alexander, J. S., R. C. Wilson and W. R. Green (2012). "A brief history and summary of the effects of river engineering and dams on the Mississippi River system and delta." U.S. Geological Survey Circular 1375: 43.

Anderson, J. L. (1983). "Proterozoic anorogenic granite plutonism of North America."

Anselmetti, F. S., D. A. Hodell, D. Ariztegui, M. Brenner and M. F. Rosenmeier (2007). "Quantification of soil erosion rates related to ancient Maya deforestation." Geology 35(10): 915-918.

Aslan, A. and W. J. Autin (1998). "Holocene flood-plain soil formation in the southern lower Mississippi Valley: implications for interpreting alluvial paleosols." Geological Society of America Bulletin 110(4): 433-449.

Aslan, A., W. J. Autin and M. D. Blum (2005). "Causes of river avulsion: insights from the late Holocene avulsion history of the Mississippi River, USA." Journal of Sedimentary Research 75(4): 650-664.

Balgord, E. A., W. A. Yonkee, M. L. Wells, A. Gentry and A. K. Laskowski (2021). "Arc tempos, tectonic styles, and sedimentation patterns during evolution of the North American Cordillera: Constraints from the retroarc detrital zircon archive." Earth-Science Reviews 216: 103557.

Barnes, M., E. Anthony, I. Williams and G. Asquith (2002). "Architecture of a 1.38–1.34 Ga granite–rhyolite complex as revealed by geochronology and isotopic and elemental geochemistry of subsurface samples from west Texas, USA." Precambrian Research 119: 9-43.

Benyon, C., A. Leier, D. A. Leckie, A. Webb, S. M. Hubbard and G. Gehrels (2014). "Provenance of the Cretaceous Athabasca Oil Sands, Canada: Implications for continental-scale sediment transport." Journal of Sedimentary Research 84(2): 136-143.

Bickford, M. and W. Van Schmus (1985). Discovery of two Proterozoic granite-rhyolite terranes in the buried midcontinent basement: The case for shallow drill holes. Observation of the Continental Crust through Drilling I, Springer: 355-364.

Black, L. P., S. L. Kamo, I. S. Williams, R. Mundil, D. W. Davis, R. J. Korsch and C. Foudoulis (2003). "The application of SHRIMP to Phanerozoic geochronology; a critical appraisal of four zircon standards." Chemical Geology 200(1-2): 171-188.

Blum, M. and M. Pecha (2014). "Mid-Cretaceous to Paleocene North American drainage reorganization from detrital zircons." Geology 42(7): 607-610.

Blum, M. D. and H. H. Roberts (2012). "The Mississippi delta region: past, present, and future." Annual Review of Earth and Planetary Sciences 40: 655-683.

Blum, M. D. and H. H. Roberts (2012). "The Mississippi Delta Region: Past, Present, and Future." Annual Review of Earth and Planetary Sciences 40(1): 655-683.

Briere, M. D. and K. Gajewski (2020). "Human population dynamics in relation to Holocene climate variability in the North American Arctic and Subarctic." Quaternary Science Reviews 240: 106370.

Campbell, C. (1998). "Late Holocene lake sedimentology and climate change in southern Alberta, Canada." Quaternary Research 49(1): 96-101.

Campbell, I. D., C. Campbell, M. J. Apps, N. W. Rutter and A. B. Bush (1998). "Late Holocene∼ 1500 yr climatic periodicities and their implications." Geology 26(5): 471-473.

Castelltort, S. and J. Driessche (2003). "How plausible are high-frequency sediment supply-driven cycles in the stratigraphic record?" Sedimentary Geology 157: 3-13.

Clift, P. D. and L. Giosan (2014). "Sediment fluxes and buffering in the post-glacial Indus Basin." Basin Research 26(3): 369-386.

Clift, P. D., L. Giosan, J. Blusztajn, I. H. Campbell, C. M. Allen, M. Pringle, A. Tabrez, M. Danish, M. M. Rabbani, A. Carter and A. Lückge (2008). "Holocene erosion of the Lesser Himalaya triggered by intensified summer monsoon." Geology 36(1): 79–82.

Clift, P. D., E. D. Olson, A. Lechnowskyj, M. G. Moran, A. Barbato and J. M. Lorenzo (2019). "Grain-size variability within a mega-scale point-bar system, False River, Louisiana." Sedimentology 66(2): 408-434.

Constenius, K. N. (1996). "Late Paleogene extensional collapse of the Cordilleran foreland fold and thrust belt." Geological Society of America Bulletin 108(1): 20-39.

Corfu, F., T. E. Krogh, Y. Y. Kwok and L. S. Jensen (1989). "U–Pb zircon geochronology in the southwestern Abitibi greenstone belt, Superior Province." Canadian Journal of Earth Sciences 26(9): 1747-1763.

Dahl, P. S., D. K. Holm, E. T. Gardner, F. A. Hubacher and K. A. Foland (1999). "New constraints on the timing of Early Proterozoic tectonism in the Black Hills (South Dakota), with implications for docking of the Wyoming province with Laurentia." Geological Society of America Bulletin 111(9): 1335-1349.

Dalziel, I. W. (1991). "Pacific margins of Laurentia and East Antarctica-Australia as a conjugate rift pair: Evidence and implications for an Eocambrian supercontinent." Geology 19(6): 598-601.

DeCelles, P. G. (2004). "Late Jurassic to Eocene evolution of the Cordilleran thrust belt and foreland basin system, western USA." American Journal of Science 304(2): 105-168.

Dickinson, W. R. (2004). "Evolution of the North American cordillera." Annu. Rev. Earth Planet. Sci. 32: 13-45.

Drake Jr, A. A., A. Sinha, J. Laird and R. Guy (1989). "The taconic orogen." The Appalachian-Ouachita orogen in the United States: Boulder, Colorado, Geological Society of America, Geology of North America 2: 101-177.

Durkin, P. R., S. M. Hubbard, R. L. Boyd and D. A. Leckie (2015). "Stratigraphic expression of intra-point-bar erosion and rotation." Journal of Sedimentary Research 85(10): 1238-1257.

Ensminger, P. A. (1999). Bathymetric survey and physical and chemical-related properties of False River, Louisiana, June and July 1998. Water-Resources Investigations Report. USGS Numbered Series.

False River Watershed Study (2013). False River Watershed Study: Discharge Bayou and the Chenal Drainage Network Assessment. Department of Natural Resources and False River Watershed Coalition.

Farrell, K. M. (1987). "Sedimentology and facies architecture of overbank deposits of the Mississippi River, False River region, Louisiana."

Fedo, Nesbitt and Young (1995). "Unraveling the effects of potassium metasomatism in sedimentary rocks and paleosols, with implications for paleoweathering conditions and provenance." Geology 23: 921–924.

Fedo, C. M., H. Wayne Nesbitt and G. M. Young (1995). "Unraveling the effects of potassium metasomatism in sedimentary rocks and paleosols, with implications for paleoweathering conditions and provenance." Geology 23(10): 921-924.

Fenstermaker, C. (2013). "False River Watershed Study."

Fildani, A., M. P. McKay, D. Stockli, J. Clark, M. Dykstra, L. Stockli and A. Hessler (2016). "The ancestral Mississippi drainage archived in the late Wisconsin Mississippi deep-sea fan." Geology 44(6): 479-482.

Fildani, A., M. P. McKay, D. Stockli, J. Clark, M. L. Dykstra, L. Stockli and A. M. Hessler (2016). "The ancestral Mississippi drainage archived in the late Wisconsin Mississippi deep-sea fan." Geology 44(6): 479-482.

Fisk, H. (1947). "Geology of the Mississippi Valley Region."

Fisk, H. N. (1944). Geological investigation of the alluvial valley of the lower Mississippi River. Vicksburg, Mississippi, Mississippi River Commission,: 78.

Folk, R. L. (1954). "The distinction between grain size and mineral composition in sedimentary rock nomenclature." Journal of Geology 62(4): 344-359.

Fuchs, M. and L. Owen (2008). "Luminescence dating of glacial and associated sediments: review, recommendations and future directions." Boreas 37(4): 636-659.

Galbraith, R. F. and R. G. Roberts (2012). "Statistical aspects of equivalent dose and error calculation and display in OSL dating: an overview and some recommendations." Quaternary Geochronology 11: 1-27.

Gehrels, G., W. Dickinson, G. Ross, J. Stewart and D. Howell (1995). "Detrital zircon reference for Cambrian to Triassic miogeoclinal strata of western North America." Geology 23: 831-834.

Gehrels, G. E. (2000). "Introduction to detrital zircon studies of Paleozoic and Triassic strata in western Nevada and northern California." Special Paper of the Geological Society of America 347: 1-17.

GeoSepServices. "Mineral Separations." GeoSep Services Quality Mineral Separations and Analytical Services: Fission Track and Zircon UPb, from geoseps.com/services-provided/mineral-separations/. .

Granet, Chabaux, Stille, France-Lanord and Pelt (2007). "Time-scales of sedimentary transfer and weathering processes from U-series nuclides: Clues from the Himalayan rivers." Earth and Planetary Science Letters 261(3): 389-406.

Gregory, B., A. D. Herrmann, T. Ireland and P. D. Clift (2022). "Testing the applicability of zircon U-Pb dating as a provenance method in a highly altered river system, Mississippi-Missouri River, USA." Basin Research 34: 251– 273.

Grootes, P. M. and M. Stuiver (1997). "18O/16O variability in Greenland snow and ice with 103 to 105 yr time resolution." Journal of Geophysical Research 102: 26,455–426,470.

Heimann, D. C., L. A. Sprague and D. W. Blevins (2011). Trends in suspended-sediment loads and concentrations in the Mississippi River Basin, 1950-2009, US Department of the Interior, US Geological Survey.

Herron, M. (1988). "Geochemical Classification of Terrigenous Sands and Shales from Core or Log Data." Journal of Sedimentary Research - J SEDIMENT RES 58.

Hoffman, P. F. (1988). "United Plates of America, The Birth of a Craton: Early Proterozoic Assembly and Growth of Laurentia." Annual Review of Earth and Planetary Sciences 16(1): 543-603.

Holmquist, J. R., R. K. Booth and G. M. MacDonald (2016). "Boreal peatland water table depth and carbon accumulation during the Holocene thermal maximum, Roman Warm Period, and Medieval Climate Anomaly." Palaeogeography, Palaeoclimatology, Palaeoecology 444: 15-27.

Hülse, P. and S. J. Bentley Sr (2012). "A 210Pb sediment budget and granulometric record of sediment fluxes in a subarctic deltaic system: the Great Whale River, Canada." Estuarine, Coastal and Shelf Science 109: 41-52.

IPCC., A. S. (2007). "Climate change 2007: synthesis report." Summary fo r Policymakers.

Karegar, M. A., T. H. Dixon and S. E. Engelhart (2016). "Subsidence along the Atlantic Coast of North America: Insights from GPS and late Holocene relative sea level data." Geophysical Research Letters 43(7): 3126-3133.

Karlstrom, K. E., S. S. Harlan, M. L. Williams, J. McLelland, J. W. Geissman and K.-I. Ahall (1999). "Refining Rodinia: Geologic evidence for the Australia–western US connection in the Proterozoic." GSA Today 9(10): 1-7.

Kesel, R. H. (2008). "A revised Holocene geochronology for the Lower Mississippi Valley." Geomorphology 101(1-2): 78-89.

Labrecque, P. A., J. L. Jensen, S. M. Hubbard and H. Nielsen (2011). "Sedimentology and stratigraphic architecture of a point bar deposit, Lower Cretaceous McMurray Formation, Alberta, Canada." Bulletin of Canadian Petroleum Geology 59(2): 147-171.

Lanphere, M. A. and H. Baadsgaard (2001). "Precise K–Ar, 40Ar/39Ar, Rb–Sr and U/Pb mineral ages from the 27.5 Ma Fish Canyon Tuff reference standard." Chemical Geology 175(3-4): 653-671.

Laskowski, A. K., P. G. DeCelles and G. E. Gehrels (2013). "Detrital zircon geochronology of Cordilleran retroarc foreland basin strata, western North America." Tectonics 32(5): 1027-1048.

Lechnowskyj, A. (2015). The Stratal Architecture of the False River Point Bar (Lower Mississippi River, LA), LSU.

Leopold, D. J., G. R. Parker and W. T. Swank (1985). "Forest development after succesive clearcuts in the Southern Appalachians." Forest Ecology and Management 13(1-2): 83-120.

Lewis, S. L. and M. A. Maslin (2015). "Defining the Anthropocene." Nature 519(7542): 171-180.

Mason, C. C., A. Fildani, T. Gerber, M. D. Blum, J. D. Clark and M. Dykstra (2017). "Climatic and anthropogenic influences on sediment mixing in the Mississippi source-to-sink system using detrital zircons: Late Pleistocene to recent." Earth and Planetary Science Letters 466: 70-79.

Mayer, L. M. and S. P. Gloss (1980). "Buffering of silica and phosphate in a turbid river 1." Limnology and Oceanography 25(1): 12-22.

Meade, R. H. and J. A. Moody (2010). "Causes for the decline of suspended-sediment discharge in the Mississippi River system, 1940–2007." Hydrological Processes 24(1): 35-49.

Meade, R. H. and J. A. Moody (2010). "Causes for the decline of suspended-sediment discharge in the Mississippi River system, 1940–2007." Hydrological Processes: An International Journal 24(1): 35-49.

Montgomery, D. R. (2007). Dirt: The erosion of civilizations. Berkeley, University of California Press.

Moores, E. (1991). "Southwest US-East Antarctic (SWEAT) connection: a hypothesis." Geology 19(5): 425-428.

Moossen, H., J. Bendle, O. Seki, U. Quillmann and K. Kawamura (2015). "North Atlantic Holocene climate evolution recorded by high-resolution terrestrial and marine biomarker records." Quaternary Science Reviews 129: 111-127.

Muehlberger, W. R., R. E. Denison and E. G. Lidiak (1967). "Basement rocks in continental interior of United States." AAPG Bulletin 51(12): 2351-2380.

Mueller, P. A., A. L. Heatherington, J. L. Wooden, R. D. Shuster, A. P. Nutman and I. S. Williams (1994). "Precambrian zircons from the Florida basement: A Gondwanan connection." Geology 22(2): 119-122.

Murray, A. S. and A. G. Wintle (2000). "Luminescence dating of quartz using an improved single-aliquot regenerative-dose protocol." Radiation measurements 32(1): 57-73.

Murray, A. S. and A. G. Wintle (2003). "The single aliquot regenerative dose protocol: potential for improvements in reliability." Radiation measurements 37(4-5): 377-381.

Nittrouer, J. A. and E. Viparelli (2014). "Sand as a stable and sustainable resource for nourishing the Mississippi River delta." Nature Geoscience 7(5): 350.

Paola, C., P. L. Heller and C. L. Angevine (1992). "The large-scale dynamics of grain-size variation in alluvial basins, 1: Theory." Basin Research 4(2): 73-90.

Paola, C., P. L. Heller and C. L. Angevine (1992). "The large-scale dynamics of grain-size variation in alluvial basins, 1: Theory." Basin research 4(2): 73-90.

Park, H., D. L. Barbeau Jr, A. Rickenbaker, D. Bachmann-Krug and G. Gehrels (2010). "Application of foreland basin detrital-zircon geochronology to the reconstruction of the southern and central Appalachian orogen." The Journal of Geology 118(1): 23-44.

Pearce, N. J., W. T. Perkins, J. A. Westgate, M. P. Gorton, S. E. Jackson, C. R. Neal and S. P. Chenery (1997). "A compilation of new and published major and trace element data for

NIST SRM 610 and NIST SRM 612 glass reference materials." Geostandards newsletter 21(1): 115-144.

Percival, J., T. Skulski, M. Sanborn-Barrie, G. Stott, A. D. Leclair, M. T. Corkery and M. Boily (2012). "Geology and tectonic evolution of the Superior Province, Canada." Geological Association of Canada Special Paper 49: 321-378.

Prescott, J. R. and J. T. Hutton (1994). "Cosmic ray contributions to dose rates for luminescence and ESR dating: large depths and long-term time variations." Radiation measurements 23(2-3): 497-500.

Rafferty, J. P. (2014). Medieval Warm Period. Encyclopedia Britannica,.

Renne, P. R., C. C. Swisher, A. L. Deino, D. B. Karner, T. L. Owens and D. J. DePaolo (1998). "Intercalibration of standards, absolute ages and uncertainties in 40Ar/39Ar dating." Chemical Geology 145(1-2): 117-152.

Rhodes, E. (2011). "Optically Stimulated Luminescence Dating of Sediments over the Past 200,000 Years." Annual Review of Earth and Planetary Sciences 39: 461-488.

Rittenour, T. M. (2008). "Luminescence dating of fluvial deposits: applications to geomorphic, palaeoseismic and archaeological research." Boreas 37(4): 613-635.

Rittenour, T. M. (2018). "Dates and Rates of Earth-Surface Processes Revealed using Luminescence Dating." Elements 14(1): 21-26.

Rodgers, J. (1971). "The taconic orogeny." Geological Society of America Bulletin 82(5): 1141-1178.

Romans, B. W., S. Castelltort, J. A. Covault, A. Fildani and J. P. Walsh (2016). "Environmental signal propagation in sedimentary systems across timescales." Earth-Science Reviews 153: 7–29.

Ross, G. M. and M. Villeneuve (2003). "Provenance of the Mesoproterozoic (1.45 Ga) Belt basin (western North America): Another piece in the pre-Rodinia paleogeographic puzzle." Geological Society of America Bulletin 115(10): 1191-1217.

Saucier (1969). Geological Investigation of the Mississippi River area, Artonish to Donaldsonville, LA. U. S. A. C. o. Engineers. Waterways Experiment Station, Vicksburg, Mississippi.

Saucier, R. and J. Snead (1989). "Quaternary Geology of the Lower Mississippi Valley (Map at 1: 1,100,000)." Louisiana Geological Survey, Baton Rouge.

Singh, M., M. Sharma and H. J. Tobschall (2005). "Weathering of the Ganga alluvial plain, northern India: implications from fluvial geochemistry of the Gomati River." Applied Geochemistry 20: 1-21.

Sláma, J., J. Košler, D. J. Condon, J. L. Crowley, A. Gerdes, J. M. Hanchar, M. S. Horstwood, G. A. Morris, L. Nasdala and N. Norberg (2008). "Plešovice zircon—a new natural reference material for U–Pb and Hf isotopic microanalysis." Chemical Geology 249(1-2): 1-35.

Southgate, D. and M. Whitaker (1992). "Promoting resource degradation in Latin America: tropical deforestation, soil erosion, and coastal ecosystem disturbance in Ecuador." Economic development and cultural change 40(4): 787-807.

Stacey, J. t. and J. Kramers (1975). "Approximation of terrestrial lead isotope evolution by a two-stage model." Earth and planetary science letters 26(2): 207-221.

Stauffer, M. (2006). "Trans-Hudson Orogen." The Encyclopedia of Saskatchwen: 530.

Steiger, R. H. and E. Jäger (1977). "Subcommission on geochronology: convention on the use of decay constants in geo-and cosmochronology." Earth and planetary science letters 36(3): 359-362.

Sternberg, H. O. r. (1956). "A Contribution to the Geomorphology of the False River Area, Louisiana." LSU Historical Dissertations and Theses. 156.

Sternberg, H. O. R. (1956). A Contribution to the Geomorphology of the False River Area, Louisiana, Louisiana State University and Agricultural & Mechanical College.

Sundell, K. and J. E. Saylor (2017). "Unmixing detrital geochronology age distributions." Geochemistry Geophysics Geosystems 18: 2872–2886.

Syvitski, J. and J. Milliman (2007). "Geology, Geography, and Humans Battle for Dominance over the Delivery of Fluvial Sediment to the Coastal Ocean." Journal of Geology 115.

Taylor, S. R. and S. M. McLennan (1995). "The geochemical evolution of the continental crust." Reviews of geophysics 33(2): 241-265.

US Army Corps of Engineers (2017). History of the Lower Mississippi Levee System.

Vermeesch, P. (2013). "Multi-sample comparison of detrital age distributions." Chemical Geology 341: 140–146.

Vermeesch, P. (2018). "IsoplotR: A free and open toolbox for geochronology." Geoscience Frontiers 9(5): 1479-1493.

Wang, S., B. Fu, S. Piao, Y. Lü, P. Ciais, X. Feng and Y. Wang (2016). "Reduced sediment transport in the Yellow River due to anthropogenic changes." Nature Geoscience 9(1): 38-41.

Wanner, H., J. Beer, J. Bütikofer, T. J. Crowley, U. Cubasch, J. Flückiger, H. Goosse, M. Grosjean, F. Joos and J. O. Kaplan (2008). "Mid-to Late Holocene climate change: an overview." Quaternary Science Reviews 27(19-20): 1791-1828.

Wanner, H., J. Beer, J. Bütikofer, T. J. Crowley, U. Cubasch, J. Flückiger, H. Goosse, M. Grosjean, F. Joos, J. O. Kaplan, M. Küttel, S. A. Müller, I. C. Prentice, O. Solomina, T. F. Stocker, P. Tarasov, M. Wagner and M. Widmann (2008). "Mid- to Late Holocene climate change: an overview." Quaternary Science Reviews 27(19): 1791-1828.

Whitmeyer, S. J. and K. E. Karlstrom (2007). "Tectonic model for the Proterozoic growth of North America." Geosphere 3(4): 220-259.

Wiedenbeck, M., J. M. Hanchar, W. H. Peck, P. Sylvester, J. Valley, M. Whitehouse, A. Kronz, Y. Morishita, L. Nasdala and J. Fiebig (2004). "Further characterisation of the 91500 zircon crystal." Geostandards and Geoanalytical Research 28(1): 9-39.

Williams, L. E. and R. A. Thomas (1982). "The Early/Middle Woodland Period in New Jersey (ca. 1000 BC-AD 1000)." RUTGERS·: 1982.

Wintle, A. G. and A. S. Murray (2006). "A review of quartz optically stimulated luminescence characteristics and their relevance in single-aliquot regeneration dating protocols." Radiation measurements 41(4): 369-391.

VITA

Nikki grew up in New Orleans, Louisiana and graduated from Louisiana State University in May 2020 with a B.S. in Geology. There she conducted research with Dr. Clift and contributed to two research articles titled “A Late Eocene-Oligocene Through-Flowing River Between the Upper Yangtze and South China Sea” and “Large-scale mass wasting on the Miocene continental margin of western India”. Then she began her graduate degree at Louisiana State University in Fall of 2020 and plans to be completed in May of 2022.